Sensors and Materials

Mary McCarrick B.Sc

Thesis for the degree of

Doctor of Philosophy

submitted to

Dublin City University

School of Chemical Sciences

January 1995

Supervisor :- Dr Dermot Diamond

I hereby certify that this material, which I now submit for assessment on the programme of study leading to the award of Doctor of Philosophy is entirely my own work and has not been taken from the work of others save and to the extent that such work has been cited and acknowledged within the text of my work.

Signed: Mary McCarrick **ID No.:** 91700515

Mary McCarrick

Date: 26-2-95

To my Parents

Denis and Agnes.

Acknowledgements

Primarily I thank my supervisor Dr Dermot Diamond for his patience, enthusiasm and good humoured support throughout the last three years and especially during the preparation of this thesis. Many thanks to Dr Steve Harris for synthesising the majority of compounds on which I worked, and for his amenability to my many questions on calixarenes.

I would also like to thank Prof. M.A. McKervey and his students G. Barrett and M. Moran for the synthesis of three of the compounds examined and for their collaboration on this work. Thanks to Dr Padraig James for his help with the NMR studies.

My time spent in Abo Akademi in Finland, on the Erasmus Programme was a beneficial period thanks to the supervision of Prof. Ari Ivaska, Prof. A. Lewenstam and Dr Johan Bobacka. I also appreciate the help of Annette, Illka, Mikael, Johan, Anna-Lenna Marit and Pia who contributed to making the "Finland Experience" such a memorable time for me.

Thanks to all of the technical staff of the chemistry department and especially Mick Burke and Damien McGuirk for their help with the NMR studies.

Thanks to Amagruss Electrodes, Eolas, and Louth County Council for financial support.

This is the tricky bit- anyone who I should mention and don't, I'll see you on court. Thanks to all of the postgrads past and present, for all of the interesting discussions. Here's to the socialites from those mind-bending Ag22 days, Catherine, Eithne, Eva, Aisling, Ann-Sofi (the honorary Paddy) and of course to the radiator, with special thanks to Fiona and Teresa for the laughs and cries (not mentioning anyone in particular) and for all of their help in getting this thesis together. J118 where spontaneity was the name of the game, was made conducive to work! with the help of Mickey and Declan. Thanks also to the other members of my group, Patxi, Suzanne, Tom, Paddy, Margaret and the one-man group, Joe. The Friday basketball people, Dave, Mark, Stina, John, Orla and Farmer were only deadly. Many thanks for the friendship and entertainment value provided by Adrienne, Siobhan, Helen, Sean, Elaine, Kevin, Mags, Miriam and Mary O'.

Finally I would like to thank my parents Denis and Agnes for their love, friendship and tireless encouragement throughout my years in education, and my brothers Ian, Denis and Kevin for helping out and putting up with me over the last few months, (I promise I'll be nice from now on).

Table of Contents

	Page No.
Title Page	i
Declaration	ii
Dedication	iii
Acknowledgements	iv
Table of Contents	v
Abstract	x
Publications	xi

Chapter 1:- Literature

1.1 Neutral Carrier Ionophores	1
1.1.1 Mode of Complexation	1
1.1.2 Neutral Ionophores	2
1.1.3 Crown-Ethers	3
1.1.4 Cryptands	4
1.1.5 Spherands	4
1.2 Calixarenes	6
1.2.1 Historical	7
1.2.2 Calixarene Nomenclature	9
1.2.3 Modified Calixarenes	10
1.2.4 Calixarenes and Complexation	11
1.3 Optical Sensors	13
1.4 Chromoionophores	14
1.4.1 Neutral Chromoionophores	15
1.4.2 Ionisable Chromoionophores	16
1.4.3 Chromogenic Crown Ethers	16
1.4.4 Chromogenic Spherands	20
1.4.5 Chromogenic Calixarenes	21
1.5 Methods Employed with Chromophores	24
1.5.1 Cation Inclusion Examination by ^{1}H NMR Spectroscopy	24
1.5.2 Cation Induced Colour Change Examination by UV-Vis Spectroscopy	24
1.5.3 Cation Selectivity Determination	25
1.5.4 pK_a Determination	26
1.6 Importance of Li^+ Analysis	27
1.7 Trimethylamine	29
1.8 References	30

Chapter 2:-Methods and Materials

2.1 Materials 36
2.2 Instrumentation 36
2.3 Nitrophenol Chromoionophores (Ligands 1, 2, & 3) 36
2.3.1 Effect of Complexation on UV-VIS Absorbance 36
2.3.2 Selectivity Coefficient Determination 37
2.3.3 Optimum Base Concentration Determination 38
2.3.4 Effect of Solvent Variation on UV-Vis Spectra 38
2.3.5 Two Phase Examination of Ligands 38
2.3.6 Complexation Studies 39
2.4 Calix[4]arene with Chromophore Within Cavity (Ligand 4) 39
2.4.1 Effect of Complexation on UV-Vis Spectra 39
2.4.2 Selectivity coefficient Determination 40
2.4.3 ^{1}H NMR Complexation Studies 40
2.5 Nitrophenylazophenol Ionophores (Ligands 5, 6, 7, 8, & 9) 40
2.5.1 Effect UV-Vis Absorbance Spectra of Ligand Complexation 40
2.5.2 Selectivity Coefficient Determination 41
2.5.3 Solvent Choice for Two Phase Examinations 41
2.5.4 Two Phase Examination of Ligands 41
2.5.5 Complexation Studies 41
2.6 Assessment of Ligand 4 for The Rapid Colorimetric Detection of Trimethylamine 42
2.6.1 Liquid Phase Experiments 42
2.6.2 Preparation of Test Strips based on the Ligand 42
2.6.3 Preparation of Sealed Test Strips 43

Chapter 3:- Nitrophenol Ligands

3.1 Introduction 45
3.2 Mechanism of Colour Generation:- 48
3.3 Base Concentration Optimisation 50
3.4 Effect of Different Concentrations of Alkali Metals on Absorbance Spectra. 51
3.4.1 Ligand 1 51
3.4.2 Ligand 2 Monochromogenic Ligand 56

3.4.3 *Ligand 3 (C_{18}) One Phase Examination* 59
3.5 Selectivity Coefficient Determination 63
3.6 Solvent Variation 65
3.7 NMR Complexation Studies 68
3.8 Two Phase Studies 76
3.9 Ligand 4 84
3.9.1 Base Optimisation 84
3.9.2 Effect of Metal Ion Concentration Variation (Single-Phase) 84
3.9.3 Interference Studies 90
3.9.4 NMR Complexation Study 92
3.10 Discussion 98
3.11 Conclusion 111
3.12 References 113

Chapter 4:- Nitrophenylazophenol Calix[4]arenes

4.1 Introduction 116
4.2 Structures of Compounds Under Examination 120
4.3 Mode of Action 122
4.4 Absorbance Spectra of Ligands 5-9 122
4.4.1 Introduction 122
4.4.2 Ligand 5 123
4.4.3 Ligand 6. 125
4.4.4 Ligand 7 128
4.4.5 Ligand 8 and 9 131
4.5 Selectivity Determination 134
4.6 Two Phase Analysis of Nitrophenylazophenol Ligands 5 to 9 138
4.6.1 Choice of Water Immiscible Solvent 138
4.7 NMR Complexation Studies 143
4.8 Discussion 146
4.9 Gaseous Amine Detection 155
4.10 Liquid Phase Experiments 156
4.11 Test Strip Results 161
4.12 Covered Test Strips 164
4.13 Discussion 165
4.14 Overall Conclusion 166
4.15 References 167

Chapter 5:-The Development of Novel Solid Contact Ion-Selective Electrodes

5.1 Project Aim 170

5.2 Theory and Literature 170

5.2.1 Introduction 170

5.2.2 Potentiometry 170

5.2.3 Conventional Ion-Selective Electrodes 171

5.2.4 Activity Coefficients 173

5.2.5 Membrane Potentials 174

5.2.5.1 Boundary Potential 175

5.2.5.2 Diffusion Potential 177

5.2.5.3 The Complete Membrane Potential 178

5.2.6 Ion-Selective Membrane Components 178

5.2.7 Cation Selectivity 179

5.2.8 Neutral Carrier ISEs 179

5.2.9 Coated Wire Electrodes (CWE) 180

5.2.10 Solid Contact ISEs 184

5.2.11 Conducting Polymers 185

5.2.11.1 Introduction 185

5.2.11.2 Charge Conduction in Metals and Semiconductors 188

5.2.11.3 Doping 189

5.2.11.4 Synthesis of Conducting Polymers 189

5.2.12 Analytical Applications of Conducting Polymers 192

5.3 Experimental 196

5.3.1 Reagents 196

5.3.2 Electrode Nomenclature 196

5.3.3 Electrode Fabrication and Measurements:- 197

5.3.3.1 Electropolymerisation of PT and POT 197

5.3.3.2 Application of ISE Cocktail to the Solid Contact 198

5.3.3.3 Preparation of Coated Wire Electrodes 199

5.3.3.4 Preparation of Single Piece Ion-Selective Electrodes 199

5.3.4 Potentiometric Measurements 200

5.3.4.1 Potentiometric Measurements of Polymer Electrodes 200

5.3.4.2 Potentiometric Measurements of PVC Coated Electrodes 201

5.3.4.3 Single-Piece Ion-Selective Electrodes 201

5.3.5 Estimation of Selectivity Coefficients 202

5.3.5.1 Separate Solution Method 203

5.3.5.2 Mixed Solution Method 206
5.3.5.3 Selectivity Coefficient Determination for SCISEs, CWEs, and Single Piece Electrodes 206
5.3.6 Redox Responses 206
5.4 Results and Discussion 208
5.4.1 Comparison of Lithium Selective Solid-Contact Electrodes and Coated Wire Electrodes. 208
5.4.1.1 Pt/PT and Pt/POT 208
5.4.1.2 Ionic Response of Pt/PT/PVC(Li^+), Pt/POT/PVC(Li^+) and Pt/PVC(Li^+) 210
5.4.2 Time Response 213
5.4.3 Stability 213
5.4.4 Oxygen Dependence 217
5.4.5 Redox Response 218
5.4.6 Effect of Conditioning Solution on Electrode Response 219
5.4.7 Conclusion 220
5.5 Comparison of Chloride Selective Solid Contact Electrodes and Coated Wire Electrodes 221
5.5.1 Ionic Response 221
5.5.2 Stability 224
5.5.3 Oxygen Study 227
5.5.4 Redox Response 227
5.5.5 Conclusion 228
5.6 Discussion to sections 5.4 and 5.5, Solid Contact Lithium and Chloride Selective Electrodes. 229
5.7 Hybrid-Film Electrodes 233
5.7.1 Ionic Response 234
5.7.1.1 Single Piece Electrodes on Platinum. 234
5.7.1.2 Single Piece POT Electrodes Using Glassy Carbon as Substrate. 236
5.7.2 Stability 241
5.7.3 Oxygen Dependence 243
5.7.4 Redox Response 244
5.8 Hybrid-Film Electrode containing Chloride ionophore, GC/15%POT,85%PVC(Cl^-). 245
5.9 Overall Discussion 246
5.10 Conclusion 248
5.11 References 249

Sensors and Materials

Mary McCarrick

School of Chemical Sciences,
Dublin City University.

Abstract

The development of ionophores offering alternative modes of transduction of cation inclusion has evoked much recent interest. The first four chapters of this thesis deal with one such set of ionophores, namely chromogenic calix[4]arenes, which can exhibit a significant change in optical properties upon complexation with metal cations in the presence of a suitable base. All of the chromogenic compounds examined are ionisable chromoionophores which rely on the deprotonation of a phenolic group for colour generation.

Chapter 1:- This chapter offers a comprehensive introduction to ionophores with particular attention being paid to chromoionophores.

Chapter 2:- This chapter outlines the methods and materials used in the examination of the novel chromogenic calixarenes.

Chapter 3:- This chapter describes four novel calix[4]arenes bearing either one or four nitrophenol chromogenic groups. All compounds were examined as cation selective ionophores capable of exhibiting significant colour changes upon complexation with Li^+, and to a lesser extent with Na^+, in the presence of a suitable base.

Chapter 4:- This chapter concentrates on assessing another series of novel chromogenic calix[4]arenes bearing from one to four nitrophenylazophenol chromophores as optical signalling moieties. Li^+ selectivity over Na^+ was again exhibited. The lithium complex of the tetranitrophenylazophenol ligand was additionally examined as a solid phase gaseous trimethylamine (TMA) indicator.

Chapter 5:- This chapter deals with novel solid-state ion-selective electrodes. Both coated wire electrodes (CWE) and solid contact (SC) electrodes, which combined the electronically conducting nature of electropolymerised polythiophene (PT) or polyoctylthiophene (POT) with an ionically conducting PVC/ionophore layer, were assessed as lithium- and chloride-selective electrodes. Hybrid-film electrodes (HFE) which were made by mixing chemically polymerised POT and a PVC/ionophore cocktail in THF and applying this mixture to a glassy carbon substrate were also examined as Li^+ selective electrodes.

Publications Arising From This Thesis

The work presented in this thesis has formed the basis of a number of publications, *(Papers I to VI)*, and one patent application *(Patent I)*. Chapters 1 to 4 deal with the subject of neutral carrier ionophores and their ability to be modified to allow cation inclusion to be transduced by a spectral change. The experimental results reported in Chapters 3 and 4 formed the basis of an initial screening project, to determine the main properties of nine novel chromogenic calix[4]arenes. The work described in Chapter 3 has been published in *Papers I* and *II*. The contents of Chapter 4 formed the basis of *Papers III* and *IV*. As a result of the findings on these compounds, one patent application was filed, *(Patent I)*. Chapter 5 is an examination of novel solid state lithium and chloride selective electrodes and some of the results obtained have been published in *Paper V*, and are being used in the preparation of another paper, *Paper VI*. Other work carried out during this research on a novel reference electrode material (Refex), but which is not included in the thesis has been published in *Paper VII*.

Publications

Paper I:- "Novel Chromogenic Ligands for Lithium and Sodium Based on Calix[4]arene Tetraesters". M. McCarrick, Bei Wu, S.J. Harris, D.Diamond, G. Barrett, and M.A. McKervey, J. Chem. Soc., Chem. Commun., (1992) 1287.

Paper II:- "Chromogenic Ligands for Lithium Based Calix[4]arenes Tetraesters Bearing Nitrophenol Residues". M. McCarrick, Bei Wu, S.J. Harris, D.Diamond, G. Barrett, and M.A. McKervey, J. Chem. Soc., Perkin Trans. 3, (1993) 1963.

Paper III:- "Assessment of Three AzophenolCalix[4]arenes as Chromogenic Ligands for Optical Detection of Alkali Metal Ions". M. McCarrick, S.J. Harris, and D. Diamond, Analyst, 118 (1993) 1127.

Paper IV:- "Assessment of a Chromogenic Calix[4]arene for the Rapid Colorimetric Detection of trimethylamine". M. McCarrick, S.J. Harris, and D. Diamond, J. Mater. Chem., 4,2, (1994) 217.

Paper V:- "All Solid-State Poly(vinyl chloride) Membrane Ion-Selective Electrodes With Poly(3-octylthiophene) Solid Internal Contact". J. Bobacka, M. McCarrick, A. Lewenstam, and A. Ivaska, Analyst, 119 (1994) 1985.

Paper VI:- ". J. Bobacka, M. McCarrick, A. Lewenstam, D. Diamond, and A. Ivaska. In preparation.

Patent

Patent I:- "Chromogenic Ligands and Use Thereof in Optical Sensors, S.J. Harris, M.A. McKervey, and D. Diamond, European Patent Application, lodged 6th August 1993, No. S922577.

Chapter 1 Literature

There has been increasing interest in the development of analytical methods for determining alkali metal ions because of their importance in biological processes, clinical applications, the susceptibility of rubidium and caesium to neutron activation, the production of radioactive caesium during nuclear fission processes and the possible use of lithium as a fusion fuel. The traditional methods for alkali metal analysis has been flame photometry or atomic absorption/emission spectrometry with inductively coupled plasma spectrometry being used more recently for caesium analysis [1]. Flame photometric measurements are subject to ceratin disadvantages such as speed, maintenance and cost. The development of analytical techniques for cation analysis which could offer an improvement to this method has been sought.

1.1 Neutral Carrier Ionophores

The discovery of the ionophoric capabilities of neutral carrier molecules for alkali metal cations such as Na^+ and K^+ in clinical assays has led to their determination by potentiometry using ion-selective electrodes. Ionophores are molecular receptors which are capable of forming stable lipophilic complexes with charged hydrophilic species such as Li^+, Na^+, K^+, Ca^{2+}, etc. and which are capable of transporting them into lipophilic phases across natural or artificial membranes. Neutral carrier ionophores are uncharged lipophilic molecules capable of selectively transporting metal ions across a hydrophobic membrane.

1.1.1 Mode of Complexation

A number of principles have been developed from the study of macrocyclic cationic receptive molecules like those described earlier. The structural recognition between host and guest is controlled by:

i. The Complementarity Principle [2], which states that "in order to complex, hosts must have binding sites which co-operatively contact and attract binding sites of guests without generating strong non-bonded repulsions".
ii. The Principle of Preorganisation, which in its original formulation states that "the smaller the changes in organisation of host, guest, and solvent required for complexation the stronger will be the binding".

Common to all of the macrocycles used in the cationic recognition is the electrostatic interaction of the cation and the free electrons of heteroatoms such as oxygen, sulphur and nitrogen which form a hydrophilic cavity away from the lipophilic remainder of the molecule. The number of heteroatoms available for such interaction is dependent on the class of macromolecule and the relative conformation which it assumes either during synthesis or upon contact with the metal cation.

1.1.2 Neutral Ionophores

The first reference to neutral carriers was by Moore and Pressman in 1964 [3], where they reported the potassium ion binding ability of the naturally occurring antibiotic Valinomycin. Almost a decade later the huge analytical potential of the molecules as a highly selective potassium complexing agent was realised by Stefanac and Simon [4].

Other similar natural systems investigated during the early stages of this new area of chemistry include the macrotetrolides which are NH_4^+ specific. A selection of these is shown in Figure 1.1.

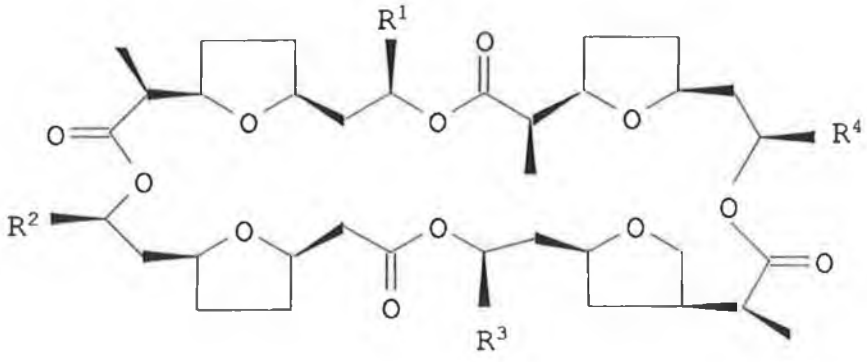

$R^1 = R^2 = R^3 = R^4 = CH_3$	**1.(i)** Nonactin
$R^1 = R^2 = R^3 = CH_3$ $R^4 = C_2H_5$	**1.(ii)** Monactin
$R^1 = R^3 = CH_3$ $R^2 = R^4 = C_2H_5$	**1 (iii)** Dinactin
$R^1 = CH_3$ $R^2 = R^3 = R^4 = C_2H_5$	**1 (iv)** Trinactin
$R^1 = R^2 = R^3 = R^4 = C_2H_5$	**1 (v)** Tetranactin

Figure 1.1:- *A selection of macrotetrolides.*

1.1.3 Crown-Ethers

While the naturally occurring antibiotics were being investigated synthetic compounds with alkali and alkaline earth metal ion complexing properties were obtained by Pedersen in 1967, and were called crown ethers [5], because of the resemblance of the molecular model of the first member of this series to a crown. The [18]crown-6 macrocycle (Figure 1.2) binds potassium in preference to the other alkali metal ions.

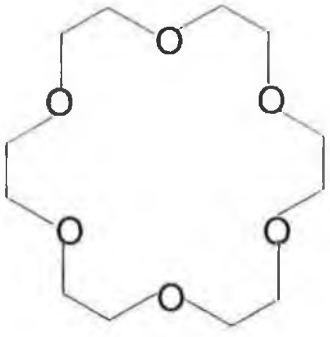

1 (vi)

Figure 1.2:- *[18]crown-6 [5].*

Crystal structures of [18]crown-6 and its K^+SCN^- complex have been obtained [6] and show that the host and its complex have different conformational organisations. The free host does not have a cavity or a "crown" shape as the potential cavity is filled with two inward turning CH_2 groups only. However, upon interaction with the K^+ guest the cavity becomes organised and an interaction occurs between the oxygen atoms and the guest. Cation selectivity is dependent on charge, size and electronic structure of the cations as well as the nature of the counterion [7].

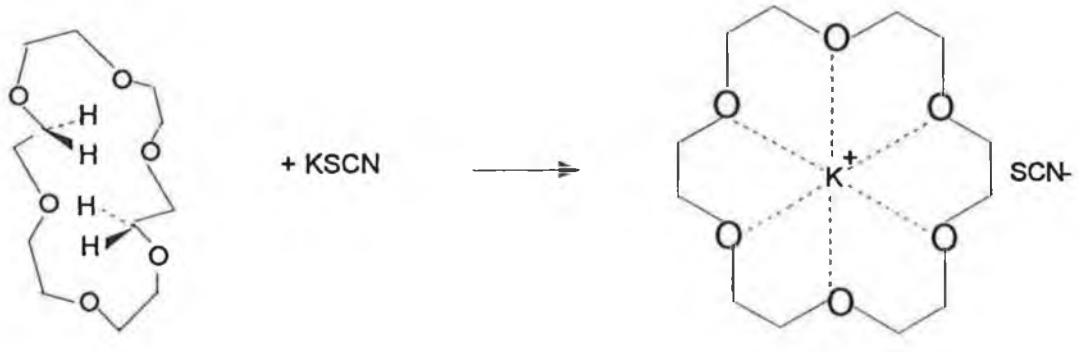

1 (vii) **1 (viii)**

Figure 1.3:- *[18]crown-6 and its K^+SCN^- complex, [7].*

1.1.4 Cryptands

The first purpose built molecules to mimic the ionophoric properties of the antibiotics were the cryptands synthesised by Lehn [8]. The cryptands differ from most crown ethers in their bicyclic nature, containing intramolecular cavities with 3 dimensional shaped "crypts" in which the bridges contain oxygen or sulphur atoms with nitrogen atoms acting as the bridgeheads e.g. [2,2,2] cryptand does not have a cavity in its uncomplexed state but reorganises upon complex formation with K^+ so that a potassium ion-occupied cavity develops lined with 28 electrons [6], (Figure 1.4). Complexes formed between these macrobicyclic ligands and alkaline earth metals [9] display enhanced stabilities with respect to the corresponding crown ether complexes [10].

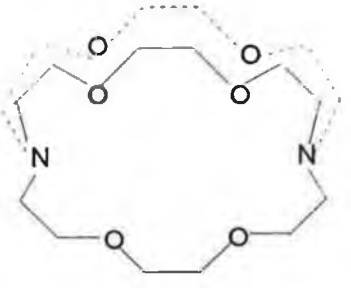

1 (ix)

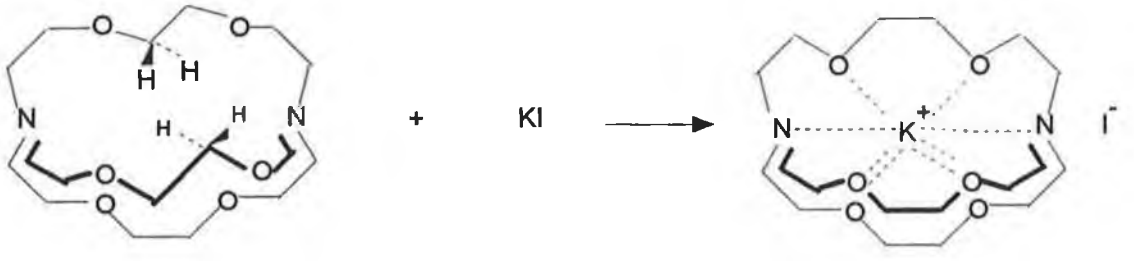

1 (x) 1 (xi)

Figure 1.4:- 1(ix) A [2.2.2] cryptand, 1(x) its conformation, and 1(xi) its K^+I^- complex, [6].

1.1.5 Spherands

In the 1970's Cram and co-workers developed a class of rigid hosts which were highly preorganised for complexation during synthesis. The first set of molecules in this class are known as spherands [11]. These are very powerful and highly

discriminating binders of Na^+ and Li^+ [12]. Figure 1.5 shows the structure of a six membered spherand and its Li^+ complex. The six oxygens of the six methoxy groups are held in a perfect octahedral arrangement by their attachment of six interconnected aromatic rings each attached to one another at their 2,6- positions. Their cavities are too small to be filled either by parts of the host itself or solvent molecules and can only be filled by simple monatomic ions. Another class of molecules stemming from the spherands is the hemispherand [13]. Hemispherands are hosts in which at least half of its structure is composed of units unable to fill their own potential cavities by conformational reorganisation.

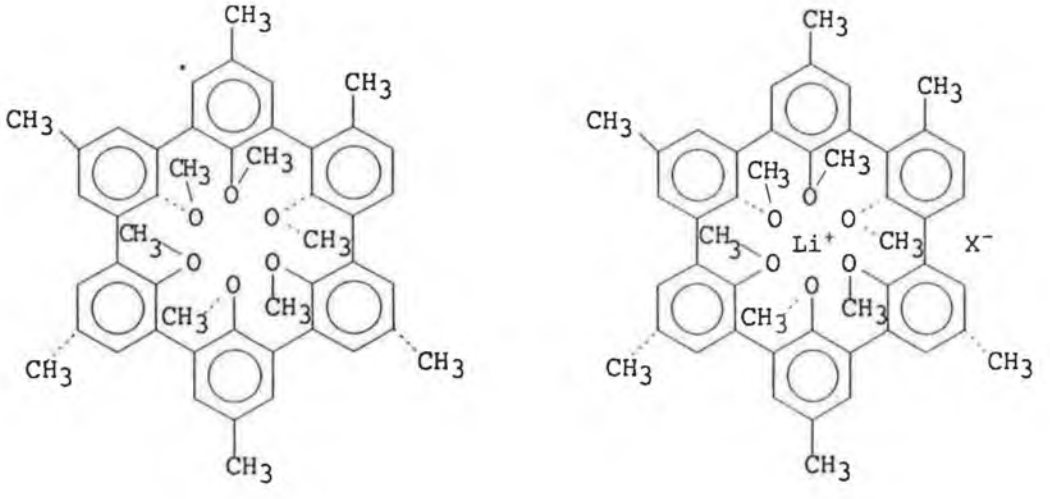

1 (xii) **1 (xiii)**

Figure 1.5:- A spherand and a spherand lithium salt complex [12].

Other hosts have been reported which have varying degrees of structural organisation, including podands [14], lariat ethers [15], cryptophanes [16], and the related speleands [17]. See Figure 1.6. On the "picrate salt extraction scale" defined by Cram [18], the complexing power of synthetic receptors towards the alkali metal cations falls in the following order, spherands > cryptaspherands > cryptands > hemispherands > coronands > crown ethers > podands > solvents.

The focus of our attention with macrocyclic ionophores was on calixarenes which are defined as [1n] metacyclophanes [19] and are products of phenol formaldehyde condensations.

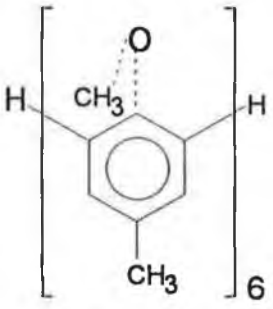

1 (xiv)
Podand [14]

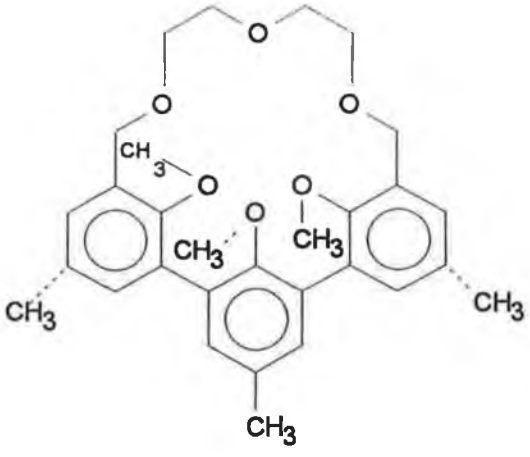

1 (xv)
Hemispherand [13]

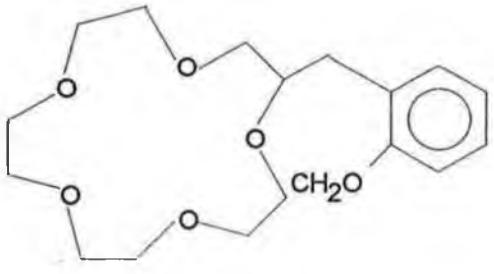

1 (xvi)
Lariat Ether [15]

Figure 1.6:- *Selection of neutral-carrier ionophores*

1.2 Calixarenes

The term calixarene was coined in 1975 by David Gutsche who perceived a similarity between the shape of a Greek vase called a calix crater and the molecular model of the cyclic oligomers produced by the condensation of *p*-substituted phenols with formaldehyde.

1.2.1 Historical

The study of phenol formaldehyde chemistry first appeared in the literature in 1872 when Adolph Von Baeyer published his work describing that phenol condenses with formaldehyde in the presence of a mineral acid to produce a resinous tar [20]. His inability to isolate pure materials from these reactions prevented a characterisation of these materials.

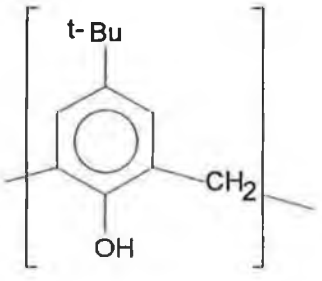

1 (xvii)

Figure 1.7 :- *General structure of calixarenes.*

A number of other chemists attempted to elucidate the structures of the resinous tars and find practical applications for their interesting properties, but it was not until Leo Baekeland discovered the preparation of the tough, resilient resin (marketed under the tradename "Bakelite") from this phenol-formaldehyde reaction [21] that interest in this area grew substantially again owing to the tremendous success of this phenoplast.

In 1942 an investigation of the "curing" phase of the phenol formaldehyde process by Alois Zinke and his co-worker Erich Ziegler was begun. The study involved simplifying the problem of variability in product conformations, by looking not at phenol but at *p*-substituted phenols. Phenol itself reacts at the *ortho* and *para* positions to form highly cross-linked polymers in which each phenolic residue is attached to three other residues. A *para* alkyl phenol, can react only at the two *ortho* positions thereby reducing the cross-linking possibilities of the formation of a linear polymer. The base induced reaction of formaldehyde and *p-tert*-butyl phenol first described in 1941 [22] yielded a crystalline product that decomposed above 300 °C and in 1944 [23] a cyclic tetrameric structure was postulated for this product, (Figure 1.8).

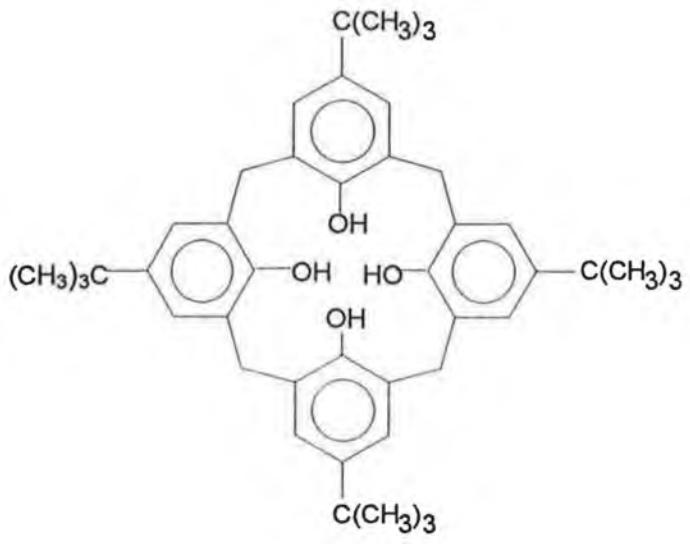

1 (xviii)

Figure 1.8 *:- p-tert-butyl calix[4]arene, [23].*

Zinke and co-workers in the following years produced a series of compounds from *p*-methyl, *p-tert*-butyl, *p-tert*-pentyl, *p*-(1,1,3,3 tetramethylbutyl)-phenol, to which cyclic tetrameric conformation was attributed.

In 1955 John W. Cornforth was interested in the preparation of tuberculostatic substances and among the compounds tested were the Zinke products which had been presented in the literature in 1944 [23] . However on repeating Zinke's reaction starting with *p-tert*-butylphenol, two materials rather than a single product were isolated. Both possessed the physical and chemical properties of a cyclic oligomer but with somewhat different melting points. Cornforth proposed that the compounds are diasterioisomers arising from hindered rotation of the phenolic nuclei around the methylene linkage [24]. He therefore concluded that the Zinke reaction produces only cyclic tetramers. This however was later disproved in the 1970's with a combination of ^{1}H, ^{13}C NMR and mass spectroscopy to be in fact a combination of cyclic octamer and hexamer [25-27].

David Gutsche's association with the Petrolite Corporation in Missouri, which was involved in the development of cyclic oligomers for use as demulsifiers for crude oil, led to an awareness of phenol-formaldehyde chemistry in general and cyclic oligomeric chemistry in particular. So when Gutsche became interested in the newly emerging area of bioorganic chemistry, in the 1970's, known as enzyme mimics, the Zinke cyclic tetramers sprang to mind as potential molecular

baskets. Initially Gutsche's group set about dealing with the scope of the phenol-formaldehyde cyclisation reaction to determine which phenols reacted to yield high melting products and which did not. Following the reassignment of the Zinke products to cyclic hexamers and octamers, further examination of the one-step process of the *p-tert*-butyl-phenol reaction was carried out by the group [28]. Reaction variables such as changes in solvents, bases, and reactant ratios led to the development of a number of recipes that now permit the cyclic tetramer, cyclic hexamer and cyclic octomer from *p-tert*-butyl phenol to be easily prepared in good yield.

These compounds are now among the most accessible synthetic macrocyclic baskets and have commanded the attention of many research groups worldwide. The recent publication of two books devoted solely to the subject of calixarenes and their applications [29, 30] and the host of journal publications and patent applications on the subject illustrate the huge potential envisaged by this class of macrocycles.

1.2.2 Calixarene Nomenclature

The number of aryl groups is indicated by the insertion of the number between the calix and the arene e.g. calix[4]arene, denotes the cyclic tetramer. Then to indicate from which phenol the calixarene is derived the *p*-substituent is designated by name e.g. the cyclic tetramer from *p-tert*-butylphenol is called *p-tert*-butylcalix[4]arene. There are five members of the series ranging from the relatively rigid calix[4]arene to the much larger and more flexible octameric calix[8]arene. The odd numbered pentamers and heptamers are however much less accessible than the other three.

The parent *p-tert*-butyl calix[n]arenes are white crystalline materials characterised by high melting points e.g. *p-tert*-butyl calix[4]arene m.p. 342-344°C and low solubility in organic solvents. It was Cornforth who first suggested that four discrete conformational isomer forms of the calix[4]arene exist [24]. It is now recognised that the various conformations of a calix[4]arene are readily inter-convertible and Gutsche has designated them as "cone", "partial cone", "1, 2 -alternate cone" and "1, 3 - alternate cone" [31], (Figure 1.9). The 1, 2 alternate cone conformation is encountered much less frequently [32].

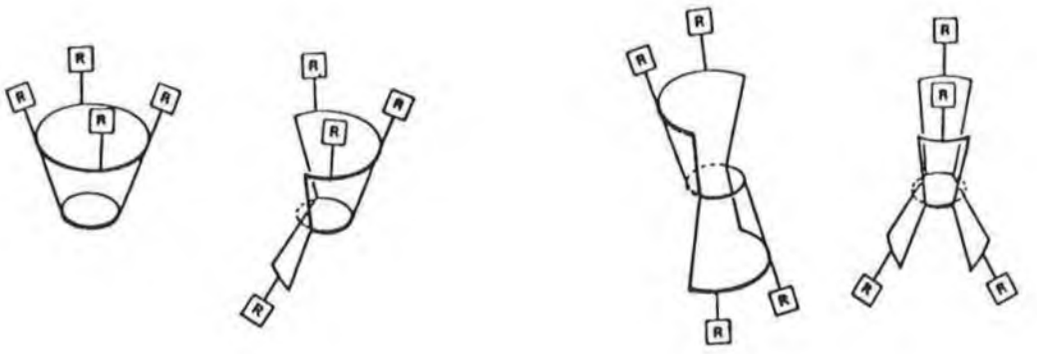

1 (xix)	1 (xx)	1 (xxi)	1 (xxii)
Cone	Partial Cone	1,2-Alternate	1,3-Alternate

Figure 1.9:- *Pseudo 3-dimensional representation of the conformers of calix[4]arenes [29].*

1.2.3 Modified Calixarenes

The parent *p-t*-butylcalixarenes have very little ionophoric activity for alkali metal cations, shown by their inability to transport these ions from neutral aqueous solution through a chloroform membrane [33, 34, 35] because there are not sufficient numbers of electron rich heteroatoms available for binding. Only when the source phase is the basic metal hydroxide is transport observed, phase transfer then being coupled to phenoxide ion formation [35]. However, these structures may be used as a platform onto which groups of ion-binding substructures may be assembled. The "lower" rims of phenol derived calixarenes are already functionalised with hydroxyl groups which provide excellent sites for the introduction of other moieties which have been found to increase the ionophoric nature of the molecules [36].

McKervey et al., introduced methyl and ethyl esters to calix[4, 6 and 8] arenes at this phenolic position and found a size related selectivity pattern, with the calix[4]arenes being selective for Na^+ and the calix[6]arenes preferentially extracting K^+, Rb^+, and Cs^+ ions. The introduction of the ester groups in the presence of excess acylating agents, lowered the conformational mobility of the molecules thereby freezing the molecule into one of the four conformations i.e. the cone. The melting point of the molecules can also in some cases be lowered significantly by lower rim substitution e.g. the tetramethyl (and tetrabenzyl ethers

of *p-tert*-butyl calix[4]arene have m.p. 226-228 °C and 230-231 °C respectively compared to m.p. 342-344'C for the unsubstituted *p-tert*-butyl calix[4]arene.

Substituents have also been introduced onto the "upper rim" of calixarenes via modification of the *p*-alkyl group by several methods [29]. Modification of the *p*-sustituents has been shown to increase the solubility in a variety of organic solvents and in extreme cases render them soluble in water e.g. sulphonated, and trimethylammmonium chloride calixarenes [37, 38].

1.2.4 Calixarenes and Complexation

It was hoped that lower rim phenolic functional group modification of calix[4]arenes, to produce derivatives containing carbonyl groups, in the form of pendent ester and ketone groups would result in efficient ligating groups in much the same way that ester groups participate in ion-binding with natural receptors such as valinomycin. Arnaud-Neu et al. [39] successfully synthesised a number of tetrameric derivatives containing either ester or ketone pendants, (Figure 1.10) and characterised them by X-ray crystallography.

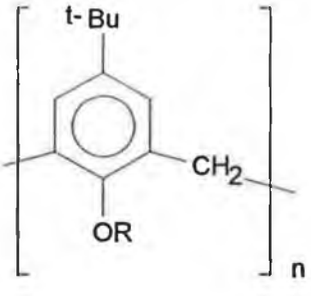

1 (xxiii) R = CH_2COCH_3 Ketone.
1 (xxiv) R = CH_2COOCH_3 Ester

Figure 1.10:- *Lower-rim functionalised calix[4]arenes, [39].*

The tetrameric structures exist in a very rigid cone conformation with the polar substituents mutually "syn" with respect to the macro ring i.e. grouped together at one end of the cavity, and the hydrophobic moieties directed towards the upper rim thus conferring a high degree of preorganisation on the molecules **1(xxv)**. The molecules are frozen into the cone conformation during synthesis. X-ray crystal structures for a calix[4]arene and a calix[6]arene are shown below.

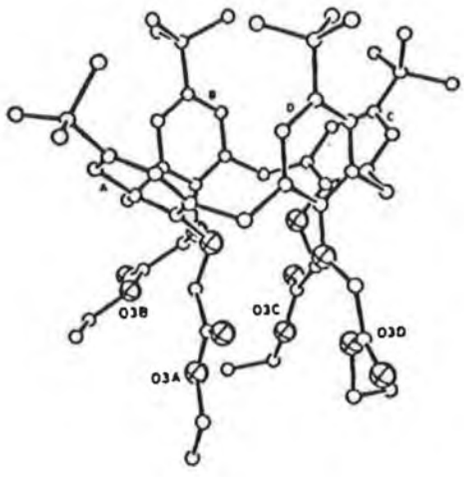

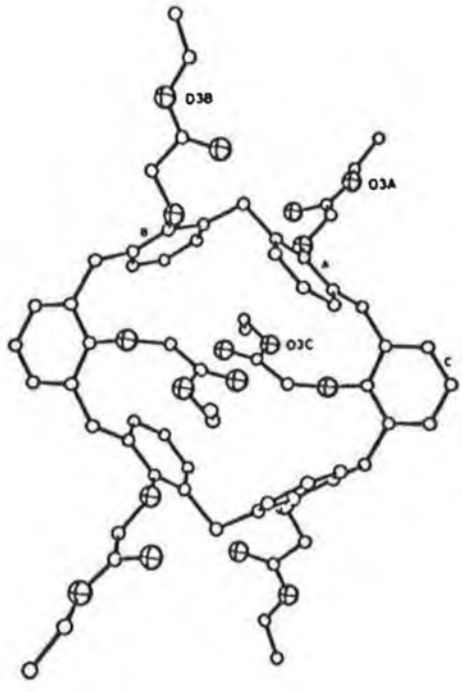

1 (xxv) **1 (xxvi)**

Figure 1.11:- *X-ray crytal structures of (a) the p-t-butyl-tetraethylester calix[4]arene and (b) the hexaethylester calix[6]arene. Carbon and oxygen atoms are shown as spheres of arbitary radius, oxygen atoms are larger and marked with a cross [39].*

The *t*-butyl-tetraethyl ester calix[4]arene exhibits a distorted cone structure with two of the opposing aromatic rings essentially parallel, while the other two rings are almost normal to one another. This can be seen in **1 (xxv)** where the aromatic rings B and D are almost parallel to each other and rings C and A are tilted at an angle away from the plane B and D. The same sort of distorted cone shape is observed in the *p-t*-butyl-tetramethylketone calix[4]arene. These molecules were found to exhibit cation binding properties. The encapsulation of an alkali metal occurs with the cation being centrally located within the hydrophilic cavity defined by the four ester/ketone groups and supported electrostatically by the four ethereal oxygen atoms and the four carbonyl oxygen atoms [39, 40] (Figure 1.12).

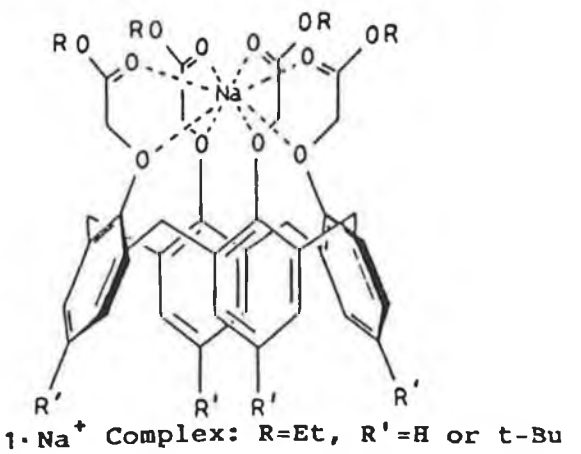

1·Na^+ Complex: R=Et, R'=H or t-Bu

Figure 1.12:- *Encapsulation of an alkali-metal cation by a tetrameric calixarene ester or ketone, R = Et, R' = H or t-But*

Further modifications of the phenolic groups and changes in the substituents bonded to the heteroatoms used have been carried out by numerous groups verifying the role played by phenolic and carbonyl oxygen atoms as receptor sites in forming complexes with alkali and alkaline earth metals. Variations in cation selectivity occur with modifications of both the lower rim phenolic groups and upper rim *t*-butyl group and have been described in depth in a number of publications [41-43].

1.3 Optical Sensors

Traditionally the transduction of metal ions using calixarenes has been by potentiometry where the first attempts to produce a sodium ion-selective electrode (ISE) involved the use of methyl and ethyl esters in liquid membrane electrodes [44] containing the methyl ester [45]. However recently increasing interest has been shown in the development of sensors utilising optical transduction. The term optrode or optode has been given to such devices, which offer attractive features relative to conventional electrodes which were outlined by Seitz in 1984 [46] and Narayanaswamy and Russell in 1986 [47].

The increased interest in optical sensors was sparked both by the progress in the development of optical hardware and by the hope of eliminating certain disadvantages of electrochemical sensors. They allow continuous remote

monitoring and can measure concentrations without significantly perturbing the sample, a very useful feature for process control applications. Because the signal is optical it is not subject to electrical interferences. No "reference electrode" is required since internal referencing can be carried out by ratioing the signal at the optimum analytical wavelength with that of a reference wavelength at which the analyte does not absorb. The ratio of the two wavelength intensity signals can be used to correct for any optical variations. The reagent phase does not have to physically contact the fibre optic, so the use of the reagent phase on a disposable basis could be practical.

The main stumbling block to the development of optical chemical sensors so far has been finding suitable immobilisable layers which have the potential to change their optical properties upon interaction with the analyte of interest. Numerous types of chemical sensing layers have been developed. A ligand (ion carrier, ionophore, indicator, complexing agent) is used as the sensing or analyte binding layer and the optical signal is generated upon interaction of the carrier with the analyte, whereupon the carrier itself or an additional compound (chromoionophore, fluoroionophore, indicator dye), changes its optical properties upon complexation with a different ion. To date, the electrically neutral and lipophilic ionophores which are widely used as the selective compounds in ion-selective electrodes, have commanded most attention for ion-selective optodes.

With the mode of complexation of the macrocycles established it became clear that by varying the nature of the pendant groups other properties could be built into these molecules. Among the neutral carrier ionophores examined for chromogenic applications were crown ethers, spherands, hemispherands and corands with calix[4]arenes only recently being synthesised with chromogenic indicator systems attached.

1.4 Chromoionophores

The strategy for designing a cation-responsive dye has been outlined in reviews and can involve cation extraction by a neutral dye [48], or an ionisable dye [49]. Chromoionophores for cation complexation are of two types, neutral and ionisable, and are summarised in the following equations [50].

Ion + Chromoionophore	⇌	Complex	*Colour Change*
Neutral: $CI + M^+$	⇌	$CI.M^+$	" "
Ionisable: $CIH + M^+$	⇌	$CI^-.M^+ + H^+$	" "

Figure 1.13:- Different types of chromoionophores.

Neutral chromoionophores (CI) contain a polarised chromophore linked to the ionophore. The positive cation charge influences the donor heteroatoms (O, N, S) as previously discussed and their electronic surroundings by ion-dipole forces. If one of the heteroatoms is a constituent of a mesomeric system such as the N atom in **1(xxviii)**, the electronic disturbance propagates through the whole (n and π) system. Due to different influences on the ground and photoexcited states of the neutral chromoionophoric compounds by cations, changes occur in the absorption spectra. These "dyes" have electron donor and acceptor sites within a molecule so that the charge transfer from the donor to acceptor according to electronic excitation gives rise to their strong visible light absorption [48]. The interaction of metal ions with the dye molecule in a manner to stabilise the localised charge on the donor site leads to hypsochromic shifts of the charge transfer band. Conversely the interaction to stabilise the charge on the acceptor site results in a bathochromic shift.

Ionisable chromoionophores (CIH) ionise in the presence of a bound cation if the pH is appropriate with the resulting change in absorption spectrum usually greater than for a neutral chromoionophore and the absorption spectrum of the complex $CI^-.M^+$ shows a shift to longer wavelength compared with the spectrum of the ionisable chromophore CIH.

1.4.1 Neutral Chromoionophores

The development of molecular combined neutral carrier dyes with high "colour sensitivity" to complexed cations began with crown ethers in the 1970's with Dix and Vogtle [51] synthesising a series of neutral chromoionophores and Takagi et al. synthesising a series of ionisable chromophoric crown ethers [52].

In Dix and Vogtle's work the electron donor or acceptor part of the chromophore was actually incorporated into the crown ether ring with one such example shown below in Figure 1.14.

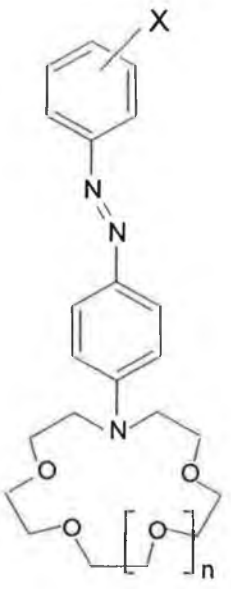

1 (xxviii)

Figure 1.14:- Neutral crown ether chromoionophore [51].

Changes in the absorption spectra occur due to electrostatic interactions between the complexed cations and the chromophore dipoles with different λ_{max}. values being observed for different extents of complexation. The largest band shifts are produced by the cation which optimally fills out the ligand cavity.

1.4.2 Ionisable Chromoionophores

Nine ionisable chromogenic calix[4]arenes are examined in the work to be presented here, all of which possess ionisable phenolic groups, (Chapter 3 and 4).

1.4.3 Chromogenic Crown Ethers

Takagi et al. in 1977 synthesised the first coloured crown ether anions [52, 53], where mono (Figure 1.15) and diprotonic chromophores were set into a crown skeleton in such a way that the complexation of positively charged metal ions was accompanied by the dissociation of protons of the chromophore. The colour effect with such chromoionophores is primarily due to the spectral differences of

the protonated and deprotonated species with very little difference being observed between the absorption spectra of different cations. Extraction studies of metal ions from an aqueous phase into a basic-chloroform layer which housed the chromogenic ligands resulted in an ease of extraction order of $K^+ > Rb^+ > Cs^+ > Na^+ >> Li^+$ being obtained and resulted in a method for the photometric determination of 10-800 ppm of K^+.

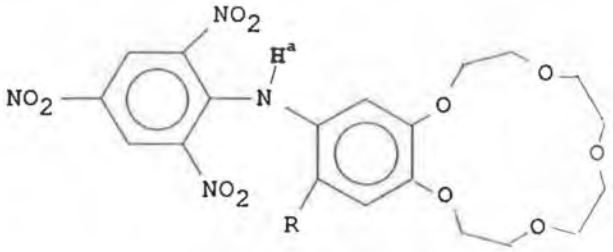

1 (xxix) R=H
1 (xxx): R=NO_2
1 (xxxi) R=Br

[a] = Labile proton

Figure 1.15:- *Picrylaminobenzene[15]crown-5 derivatives [49].*

Further work on the examination of the effect of variation in chromophore substituents e.g. nitrile or trifluoromethyl for nitro, of these picrylaminobenzene[15]crown-5 derivatives was carried out by Pacey et al. [54] to try and increase the spectral separation of the HL and L^- species making the effective molar absorptivity for L^- greater and improving the reagent sensitivity. The addition of a trifluoromethyl group was found to improve aqueous solubility and one of the molecules bearing this group was found to behave as a potassium selective colorimetric crown ether. The analytical range which the analysis covered was within the normal 137-207 ppm K^+ range for human blood serum. The results obtained with this system were comparable with those obtained by atomic absorption spectrometry of the same sample.

Lariat ethers bearing a similar monobasic amine linkage were also examined and proved to have better extraction ability for alkali metal cations, however this was at the expense of reduced cation selectivity [55].

In 1981 Misumi et al. incorporated a second type of ionisable chromophore into a crown ether system [56], namely a dinitrophenylazophenol group, **(xxxii)** with in this instance, the ionisable phenolic proton, being sited within the crown cavity.

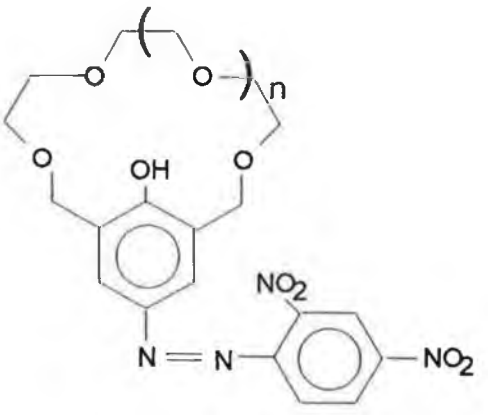

1 (xxxii)

Figure 1.16:- "Crowned" dinitrophenylazophenol [56].

Pyridine was the base used in this work to facilitate the uptake of the phenolic proton upon preferential lithium complexation. A colour change from yellow to purple-red was observed upon complexation, with Li^+, when n =1. A number of factors were deemed to be crucial for lithium induced colour generation, such as

1. cavity size of the crown ether unit,
2. acidity constant of the azophenol group,
3. basicity of the added amine and
4. polarity of solvent.

Coordination of the dissociated phenol with the Li^+ cation, along with the restrictive cavity size, were thought to be the main reasons why complexation with other metal alkali metal salts was precluded.

Alder et al. [57] developed a similar system for the determination of K^+ in the presence of sodium by increasing n to 2 and attaching this reagent to an optical fibre, by dipping the fibre (which had been coated with Amberlite XAD-2 resin and encapsulated with porous PTFE membrane), in a 0.1 % methanol solution of the crown compound. A potassium sensor capable of determining aqueous potassium ions in the range 10^{-3}-10^{-1} M aqueous resulted. However the K^+/Na^+ selectivity of 6.4 was not sufficient for clinical use. Further work by Sutherland et al. has been carried out on K^+ and Na^+ determination in the presence of other clinically important cations by optical methods, using other macrocycles and will be referred to later.

Work on chromoionophores bearing the dinitrophenylazophenol chromophore continued with Misumi et al. [58], with the aim of obtaining an amine selective complexation coloration. The coloured complexes of these crowns with metal or

ammonium ion are differentiated from simple ion-dipole type complexes by an additional binding force, namely, coulombic interaction between the phenolate anion, housed in the central hydrophilic crown cavity and the guest cation. A number of these nitrophenylazophenol crowns were found to be capable of producing colour changes with primary, secondary and tertiary amines. Coloration was found to be related to the structure of the complex rather than to the relative basicity of the amines. Figure 1.17 shows one of the dinitrophenylazophenol crowns described in this paper which apart from the chromophore also contains the nitrogen of a pyridine ring in the crown cavity. Variations in absorption λ_{max} were observed for the different classes of amines i.e. primary amines result in absorption between 574-586 nm while secondary and tertiary amine systems absorbed between 602-606 nm.

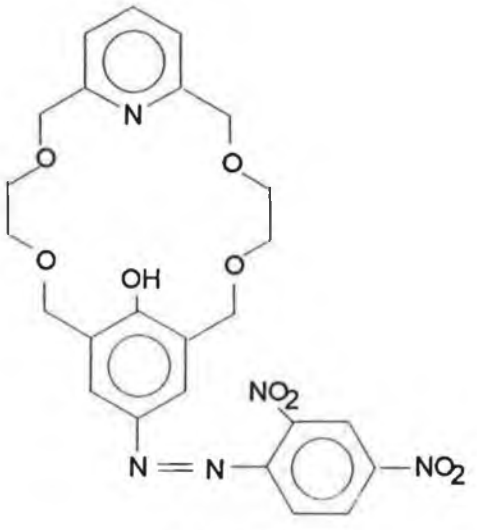

1 (xxxiii)

Figure 1.17:- Amine selective "crowned" dinitrophenylazophenol [58].

In 1988 Van Gent et al. [59] used a [15]crown-5 incorporating a phenol, onto which was attached an ethenylmethylquinolonium iodide moiety, with again a phenolic hydroxyl group sited in the crown cavity. In this work the importance of the coulombic interaction between the phenolate anion, along with electrostatic interaction with the crown oxygens, for cation selectivity was expressed. Complexation with Ca^{2+} caused the greatest λ_{max} shift in the absence of a base and was suggested as being indicative of the Ca^{2+} ion being compatible with the cavity size and thereby in close contact with the phenolate anion. Such cation anion interactions in the cavity of macrocycles have been described as saltexes [60].

1.4.4 Chromogenic Spherands

In 1986 Cram et al. introduced the highly preorganised spherands to the world of chromogenic cation analysis. A chromogenic spherand which acted as a lithium-specific chromogenic indicator system for solid lithium salts of soft anions such as LiBr, LiI or $LiClO_4$ but was too weak for that of solid LiF, $LiNO_3$ and Li_2SO_4, was described [18]. This compound bore a dinitrophenylazophenol chromophore with the chromophoric phenol group acting as part of the spherand backbone. Subsequently a six membered spherand incorporating a dinitrophenylazophenol moiety was synthesised and its high Li^+ binding power seen by its non-chromogenic analogue was found to be maintained [61]. The pK_a of the phenolic proton varied depending on which cation was complexed with the ligand. The lowest pK_a of 5.9 was found for the Li^+ complex compared to values of 6.9, 12.7, and 13 for the Na^+, K^+ complexes and the free ligand respectively. The sodium complex of one such chromogenic spherand is shown in Figure 1.18.

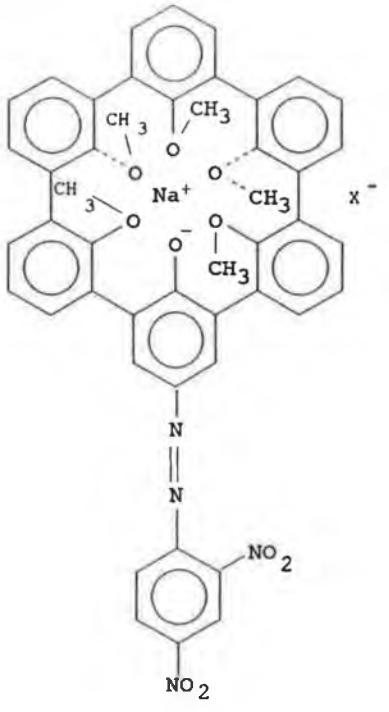

1(xxxiv)

Figure 1.18:- *Complex formed between metal cation and dinitrophenylazophenol spherand [61].*

Cram et al.'s interest in chromoionophores continued with results for Na^+ and K^+ selective cryptaspherands published in 1989 [62]. The molecules synthesised were targeted because of the selective nature of their analogous non-chromogenic cryptaspherands for either Na^+ or K^+. The picrylamine groups attached to one of

the spherand rings acted as the chromophore with the inclusion of a cation in the central cavity being sufficient to increase the acidity of the monobasic amine proton selectivities of greater than 1000 for both $[K^+]/[Na^+]$ and $[Na^+]/[K^+]$ were obtained with these new compounds.

In 1992 two groups described chromogenic cryptands which showed excellent lithium over sodium selectivities [63, 64]. Sholl et al. reported a Li^+:Na^+ selectivity ratio of ca. 10^4 on the basis of the spectroscopic response at pH 9. No response to Na^+ was seen even at a 1M NaCl concentration. Zazulak et al. reported an association constant of 3200 M^{-1} in 10 % DEGMEE/TMA(OH) (diethylene glycol monoethyl ether / tetramethyl ammonium hydroxide) for a lithium chromgenic cryptand complex, but could not obtain a value for Na^+ or K^+ due to the lack of a chromogenic response. Both sets of compounds contained a phenolic hydroxy group in the central cavity, attached to a nitrophenylazophenol group.

1.4.5 Chromogenic Calixarenes

In 1984 Bohmer et al. described a lithium specific colour change for a calix[4]arene which had not been functionalised at the hydroxyl group on the phenolic units. However, the calixarenes examined contained one hydroxylnitrophenylene unit [65].

The first report of the incorporation of the nitrophenylazophenol into a calix[4]arene structure appeared in 1989 [66] (Figure 1.19a). The pK_a values of each of the phenolic protons of a tetrachromogenic derivative were evaluated.

$$CalixH_4 \rightleftharpoons CalixH_3^- + H^+ \qquad pK_{a1} = 0.5$$

$$CalixH_3^- \rightleftharpoons Calix\ H_2^{2-} + H^+ \qquad pK_{a2} = 2.0$$

$$Calix\ H_2^{2-} \rightleftharpoons Calix\ H^{3-} + H^+ \qquad pK_{a3} = 10.0$$

$$Calix\ H^{3-} \rightleftharpoons Calix^{4-} + H^+ \qquad pK_{a4} = 13.0$$

where H^+ is the acid proton removed from the phenol groups.
The marked pK_a split was explained by the strong hydrogen-bonding interactions characteristic of calix[4]arenes. The cation binding capabilities of a monochromogenic calix[4]arene bearing one nitrophenylazophenol group with

the phenolic hydroxyl group sited in the central hydrophilic cavity was later examined by the same group [67] (1xxxvi).

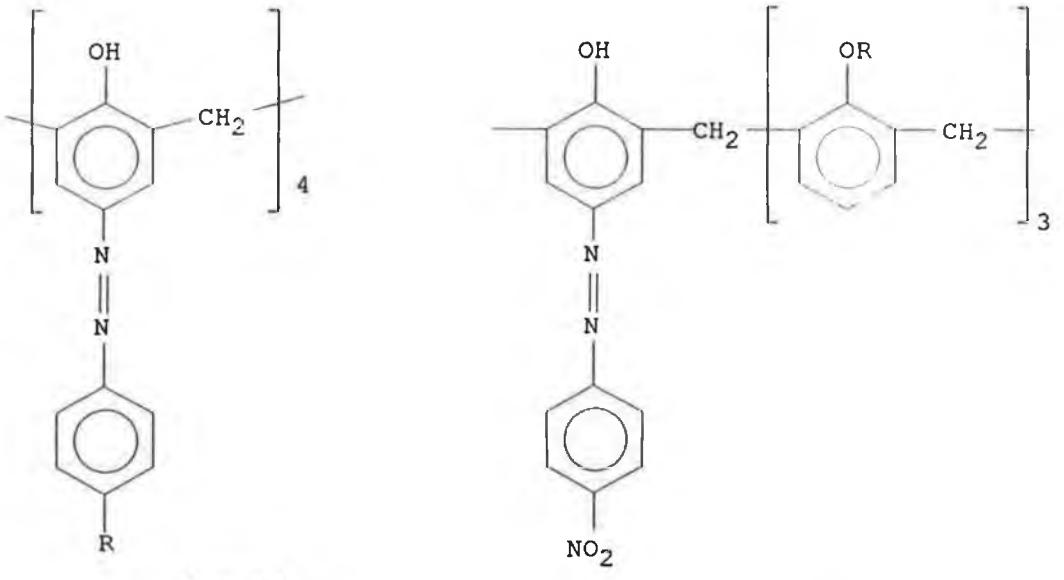

1(xxxv) **1(xxxvi)**

Figure 1.19:-(a) Tetra-nitrophenylazophenol Calix[4]arene and (b) Mono-nitrophenylazophenol Calix[4]arene.

This compound displayed Li^+ over Na^+ selectivity in the presence of imidazole which was added to facilitate the metal induced proton dissociation. Complexation was again thought to occur with Li^+ acting as a counter-cation for the azophenolate anion as well as interacting by electrostatic interaction with the three phenolic and carboxylic oxygens. A similar molecule which contained a 2,4-dinitrophenylazophenol group rather than a 4-nitrophenylazophenol group was described by Nakamoto et al. and was also found to display Li^+ specific coloration in the presence of triethylamine [68].

Sutherland et al. used the same chromophore in a tetrameric bridged structure (1xxxi) [69, 70] which had previously been shown to display K^+ selectivity in its purely ionophoric form [71]. The sensitivity to K^+ at a given pH was found to be susceptible to alteration by varying the pK_a of the azophenol chromophore through a change in the substitution pattern of the chromogenic aromatic group. It was found that improved extraction ability for K^+ from a buffered pH aqueous solution to $CHCl_3$ was demonstrated when the chromogenic moiety was a dinitrophenylazophenol as opposed to the nitrophenylazophenol. The addition of a second electron withdrawing NO_2 group would appear to have the ability to give further stabilisation to the deprotonated phenolic form of the chromogenic

moiety [69]. A reduction in the size of the bridge of the calix[4]arene from 5 to 4 (OCH_2) groups was found to change the cation for which the molecule was selective, to Na^+, with very little response to K^+ [70]. K^+ over Na^+ selectivity which was adequate for physiological samples was obtained.

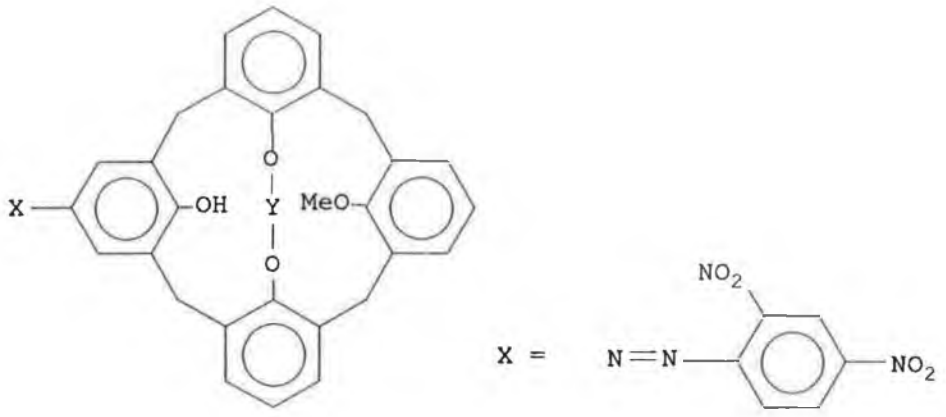

Y = $OCH_2(CH_2OCH_2)_3CH_2O$

1(xxxvii)

Figure 1.20:- *Bridged chromogenic calix[4]arene [69].*

The neutral indoaniline chromophore has been used most recently in conjunction with calixarenes for cation analysis [72, 73]. Kubo et al. described a Na^+ selective calix[4]arene tetraester. A bathochromic shift was observed upon complexation with the Na^+ cation and was explained in terms of the well tailorerd electrostatic interactions existing between Na^+ cation surrounded by OCH_2COO^- groups and the indoaniline carbonyl oxygen segment [72]. A 1, 3 bis indoaniline calix[4]arene has been found to display Ca^{2+} induced colour change with greater than a 100 nm bathochromic wavelength upon interaction with Ca^{2+}, [73]. The preferential binding of Ca^{2+} compared to Na^+ which have similar ionic radii is attributed to the higher charge density of the Ca^{2+} which should interact more strongly with polar donor groups, especially those of the two quinone oxygens.

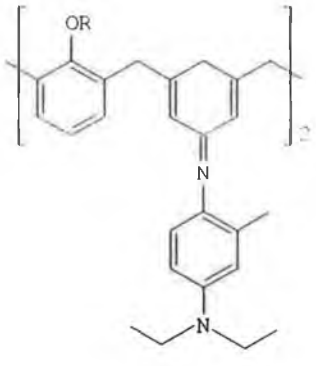

1(xxxviii) R = CH_2CO_2Et

Figure 1.21:- *1,3-Bis(indoaniline) derived Calix[4]arene [73].*

1.5 Methods Employed with Chromophores

1.5.1 Cation Inclusion Examination by ^1H NMR Spectroscopy

The inclusion of cations into chromogenic ionophores has been examined by ^1H NMR spectroscopy. The chromoionophore is generally dissolved in $CDCl_3$ and a ^1H NMR spectrum is obtained before incremental concentrations of the salts of interest are added, usually 0.5, 1.0, 2.0 mole equivalents, and the spectral shifts are observed. For 1:1 stoichiometric complexes no further spectral shifts are observed after a 1 M equivalent has been added. The most dramatic spectral shifts are observed for the most selective cations, with complexation exerting a stronger force on the ligands thus perturbing the NMR signal to the greatest extent. This behaviour was observed by Cram et al. for their chromogenic spherand, where ^1H NMR shifts were observed for the Li^+ and Na^+ complexes, with little perturbation of the signal observed upon addition of K^+ [61].

Actual NMR spectra are shown by Jin et al. for a fluorogenic calix[4]arene system. The ligand was again dissolved in $CDCl_3$ and NaSCN salt dissolved in CD_3OD [74]. Shifts of the peaks due to the bridging methylene protons of the calix ring due to the complexed and uncomplexed forms of the ligand are observed after a 0.5 mole equivalent of salt is added. However, once a 1 mole equivalent of salt is added the bridging methylene proton peaks show no further perturbation.

The interaction of Li^+ with the phenolate anion of the mono chromogenic calix[4]arene described by Shinkai et al. [67], has been inferred by NMR spectroscopy. In their study of the δH values for the OCH_2CO methylene protons were shifted to a higher magnetic field in the presence of Na^+ with the same peaks being shifted down field in the presence of Li^+, indicative of two different types of binding occurring.

1.5.2 Cation Induced Colour Change Examination by UV-Vis Spectroscopy

Studies of the inclusion of cations into macroyclic compounds possessing ionisable chromophores followed by deprotonation causing a colour change have been carried out by using UV-Vis spectroscopy. Lipophilic bases are usually included to facilitate the metal-induced proton-dissociation. A suitable solvent

system is chosen to dissolve the ligand. To this the base i.e. imidazole, pyridine, trimethylamine, etc., is added and finally varying concentrations of metal salts are added and the UV-Vis spectrum is recorded in the range 200 - 800 nm. From this wavelength absorbance maxima (λ_{max}) and extinction coefficient (ε) values can be calculated for complexed and uncomplexed forms of the cations. The solvent employed can be critical due to the nature of the transitions involved in generating the spectrum. Because the chromophores employed are conjugated π systems and their absorbance spectra occur in the visible region of the spectrum, two types of transitions namely $n \rightarrow \pi^*$ and $\pi \rightarrow \pi^*$, are responsible for generating the signal with $n \rightarrow \pi^*$ transitions generated from the movement of unshared electrons from the heteroatoms into the conjugated ring, more polar solvents result in hypsochromic shifts. This can be explained in terms of non-bonding electrons in the ground state being stabilised relative to the excited state, by hydrogen bonding or electrostatic interaction with polar solvents and thus a higher energy input is required to move electrons to the excited state. In $\pi \rightarrow \pi^*$ transitions the excited state is more polar than the ground state and therefore dipole-dipole interactions with polar solvents will lower the energy of the excited state more than that of the ground state, resulting in bathochromic shifts in some cases (but not all), with increasing polarity. This solvent dependence is illustrated clearly by Zazulak et al. [64], and Cram et al. [61]. Solvents used for one phase examinations include methylene chloride [75], methanol [59], chloroform [58], chloroform/pyridine [56], THF/methanol [76], 10% Aqueous DEGMEE [64].

1.5.3 Cation Selectivity Determination

The selectivity of different chromogenic ligands for different cations has been determined by a number of methods. Complexation constants determined by the Benesi-Hildebrand [77] method have been employed in one phase systems [61]. Helgeson et al. [62], obtained actual selectivity values for their cryptaspherands for K^+ over Na^+ by ratioing the slope of the curve obtained with aqueous solutions of 140 mM NaCL and varying concentrations of KCl between 1 and 10 mM, and the curve obtained with a background concentration of 4 mM KCl with varying NaCl concentrations between 0 and 200 mM.

In two phase systems where the ligand is dissolved in an organic phase and the metal salt is introduced in an immiscible aqueous phase, extraction coefficients

have been employed for determining cation selectivity. Sutherland et al. [71], calculated the extraction coefficient (see equations **1.1** and **1.2**) of cations from an aqueous phase into chloroform in a pH controlled environment and ratioed the interfering ion K_e with that of the primary ion, to obtain a selectivity measurement.

$$[M^+]_{aq} + [ClH]_{org} \rightleftharpoons [H^+]_{aq} + [M^+Cl^-]_{org} \qquad \textbf{(1.1)}$$

$$K_e = \frac{[H^+]_{aq}[M^+Cl^-]_{org}}{[M^+]_{aq}\,[ClH]_{org}} \qquad \textbf{(1.2)}$$

where M^+ = primary ion.
The various parameters were measured by UV-Vis spectroscopy at the protonated and deprotonated λ_{max}.

1.5.4 pK_a Determination

The evaluation of the pK_a of the dissociating protons with various metal cations is also a useful indicator of cation selectivity. The lower the pK_a of these protons to a particular metal cation, the more easily the dissociating proton will be removed and hence less basic conditions can be used to facilitate proton dissociation for select cations. A number of publications have described a variation in pK_a values for the dissociating protons of ionisable chromoionophores. Cram et al. found with their chromoionophore **1**(xxxiv) that the $HL.Na^+$ and $HL.Li^+$ were much stronger acids than the free, uncomplexed ligand HL and there was also a difference in the acidity of both of these complexes, i.e. $HL.Li^+$, $pK_a = 5.9$, $HL.Na^+$, $pK_a = 6.9$, HL $pK_a = 13.0$, [61]. The different forms of the ligand are

- HL = protonated ligand,
- L^- = deprotonated ligand,
- $L^-.M^+$ = deprotonated complex,
- $LH.M^+$ = protonated complex.

pK_a measurements were carried out in 80% dioxane-20% water. In these pK_a determinations the concentrations of protonated and deprotonated indicator were adjusted by incremental additions of solutions of HCl or base where necessary until concentrations of the protonated and deprotonated indicators equalled one

another. The pH's of the resulting solutions were taken. The observed readings were adjusted with ionic activity factors that correct for ionic strength changes in water-dioxane mixtures. Further pK_a studies involving some of the same authors [62, 78] were based on the following equations, (**1.3-1.6**).

$$pK_a = pH + \log (HL/L^-) \qquad \textbf{(1.3)}$$

$$\frac{HL}{L^-} = \frac{A_{a\lambda}\varepsilon_{L^-,\,b\lambda} - A_{b\lambda}\varepsilon_{L^-,a\lambda}}{A_{a\lambda}\varepsilon_{HL,\,a\lambda} - A_{b\lambda}\varepsilon_{HL,b\lambda}} \qquad \textbf{(1.4)}$$

$$\frac{A_{a\lambda}}{l} = \varepsilon_{HL,\,a\lambda}[HL] + \varepsilon_{L^-,\,a\lambda}[L^-] \qquad \textbf{(1.5)}$$

$$\frac{A_{b\lambda}}{l} = \varepsilon_{HL,\,b\lambda}[HL] + \varepsilon_{L^-,\,b\lambda}[L^-] \qquad \textbf{(1.6)}$$

where HL is the protonated chromoionophore, L^- is the deprotonated chromoionophore, A is the observed absorbance at $a\lambda$ (wavelength maxima of HL) or $b\lambda$ (wavelength maxima of L^-), ε is the molar absorptivity and l is the light path length in centimeters. Spectra were obtained for solutions of the ligand in its completely protonated form i.e. 0.02 M HCl added to suppress ionisation of the dissociating proton, and in its completely ionised form i.e. in the presence of 0.02 M TMAOH, and also in media buffered to known pH's. From the spectral data the pK_a values were calculated.

1.6 Importance of Li^+Analysis

Lithium therapy is the most widely used treatment for the control of recurrent depression or manic depression. It is administered as Li_2CO_3 and monitoring of lithium concentration during treatment is required in order to secure a therapeutic effect and to avoid an overdose of lithium which could lead to fatal poisoning [79]. There is a narrow gap between therapeutic and toxic levels, see Figure 1.22.

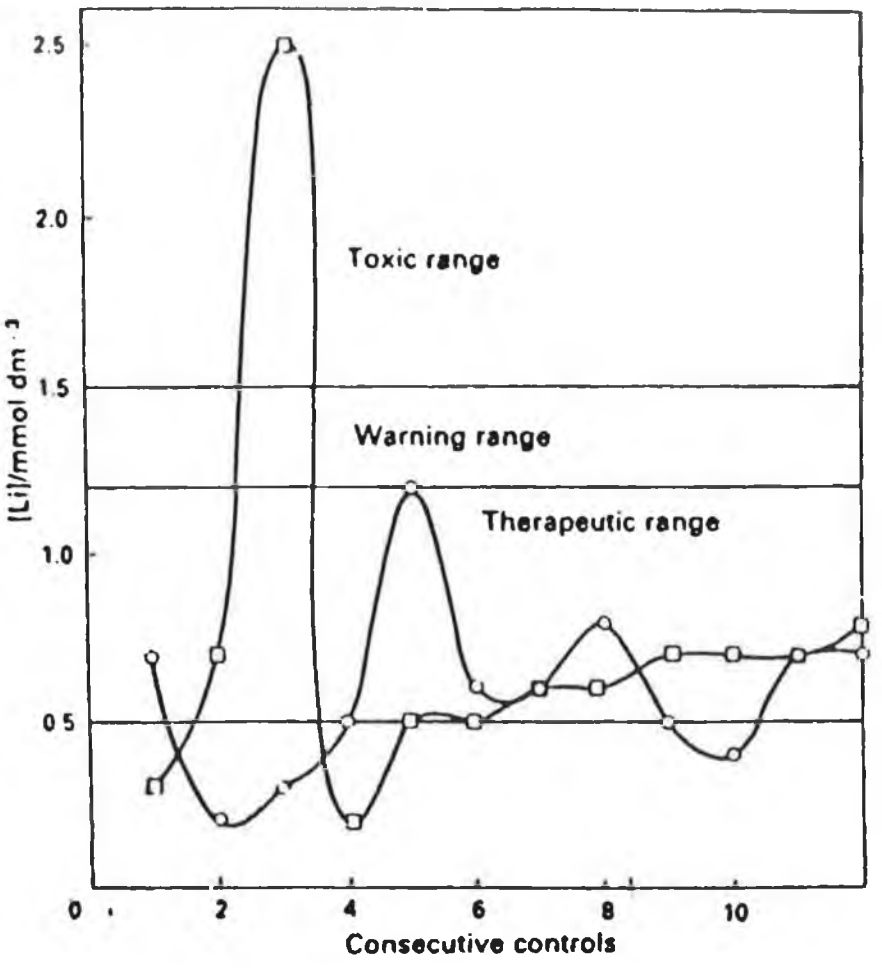

Figure 1.22 *:- Example of serum Lithium Concentration Control Chart, for monitoring of* Li^+ *levels during therapy [89].*

For the treatment to be therapeutic serum lithium levels should be maintained between 0.5 and 1.0 mM. At between 2.0 and 2.5 mM, adverse side-effects appear and at higher levels death. The effect of doses of Li_2CO_3 are patient specific and therefore serum levels must be constantly monitored. A facile assay for blood samples from patients receiving lithium salts is clinically desirable to eliminate the use of AA which is more time consuming and expensive. A clinical lithium analyser based on ISEs is available for potentiometric analysis, but there is room for improvement [80].

There has been much recent interest in the development of a neutral carrier ionophore which could be applied to this application. Sodium is the main ionic interferent in blood fluid assays, being present at 1400 times higher concentrations than the lowest level of 0.1 mM lithium. Along with the neutral

chromoionophores exhibiting Li^+ selectivity [56, 61, 63-68] a number of other ionophores have been examined for ISE electrode capabilities.

The ionophores used have been the cyclic crown-ethers or the non-cyclic polyether diamide carriers and polypropoxylate adducts and these have been reviewed [81]. Work has continued with all types of ionophores [82-86] including the natural antibiotics [87, 88]. Parker et al. in 1991 described a di-*n*-butylamide14-crown-4 derivative which had superior Li^+ over Na^+ selectivities i.e. Log $k^{pot}_{Li,Na}$ = - 3.25 and -2.92, to anything previously reported [89]. The electrode also functioned satisfactorily in serum, exhibiting a fast response time (10-15s), had minimal protein interference and had a lifetime of 50 d which is acceptable for such an electrode.

1.7 Trimethylamine (TMA)

TMA is a degradation product of the reaction of bacteria such as *Pseudomanas* upon trimethylamine oxide in marine fish after death [90]. Its detection, along with other amines, has been used as a means of determining fish freshness. Traditionally fish freshness has been assessed by olfactory analysis [91], but this is both time consuming and expensive. Colorimetric methods have also been employed and developed successfully, and can distingiush between TMA and dimethyl amine (DMA) [92-94], both of which are generated (along with other volatile amines and sulphides) as the fish spoils [90]. However, these methods require time consuming mincing of the fish followed by solvent extraction before analysis. More recently Gastec detector tubes, containing crystals which change colour as they react with a specific gas or vapour, have been developed and used in amine analysis of the gill air of fish [95], with amines being determined in a concentration range of 0.05 to 5 ppm. These tubes are attached to a pump and a specific volume of gas is analysed. GC analysis of amines produced by fish has also been used to distinguish between TMA and DMA and to quantify the levels at which each are present [96]. Another approach investigated for TMA analysis involves the use of semiconductor gas sensors containing ruthenium. Such sensors were found to respond well to 50 ppm TMA and were used to determine the freshness of Japanese saurel [97, 98]. All of these methods, while not all destructive, do involve a certain degree of handling of the samples or involve some form of instrumentation. The development of a non-instrumental indicator system which would respond quickly to gaseous amines could obviously be of great benefit to the food industry.

1.8 References

1. H. Vanhoes, C. Vandecasteele, J. Versieck and R. Dans, Anal. Chem., 61 (1989) 1851.
2. D.J. Cram, G.M. Lein, J. Am. Chem. Soc., 107 (1985) 3657.
3. C. Moore and B.C. Pressman, Biochem., Biophys. Res. Commun., 15 (1964) 562.
4. Z. Stefanac and W. Simon, Microchem. J., 12 (1967) 125.
5. C. J. Pedersen, J.Am. Chem. Soc., 89 (1967) 7017.
6. D.J. Cram and K.N. Trueblood, Top. Curr. Chem., 98 (1981) 43.
7. C.J. Pedersen and H.K. Frensdorf, Angew. Chem. Int. Ed. Engl., 11 (1972) 16.
8. B. Dietrich, J.M. Lehn, J.P Sauvage, Tett. Lett., (1969) 2885.
9. B. Dietrich, J.M Lehn, and J.P. Sauvage, Tett. Lett., (1969) 2889.
10. J.M. Lehn and J.P. Sauvage, J. Am. Chem. Soc., 97 (1975) 6700.
11. G.M. Lein, D.J. Cram, T. Kaneda, R.C. Helgeson, G.M. Lein, J. Am. Chem. Soc., 101 (1979) 6752.
12. D.J. Cram, T. Kaneda, R.C. Helgeson, S.B. Brown, C.B. Knobler, E. Maverick, K.N. Trueblood, J. Am. Chem. Soc., 107 (1985) 3645.
13. K.E. Koenig, G.M Lein, P. Stuckler, T. Kaneda, D.J. Cram, J. Am. Chem. Soc., 101 (1979) 3553.
14. F. Vogtle and E. Weber, Angew. Chem., Int. Ed.Engl., 18 (1979) 753.
15. G. W. Gokel, D.M. Dishong and C. J. Diamond, J. Chem. Soc., Chem. Commun., (1980) 1053.
16. J. Canceill, L. Lancombe and A. Collet, J. Am. Chem. Soc., 107 (1985) 6993.
17. J. Canceill, A. Collet, J. Gabard, F. Kotzyba-Hibert and J.M Lehn, Helv. Chim. Acta, 65 (1982) 1894.
18. D.J. Cram, Angew. Chem., Int. Ed. Engl., 25 (1986) 1039.
19. D.J. Cram and H. Steinberg, J. Am Chem. Soc., 73 (1951) 5691.
20. A. Baeyer, Ber., 5 (1872) 25.
21. L.H. Baekeland, U.S. Patent 942, October (1908) 699.
22. A. Zinke and E. Ziegler, Ber., B74 (1941) 1729.
23. A. Zinke and E. Ziegler, Ber., 77 (1944) 264.
24. J.W. Cornforth, P. D'Arcy Hart, G.A. Nicholls, R.J.W. Rees and J.A. Stock, Br. J. Pharmacol., 10 (1955) 73.

25. H. Kammerer, G. Hapel and F. Caesar, Makromol. Chem., 162 (1972) 179.

26. G. Happel, B. Mathiasch, and H. Kammerer, Makromol. Chem., 176 (1975) 3317.

27. J.H. Munch, Makromol. Chem., 178 (1977) 69.

28. C.D. Gutsche and R. Muthukrishnan, J. Org. Chem., 43 (1978) 4905.

29. C. D. Gutsche "*Calixarenes*", Monographs in Supramolecular Chemistry, Vol. 1, R.S.C. Cambridge (1989).

30. J. Vicens and V. Bohmer, (edts.), "*Calixarenes - A Versatile Class of Macrocyclic Compounds*", Topics in Inclusion Science, Kluwer Academic Publishers, (1991).

31. C.D. Gutsche, B. Dhawam, J.A. Levine, K.H. No, L.J Bauer, Tetrahedron, 39 (1983) 409.

32. L.C. Groenen, J.D. Van Loon, W. Verboom, S. Harkema, A. Casnati, R. Ungaro, A. Pochini, F. Ugozzoli , R.N. Reinhoudt, J. Am. Chem. Soc., 113 (1991) 2385.

33. R.M. Izatt, J.D. Lamb, R.T. Hawkins, P.R. Brown, S.R. Izatt and J.J. Christensen, J. Am. Chem. Soc., 105 (1983) 1782.

34. A. Arduini, A. Pochini, S. Reverberi, and R. Ungaro, J. Chem. Soc., Chem. Commun., (1984) 981.

35. C. Alfieri, E. Dradi, A. Pochini, R. Ungaro, and G.D. Andreetti, J. Chem. Soc., Chem. Commun., (1983) 1075.

36. M.A. McKervey, E.M. Seward, G. Ferguson, B. Ruhl, S.J. Harris, J. Chem. Soc., Chem. Commun., (1985), 389.

37. S. Shinkai, H. Kawabata, T. Arimura, T. Matsuda, H. Satoh and O. Manabe, J. Chem. Soc. Perkin Trans. 1, (1989) 1073.

38. S. Shinkai, Y. Shirahama, T. Tsubaki and O. Manabe, J. Chem. Soc. Perkin Trans. 1, (1989) 1859.

39. F. Arnaud-Neu, E.M. Collins, M. Deasy, G. Ferguson, S.J. Harris, B. Kaitner, A.J. Lough, M.A. McKervey, E. Marques, B.L. Ruhl, M.J. Schwing -Weill, E.M. Seward, J. Am. Chem. Soc., 111 (1989) 8681.

40. A. Arduini, A. Pochini, S. Reverberi, R. Ungaro, C.D. Andreetti, F. Ugozzoli, Tetrahedron, 42 (1986) 2089.

41. G. Barrett, V. Bohmer, G. Ferguson, J.F.Gallagher, S.J. Harris, R.G. Leonard, M.A. McKervey, M. Owens, M. Tabatabai, A. Vierengel, W. Vogt, J. Chem. Soc., Perkin Trans 2, (1992) 1595.

42. F. Arnaud-Neu, G. Barrett, S. Cremin, M. Deasy, G. Ferguson, S.J. Harris, A.J. Lough, L. Guerra, M.A. Mc Kervey, M.J. Schwing-Weil, P. Schwinte, J. Chem. Soc., Perkin Trans 2, (1992) 1119.

43. E.M. Collins, M.A. McKervey, E. Madigan, M.B. Moran, M.Owens, G. Ferguson, S.J. Harris, J. Chem. Soc., Perkin Trans 1, (1991) 3137.

44. D. Diamond, in M.R. Smyth and J.G. Vos, (edts.), "*Electrochemistry, Sensors and Analysis*", Analytical Chemistry Symposium Series, Volume 25, Elsevier, Amsterdam, (1986) 155.

45. D. Diamond, G. Svehla, E.M. Seward, M.A. McKervey, Anal. Chim. Acta, 204 (1988) 223.

46. W.R. Seitz, Anal. Chem., 56 (1984) 16A.

47. R. Narayanaswamy, D.A. Russell, Proc. of the 2nd Int. Meeting on Chem.Sensors, Bordeaux (1986).

48. H.G. Lohr, and F. Vogtle, Acc. Chem. Res., 18 (1985) 65.

49. M. Takagi and K. Ueno, Top. Curr. Chem., 121 (1984) 39.

50. R.E. Moss, I.O. Sutherland, Anal. Proc., 25 (1988) 272.

51. J. P. Dix, and F. Vogtle, Angew. Chem. Int. Ed. Engl., 17 (1978) 857.

52. M. Takagi, H. Nakamura, and K. Ueno, Anal. Lett., 10 (1977) 1115.

53. H. Nakamura, M. Takagi, and K. Ueno, Talanta, 26 (1979) 921

54. B.P. Bubnis, J.L. Steger, Y.P. Wu, L.A. Meyers and G.E. Pacey, Anal. Chim. Acta, 139 (1982) 307.

55. B. P. Bubnis, and G. E. Pacey, Tett. Lett., 25, 11 (1984) 1107.

56. T. Kaneda, K. Sugihara, H. Kamiya, and S. Misumi, Tett. Lett., 22, 44 (1981) 4407.

57. J.F. Alder, D.C. Ashworth, R. Narayanaswamy, R.E. Moss and I.O. Sutherland, Analyst, 112 (1987) 1191.

58. S. Misumi, and T. Kaneda, J. Incl. Phenom. and Molec. Rec. in Chem., 7 (1989) 83.

59. J. Van Gent, E.J.R. Sudholter, P.V. Lambeck, T.J.A. Popma, G. J. Gerritsma, and D.N. Reinhoudt, J. Chem. Soc., Chem. Commun., (1988) 893.

60. T. Kaneda, Y. Ishizaki, S. Misumi, Y. Kai, G. Hirao, and N. Kasai, J. Am. Chem. Soc., 110 (1988) 2970.

61. D.J. Cram, R.A. Carmack and R.C. Helgeson, J. Am. Chem. Soc., 110 (1988) 571.

62. R.C. Helgeson, B.P. Czech, E. Chapoteau, C.R. Gebauer, A. Kumar and D.J. Cram, J. Am. Chem. Soc., 111 (1989) 6339.

63. A.F. Sholl, I.O. Sutherland, J. Chem. Soc., Chem. Commun., (1992) 1716.

64. W. Zazulak, E. Chapoteau, B.P. Czech, and A. Kumar, J. Org. Chem., 57 (1992) 6720.

65. V. Bohmer, E. Schade, and W. Vogt, Makromol. Chem., Rapid Commun. 5, (1984), 221.

66. S. Shinkai, K. Araki, J. Shibata, D. Tsugawa and O. Manabe, Chem. Lett., (1989) 931.

67. H. Shimizu, K. Iwamoto, K. Fujimoto and S. Shinkai, Chem. Lett., (1991) 2147.

68. Y. Nakamoto, T. Nakayama, T. Yamagishi, S. Ishida, Workshop on Calixarenes and Related Compounds, Mainz, Germany, August 28-30, (1991) Poster1.

69. A.M. King, C.P. Moore, K.R.A. Sandanayke and I.O. Sutherland, J. Chem. Soc., Chem. Commun., (1992) 582.

70. K.R.A.S. Sandanayake, and I.O. Sutherland, Sens. and Act. B, 11, (1993) 331.

71. E. Ghidini, F. Ugozzoli, R. Ungaro, S. Harkema, A. Abu El-Fadl and D. N. Reinhoudt, J. Am. Chem. Soc., 112 (1990) 6979.

72. Y. Kubo, S. Hamaguchi, K. Kotani, K. Yoshida, Tett. Lett., 32, 50 (1991) 7419.

73. Y. Kubo, S. Hamaguchi, K. Yoshida and S. Tokita, J. Chem . Soc., Chem. Commun., (1993) 305.

74. J. Jin, K. Ichikawa, T. Koyana, J. Chem. Soc., Chem. Commun., (1992) 499.

75. S. Ogawa, R. Narushima, Y. Arai, J. Am. Chem. Soc., 106 (1984) 5760.

76. S. Shinkai, K. Araki, J. Shibata, D. Tsugawa and O. Manabe, J. Chem. Soc., Perkin Trans. 1, (1990) 3333.

77. H. Benesi, J. H. Hildebrand, J. Am. Chem. Soc., 71 (1949) 2703.

78. B.P. Czech, E. Chapoteau, W. Zazulak, C.R. Gebauer, and A. Kumar, Anal. Chim. Acta, 241 (1990) 127.

79. A. Amdisen, in *"Handbook of Lithium Therapy"*, edt. F.N. Johnson, M.T. P. Press Lancaster, (1986) Ch. 2.

80. W. Mc Curdy, Clin. Chem., 34 (1988) 476.

81. V.P.Y. Gadzekpo, G.J. Moody, J.D.R. Thomas, and G.D. Christian, Ion Selective Electrode Rev., 8 (1986) 173.

82. H. Sugihara, T. Okada, and K. Hiratini, Anal. Chim. Acta, 182 (1986) 275.

83. A.S. Attiyat, G.D. Christian, R.Y. Xie, X. Wen, and R.A. Bartsch, Anal. Chem., 60 (1988) 2561.

84. .E. Metzger, R. Bohmer, W. Simon, D. J. Vonderschmitt and K. Gautschi, Anal. Chem., 59 (1987) 1600.

85. K. Kimura, H. Oishi, T. Miura and T. Shono, Anal. Chem., 59 (1987) 223.

86. C.W. Beswick, G.J. Moody, and J.D.R. Thomas, Anal. Proc., 26 (1989) 2.

87. K. Suzuki, K. Tohda, M. Tominaga, K. Tatsuta, and T. Shirai, Anal. Lett., 20, 6 (1989) 927.

88. K. Tohda, K. Suzuki, N. Kosuge, K. Watanabe, H. Nagashima, H. Inoue, and T. Shirai, Anal. Chem., 62 (1990) 936.

89. R. Kataky, P. E. Nicholson, D. Parker, and A.K. Covington, Analyst, 116 (1991) 135.

90. C.K. Simmonds, and E.C. Lamprecht, in *"Microbiology of Frozen Foods"* edt. R.K. Robinson, Elsevier Applied Science Publishers London and New York, (1985), pp 169-208.

91. J.M Shewan, R.G. McIntosh, C.G. Tucker, and A.S.C. Ehrenburg, J. of the Science of Food and Agriculture, 4 (1953) 283.

92. W.J. Dyer, J. of the Fisheries research Board of Canada, 6 (1945) 351.

93. W.J. Dyer, J. of the Fisheries research Board of Canada, 7 (1950) 576.

94. W.J. Dyer, Journal of the Association of Official Agricultural Chemists, 42 (1959) 292.

95. N.J.C. Strachan, and F.J. Nicholson, Int. J. Food Sc. and Tech., 27 (1992) 261.

96. R.I. Perez Martin, J.M. Franco, P. Molist, and J.M. Gallardo, Int. J.of Food Sc. and Tech., 22 (1987) 509.

97. M. Egashira, Y. Shimizu, and Y. Takao, Chem. Lett., (1988) 389.

98. M. Egashira,Y. Shimizu, and Y. Takao, Sens. and Act., B, 1, (1990) 108.

Chapter 2

Methods and Materials

2.1 Materials

The reagents and materials were obtained from the following sources: Analar grade chlorides of lithium, sodium and potassium were supplied by Riedel De Haen, perchlorate salts of the same cations were supplied by Aldrich, sodium thiocyanate was obtained from Riedel De Haen, lithium thiocyanate from Aldrich and potassium thiocyanate from Merck. The lipophilic bases triethylamine (TEA), tridodecylamine (TDDA), and morpholine were purchased from Merck, Riedel De Haen and Aldrich respectively. Spectroscopic grade tetrahydrofuran (THF) was supplied either by Fluka, Romil, or Aldrich, whereas HPLC grade solvents, acetonitrile, methanol, butan-1-ol, butanone, butan-2-ol, 1,1,1 trichloroethane were obtained from Labscan. The deuterated solvents of chloroform and methanol were obtained from Aldrich. All salt solutions were made up in distilled, deionised (Milli-Q grade) water.

2.2. Instrumentation

The ultraviolet-visible (UV-Vis), nuclear magnetic resonance (NMR) and infrared (IR) spectra were obtained with a Hewlett Packard 8452A diode array spectrophotometer, a Brucker AC-400 spectrometer, and a Perkin-Elmer 983G spectrophotometer, respectively. All UV-Vis experiments were carried out in a quartz cuvette and the instrument was blanked in the solvent in which the ligands had been dissolved.

2.3 Nitrophenol Chromoionophores (Ligands 1, 2, & 3)

2.3.1 Effect of Complexation on UV-VIS Absorbance

Solutions of the ligands were made up in THF, (Ligand 1 and 3 at $5x10^{-5}$M, and Ligand 2 at $7x10^{-5}$M). 2.5 mL aliquots of these solutions were taken and liquid morpholine was added in the following amounts, 20 μL for Ligands 1, and 3, 45 μL for Ligand 2. Incremental concentrations of the aqueous metal perchlorates of lithium and sodium were added to give final concentrations in the range 10^{-1} to 10^{-6} M. Potassium perchlorate was added to give concentrations in the range 10^{-6} to $4x10^{-3}$ M. The exact volumes and concentrations of $MClO_4$ (where M =

Li, Na, or K) to give the required final concentrations are shown in Table 2.1. The UV-Vis spectra of the solutions were obtained between 800 and 300 nm.

Table 2.1:- Table of volumes of aqueous $MClO_4$ added to 2.5 mL aliquots of Ligands 1 - 9 dissolved in organic solvents (THF, butanol, MeOH - see individual experiments for details) to give the desired final $MClO_4$ concentration in the aliquot for UV-Vis spectroscopy experiments.

Initial $[MClO_4]_{(aq)}$ mol dm^{-3} M=Na, Li	Volume (μL) $MClO_{4(aq)}$ added to Ligand Soln. M=Na, Li	Initial $[KClO_4]_{(aq)}$* mol dm^{-3}	Volume (μL) $KClO_{4(aq)}$ added to Ligand Soln.	$[MClO_4]$ in Ligand Soln. mol dm^{-3} M = Na, Li, K.
10^{-3}	2.5	10^{-3}	2.5	10^{-6}
10^{-2}	2.5	10^{-2}	2.5	10^{-5}
10^{-1}	2.5	10^{-1}	2.5	10^{-4}
1	2.5	10^{-1}	2.5	10^{-3}
—	—	10^{-1}	50	$2x10^{-3}$
—	—	10^{-1}	100	$4x10^{-3}$
5	5	—	—	10^{-2}
5	50	—	—	10^{-1}

* Limited solubility of $KClO_4$ necessitated a different experimental design. While this complicated the interpretation of the results it is unfortunately unavoidable.

2.3.2 Selectivity Coefficient Determination

In order to determine selectivity coefficients in this one phase system, a series of experiments was set up as above, with the final lithium perchlorate concentration being varied in the range 10^{-1} to 10^{-6} M, in a fixed background concentration i.e. 10^{-2} or 10^{-3} M, of interfering ion in the form of sodium perchlorate. Spectra were obtained from 800-300 nm and graphs of absorbance at 424 nm (the λ_{max} of the deprotonated complex) versus the log of the concentration of lithium perchlorate concentration drawn. At high concentrations, the sodium ion has the effect of reducing the response of the ligand to lithium at lower concentrations as it dominates the complexation process with the ligand and swamps any lithium ion effects. However, at higher lithium ion concentrations, a response will be

observed because of greater affinity of the ligand for lithium ions. From these graphs, selectivity coefficients can be estimated from the ratio of the sodium and lithium ion concentrations at the intersection of the sodium and lithium dominant response regions of the curves.

2.3.3 Optimum Base Concentration Determination

To solutions of the ligands in THF at the concentrations previously mentioned, aqueous lithium perchlorate was added to give a final concentration of 10^{-3} M, i.e. 2.5 μL of 1 M $LiClO_4$ was added to 2.5 mL of sample. Morpholine was then added with incremental increases in concentration to give final morpholine concentraions in the range 0.023 M to 0.597 M. Spectra were recorded in the range 800 - 300 nm. A graph of absorbance at 424 nm versus the log of morpholine concentration was plotted and the end point of the titration calculated.

2.3.4 Effect of Solvent Variation on UV-Vis Spectra

Ligand 1 was examined for spectral changes with a variation in the solvent in which the ligand was dissolved. Method 2.3.1. was followed as before with methanol being used in place of THF as the solvent. Changes in the spectra between the two different solvents were noted and λ_{max} changes were calculated.

2.3.5 Two Phase Examination of Ligands

For two-phase experiments, 20 μL of TDDA were added to 2.5 mL aliquots of $5x10^{-5}$ M solutions of each of the ligands made up in butan-1-ol. To these, 2.5 mL of water were added. Incremental concentrations of metal perchlorates were then added to the lower, aqueous phase to give final aqueous phase concentrations in the range 10^{-1} to 10^{-6} M (see Table 2.1 for volumes used). Spectra were taken of both phases after the two layers had been allowed to separate (i.e. approximately 15 minutes). Preliminary examinations of suitable water immiscible solvents will be described with the nitrophenylazophenol ligands.

2.3.6 Complexation Studies

An investigation of cation inclusion in the calix[4]arene ring was carried out by ^{1}H NMR titrations. The ^{1}H NMR spectra of the free and complexed forms of the ligands were obtained in $CDCl_3$ at room temperature. Sodium thiocyanate was added as aliquots from a 1.0 M solution in CD_3OD directly to the $CDCl_3$ solution of the ligand in an NMR tube to give the metal:ligand ratios shown in Table 2.2.

Table 2.2 NMR Titrations

R (R=[NaSCN]/[Lig]*)	Total Vol. NaSCN** Added
(a) R = 0.0	0.00
(b) R = 0.5	1.25
(c) R = 1.0	2.50
(d) R = 2.0	5.00

* [Lig] = $5x10^{-3}$ M dissolved in $CDCl_3$.

** NaSCN dissolved in CD_3OD

Shifts in certain NMR signals are associated with cation complexation with calix[4]arenes and these were examined with the spectra obtained. These will be discussed in detail later.

2.4 Calix[4]arene with Chromophore Within Cavity (Ligand 4)

2.4.1 Effect of Complexation on UV-Vis Spectra

A $5x10^{-5}$ M solution of ligand 4 was made up in THF. To 2.5 mL aliquots of this solution 12.5 μL of morpholine were added i.e. 6 x 10^{-2} M morpholine. This concentration was arrived at by following Method 2.3.3. Incremental changes of aqueous metal perchlorates of lithium, sodium and potassium were added, with the volumes used in Table 2.1 again being used. Spectra were recorded from 800-300 nm.

2.4.2 Selectivity Coefficient Determination

Selectivity coefficients were obtained using method 2.3.2 for lithium over sodium selectivity, with 10^{-3}M lithium perchlorate being used as the interfering ion concentration. Sodium over lithium selectivity studies were also carried out, using a constant background lithium perchlorate concentration of 10^{-3} M. Sodium over potassium selectivity was examined by introducing a fixed volume of $KClO_4$ made up in acetonitrile, to give a final $KClO_4$ concentration of 10^{-2} M, or a fixed volume of aqueous $KClO_4$ to give final $KClO_4$ concentration of 4 mM.

2.4.3 ^{1}H NMR Complexation Studies

^{1}H NMR complexation studies were carried out by method 2.3.7 with the concentration of Ligand 9 being 2.5 x 10^{-3} M. Sodium was introduced as its perchlorate salt, and similar studies were conducted for lithium and potassium using perchlorate and thiocyanate salts respectively. KSCN was used in place of $KClO_4$ because of the lack of solubility of $KClO_4$ in CD_3OD.

2.5 Nitrophenylazophenol Ionophores (Ligands 5, 6, 7, 8, & 9)

2.5.1 Effect UV-Vis Absorbance Spectra of Ligand Complexation

5x10^{-5} M solutions of ligands 5, 7, 8, and a 6x10^{-5} M solution of ligand 6, were made up in THF. A 10^{-4} M solution of Ligand 9 was also examined. 2.5 mL aliquots of each ligand solution were taken and to this 100 μL of tri-n-dodecylamine (TDDA) was added, (50 μL in the case of Ligand 6). Incremental concentrations of aqueous metal perchlorates of lithium, and sodium were added as before to give final metal perchlorate concentrations of 10^{-6} M to 0.1 M. The same volumes of aqueous solutions described in table 2.1 were used. After gently shaking, the clear yellow ligand solution changed colour to red immediately, with the intensity of the resultant colour being dependent on the metal perchlorate concentration. This colour change was examined using UV-Vis spectroscopy in the range 800-300 nm.

2.5.2 Selectivity Coefficient Determination

In order to determine selectivity coefficients for lithium against sodium, a series of experiments was set up as above, with the final lithium perchlorate concentration being varied in the range 10^{-6} to 10^{-1} M, in a fixed background concentration of interferent (0.05 M and 0.1 M sodium perchlorate). Spectra were obtained from 300-800 nm and graphs of absorbance at 520 nm versus the log of the concentration of lithium perchlorate concentration drawn.

2.5.3 Solvent Choice for Two Phase Examinations

To 2.5 mL of 5 x 10^{-5} ligand 4 in each of the following solvents: dichloroethane, butan-1-ol, butanone, 1,1,1 trichloroethane, butan-2-ol, 20 μL of triethylamine (TEA) were added. Any colour changes which occured were noted. 2.5 mL of water were added and again any resulting colour changes in either layer were noted. Finally 2.5 μL of 1 M $LiClO_4$ were added to the aqueous phase. After the two phases had been shaken and subsequently allowed to re-separate, colour changes in each layer were observed. For comparative purposes, blank experiments were carried out for each solvent containing everything except the lithium perchlorate.

2.5.4 Two Phase Examination of Ligands

After butan-1-ol had been chosen as the most suitable water immiscible solvent, two-phase experiments were carried out where 100 μL of TDDA was added to 2.5 mL aliquots of 5x10^{-5} M solutions of each of the ligands made up in butan-1-ol. To these, 2.5 mL of water were added. Incremental concentrations of metal perchlorates were then added to either the upper organic layer or to the lower, aqueous phase to give final concentrations in the range 10^{-1} to 10^{-6}M for the phase into which the salt was introduced. Spectra were taken of both phases.

2.5.5 Complexation Studies

An investigation of cation inclusion in the calix[4]arene ring was carried out by ^{1}H NMR titrations using the method outlined in method 2.3.7.

2.6 Assessment of Ligand 4 for The Rapid Colorimetric Detection of Trimethylamine

2.6.1 Liquid Phase Experiments

2.5 mL of a solution containing $5x10^{-5}$ M of **5** and 1 M $LiClO_4$ in butan-1-ol was placed in a test tube in a gas tight vessel. Fixed volumes between 0.2 and 50 μL of a 25% w/v aqueous TMA solution were injected into a 550 mL capacity vessel through a supa seal cap, ensuring that none of the liquid entered the test tube containing the indicator solution, giving maximum final TMA concentrations in the approximate range of 0.1 to 25.0 ppm*, assuming all TMA passes into the gas phase. The vessel was heated gently in a 50°C oven to aid the evolution of TMA from the aqueous solution into the gaseous form. After reaction, samples of the solution were removed in order to obtain the UV-Vis spectra. For TMA concentrations below 1 ppm, injections were made from a 1/10, or a 1/100 dilution of the 25% $TMA_{(aq)}$ stock solution.

2.6.2 Preparation of Test Strips based on the Ligand

Using filter paper as the support (Whatman no.1, 4.25 cm disc), the complexed calixarene was immobilised by carefully adding 0.2 mL of a tetrahydrofuran (THF) solution which was $6x10^{-4}$ M in ligand **5** and 0.1M in $LiClO_4$ onto the paper. Evaporation of the THF yielded a paper with a yellowish tinge. Test strips prepared in this manner were placed in a gas-tight vessel of capacity 2.71 L, and varying volumes of TMA were injected through a supa-seal cap to give final TMA concentrations of 0.010 to 50 ppm.

---

* Gaseous TMA concentrations were calculated as follows

1. 25% w/v aqueous TMA = 25 g of TMA /100 mL aqueous TMA solution = 0.25 mg/ μL
2. 1 mg TMA = 4 μL of 25 % $TMA_{(aq)}$
3. 1 ppm TMA = 4 μL of 25% $TMA_{(aq)}$ /L of gas tight chamber
4. 1 ppm TMA in 550 mL (Capacity of gas tight chamber) = 4 μL x (550mL/1000 mL)

2.6.3 Preparation of Sealed Test Strips

Method 2.6.2 was followed, and after evaporation of THF, the strips were covered with a film of low density polyethylene (LDPE).

Chapter 3

Nitrophenol Ligands

3.1 Introduction

In both this chapter and in Chapter 4, nine chromogenic calix[4]arenes are characterised as part of an initial screening process to determine the feasibility of using some of these chromogenic calixarenes as optical cation or amine sensor components and thereby allow patenting of any class of compound which was seen to have the desired analytical characteristics. Ligands 1, and 2 were synthesised by Geraldine Barrett, and Ligand 4 was synthesised by Mary Moran, under the supervision of Prof. M.A. McKervey, at the Queen's University, Belfast. Ligand 3 was synthesised by Dr Stephen J. Harris at D.C.U.

The cation binding and extraction ability of calix[4]arenes is well known [1]. Calix[4]arenes, the subjects of this work have been shown to display preferential uptake of the smaller cations of the alkali metal series, such as sodium, potassium and to a certain extent lithium [2]. The incorporation of known chromophores into the calixarene structure or the attachment of such moieties as pendent groups to the calixarenes is an approach which can offer an effective means of cation inclusion transduction in the form of a spectral/colour change. Arnaud-Neu et al [2] carried out an extensive study of alkyl calixaryl esters and ketones with a number of variations of R and R' groups (see structure **3 (i)**).

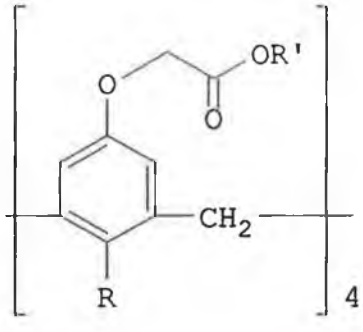

3 (i) Calix[4]arene tetraester.

Even relatively minor changes in the R' groups produced changes in cation extraction abilities of the calixarenes. One example of this was the attachment of a *tert*-butyl group in place of an ethyl group in the R' position, which resulted in the ability of the molecule to extract K^+ increasing with no significant decrease in Na^+ extraction. A possible explanation for this phenomenon was the enlargement

of the polar cavity due to steric interference between the bulky *tert*-butyl substituents [2]. So the attachment of nitrophenol chromophores in this R' position will result in a selectivity pattern which is difficult to predict exactly. Since all the molecules are tetramers of the tetraester type, complexation ability would be expected with the smaller cations i.e Li^+, Na^+ and K^+ as opposed to Cs^+ or Rb^+ which have shown preferential uptake by calix[6]arenes.

Ligands 1 to 3 have ester groups attached to the phenolic oxygens of the calixarene backbone, with either 1 or 4 nitrophenol chromogenic moieties attached as pendent groups to the CH_2 of these ester groups. Ligand 4 unlike ligands 1 and 3 actually has the chromogenic moeity built into the calix[4]arene structure with the nitrophenol group making up one of the aromatic rings of the calix[4]arene annulus. In Ligands 1 to 3 the nitro group of the nitrophenol chromogenic moiety is *ortho* to the dissociating phenolic group whereas in Ligand 4 it is in the *para* position. The nitrophenol moiety with the phenol group in the *ortho* position relative to the nitro group, has been used as an indicator [3] and shows a colour change from colourless to yellow in the pH range 5.0 to 7.0 (pK_a 7.17). The *para* nitrophenol molecule has been found to change colour over a pH range of 5.6 to 7.6 (pK_a 7.15) [3].

In both Ligands 1 and 2, the tetra and monochromogenic ligands respectively, *tert*-butyl groups occupy the *para* position of the calixarene backbone. With Ligand 3 (another tetrachromogenic ligand), a long-chain C_{18} group, introduced to enhance the lipophilicity of the molecule, occupies this position. Ligand 4 is another monochromogenic compound, with three *t*-butyl groups occupying the *para* position of the remaining aromatic rings, and as was previously stated, the chromogenic portion of the molecule forms an integral part of the calix[4]arene backbone. Like the other monochromogenic ligand (Ligand 2) the remaining aromatic rings of the calixarene backbone possess ethyl ester moieties. The ethyl ester moieties attached to the phenolic oxygens of the calixarene backbone offer the heteroatoms (in particular carbonyl oxygen atoms), required for electrostatic interaction with the complexing cation as described in Chapter 1 section 1.3.4.

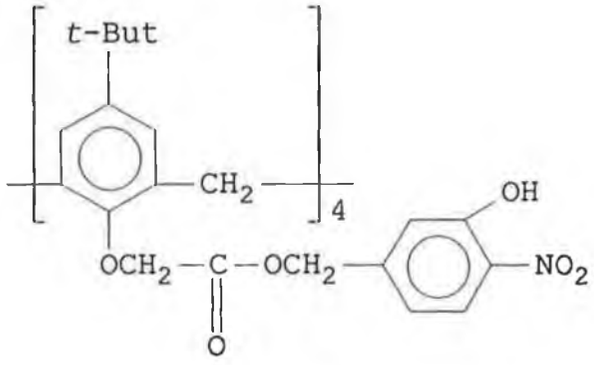

3 (ii) Ligand **1**

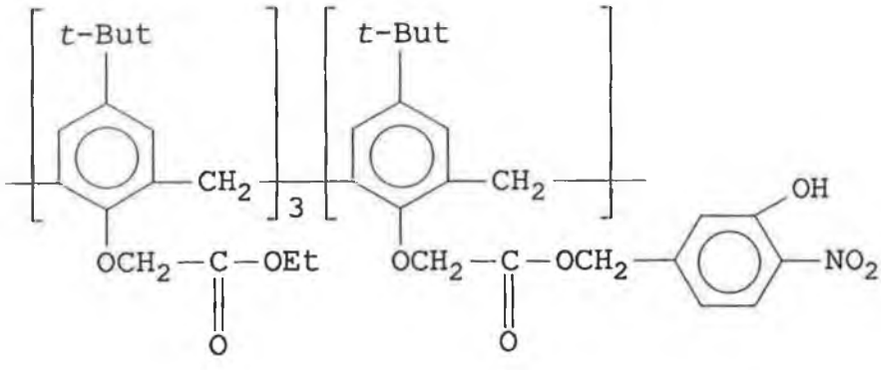

3 (iii) Ligand **2**

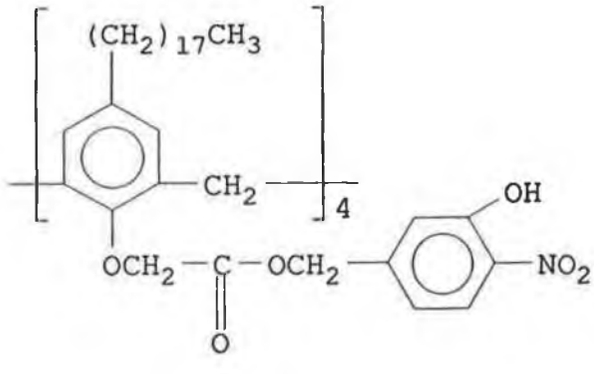

3 (iv) Ligand **3**

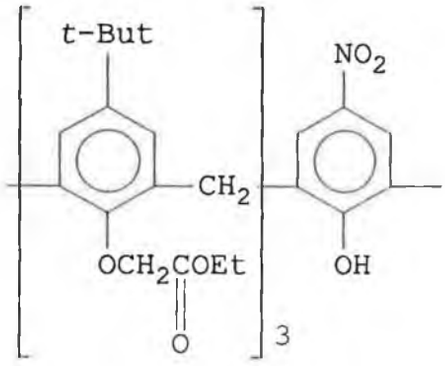

3(v) Ligand 4

3.2 Mechanism of Colour Generation

All of the above ligands, and those to be discussed in Chapter 4 belong to a series of ionisable chromogenic materials in which the colour generation process essentially arises from deprotonation of the acidic chromophore (-COH), where C represents the chromogenic portion of the ligand and OH represents the ionisable phenolic group on this moiety, attached near the ligand (L-) polar cavity (see equation **(3.1)** below. In previous experiments [4-11] it has been demonstrated that this approach could be used to detect a variety of alkali metal cations, represented here as (M^+) in solution and therefore have the potential for incorporation into an optical sensor for these ions. In all of the previously mentioned ionisable chromoionophores [4-11] the dissociating phenolic group was actually sited within the hydrophobic cavity of the calixarene [8-11], the spherand [5], the crown ether [6, 7] and the cryptand [4]. Usually with these materials, formation of the metal-ligand complex by itself does not generate the colour change because a proton receptor is required for the acid-base colour generating reaction:

$$\text{L-COH} + M^+ \rightleftharpoons \text{LM}^+\text{-COH} \qquad (3.1)$$

$$\beta = \frac{[\text{LM}^+\text{-COH}]}{[\text{L-COH}]\,[M^+]} \qquad (3.2)$$

where β is the stability constant for complexation.

Complexation in the absence of any chromogenic indication of deprotonation can be confirmed by ^{1}H NMR spectroscopy. However, the positively charged metal

ion in the ligand cavity increases the acidity of the ionisable chromophores and in the presence of a suitable base (B) these are more easily deprotonated, shifting their absorbance maxima to longer wavelengths in the process:

$$LM^{+}\text{-}COH + B \rightleftharpoons LM^{+}\text{-}CO^{-} + BH^{+} \qquad \textbf{(3.3)}$$

$$K_{a(C)} = \frac{[LM^{+}\text{-}CO^{-}]\,[BH^{+}]}{[LM^{+}\text{-}COH]\,[B]} \qquad \textbf{(3.4)}$$

where $K_{a(C)}$ is the acid dissociation constant for the deprotonation of the complex.

Hence for metal-ion detection, the base must be chosen carefully because if it is too strong, deprotonation of the ligand may occur independently of the presence of metal ion:

$$L\text{-}COH + B \rightleftharpoons L\text{-}CO^{-} + BH^{+} \qquad \textbf{(3.5)}$$

$$K_{a(L)} = \frac{[L\text{-}CO^{-}]\,[BH^{+}]}{[L\text{-}COH]\,[B]} \qquad \textbf{(3.6)}$$

where $K_{a(L)}$ is the acid dissociation constant for the deprotonation of the free ligand.

The ideal base will therefore react with the complex but not with the free ligand, hence enabling the metal ion to be detected optically.

As the inclusion of a cation in the ligand cavity will render the phenolic proton more labile the acidity of the phenolic proton of the chromophore will increase, i.e.. $K_{a(C)} > K_{a(L)}$

3.3 Base Concentration Optimisation

A base titration was carried out as in Method 2.3.3, with $7x10^{-5}$ M Ligand 2, 10^{-3} M $LiClO_4$ with the concentration of morpholine being varied between 0.023 and 0.597 M. The following spectra were obtained. From this a graph of absorbance versus [Morpholine] was drawn (Figure 3.2) and a morpholine optimum concentration of 0.2 M was obtained. The optimum base concentration was considered to be the concentration which gave the greatest absorbance in the presence of 10^{-3} M $LiClO_4$, and above which no further increase in absorbance was seen.

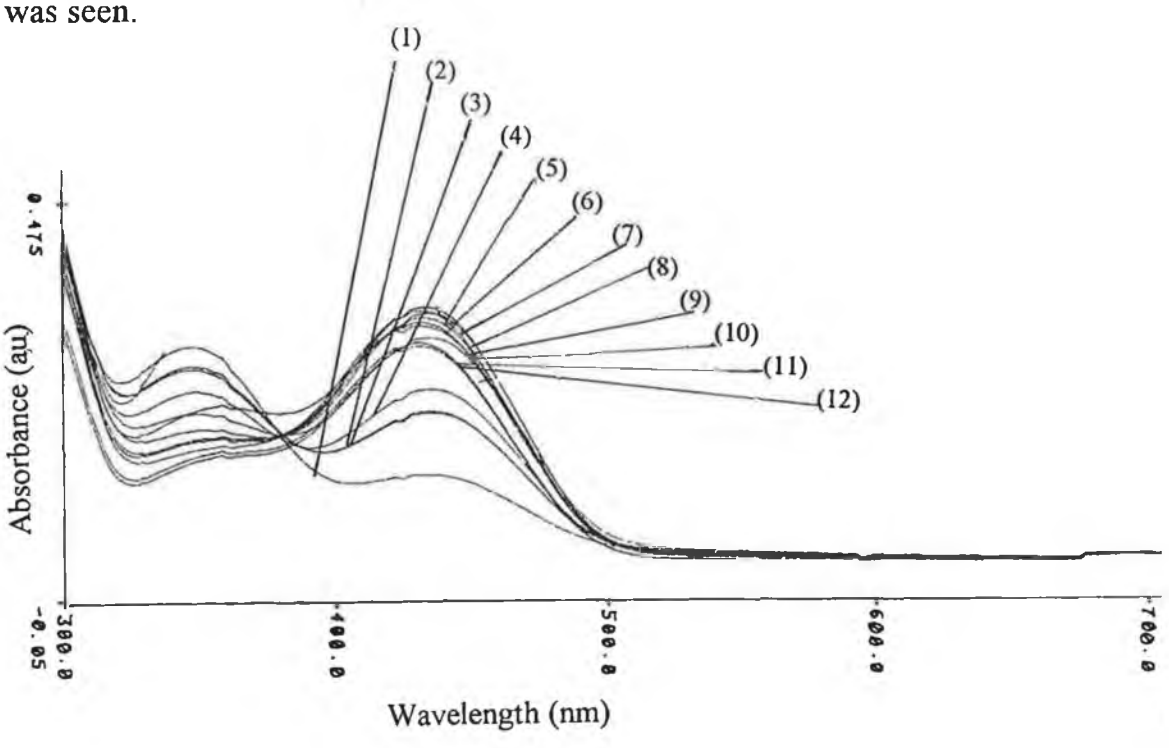

Figure 3.1:-UV-Vis spectra showing the effect of increasing morpholine concentration on the UV-Vis spectrum of 5 x 10^{-5} M Ligand 1 with 10^{-3} M $LiClO_4$, using with 0.23 M (1), 0.046 M (2), 0.069 M (3), 0.092 M (4), 0.115M (5), 0.138 M (6), 0.161 M (7), 0.207 M (8), 0.253 M (9), 0.298 M (10), 0.390 M (10) 0.482 M (11), 0.666 M (12). Method 2.3.3.

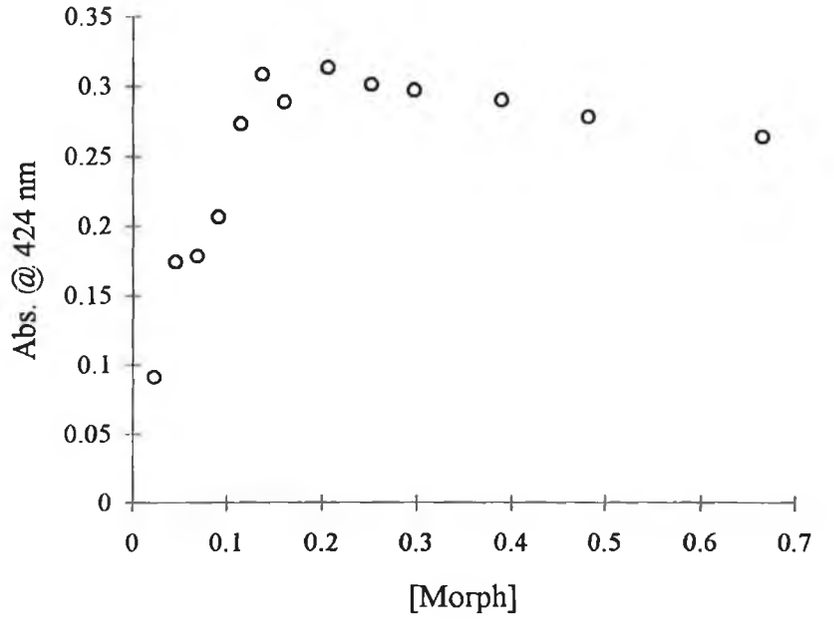

Figure 3.2:-Graph of absorbance at 424 nm versus [morpholine] for Ligand 2, drawn from data obtained from Figure 3.1.

Similarly for Ligands 1 and 3, the tetrachromogenic ligand and its C_{18} analogue of respectively, the optimum morpholine concentration was evaluated and found to be around 0.1 M for each under the conditions of the experiment.

3.4 Effect of Different Concentrations of Alkali Metals on Absorbance Spectra, in One Phase Experiments.

3.4.1 Ligand 1, One Phase.

A series of experiments was set up using the optimum morpholine concentrations to determine the ligand's spectroscopic responses to varying concentrations of the perchlorates of lithium, sodium and potassium. Method 2.3.1 was followed with incremental increases in metal perchlorate concentration in the range 10^{-6} M and 0.1 M being examined. Figures 3.3(a), (b) and (c) show the spectral response achieved for lithium, sodium and potassium respectively.

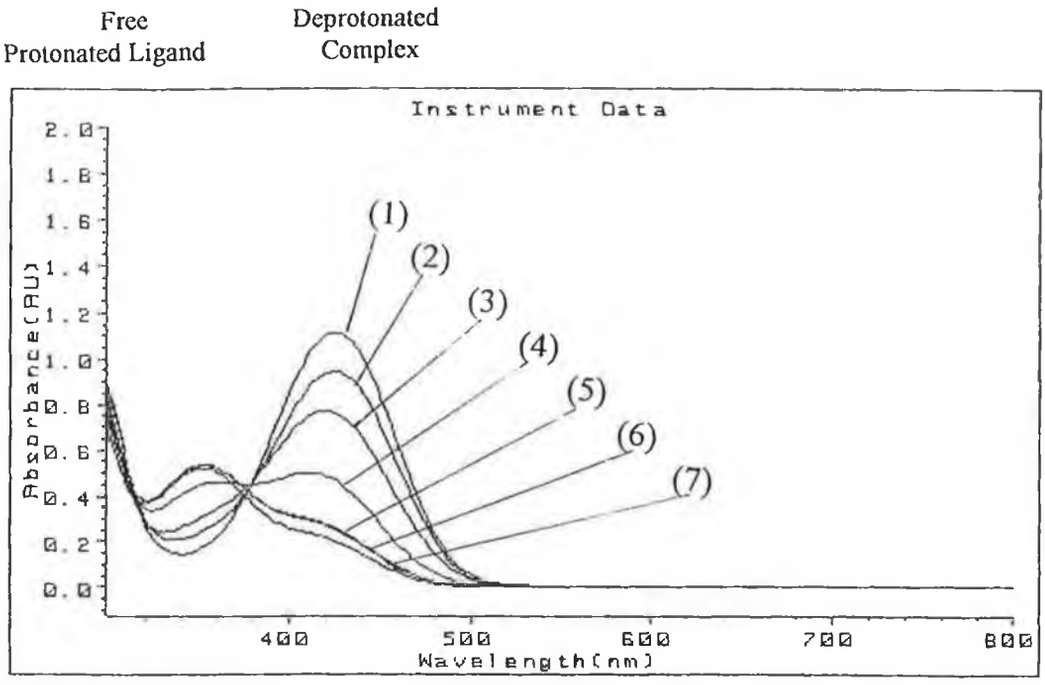

Figure 3.3 (a):- Ligand 1, lithium response

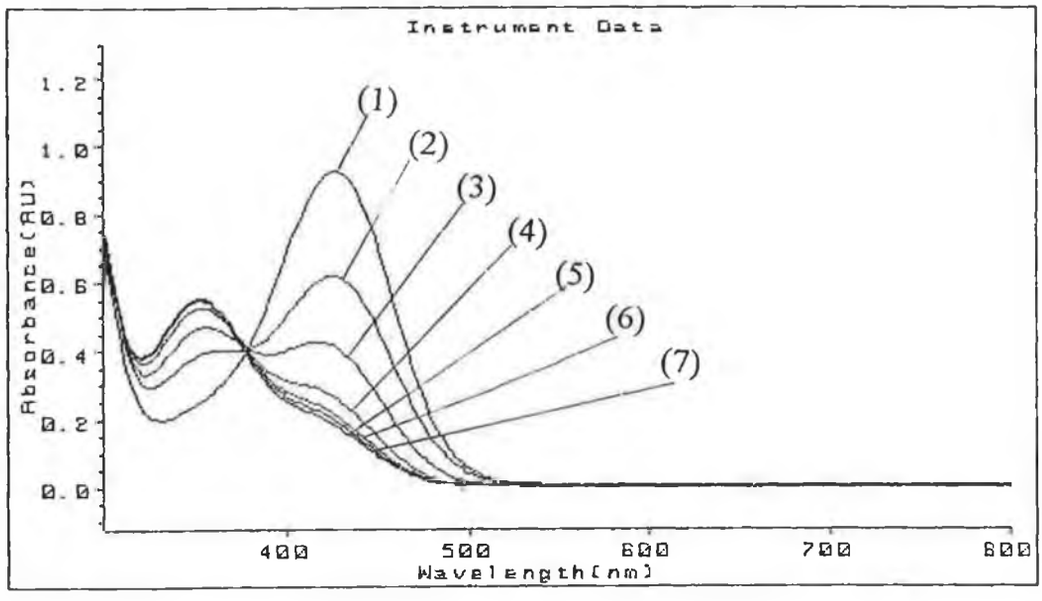

Figure 3.3 (b):-Ligand 1, sodium response.

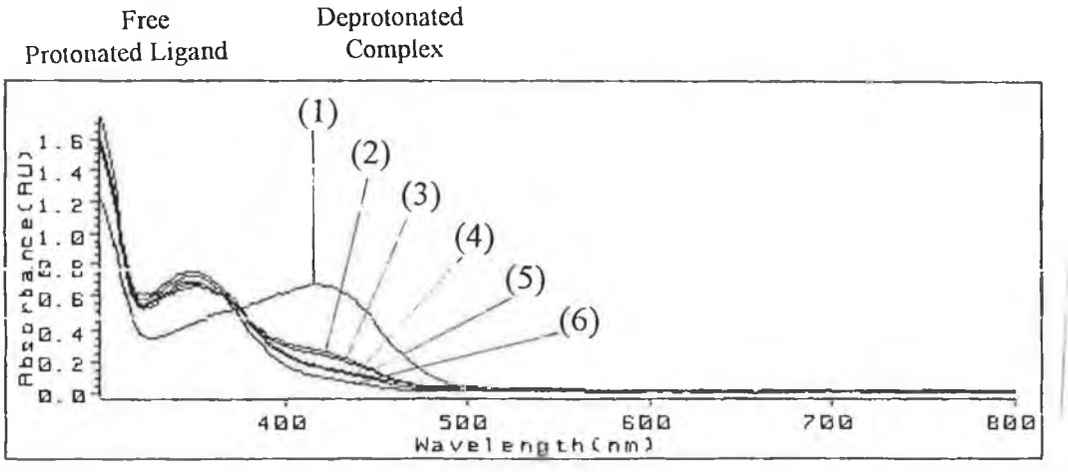

Figure 3.3 (c):-Ligand 1, potassium response.

Figure 3.3:- One-phase investigation of changes in the absorbance spectrum of 2.5 mL of a $5x10^{-5}$ M solution of Ligand 1 in THF, with 20 μL of morpholine, upon addition of aqueous (a) $LiClO_4$, (b) $NaClO_4$, with final concentrations of 0.1 (1), 10^{-2} M (2), 10^{-3} M (3), 10^{-4} M (4), 10^{-5} M (5), 10^{-6} M (6) 0 M (7) and (c) $KClO_4$, with final concentrations of, $4x10^{-3}$ M (1), $2x10^{-3}$ M (2), 10^{-3} M (3), 10^{-4} M (4), 10^{-5} M (5), 10^{-6} M (6), See Table 2.1.

Upon addition of morpholine to the ligand solution, a very slight colour change was observed indicating that the bulk of the ligand remained in the protonated form. Upon addition of the metal perchlorates a clear yellow colour was immediately observed, with the intensity of the colour being dependent on the concentration and nature of the perchlorate added. From the UV-Vis spectra in Figure 3.3 it can be seen that a λ_{max} for the protonated form of this ligand exists at 350 nm, with an extinction coefficient (ε) of 11400 L mol^{-1} cm^{-1}. The absorbance at this wavelength decreases with increasing concentrations of lithium and sodium perchlorate which coincides with an increase in absorbance at 424 nm. This wavelength corresponds to the deprotonated λ_{max} for the complexes of all three metals. Isobestic points are observed at 390 nm for all three complexes indicating the presence of two absorbing species in equilibrium with each other [12]. Since the same wavelength maxima exist for all three complexes, it indicates that lithium, sodium and potassium interact with the ligand in a similar manner with no significant differences existing in the excited states of the

different complexes, as this would result in a slight shift in the λ_{max} of the complex. This is the case with the neutral chromoionophores in which the chromogenic moiety is sited either within or in close proximity to the ionophoric cavity [13], or with ionisable chromoionophores such as Ligand 4 to be discussed here, where the dissociating phenol makes up part of the hydrophilic cavity. Inclusion of a cation results in an electronic disturbance which propagates through the whole n and π systems, with variations in the extent of interaction between different cations resulting in variations in the resulting λ_{max} of the complexes formed.

A comparison of the response of the ligands to lithium, sodium and potassium is shown in Figure 3.4, where a graph of absorbance at 424 nm versus log [metal perchlorate] is drawn.

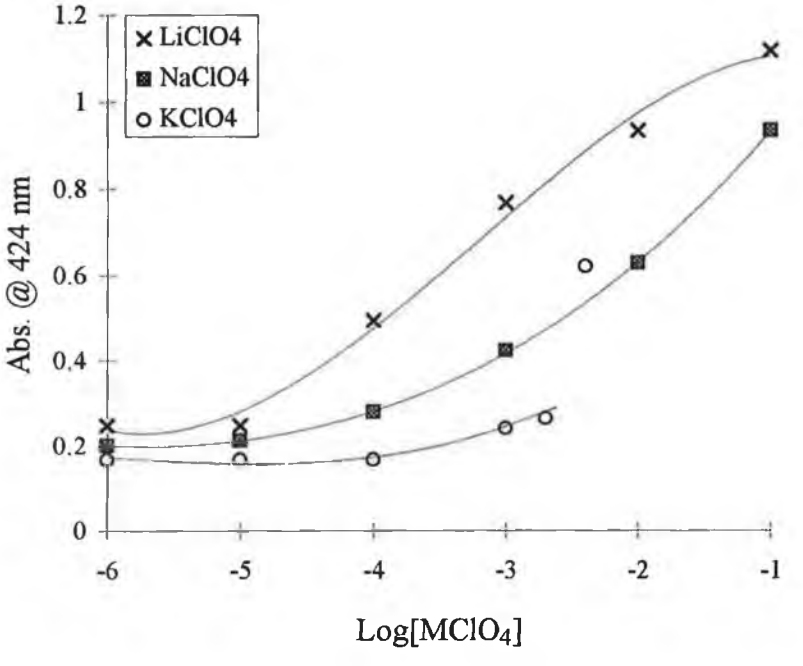

Figure 3.4:- *Comparison of absorbance at 424 nm of the lithium, sodium and potassium metal complexes of Ligand 1. Data from Figures 3.3(a), (b) and (c).*

From this graph it can be seen that a superior response to the presence of lithium compared to sodium is achieved, with practically no response to potassium attained prior to the addition of 4 mM potassium. A detection range of 10^{-4} to 10^{-2} M and a limit of detection (L.O.D.) of c. $6x10^{-5}$ M is obtained for lithium. With sodium a linear range between 10^{-4} and 10^{-2} M is also observed. However, a much reduced slope is seen in this range. The slope for the lithium response in

this region is 0.325 a.u./dec. compared to 0.178 a.u./dec. for sodium. This in effect means that small changes in lithium concentration in this range will cause larger colour/spectral changes than similar changes in sodium concentration. The lithium curve suggests a slight levelling off effect or a decrease in slope above 10^{-2} M, whereas the slope of the sodium response curve increases above 10^{-2} M.

Ligand 1 exhibits practically no response to potassium prior to the addition of 2 mM $KClO_4$. The minimal solubility of $KClO_4$ in water precluded an examination of a $KClO_4$ concentration above 4 mM. A maximum of 0.1 M $KClO_4$ could be dissolved in water, compared to the possibility of making 5 M solutions of both lithium and sodium perchlorate. Thus to obtain a final lithium perchlorate concentration of 0.1 M in a 2.5 mL solution of ligand the required volume of 5 M $LiClO_4$ was 50 μL, which constitutes less than a 2% overall volume increase. To obtain even a 10^{-2} M $KClO_4$ final concentration in 2.5 mL of ligand solution 0.25 mL would be required and this is equivalent to a 10% change in volume. Such a large introduction of an aqueous solution is likely to generate numerous problems which would render the data obtained difficult to compare with the data for $LiClO_4$ or $NaClO_4$.

- Firstly the combined H_2O/THF solvent would be more polar than THF on its own and therefore a λ_{max} shift would be inevitable.
- Secondly as the nature of the solvent would have been altered, the pK_a of the base (morpholine) along with the overall polarity of the solvent will be enhanced and thus deprotonation of the phenolic moieties of the chromophore would be increasingly favoured.

Control experiments carried out as above, with the exception that the same volume of water used to obtain $2x10^{-3}$ and $4x10^{-3}$ M i.e. 0.050 and 0.100 mL, was added in place of $KClO_4$, showed an absorbance at 424 nm of 0.210 and 0.274 a.u. respectively. Therefore, part of the response seen for K^+ especially in Spectrum (1) of Figure 3.3 (c) is due to an enhanced proton exchange environment arising from the increase in the percentage of water. Therefore the point due to $4x10^{-3}$ M $KClO_4$ cannot be seen as being entirely due to the occurrence of K^+ complexation but is due in part to solvent environment changes, as the volume of water added to obtain this point is much larger than any of the others. Despite these complications, it is clear that the overall order of response for Ligand 1 in these initial screening experiments is $Li^+ > Na^+ > K^+$.

3.4.2 Ligand 2 ,Monochromogenic Ligand

The following spectra were obtained with $7x10^{-5}$ M Ligand 2 and 0.2 M morpholine with the metal perchlorate concentrations again being varied from 10^{-6} M to 10^{-1}M. The spectra obtained for the response to lithium, sodium and potassium are shown in Figure 3.5 (a), (b) and (c) respectively.

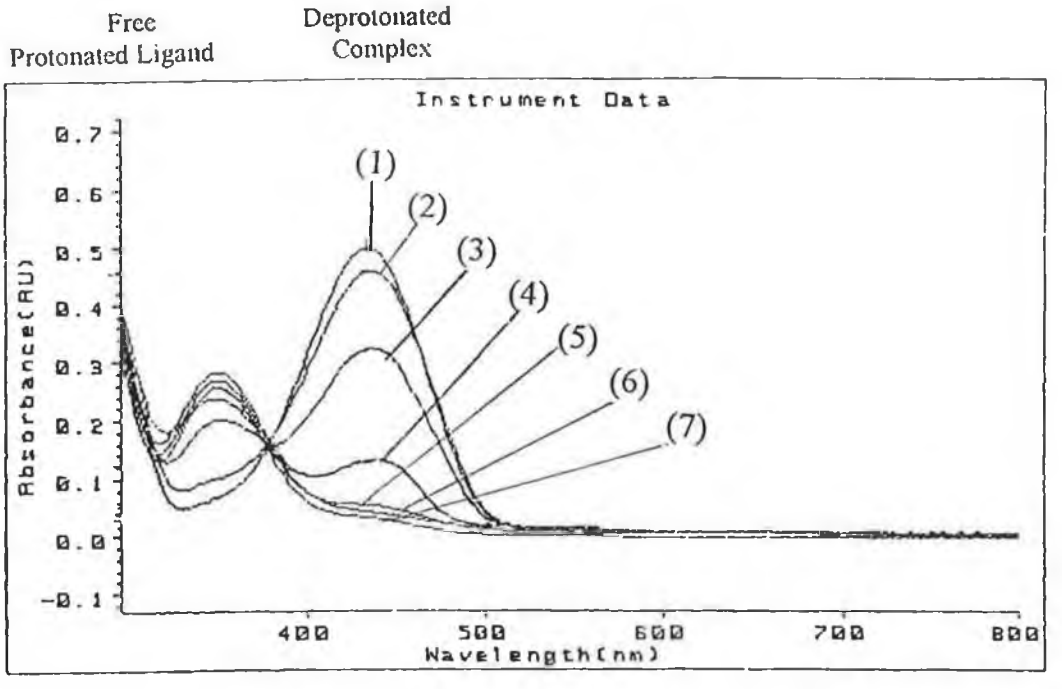

Figure 3.5 (a):-Ligand 2, lithium response.

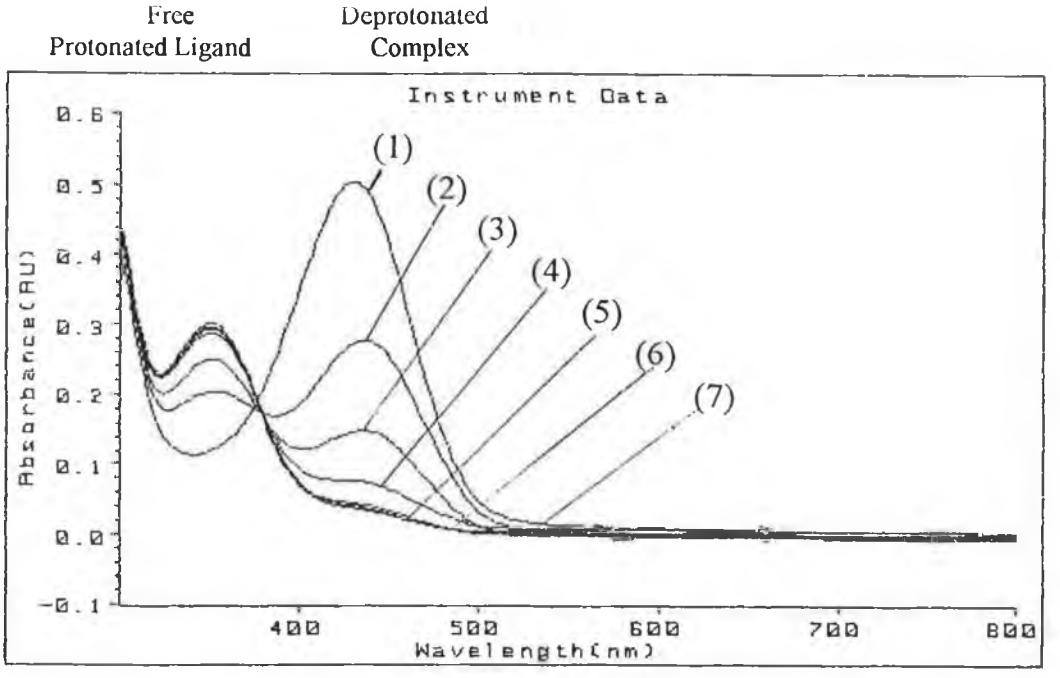

Figure 3.5 (b):- *Ligand 2, sodium response.*

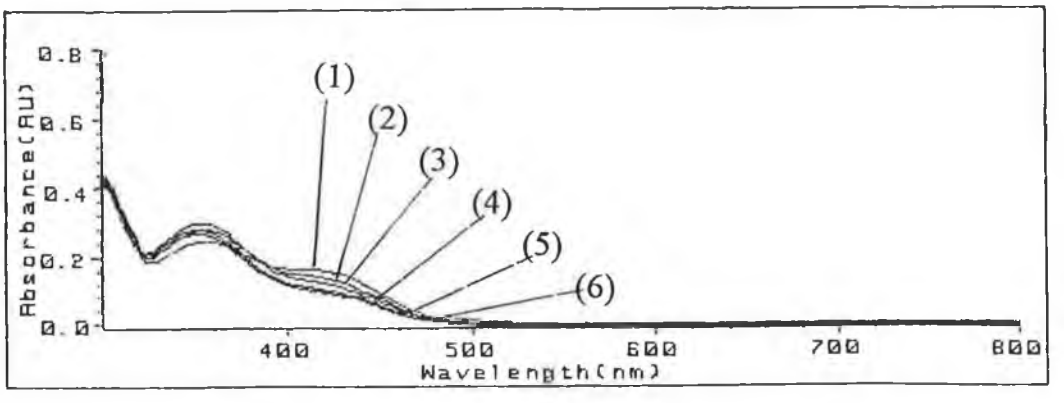

Figure 3.5 (c):- *Ligand 2, potassium response.*

Figure 3.5:- *One-phase investigation of changes in the absorbance spectrum of 2.5 mL of a $7x10^{-5}$ M solution of Ligand 2, in THF, with 45 μL of morpholine, upon addition of aqueous (a) $LiClO_4$, (b) $NaClO_4$, with final concentrations of 0.1 (1), 10^{-2} M (2), 10^{-3} M (3), 10^{-4} M (4), 10^{-5} M (5), 10^{-6} M (6), 0 M (7) and (c) $KClO_4$ with final concentrations of $4x10^{-3}$ (1), $2x10^{-3}$ M (2), 10^{-3} M (3), 10^{-4} M (4), 10^{-5} M (5), 10^{-6} M (6), See Table 2.1.*

The bulk of Ligand 2 remains in the protonated form upon addition of morpholine. This is observed as a very slight colour change to barely yellow, with deprotonation again occuring upon complexation with the metal cations. Deprotonation upon complexation is signalled by a colour change from colourless to yellow with intensity being dependent on metal perchlorate concentration. This is witnessed in the UV-Vis spectra as an increase in absorbance at the deprotonated complex λ_{max} of 424 nm. An isobestic point is observed at 375 nm. The actual absorbance values for Ligand 2 compared to those for Ligand 1 are lower due to the presence of only one chromogenic group in Ligand 2 compared to the four of Ligand 1. However, the cation induced deprotonation observed for Ligand 2 is indicative of one deprotonation being sufficient for the effect to be observed.

Figure 3.6 shows a comparison of the absorbance at 424 nm for varying concentrations of the three metal perchlorates. Again superior cation uptake is observed for lithium perchlorate. The response curves observed for Ligand 2 with Li^+ and Na^+ are quite similar to those observed for Ligand 1. There is a rapid increase in intensity observed after 10^{-4} M $LiClO_4$ has been added.

However, the response levels off more quickly with this ligand after the initial large increase in intensity above 10^{-3} M. This levelling off in intensity is a possible indication of complete ligand deprotonation or ligand saturation. Looking more closely at spectrum 1 in Figure 3.5 (a) it can be seen that the absorbance at the protonated λ_{max} of 350 nm has depreciated to such an extent that it is now the lowest point of a trough. The possibility of a further decrease in intensity appears to be quite unlikely. Since the absorbance at this level of $LiClO_4$ is less than 0.05 a.u. This enables ε to be estimated to be 8166 L mol^{-1} cm^{-1} , if the concentration of deprotonated ligand at this concentration is estimated to be 6 x 10^{-5} M.

With $NaClO_4$ (Figure 3.6) no major change in absorbance occurs before 10^{-3} M $NaClO_4$ is reached and again the change in absorbance is largest between 10^{-2} and 10^{-1} M $NaClO_4$ indicating a difference in the maximum response region for both cations. From both Figure 3.6 and 3.5 (b) where a levelling off of the response to Na^+ is not evident at 350 nm, it would appear that saturation point has not been reached between the ligand and Na^+ at an $NaClO_4$ concentration of 0.1 M, but that the system may tolerate a further increase in $NaClO_4$ concentration. The LOD for the Li^+ complex is c. $6x10^{-5}$ M and for the Na^+

complex c. 10^{-4} M. The preferential order of cation uptake is again $Li^+ > Na^+ > K^+$.

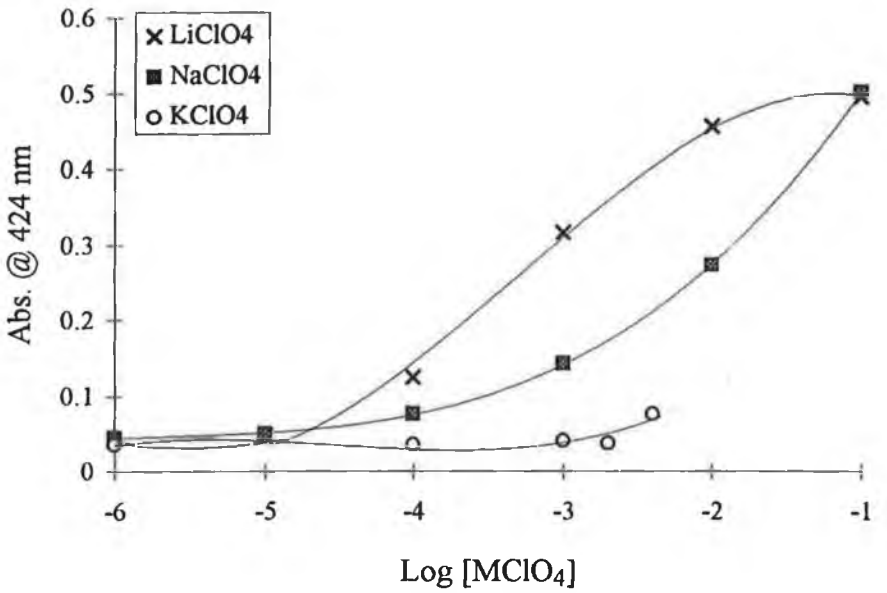

Figure 3.6:- *Comparison of the spectral response at 424 nm of each of the lithium, sodium and potassium metal complexes of Ligand* <u>2</u>. *Data obtained from Figure 3.5 (a), (b) and (c).*

3.4.3 Ligand <u>3</u> (C_{18}) One Phase UV-Vis Examination.

Ligand <u>3</u>, a tetra-chromogenic ligand which possesses C_{18} groups in the para position of the calixarene as opposed to the *tert*-butyl groups which are contained in Ligands <u>1</u> and <u>2</u> was examined as before for cation induced UV-Vis spectroscopic changes. 0.1 M morpholine in 2.5 mL of $5x10^{-5}$ M ligand was found to be the optimum base concentration. The following spectra were recorded for metal perchlorates of lithium and sodium in the concentration range 10^{-1} to 10^{-6} M, (Figure 3.7 (a), (b) and (c)).

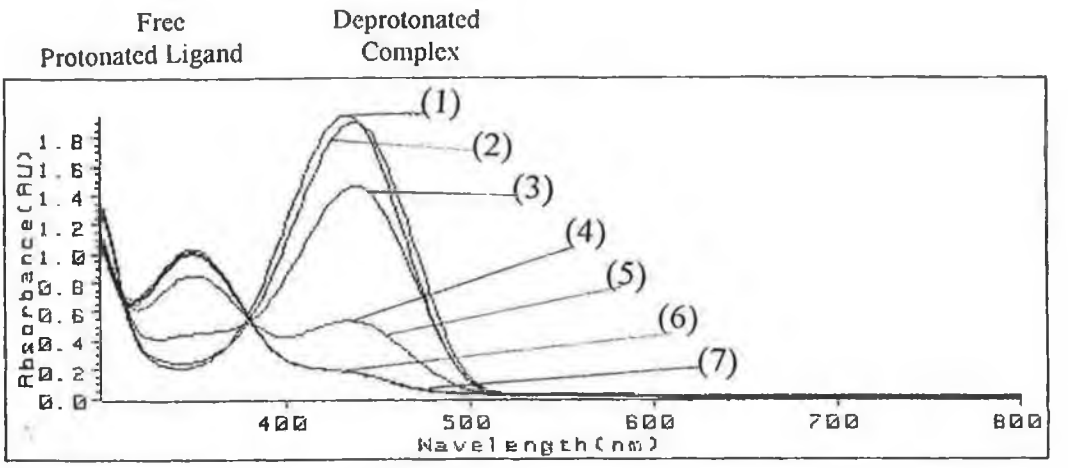

Figure 3.7 (a):- Ligand 3, lithium response.

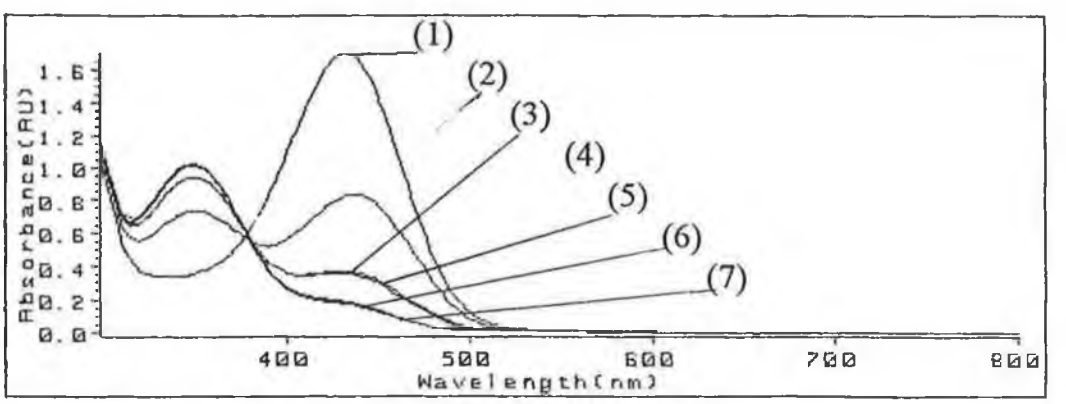

Figure 3.7 (b):- Ligand 3, sodium response.

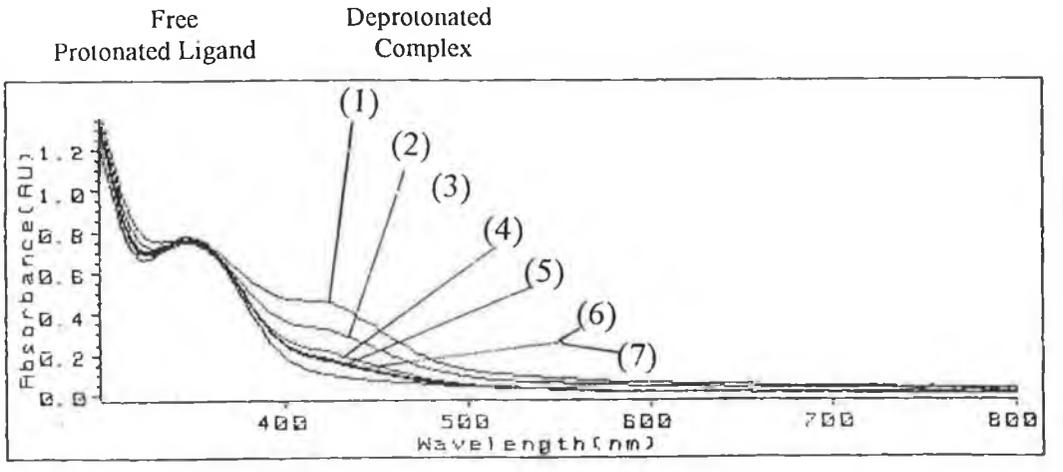

Figure 3.7 (c):- *Ligand 3, potassium response.*

Figure 3.7:- *One-phase investigation of changes in the absorbance spectrum of 2.5 mL of a $5x10^{-5}$ M solution of Ligand 3, in THF with 20 μL of morpholine, upon addition of aqueous (a) $LiClO_4$, (b) $NaClO_4$, with final concentrations of 0.1 (1), 10^{-2} M (2), 10^{-3} M (3), 10^{-4} M (4), 10^{-5} M (5), 10^{-6} M (6), 0 M (7) and (c) $KClO_4$ with final concentrations of $4x10^{-3}$ (1), $2x10^{-3}$ M (2), 10^{-3} M (3), 10^{-4} M (4), 10^{-5} M (5), 10^{-6} M (6), 0 M (7), 0 M and 0 M morpholine (8) see table 2.1.*

The protonated λ_{max} of this compound appears at 350 nm, ($\varepsilon = 2.16 \times 10^4$ L mol^{-1} cm^{-1}), with the deprotonated complex λ_{max} occuring at 424 nm. The absorbance at this wavelength increases upon addition of increasingly more concentrated solutions of metal perchlorates. An isobestic point occurs at 380 nm. The same λ_{max} of 424 nm occurs for the complexes of all three cations.

A comparison of the responses of 424 nm for the different cations in the concentration range of 10^{-6} M to 10^{-1} M is seen in Figure 3.8. From this curve it can be seen that Ligand 3 responds most favourably to the presence of lithium perchlorate. An L.O.D. of c. 3×10^{-5} M was obtained for $LiClO_4$ compared to that of 7×10^{-4} M for $NaClO_4$. A large increase in absorbance is observed between 10^{-4} M and 10^{-2} M $LiClO_4$ before a levelling off is seen. The greatest change in absorbance occurs between 10^{-4} and 10^{-3} M where a slope of 0.9 a.u./dec. is observed. For $NaClO_4$ a substantial absorbance change is not observed prior to the addition of 10^{-3} M $NaClO_4$ indicating a different linear range for these two cations. Saturation is again observed for the $LiClO_4$ curve indicating complete ligand deprotonation and a minimum ε of 3.70×10^4 L

mol^{-1} cm^{-1} was estimated, for a deprotonated complex complex concentration of 5 x 10^{-5} M. There is a difference of approximately 1 a.u. between Li^+, and Na^+ at 10^{-3} M $MClO_4$ which indicates that the ligand has the ability to distinguish between the two cations at this concentration level.

The $NaClO_4$ response curve has obviously not reached saturation point but from the depth of the trough at the protonated λ_{max} of spectrum 1 of Figure 3.7 (b) it would appear to be close to it. The largest absorbance change occurs for the Na^+ complex between 10^{-2} and 10^{-1} M, with the final absorbance with 10^{-1} M $NaClO_4$ approaching the same value observed for 10^{-1} M $LiClO_4$.

There is a slight change in absorbance for the $KClO_4$ complex between 2 and 4 mM $KClO_4$, and this is seen in the lowest curve of Figure 3.8. However the intensity remains lower than for the $NaClO_4$ complex response at similar concentrations and the role played by the changing nature of the solvent cannot be discounted. No change in the protonated λ_{max} at 350 nm is observed in this $KClO_4$ concentration range indicating poor selectivity for this ligand to K^+. The order of complexation for Ligand **3** is therefore again the same as it was for Ligands **1** and **2** of $Li^+ > Na^+ > K^+$.

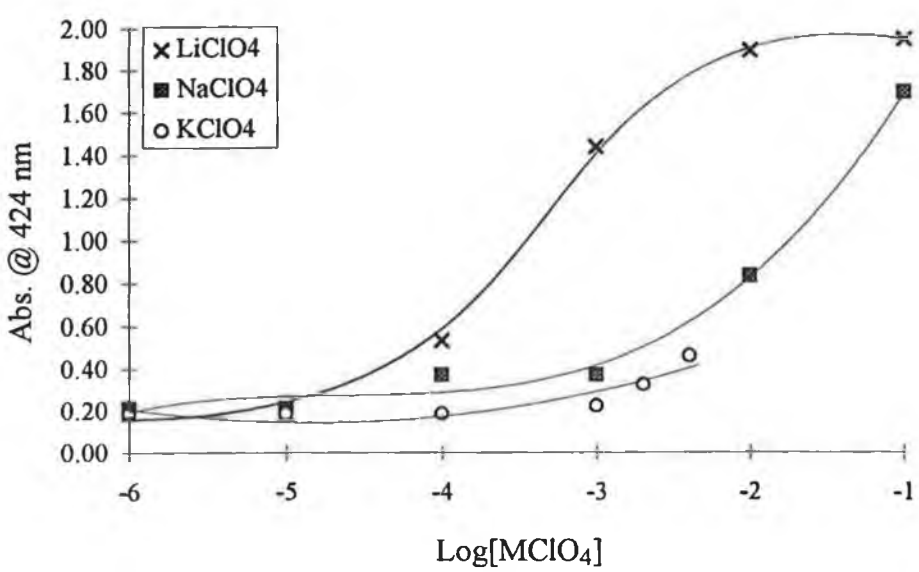

Figure 3.8:-Comparison of the spectral response at 424 nm of each of the lithium, sodium and potassium metal complexes of Ligand 3. Data obtained from Figs. 3.7 (a), (b) and (c).

3.5 Selectivity Coefficient Determination

After the establishment of preferential lithium uptake by all three ligands the next phase of the work was to determine selectivity coefficients for Li^+ over Na^+. These values were determined using Method 2.3.2 by examining the spectral response of $LiClO_4$ from 10^{-6} M to 10^{-1} M as before, except this time fixed background concentrations of the interferent were also included. Fixed interfering $NaClO_4$ concentrations of 10^{-2} and 10^{-3} M were examined. 0.1 M $NaClO_4$ was also examined as the interfering cation concentration for the determination of a selectivity coefficient for lithium over sodium. However, the absorbance of the ligands in the presence of 0.1 M $NaClO_4$ is quite similar to that of the ligands in the presence of 0.1 M $LiClO_4$, and this is clearly seen in Figures 3.4, 3.6 and 3.8. So in effect this concentration of sodium completely swamped the response of lower levels of lithium and hence no selectivity coefficient could be determined.

Figures 3.9 (a), (b) and (c) show the interference study graphs of absorbance at the deprotonated complex λ_{max} of Ligands **1**, **2** and **3** respectively in the presence of 10^{-2} M and 10^{-3} M $NaClO_4$.

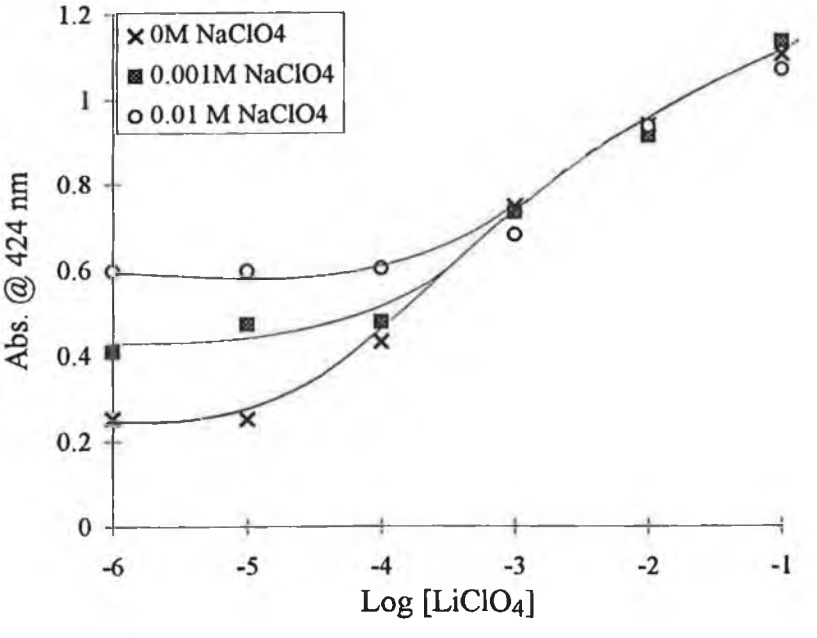

Figure 3.9(a):- Ligand 1 selectivity

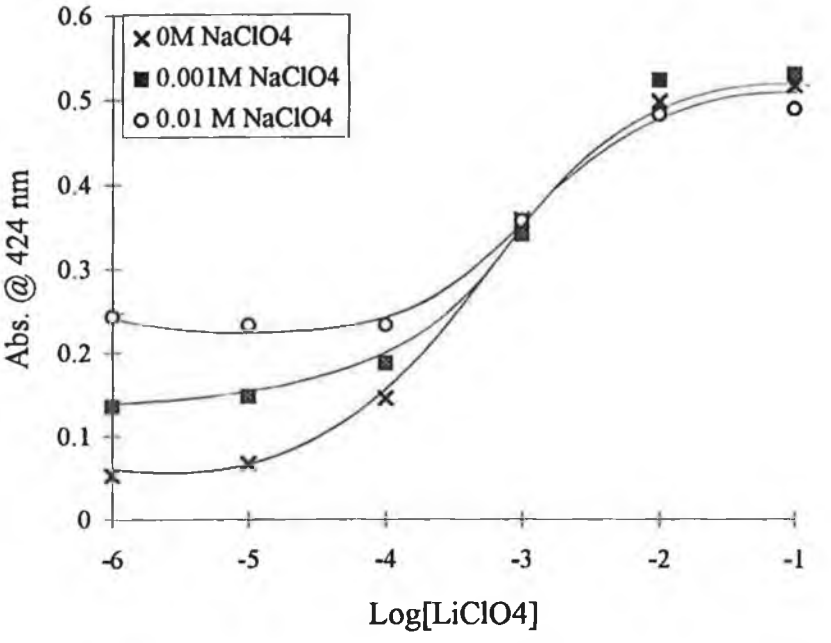

Figure 3.9 (b):- *Ligand 2 selectivity*

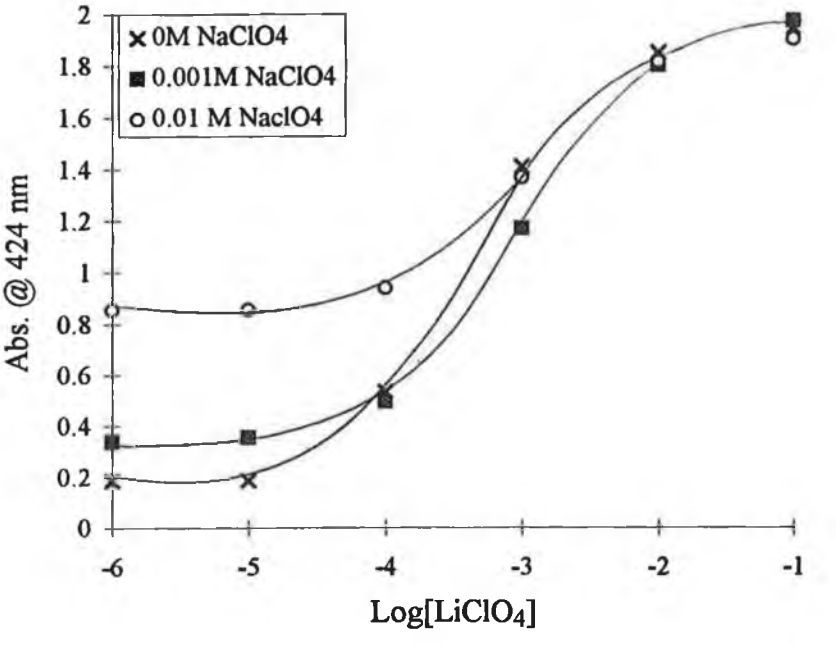

Figure 3.9:- *Ligand 3 selectivity*

Figure 3.9:- *One-phase studies of the optical response of: (a) $5x10^{-5}$ M Ligand 1 in THF with 20 μL morpholine, (b) $7x10^{-5}$ M Ligand 2 in THF with 45 μL morpholin, (c) $5x10^{-5}$ M Ligand 3 in THF with 20 μL morpholine - to additions of $LiClO_4$ in the presence of fixed (10^{-2}, 10^{-3} M) concentrations of $NaClO_4$, see Method 2.3.2.*

From these data approximate selectivity coefficients ($K_{Li, Na}$) were calculated from the intercept between the lithium response curve and the sodium interference curves via the expression $K_{Li\ Na} = C_{Na}/C_{Li}$ and are shown in table 3.1.

Table 3.1:- Selectivity Coefficients for Ligands 1-3

Ligand	$[Na^+]$ / M	K_{LiNa}
1	10^{-2}	25.1
1	10^{-3}	11.2
2	10^{-2}	34.7
2	10^{-3}	14.7
3	10^{-2}	43.1
3	10^{-3}	23.2

There is very little difference in selectivity coefficients between the mono and tetra chromogenic ligands bearing *tertiary* butyl groups in the *para* position, (Ligands 1 and 2 respectively). A slight enhancement of selectivity is observed for the tetrachromogenic ligand, Ligand 3, which bears C_{18} groups in the *para* position of the phenolic calixarene backbone. Due to the difficulties in defining accurately the straight line portions of the curves in this type of diagram (and hence the intercept), it is difficult to estimate selectivity precisely. However, it does give an approximate quantification of the relative affinity of the ligands with these ions. All three ligands show slight selectivity for lithium over sodium in the same order of magnitude.

3.6 Solvent Variation

The effect of solvent variation on the UV-Vis spectra of the deprotonated complex and protonated forms of Ligand 1 was examined to gain an insight into the types of electronic transitions involved in generating the spectra. Method 2.3.5 was followed with the solvent being varied from 100% THF to 100% methanol. A hypsochromic shift of 16 nm was observed on going from THF to methanol, see Figure 3.10(a) and (b). Figure 3.11 shows a comparison of the intensity achieved over the $LiClO_4$ concentration range at the λ_{max} of

deprotonated complex in both solvents. As well as a λ_{max} shift with increasing polarity, (dielectric constants for THF and methanol at 20° C are 7.6 and 32.63 respectively) [3], it was also noted that a stronger yellow colour was observed with the addition of morpholine, in the absence of any metal perchlorate and this is seen clearly in spectrum 3.10(b), traces (7) and (6) which are spectra of the ligand in the absence and presence of morpholine respectively, without any metal. This is indicative of a greater proportion of the ligand being in the deprotonated form (equtaion **3.1**) and that the lipophilic base, morpholine, has a lower pK_a in this solvent than it had in THF. Only above 10^{-3} M $LiClO_4$ is a more intense peak observed than that achieved with the ligand and base.

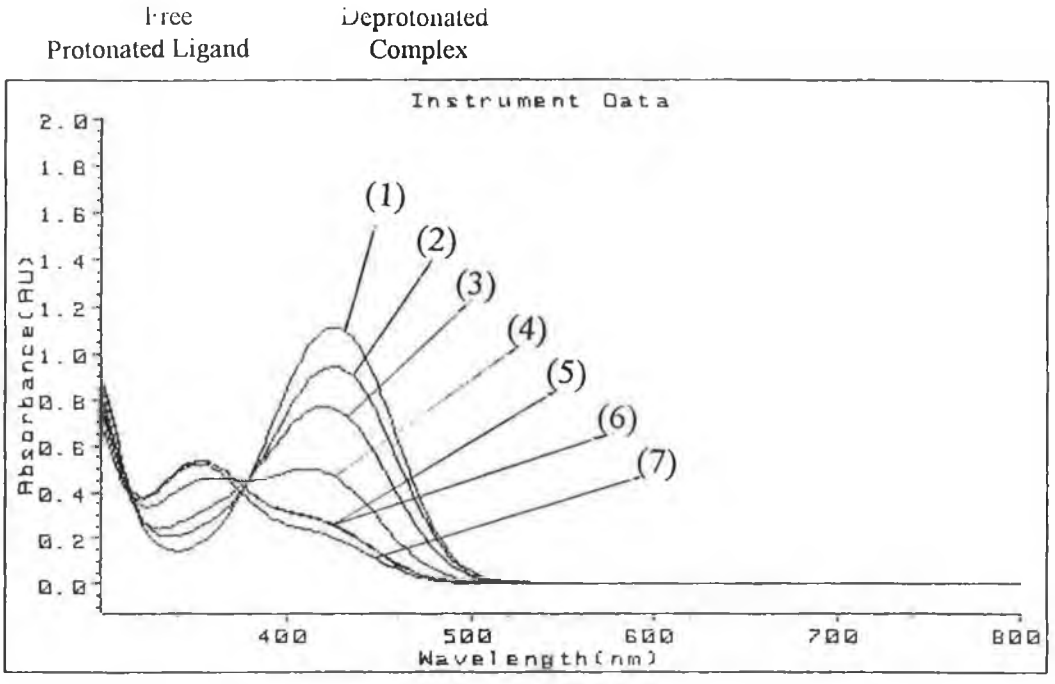

Figure 3.10 (a):-Ligand 1 in 100% THF

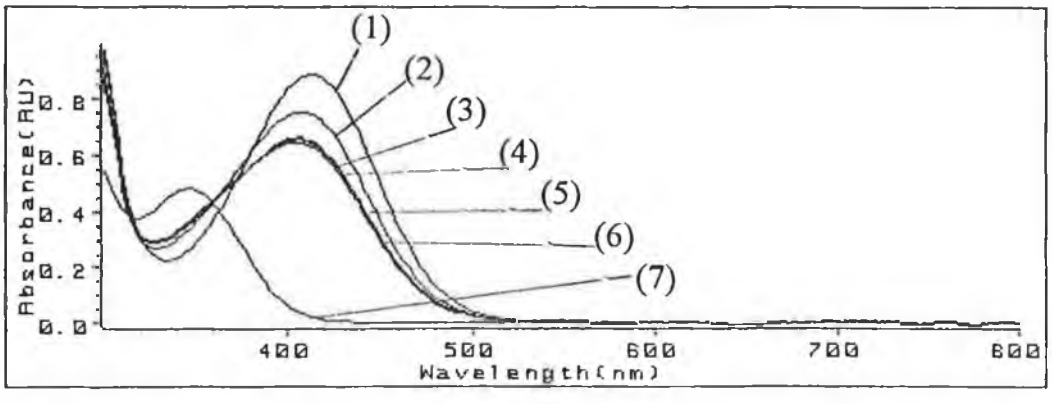

Figure 3.10 (b):- Ligand 1 in 100% Methanol.

Figure 3.10:- UV-Vis spectra of $5x10^{-5}$ M Ligand 1 and 0.1 M morpholine in (a) THF, with 10^{-1} M (1), 10^{-2} M (2), 10^{-3} M (3), 10^{-4} M (4), 10^{-5} M (5), 10^{-6} M (6), 0 M (7), and (b) methanol with 10^{-1} M (1), 10^{-2} M (2), 10^{-3} M (3), 10^{-4} M (4), 10^{-5} M (5), 0 M (6), 0 M and 0 M morpholine (7), See table 2.1 for details.

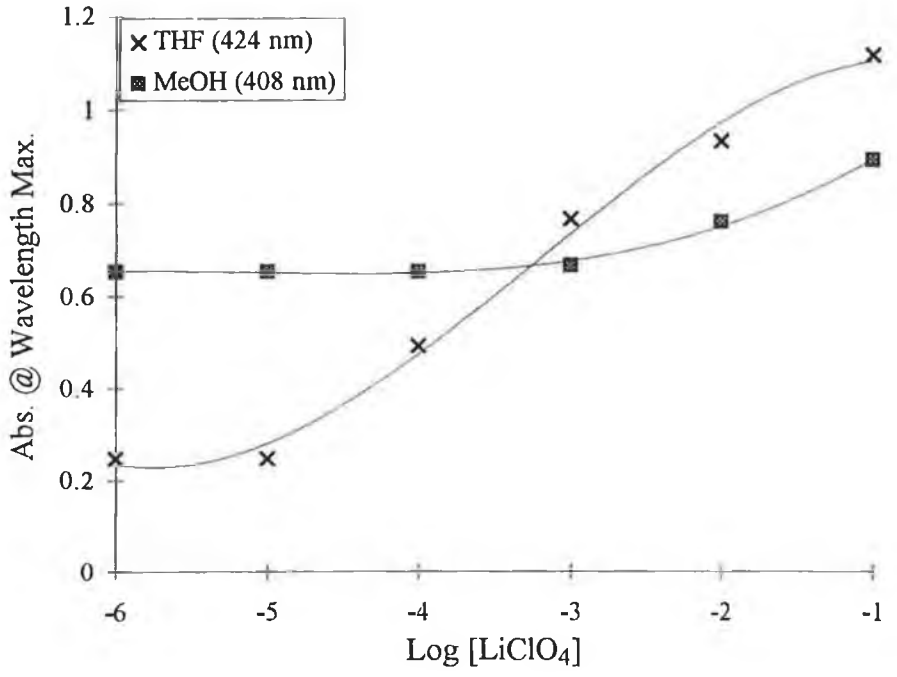

Figure 3.11:-Comparison of the spectral response of Ligand 1 to changes in $LiClO_4$ concentration in THF (424 nm) and MeOH (408 nm),with data taken from Fig 3.10(a) and (b) respectively.

3.7 NMR Complexation Studies

To confirm that complexation of the ligand with the metal cation was occurring in the absence of colour generation, as outlined in equation (**3.1**)

$$\text{L-COH} + M^+ \rightleftharpoons LM^+\text{-COH} \qquad \textbf{(3.1)}$$

NMR complexation experiments were carried out. Sodium thiocyanate was used as the complexing salt and Method 2.3.6 was followed. Calix[4]arene tetraesters of the type used in this study undergo several very characteristic changes in proton chemical shifts on complexation with alkali metal cations [14-16].

Figure 3.12 shows a series of NMR spectra obtained by Arduini et al. [16], demonstrating the effect of sodium complexation with a *t*-butyl calix[4]arene tetra-*t*-butyl ester **3(vi)** which is in a rigid cone conformation in solution. Two features are very important with cone shaped *p-t*-butyl calix[4]arenes. These are the two sets of 4H doublets associated with the non-equivalence of the bridging methylene protons H_A and H_B of the calixarene annulus (see structure **3(vii)**),

between 3 and 5 ppm, and the large single resonance due to the *t*-butyl groups on the upper rim of the calixarene at approximately 1 ppm (3.12(a)).

On introduction of NaSCN into the $CDCl_3$ solution of **3(vi)** a number of characteristic shifts in peaks occurs, 3.12(b). The highfield doublet at 3.2 ppm (H_B) has been assigned to the equatorial protons of the binding methylene protons. It is seen to experience a deshielding effect on complexation induced by confomational charges which bring the equatorial protons closer to the hydrophilic cavity and this results in a down-field shift of 0.38 ppm to 3.58 ppm. The H_A protons at 4.9 ppm, have been assigned to the axial protons, experience an upfield shift of 0.78 ppm to 4.12 ppm. This is indicative of the H_A protons becoming shielded from the effect of the aromatic ether and carbonyl oxygens which make up the polar cavity where complexation is thought to occur. The upfield shift on the H_A proton signals that these protons are sensitive to small variations in the polar environment of the aromatic ether and ester oxygens which are in close proximity. No further spectral shifts are observed when a 1:1 [Lig]:[NaSCN] relationship has been reached, (Figure 3.12(c)), and this is indicative of a 1:1, ligand : metal stoichiometry.

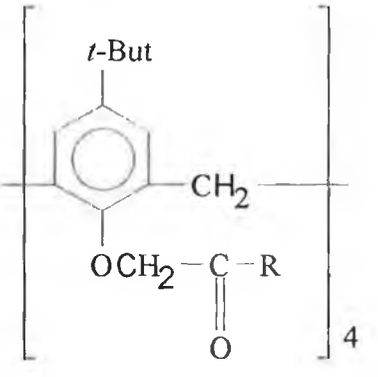

R = O-*t*-butyl

3(vi)

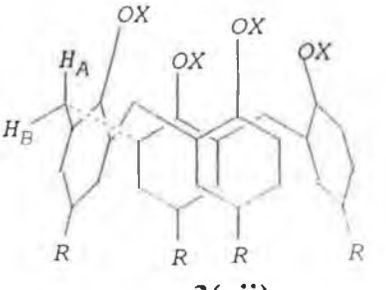

R = *p-tert*-butyl **3(vii)**

Representation of a calix[4]arene, highlighting the bridging methylene protons of the annulus (the double bonds of the aromatic rings have been omitted to aid clarity).

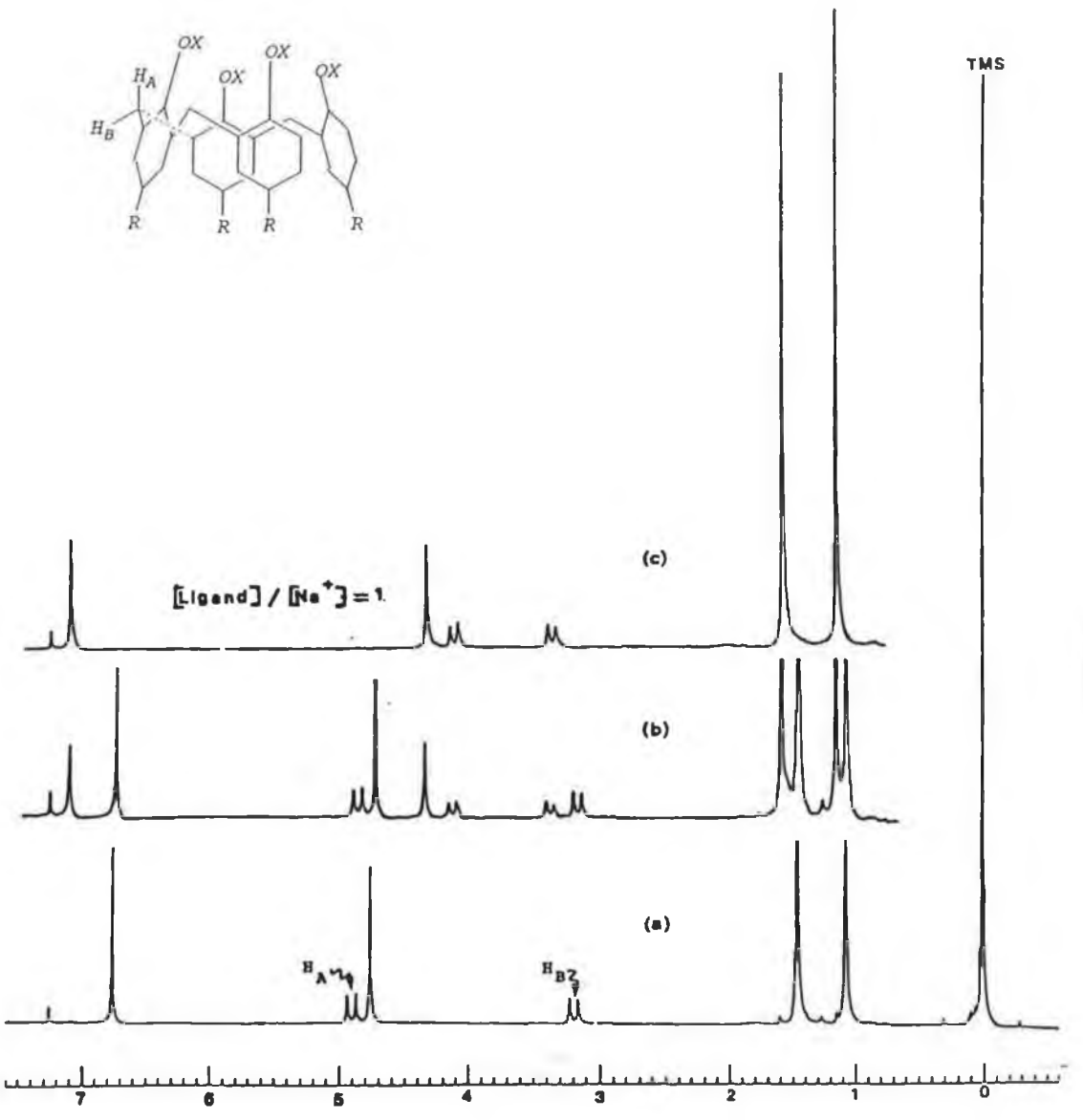

Figure 3.12:- *Encapsulation of NaSCN by* **3(vi)**. *^1H NMR spectra (200 MHz) in $CDCl_3$ at 25° C: (a) = free ligand; (b) = 40 % complex; (c) = 100 % complex; $[Ligand]_{CDCl_3} = 5 \times 10^{-2}$ M,* ***[16].***

Ligands 1 to 3 are believed to possess the cone conformation **3(viii)** in which all four aromatic rings are pointing in the same direction in solution since their immediate precursors, viz. acid chlorides **3(ix)** and **3(x)** are known to have this conformation, and the NMR spectra in Figure 3.13 confirm this for Ligand 1.

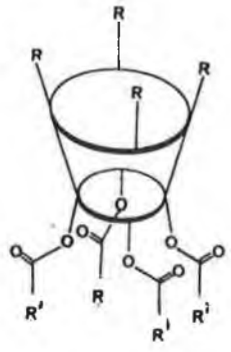

3(viii)

3-dimensional representation of a calix[4]arene in the cone conformation

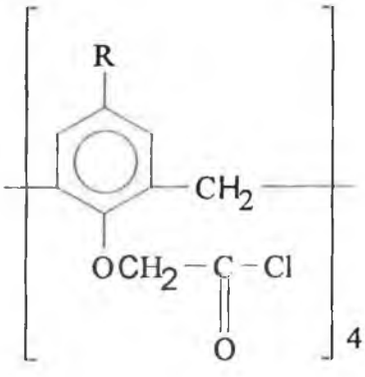

3(ix)

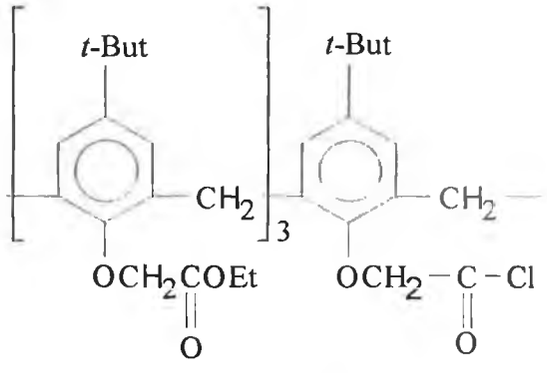

3(x)

R = But

R = $(CH_2)_{17}CH_3$

Structures of the acid chloride precursors to the chromogenic calix[4]arenes.

Figure 3.13 shows the spectra obtained with Ligand 1 in (a) the absence of metal cation and (b) in the presence of a 1 mole equivalent of NaSCN. From these spectra, it appears that Ligand 1 is a distorted cone in solution since the ^{1}H NMR spectrum reveals a cluster of peaks at between 0.84 and 1.33 ppm for the *t*-butyl groups of the upper rim. A completely symmetrical molecule would have yielded only one signal for the *t*-butyl groups, as was the case if Figure 3.12 (a). An x-ray crystal structure of a distorted cone conformational tetraamide, **3(xi)**, is

shown in structure **3(xii),** [17]. In this free ligand two opposite aromatic rings (A, C) are almost parallel to each other, and the other two (B, D) are almost perpendicular. This non-symmetrical arrangement renders the *t*-butyl groups of the *para* position of the upper calixarene rim, non-equivalent. The splitting of the *t*-butyl resonance is seen for Ligand **1** in Figure 3.13(a) at approximately 1 ppm. Preliminary molecular modelling using Hyperchem **3(xiii)** corroborates this finding. The bond distances between A and C was estimated to be 5.31 A, whereas the bond distance between B and D was estimated to be 9.25 A.

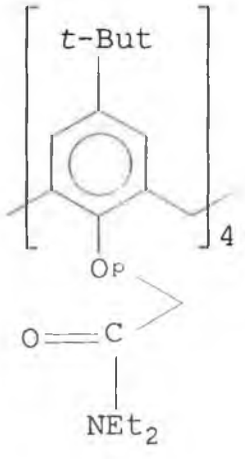

3(xi)

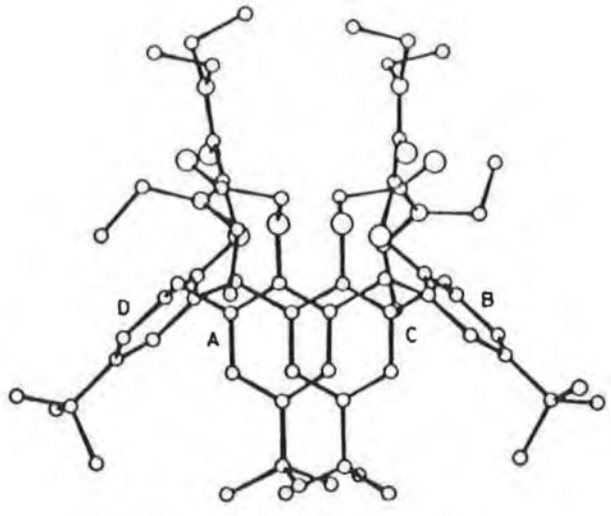

3(xii),

*Calix[4]arene tetraamide **3(xi)**, and an x-ray crystal structure of this compound, **3(xii)**, [17].*

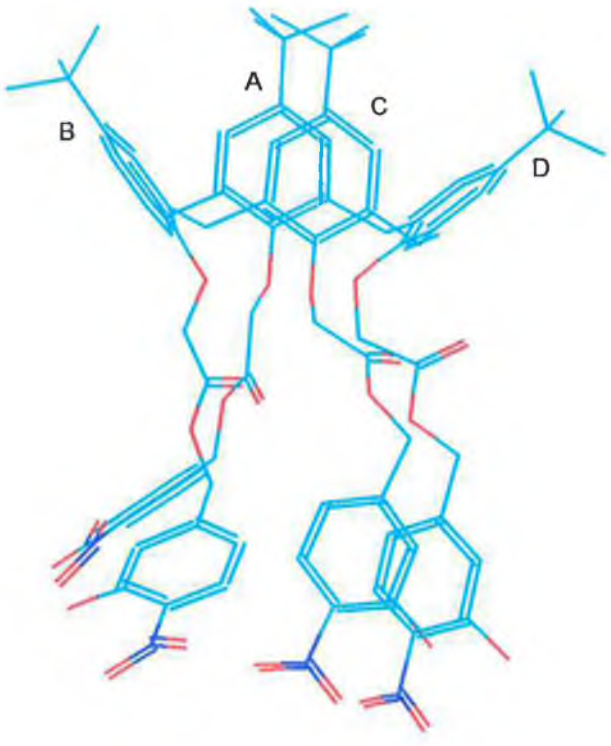

3(xiii)

Molecular Model of Ligand 1 using Hyperchem *

* Molecular Modelling performed by P. Kane at D.C.U.

Light Blue = C-C Bonds

Red = Oxygen Atoms

Dark Blue = Nitrogen Atoms

On addition of NaSCN to Ligand **1** the cluster of signals at approximately 1 ppm is replaced by a single resonance at 1.20 ppm, (Figure 3.13(b)). This simplification in the signal to a singlet is synonomous with complexation of the cation conferring a more ordered symmetry on the molecule, in which all of the *t*-butyl groups are in a similar environment. On complexation, the carbonyl oxygen atoms form part of a rigid polar cavity encapsulating the metal-ion whereas with the free ligand, the pendent groups are much more mobile, while the macrocycle itself adopts a 2-in/ 2-out conformation in which the in/out groups are dynamically changing [17].

The ^1H NMR spectrum(Figure 3.13(a)) shows a number of complex signals between 3 and 6 ppm, the region in which the characteristic H_A and H_B signals

would be expected to lie. At 3.2 ppm the identification of a H_B doublet is difficult as it would appear that signals from at least one other set of protons is occurring here. However, upon introduction of NaSCN, both a shift in these peaks to 3.4 ppm and a simplification of the signal is observed. As this is the region in which the equatorial proton H_B would be expected to appear this gives some indication that the inclusion of a cation has the effect of perturbing the positioning of the H_B proton in relation to the aromatic-ether and ester oxygens of the hydrophilic cavity and thereby deshielding it. Similarly, it is equally difficult to assign a doublet to the axial H_A protons. A set of peaks at 4.5 ppm in Figure 3.13 (A) is seen to shift to 4.3 ppm upon interaction of 1 mole equivalent of NaSCN, and this could possibly be as a result of some shielding of the H_A proton, similar to that observed in Figure 3.12 by Arduini et al. [16]. Although these assignments are only tentative, it is clear from the two spectra that the introduction of NaSCN causes a change in the environment of many of the protons of this ligand. The most convincing piece of evidence for cation inclusion was the simplification of the signals for the *t*-butyl hydrogens discussed above which indicated a more ordered symmetry for the molecule after complexation.

It must be noted that during these ^1H NMR experiments no colour change was observed, indicating that complexation occurs in the absence of base and thus without deprotonation and that the equilibrium in **(3.1)** is effectively being forced to the right. This lack of of colour/spectral change when complexation occurs in the absence of morpholine is indicative of the deprotonation of the nitrophenol being a prerequisite for colour generation. A colour change is observed only if a suitable base is available for the uptake of the phenolic proton or if the equilibrium in **(3.3)** is forced to the right. No further spectral shifts were observed after a 1 mole equivalent of NaSCN had been added and therefore it can be deduced that a 1:1 stoichiometry for the NaSCN with Ligand **1** exists and that equation **(3.1)** favours the right hand side. Other changes in the position of the aromatic protons upon complexation are consistent with data from other studies with calixarene esters [14].

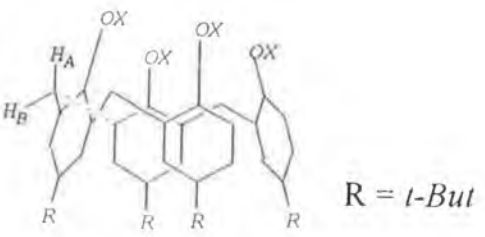

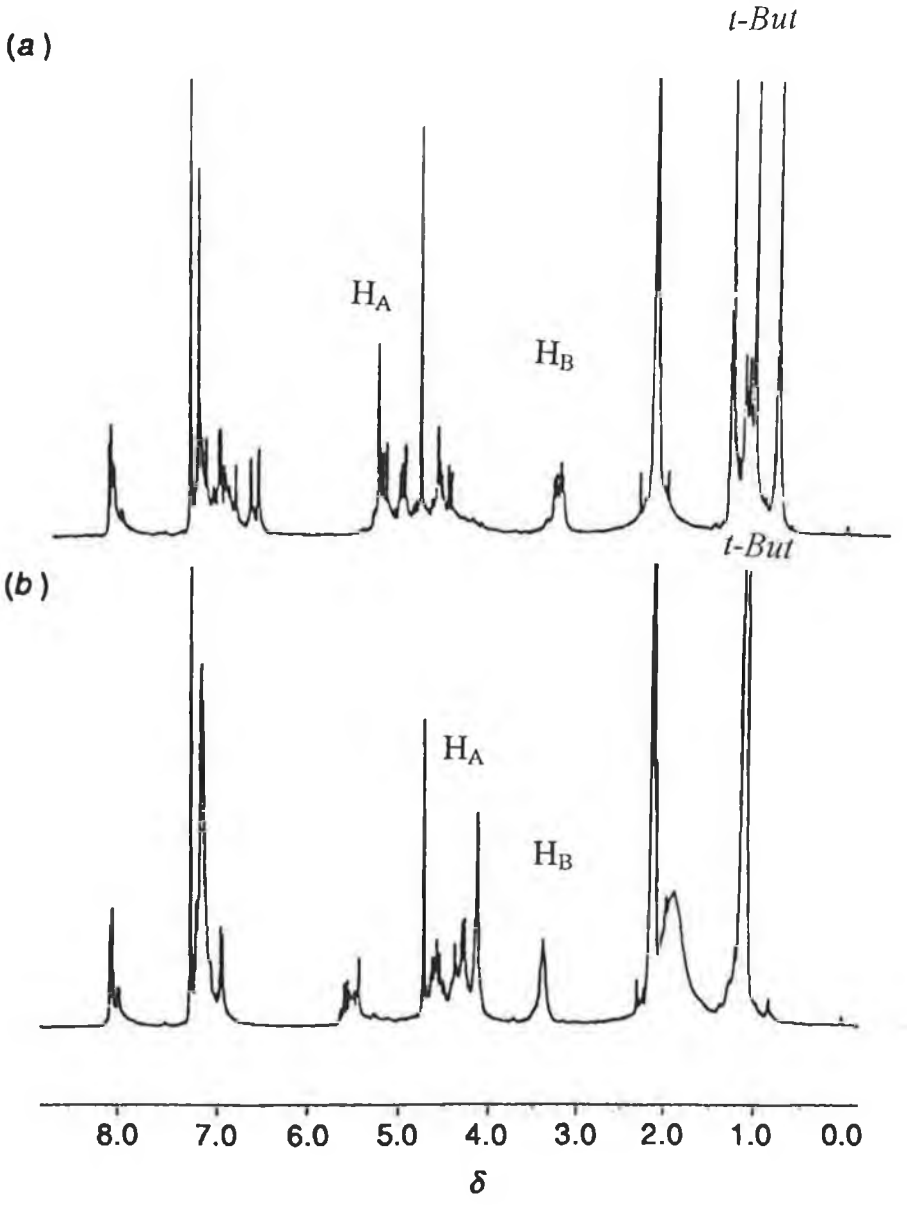

Figure 3.13:- *^1H NMR spectra of the free and complexed form of Ligand 1 in $CDCl_3$ at room temperature: (a) [NaSCN]/[1] = 0; (b) [NaSCN]/[1] = 1; where [1] = $5x10^{-3}$ M in $CDCl_3$. An aliquot from 1.0 M solution of NaSCN in CD3OD was added directly to a $CDCl_3$ solution of 1 in an NMR tube. p-tertbutyl H; H_A, and H_B. = $ArCH_2Ar$. See table 2.2.*

3.8 Two Phase Studies

On introducing a second, (aqueous), phase of deionised water into the system, it is imperative from a sensor point of view that conditions are optimised so that partition coefficients for the base and all forms of the chromogenic calixarene (complexed, complexed and deprotonated, uncomplexed) greatly favour the organic phase, as leaching of the membrane components into the aqueous phase leads to poor sensor response characteristics. A transfer of metal ions from the aqueous to the organic phase is however required. The system involves a number of equilibria with the partition coefficient of the deprotonated complex determining the extent to which the coloured species enters the aqueous phase.

TDDA, which is a more lipophilic base than morpholine, was used in the two phase work in order to maintain the base in the organic phase, thus reducing the tendency of the base to partition out into the aqueous phase and ensuring that the deprotonation of the nitrophenol group would occur in the organic phase. Method 2.3.5 was followed for the two phase examination of the ligands. The organic phase used was butan-1-ol, and the choice of this solvent will be described in Chapter 4, with the nitrophenylazophenol ligands. The ligands at concentrations of $5x10^{-5}$ M were dissolved in this organic phase, along with 20 μL of TDDA. Upon addition of 2.5 mL of water to the system (without metal perchlorates), the formation of a faint yellow colour at the interface of the water and the butan-1-ol was observed which is indicative of the deionised water (which has a much higher dielectric constant than THF) being able to support the existence of the ions formed and hence favour ligand deprotonation.

Upon addition of the metal perchlorates to the aqueous phase, an increase in colour intensity was noted in the organic phase at the higher lithium perchlorate concentrations. This colour change was monitored by UV-Vis spectroscopy with an absorbance maximum being noted at 420 nm and an isobestic point at 350 nm, (Figures 3.14 (a) and (b) for ligands 1 and 2 respectively). This strongly suggests that the metal perchlorate has been taken up from the aqueous phase and the Li^+ ion has complexed with the calixarene.

With both ligands 1 and 2, a transfer of colour due to the deprotonated complex into the aqueous phase was noted at lithium and sodium perchlorate concentrations of 10^{-1} to 10^{-3} M, with the yellow colour diffusing into and throughout the aqueous layer within minutes of addition of the $LiClO_4$ and

subsequent settling out of the two layers. UV-Vis spectra of the yellow aqueous phase gave peaks at 420 nm up to 80% the size of those obtained for the organic layer for ligand **3** (Figure 3.15(b)) and up to 20% for ligand **1**, (Figure 3.25(a)) with measurements being taken 15 minutes after the addition of the $LiClO_4$, suggesting that significant leaching of the deprotonated complex into the aqueous phase was occurring. In contrast to calix[4]arene esters which are extremely water insoluble, the movement of colour due to the complexed form of the molecule into the aqueous phase was surprising. The zwitterionic nature of the deprotonated complex, is probably an important factor influencing the transfer of colour from the organic to the aqueous phase, as the deprotonated complex possesses positive charge centred on the metal ion in the cavity, and a negative charge at the deprotonated nitrophenol chromophore, see structure (**3(xiv)**).

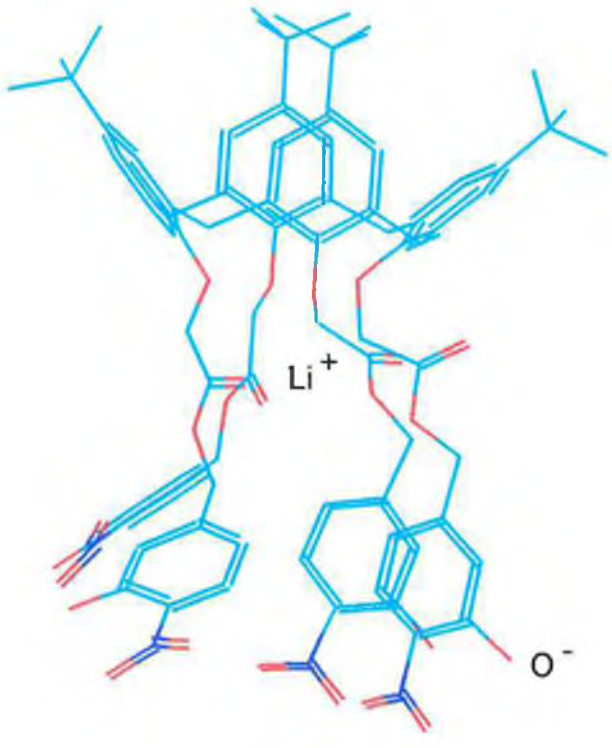

3(xiv)

Molecular Model of Ligand 1 using Hyperchem *

Light Blue = C-C bonds

Red = Oxygen atoms

Dark Blue = Nitrogen atoms

* Molecular Modelling performed by P. Kane at D.C.U.

The variable solubility of these ligands is of some interest, as most calixarenes are very water-insoluble, even when complexed with a cation. An examination of a two phase system was carried out as above using 10^{-2} M $LiClO_4$ in the absence of the base TDDA. UV-Vis spectra were taken of both phases after 24 hours and it was found that none of the protonated complex had transferred to the aqueous phase. This demonstrates the importance of the deprotonation of the chromophore in determining overall solubility.

However, with Ligands 1 and 2, it seems that the aqueous solubility can be dramatically altered, for example by variation of the pH of the aqueous phase. This was demonstrated with Ligand 1 by using 2.5 mL of 1 M HCl as the aqueous phase, in contact with 2.5 mL of an organic butanol phase, which contained TDDA, and the ligand-Li^+ complex. No colour transfer was noticed and a spectrum of the aqueous phase showed peaks for neither form of the ligand after 1 hr, (see Figure 3.16), as the complex would be predominantly in the protonated form at the aquo-butanol boundary and would hence remain insoluble in the aquo-phase. Any reprotonation of the aquo-butanol interface may also have resulted in a certain degree of decomplexation of the ligand, with the metal entering the aqueous phase.

Another experiment was carried out in which a typical two phase experiment was carried out with 10^{-2} M $LiClO_4$ added to the aqueous phase and after mixing of the two layers to generate the deprotonated complex in the organic phase HCl was added to the bottom aqueous phase to make it 10^{-2} M in HCl . Any colour which had traversed the organic/aqueous phase disappeared from the aqueous phase. On examination of the spectrum of the aqueous phase the presence of protonated ligand was found, with no trace of any of the deprotonated complexed ligand, (see Figure 3.17). This means a mode of conferring a certain degree of water solubility on these calixarenes has been obtained. Water soluble calixarenes are of interest because of their ability to interact with ions and molecules and to perform catalysis [1].

This type of pH or ion dependent solubility raises interesting possibilities for switching ion or ligand transport between phases. As deprotonation of these calixarenes is also a function of the electrochemical environment (the nitrophenol groups can be readily oxidised-reduced, and have well-defined voltammetric behaviour [18]), phase transport could in principle be controlled by means of an externally applied potential or as was demonstrated here by pH variation.

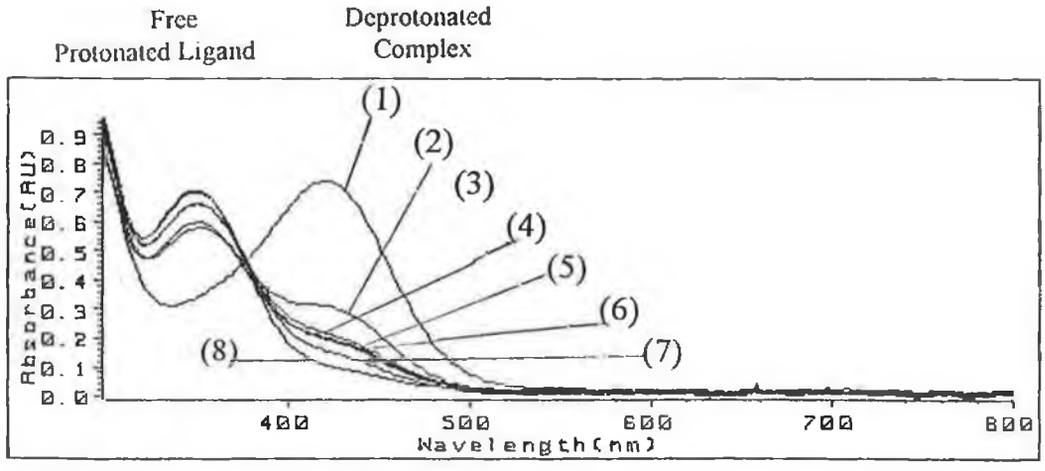

Figure 3.14 (a):- Two-phase Ligand 1, organic phase.

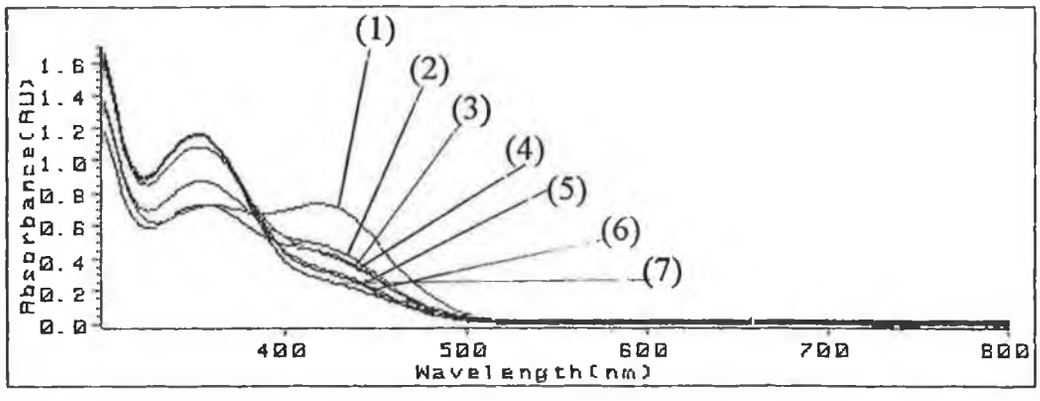

Figure 3.14 (b):-Two Phase Ligand 2, organic phase.

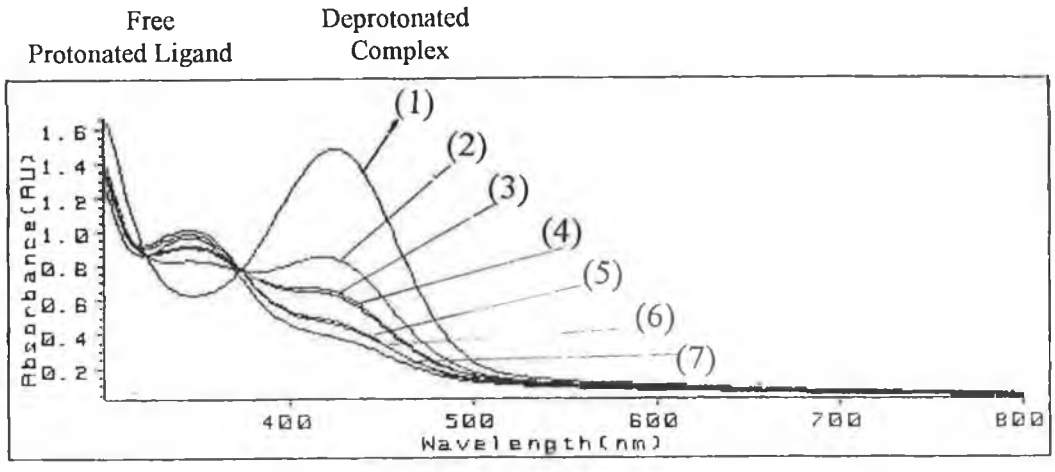

Figure 3.14 (c):- *Two-phase Ligand 3, organic phase.*

Figure 3.14:- *Two-phase studies showing changes in absorbance spectrum of the organic (butan-1-ol) phase for $5x10^{-5}$ M (a) Ligand 1, (b) Ligand 2 and (c) Ligand 3, with 20 μL of TDDA, when $LiClO_4$ was added to the aqueous phase of the two-phase system to give the following aqueous-phase concentrations: 0.1 (1), 10^{-2} (2), 10^{-3} (3), 10^{-4} (4), 10^{-5} (5), 10^{-6} (6), 0 M (7). See method 2.3.5.*

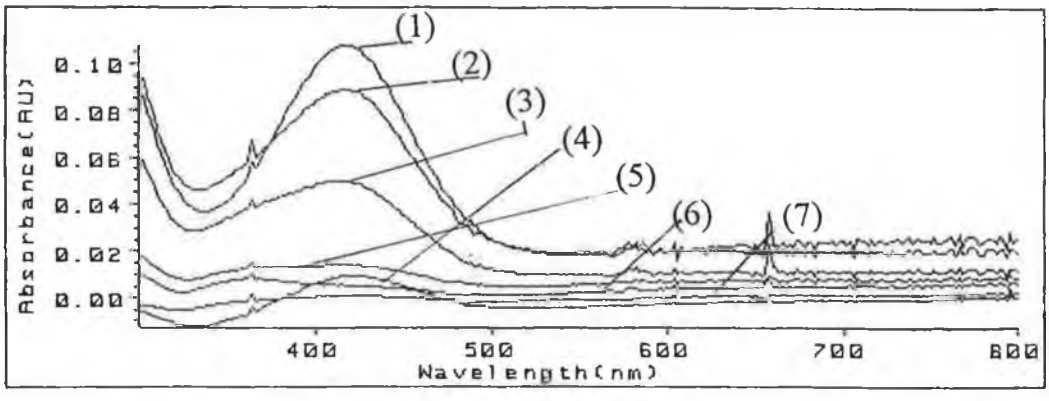

Figure 3.15(a):-*Two-phase Ligand 1 aqueous phase.*

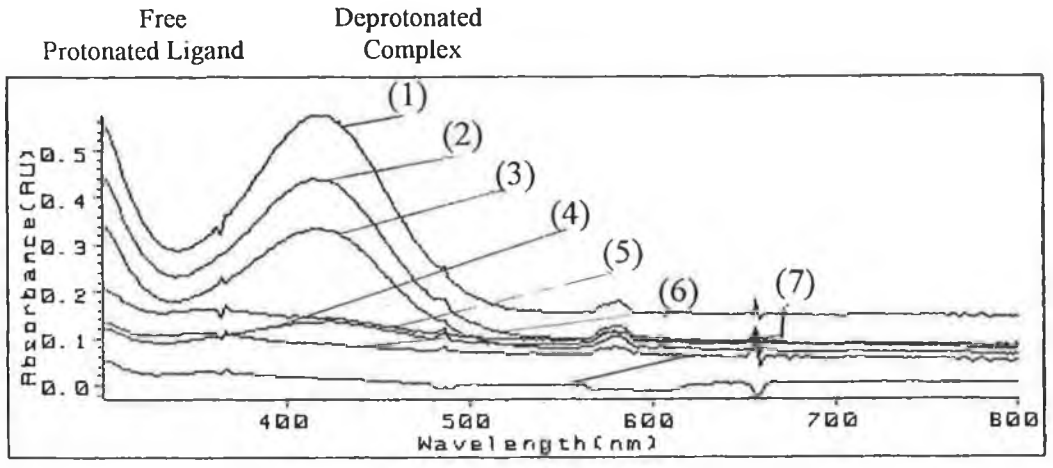

Figure 3.15(b):- *Two-phase Ligand 2 aqueous phase.*

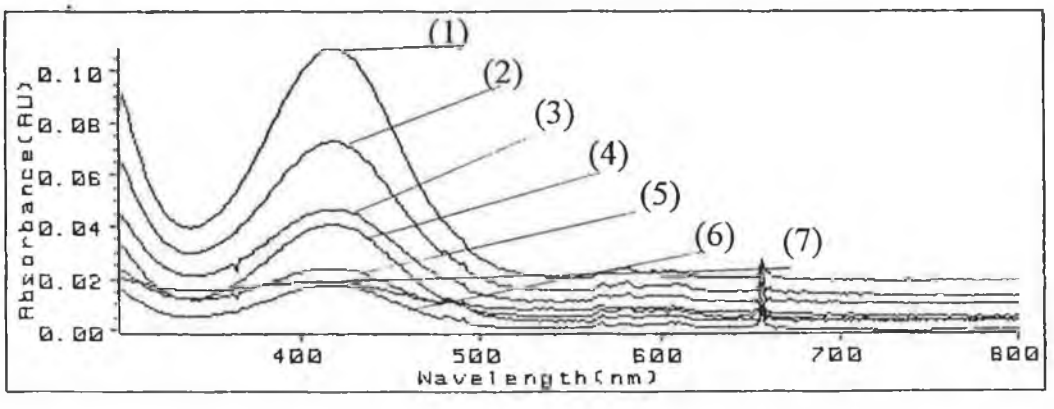

Figure 3.15(c):- *Two-phase Ligand 3 aqueous phase.*

Figure 3.15:- *Two-phase studies showing changes in absorbance spectrum of the aqueous- phase for $5x10^{-5}$ M (a) Ligand 1, (b) Ligand 2 and (c) Ligand 3, with 20 μL of TDDA, when $LiClO_4$ was added to the aqueous phase of the two-phase system to give the following aqueous-phase concentrations: 0.1 (1), 10^{-2} (2), 10^{-3} (3), 10^{-4} (4), 10^{-5} (5), 10^{-6} (6), 0 M (7). See method 2.3.5.*

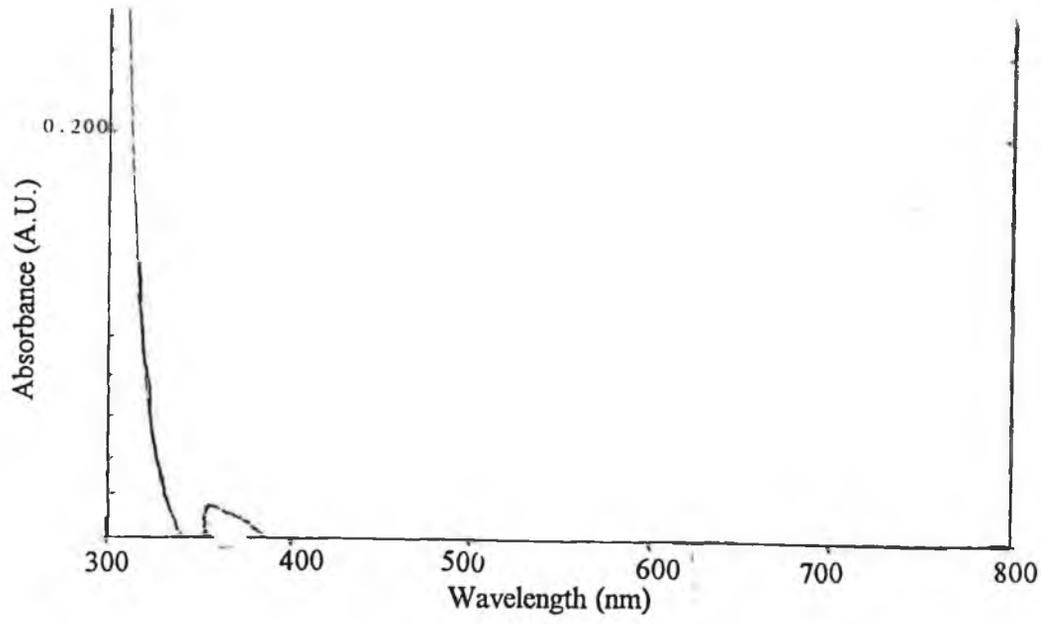

Figure 3.16:- Spectrum of the aqueous phase of a 2 phase experiment which was carried out by carefully adding 2.5 mL of a solution which was $5x10^{-5}$ M in Ligand 1, 10^{-2} M in $LiClO_4$ and 20 μL of TDDA to 2.5 mL of 1 M HCl.

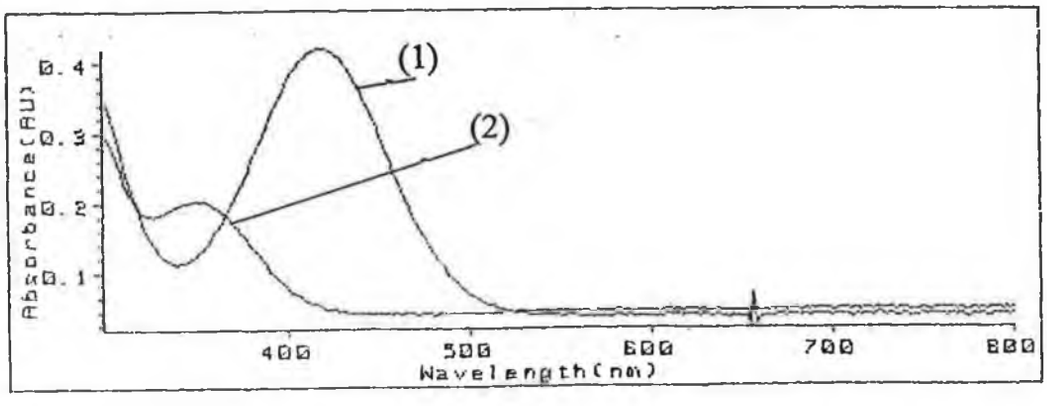

Figure 3.17:- Aqueous phase spectra, of 2 phase experiments in which (1) 2.5 mL of $5x10^{-5}$ M Ligand 1 and 20μL of TDDA were mixed with 2.5 mL of 10^{-2} M $LiClO_{4\,(aq)}$ and (2) where after the two phases had settled, HCl was added to the aqueous phase to give a final HCl concentration of 10^{-2} M.

However, for sensor applications involving the immobilisation of the ligand on a fibre optic cable, leaching of the complex into the aqueous phase is undesirable. In order to try and prevent or reduce this effect, a more lipophilic analogue (Ligand 3) bearing C_{18} groups at the *para* position in place of the *tert*-butyl groups was investigated. Unfortunately, the waxy nature of the product arising from the C_{18} groups precluded the generation of good crystals for confirmation of this molecular arrangement. However, the complexing ability, IR spectra, UV-Vis spectral changes on complexation and lack of aqueous solubility as described below is convincing evidence that the desired compound has been obtained.

Ligand 3 also demonstrated the ability to facilitate cation-transfer from the aqueous phase as illustrated in Figure 3.12c. In contrast to Ligands 1, and 2, no colour transfer from the organic (butan-1-ol) phase to the aqueous phase was noted even at the higher concentrations. From UV-Vis spectra of the aqueous phase at the three highest lithium perchlorate concentrations, peaks at 420 nm were observed with heights less than 5% of the corresponding organic phase peaks(Figure 3.15(c)). This suggests that the substitution of more lipophilic groups on the upper rim of the calix[4]arene for the *t*-butyl groups has the predictable effect of stabilising the molecule in an organic phase. Colour transfer into the aqueous phase was noticed after a few days indicating a slow, gradual leaching of the coloured complex from the organic phase.

3.9 Ligand 4

The final ligand, Ligand 4, of the "nitrophenol" group of chromogenic calixarenes, was different from the previous three ligands in that the chromogenic nitrophenol group was actually part of the central calix[4]arene cavity, rather than a pendent arm as in the other ligands examined.

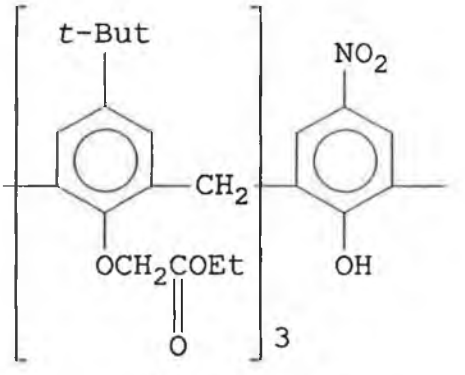

3(v) Ligand 4

3.9.1 Base Optimisation

A 5 x 10^{-5} M solution of Ligand 4 in THF, in the presence of 10^{-2} M $NaClO_4$ was used to examine the variation in absorbance at the deprotonated λ_{max} with varying morpholine concentration. A base concentration in the range 10^{-5} to 10^{-1} M was used. The optimum morpholine concentration for this system was found to be 6 x 10^{-2} M using the method described in Method 2.3.3.

3.9.2 Effect of Metal Ion Concentration Variation (Single Phase)

Method 2.4.1 was followed to examine the effect cation complexation had on the UV-Vis spectrum of this ligand. Figure 3.18(a) and (b) shows the spectra obtained with 5x10^{-5} M Ligand 4 when the $LiClO_4$ and $NaClO_4$ concentrations were incrementally increased from 10^{-6} M to 10^{-1} M in the presence of 6x10^{-2} M morpholine. Figure 3.18 (c) shows the response of Ligand 4 to $KClO_4$ in the concentration range of 10^{-6} to 4x10^{-3} M.

Visually, complexation is signalled by a colour change from colourless to yellow in the presence of morpholine. A very slight colour change to light yellow is observed when the morpholine is added prior to the addition of metal perchlorates . This again demonstrates that equilibrium (**3.5**) is primarily on the left hand side and that the pK_a of the nitrophenol is too high for significant deprotonation by the base morpholine to occur at this point. The subsequent addition of the metal perchlorates initiates deprotonation and a colour change, through the effective lowering of the pK_a of the nitrophenolic proton upon complexation with the metal ion.

From examination of the spectra of Figure 3.18 it becomes apparent that a fundamental difference in the behaviour of this chromoionophore compared to Ligands **1** to **3** exists. A variation in λ_{max} is observed for the three different complexes. The deprotonated form of the Li^+ complex $[L(Li^+)CO^-]$ is seen at 416 nm compared to a λ_{max} of 430 nm for the deprotonated form of the Na^+ $[L(Na^+)CO^-]$ and K^+ complexes. The λ_{max} of the protonated complex of Ligand **4** exists at 330 nm which is 20 nm less than that of Ligands **1** to **3**, and isobestic points are observed at 360 and 370 nm for $LiClO_4$ and $NaClO_4$ respectively. This deviation in λ_{max} is possibly related to a number of factors, with the positioning of the nitro group in relation to the phenol group being of particular significance. In Ligand **4** as was stated earlier the ionisable phenolic group is *para* to the nitro group whereas ligands **1** to **3** it is in the *ortho* position. The nitrophenol chromophores have been found to show variations in λ_{max} i.e. *para* λ_{max} 317.5, ε = 10,000; *ortho* λ_{max} 350, ε = 3,200, [19].

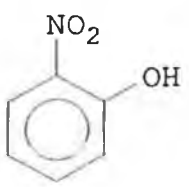

Ortho-nitrophenol
3 (xv)

Para-nitrophenol
3(xvi)

In Ligands **1** to **4** however, the aromatic chromogenic moiety is not simply di-substituted but they also have either one (Ligands **1** to **3**) or 2 (Ligand **4**) carbons of the aromatic rings occupied via their attachment to the calixarene backbone, which can also have an effect on the λ_{max} of the chromogenic group.

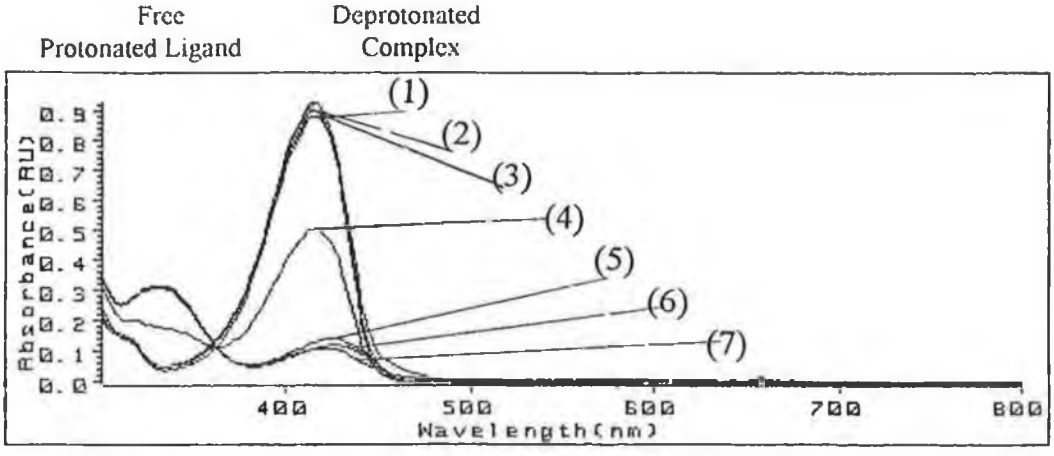

Figure 3.18(a):-Lithium response with Ligand ***4****.*

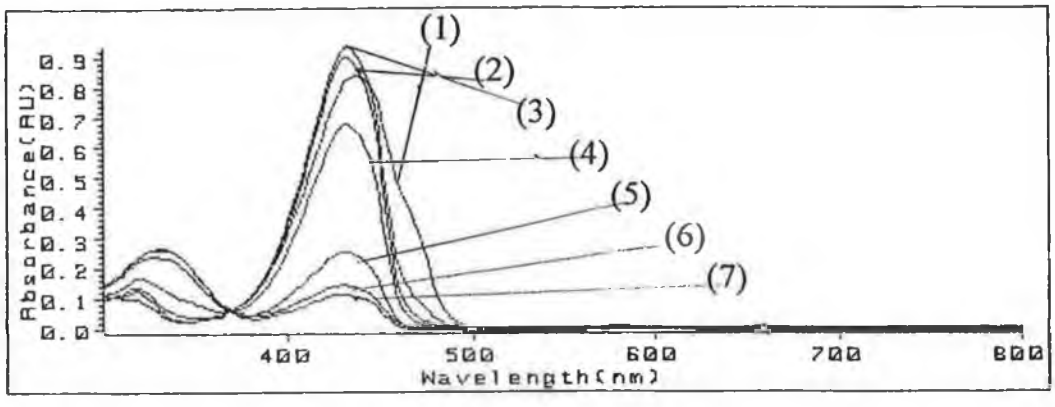

Figure 3.18(b):- Sodium response with Ligand ***4***

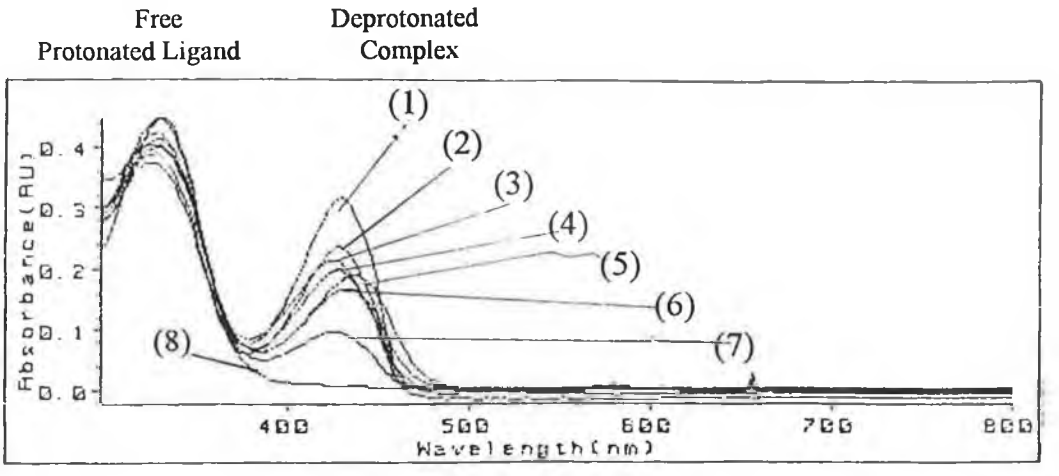

Figure 3.18(c):-Potassium response with Ligand 4

Figure 3.18:- *One-phase investigation of changes in the absorbance spectrum of 2.5 mL of a $5x10^{-5}$ M solution of Ligand 4, with $6x10^{-2}$ M morpholine, upon addition of aqueous (a) $LiClO_4$, (b) $NaClO_4$, with final concentrations of 0.1 (1), 10^{-2} M (2), 10^{-3} M (3), 10^{-4} M (4), 10^{-5} M (5), 10^{-6} M (6) and (c) with final concentrations of $4x10^{-3}$M (1), $2x10^{-3}$M (2), 10^{-3} M (3), 10^{-4}(4), 10^{-5} (5), 10^{-6} (6), 0 M (7), 0 M and 0 M TDDA (8). See table 2.1.*

Another difference in the spectra stems from a spectroscopic change for much lower $LiClO_4$ and $NaClO_4$ concentrations. A comparison of the response of Ligand 4 to the presence of Li^+, Na^+, and K^+ at the λ_{max} of each cation is shown in Figure 3.19. For both $LiClO_4$ and $NaClO_4$ there is a marked increase in absorbance between 10^{-5} and 10^{-4} M salt, with a change in absorbance of approximately 0.65 a.u. between these two concentrations. Above 10^{-3} M there is very little further change in absorbance and a decrease is seen above 10^{-2} M. For $NaClO_4$ the absorbance intensity again increases up to a concentration of 10^{-3} M before it levels off and eventually begins to decrease after a concentration of 10^{-2} M salt had been added. Another λ_{max} shift is observed for the Na^+ complex at 10^{-1} M to 436 nm. The actual form of the Li^+ and Na^+ curves is quite similar with a response to both of the cations occurring at the same concentration. A

limit of detection of less than 10^{-5} M $MClO_4$ exists (where M = Li or Na) indicating almost a 10 fold decrease in L.O.D. over Ligands 1 to 3 for Li^+ and almost a 100 fold decrease in L.O.D. for Na^+. Therefore this ligand at a concentration of $5x10^{-5}$ M is much more sensitive to both cations. Either cation could therefore be detected in the absence of the other at concentrations between ~ 10^{-5} and 10^{-3} M.

This is unlike the situation observed with Ligands 1 to 3 where a response was seen initially for $LiClO_4$ above a concentration of 10^{-4} M but no substantial response was seen for $NaClO_4$ prior to the addition of 10^{-3} M. Where an almost exponential increase in absorbance was then seen.

No clear selectivity can be seen for Ligand 4 between lithium and sodium from these response curves. However, it is clear from the curve for $KClO_4$ that in the concentration range examined there is virtually no detectable interaction between the ligand and K^+. A slight decrease in absorbance is observed but the fact that a variation in baseline is attained at the different concentration levels does cause anomalies in the results and such a small decrease may be attributed to this baseline variation. The lack of an isobestic point may also be an indication of the lack of any equilibrium being set up between the ligand and the potassium salt.

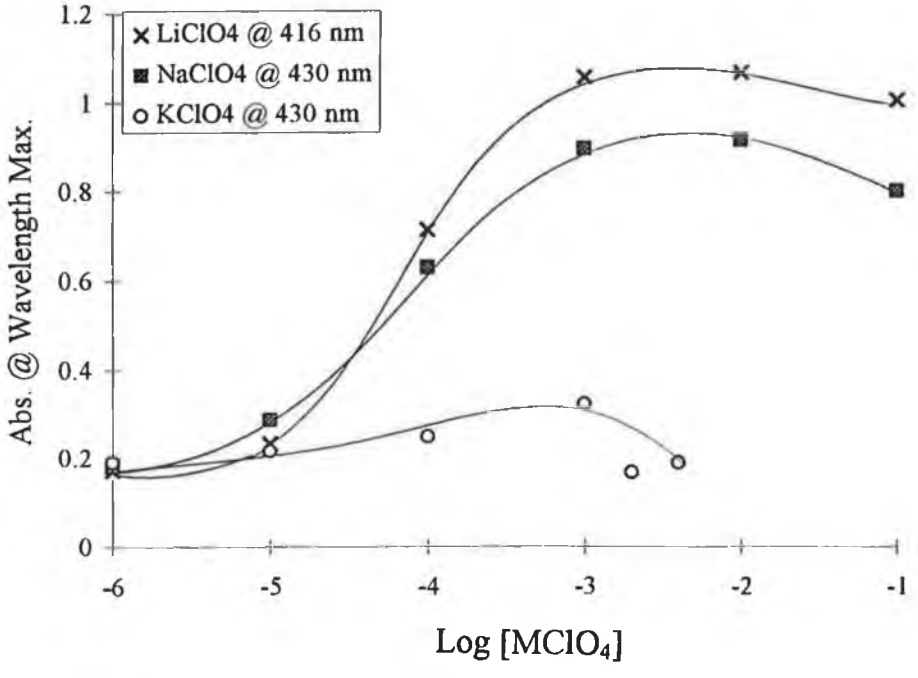

Figure 3.19:- *Comparison of the absorbance at the λ_{max} of the lithium, sodium and potassium metal complexes of Ligand 4, i.e 416 nm for $LiClO_4$ and 430 nm for $NaClO_4$ and $KClO_4$, with data from Fig 3.18 (a), (b) and (c) respectively.*

The difference in λ_{max} between the Lli^{+}-CO^{-} and the LNa^{+}-CO^{-} complexes opens up further possibilities of monitoring for different cations at different wavelengths. Figure 3.20 and 3.21 show the differences in response obtained when measurements for the presence of Li^{+} and Na^{+} were taken at 400 and 450 nm. At 400 nm a clear selectivity for Li^{+} over Na^{+} and K^{+} emerges, (Figure 3.20). These results suggest that it should be possible to use this chromoionophore for either Li^{+} or Na^{+} analysis depending on the wavelength(s) monitored. Furthermore, it may be possible to simultaneously analyse both Na^{+} and Li^{+} by monitoring the wavelength regions where both dominate the absorbance spectrum. In contrast, Figure 3.21 shows that at 450 nm the Li^{+} response is negligible and a sharp increase in intensity is observed for Na^{+} between 10^{-5} and 10^{-3} M. Again K^{+} shows no substantial response at this level.

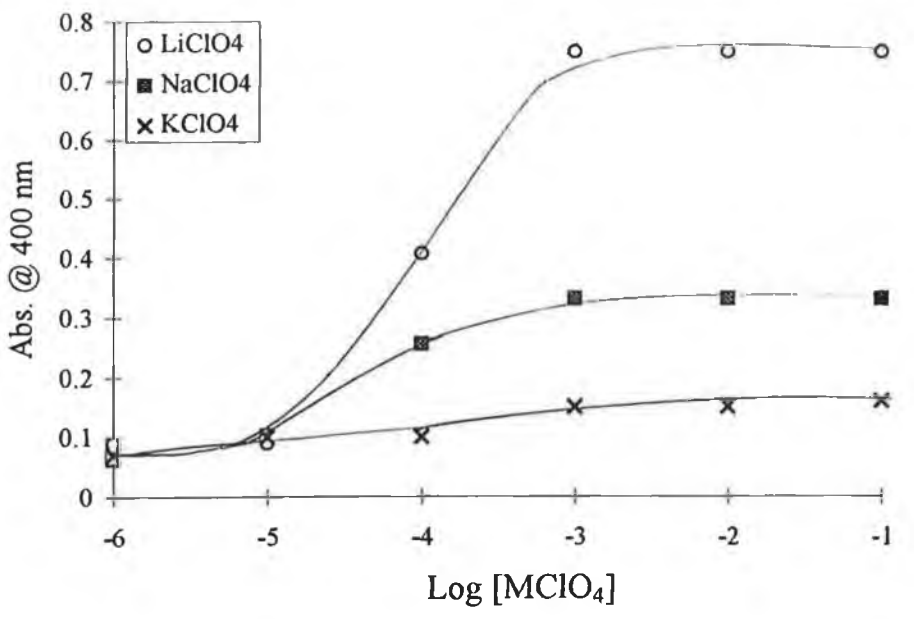

Figure 3.20:- *Comparison of the absorbance of the lithium, sodium and potassium metal complexes of Ligand* ***4****, at 400 nm, with data from Fig 3.18(a), (b) and (c) respectively.*

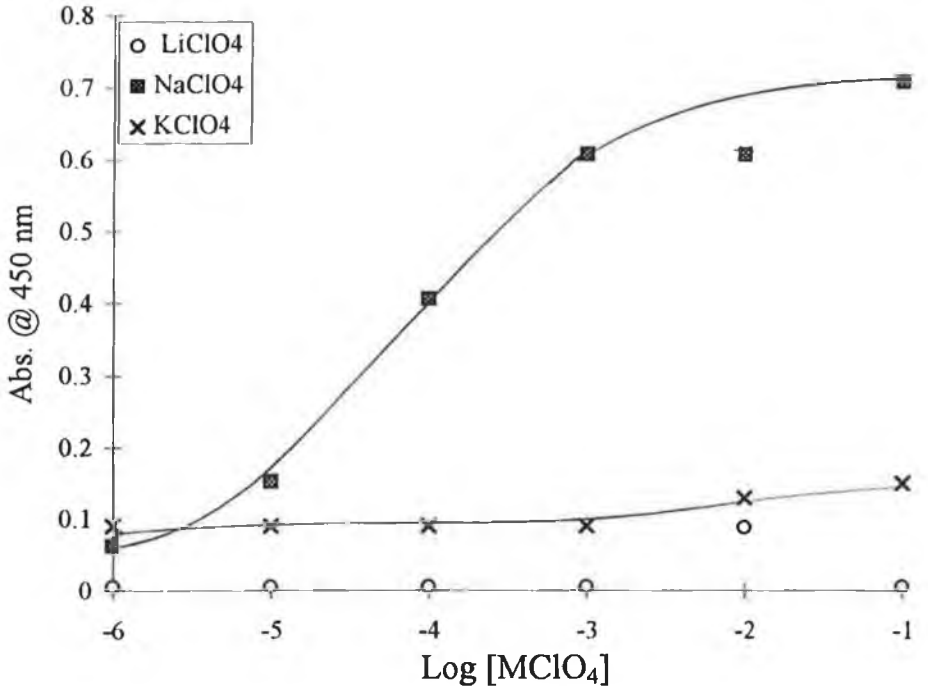

Figure 3.21:- *Comparison of the absorbance of the lithium, sodium and potassium metal complexes of Ligand* ***4****, at 450 nm, with data from Fig 3.18(a), (b) and (c) respectively.*

3.9.3 Interference Studies

Interference studies were carried out in which fixed concentrations of either Na^+ or Li^+ were added to the solutions of the corresponding primary ions. Figure 3.22 shows the spectra of solutions of 10^{-6} to 10^{-1} M $NaClO_4$ in the presence of a constant $LiClO_4$ background of 10^{-3} M. Lithium would appear to be dominating the complexation process up to 10^{-3} M with an absorbance maximum at 416 nm being observed from 10^{-6} to 10^{-3} M $NaClO_4$. Above 10^{-3} M $NaClO_4$ sodium becomes the predominant species of uptake by the ligand with a shift in λ_{max} to that of the sodium complex (430 nm). Again the 0.1M Na^+ sample shows a further bathochromic shift to 436 nm.

When a constant background of Na^+ in the presence of a varying concentration of Li^+ primary ion is examined (Figure 3.23) for standards from 10^{-6} to 10^{-4} M $LiClO_4$ the spectrum is the characteristic spectrum of a 10^{-3} M solution of $NaClO_4$, however above this lithium concentration the compound would appear to be oblivious to the presence of Na^+ and responds solely to the higher concentrations of Li^+ with a shift to the lithium complex λ_{max} at 416 nm A complete exchange of Na^+ for Li^+ would have appeared to have occurred in the

ligand. These interference study results indicate that Ligand 4 is approximately 10 times more selective for Li^+ than Na^+ but for clinical analysis of Li^+ this selectivity would not be sufficient, nor would the fact that both cations respond in a similar concentration range be advantageous.

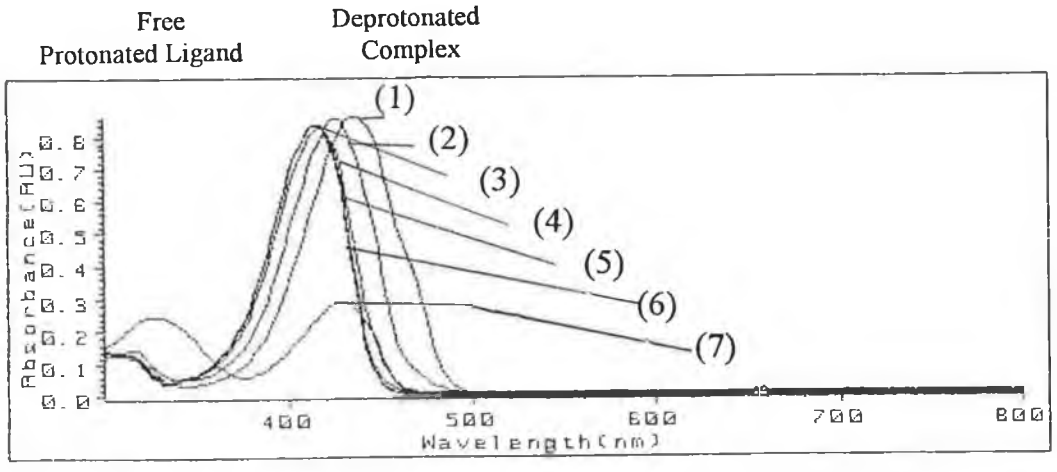

Figure 3.22:- *One-phase studies of the optical response of Ligand 4 ($5x10^{-5}$ M) in THF with $6x10^{-2}$ M morpholine - to additions of 0.1 (1), 10^{-2} M (2), 10^{-3} M (3), 10^{-4} M (4), 10^{-5} M (5), 10^{-6} M (6), 0 (7), $NaClO_4$ in the presence of 10^{-3} M $LiClO_4$.*

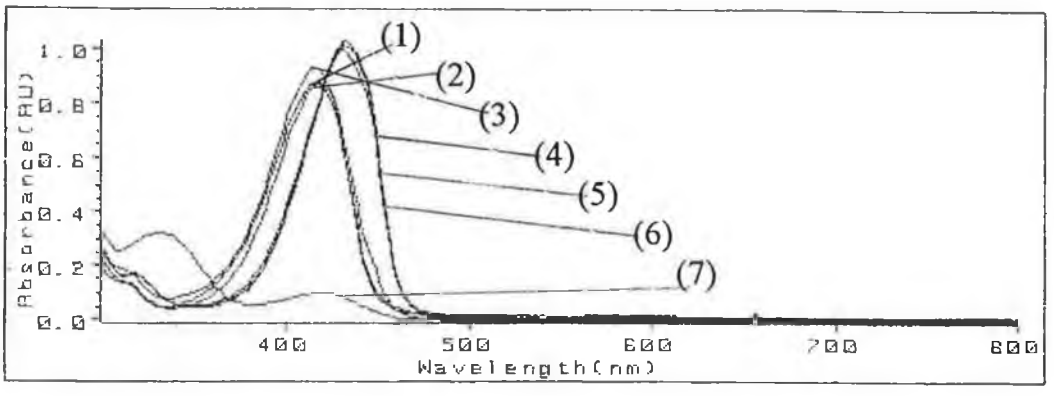

Figure 3.23:- *One-phase studies of the optical response of Ligand 4 ($5x10^{-5}$ M) in THF with $6x10^{-2}$ M morpholine - to additions of 0.1 (1), 10^{-2} M (2), 10^{-3} M (3), 10^{-4} M (4), 10^{-5} M (5), 10^{-6} M (6), 0 M (7), $LiClO_4$ in the presence of 10^{-3} M $NaClO_4$. See Method 2.4.2*

$KClO_4$ was then examined as an interferent. A final concentration of 4 mM $KClO_4$ was examined. This was obtained by the addition of 100 μL of aqueous 0.1M $KClO_4$ to 2.5 mL of $6x10^{-5}$ M Ligand 4. Figure 3.24 shows graphs of abs. at 430 nm vs. log[$NaClO_4$] in a constant background of 0 M K^+ and 4 mM K^+. A reduction in absorbance intensity was noted for all samples containing the 4 mM K^+ interferent and an actual selectivity coefficient could not be calculated. The reduction in intensity at the deprotonated complex λ_{max} when the aqueous $KClO_4$ solution was introduced again highlights the importance the choice of solvent in terms of its polarity or its ability to support ions, has on the components of the system and that it must be carefully considered.

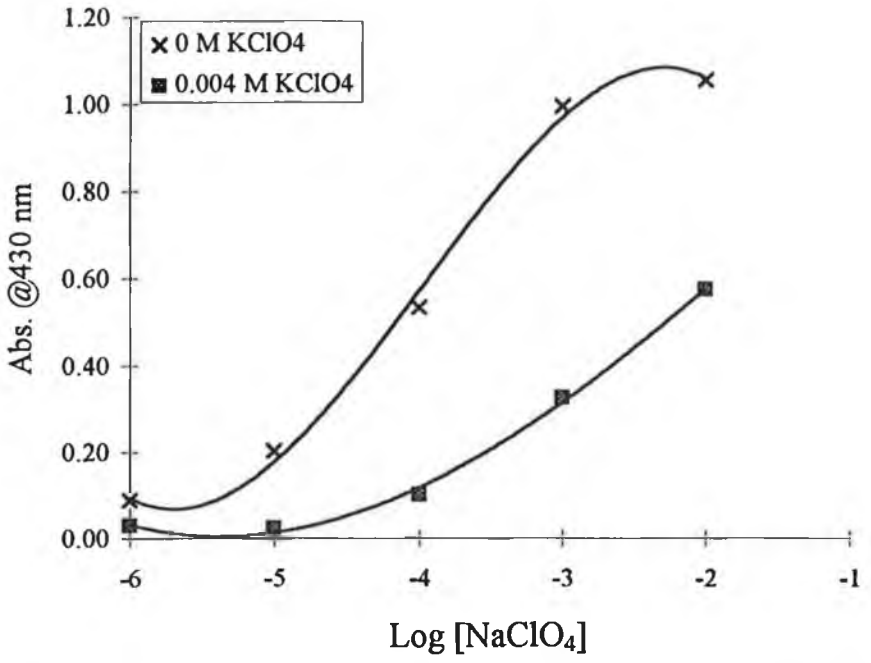

Figure 3.24:- Graphs of absorbance at 430 nm vs. log[$NaClO_4$] in a constant background of 0 M K^+ and 4 mM K^+.

3.9.4 NMR Complexation Study

NMR studies were carried out with Ligand 4 in the presence of varying concentrations of $LiClO_4$, $NaClO_4$ and KSCN. Method 2.4.3 was followed. To a ligand concentration of 25 mM in $CDCl_3$, 0, 0.5, 1.0 and 2.0 mole equivalents of metal salt in CD_3OD were added. The ligand solution at this concentration was yellow and it was observed that upon addition of CD_3OD the colour changed to light yellow. Again this is indicative of the substantial role played by the solvent on colour generation.

The NMR spectrum of Ligand 4 before the introduction of any metal salt was as expected quite similar to that obtained for the triester monoacid [2], another tetrachromogenic molecule with three ester moieties and one acidic group on the remaining aromatic rings, with a quartet observed at 3.3 ppm and a doublet at 4.5 ppm and 4.8 ppm due to the AB system of the methylene protons. The bridging methylene protons of this calix[4]arene cannot be divided into two sets of equivalent protons, i.e H_A and H_B, as was the case with Ligand 1. This is due to the fact that one of the aromatic rings making up the calixarene has an NO_2 group on place of *t*-but in the para position on the upper rim, and an unsubstituted phenol on the lower rim and would be expected to result in a more complex A, B system. A more complicated signal would also be envisaged for the *t*-but protons since, as was stated above, one of the para positions is occupied by an NO_2 group.

Upon complexation with Li^+ a number of peaks are shifted. Figure 3.25 (a) and (b) show the NMR spectra of Ligand 4 upon addition of (a) 0, and (b) 1.0 mole equivalents of $LiClO_4$ respectively. The four peaks at 3.3 ppm are split into 2 distinct doublets with a down-field shift being observed for one of these doublets. Another doublet associated with the AB system of the methylene protons at 4.8 ppm undergoes an upfield shift to 4.7 ppm. A number of peaks due to the aromatic protons also experience down field shifts. No further shifts in peaks are noticed after the addition of a 1 M equivalent of $LiClO_4$ indicating a 1:1 complexation stoichiometry. A similar explanation of the shielding and deshielding effects of the AB system offered for Ligand 1 may also be applied to these observed shifts. (See section 3.8).

Figure 3.26 (a) and (b) show the NMR spectra of Ligand 4 upon addition of (a) 0, (b) 1.0 mole equivalents of $NaClO_4$ respectively. When the ligand is complexed with Na^+, the protons of the methylene AB proton system are again shifted. The shifts observed for the aromatic protons are once again observed, however there is a further upfield shift of the doublet associated with the methylene AB system to 4.5 ppm where it merges with the peaks of the ester CH_2 protons when a 2 mole equivalent of $NaClO_4$ is added. This introduces the possibility that more than a 1:1 stoichiometry exists for the calixarene-Na^+ complex. This however, would be unusual since 1:1 stoichiometry has previously been found for sodium complexes of calix[4]arenes [16]. The continuation of spectral change after a 1 mole equivalent of $NaClO_4$ had been added may be as a result of a solvent effect on the ligand or an ionic strength effect. Previously, it has been shown that

dissimilar solvent affects can occur upon complexation with different cations of the same ligand [24].

For the complexation study with potassium the salt used was KSCN because of the lack of solubility of $KClO_4$ in CD_3OD. Figure 3.27 (a), and (b) show the NMR spectra of Ligand 4 upon addition of (a) 0, and (b) 1.0 mole equivalents of KSCN respectively. Upon complexation with K^+ the quartet remains in the same position, but the doublets at 4.5 ppm and 4.8 ppm are shifted slightly upfield. However there is very little shift in the position of the aromatic protons indicating that there is less interaction between the calix[4]arene and potassium than there was for lithium and sodium. It must be noted that some of the KSCN began precipitating out of solution almost as soon as it had been added to the NMR tube at the 0.5 mole equivalent level indicating a lack of solubility of KSCN in $CDCl_3$ at these levels. The apparent lack of compatibility of K^+ with the calixarene cavity shown in the ^1H NMR signal changes suggests that it is not being encapsulated by the molecule. For both Li^+ and Na^+ at concentrations less than a 1 mole equivalent signals for both the complexed and complexed forms of the AB system are seen in the spectrum, indicating that at room temperature, the exchange rate between the two species is slow on the NMR time scale [16].

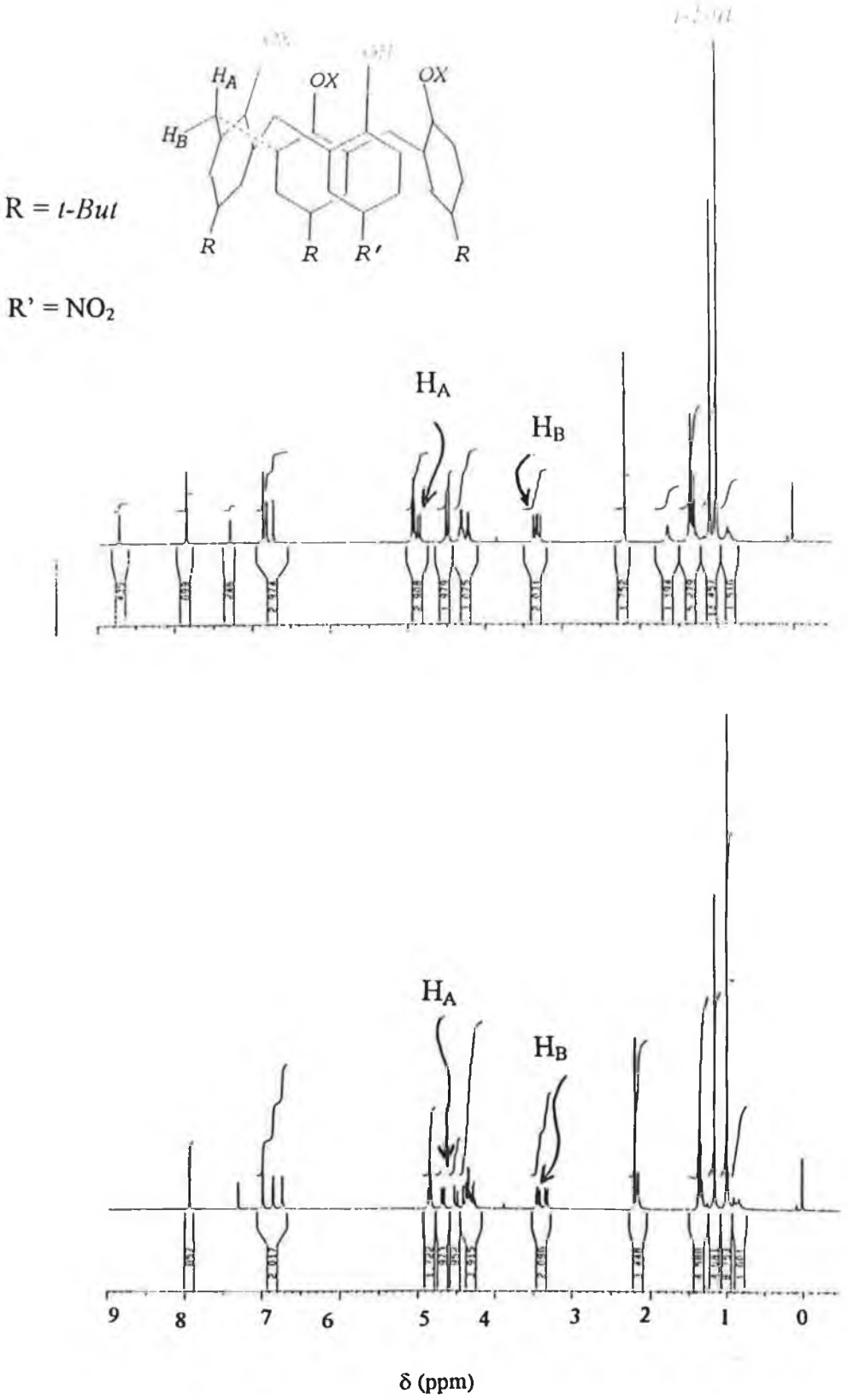

Figure 3.25:- *^1H NMR spectra of the free and complexed form of Ligand* ***4*** *in $CDCl_3$ at room temperature: (a) $[LiClO_4]/[4] = 0$: (b) $[LiClO_4]/[4] = 1$; where $[4] = 5x10^{-3}$ M in $CDCl_3$. An aliquot from 1.0 M solution of $LiClO_4$ in CD_3OD was added directly to a $CDCl_3$ solution of* ***4*** *in an NMR tube. p-tert-butyl H; H_A and H_B $ArCH_2Ar$.*

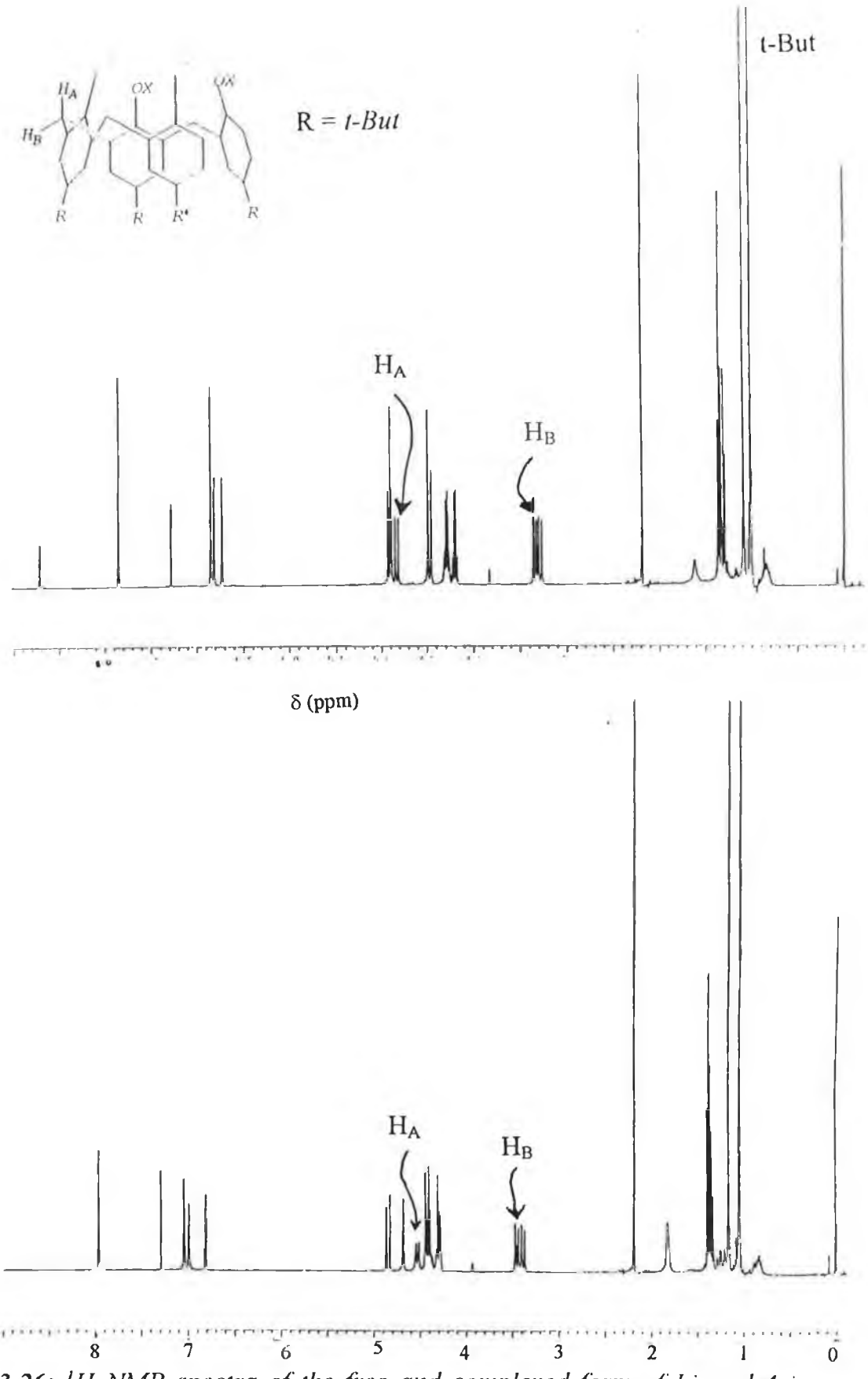

Figure 3.26:- *^1H NMR spectra of the free and complexed form of Ligand* ***4*** *in $CDCl_3$ at room temperature: (a) R = $[NaClO_4]/[4]$ =0: (b) $[NaClO_4]/[4]$ = 1; where [4] = $5x10^{-3}$ M in $CDCl_3$. An aliquot from 1.0 M solution of $NaClO_4$ in CD_3OD was added directly to a $CDCl_3$ solution of* ***1*** *in an NMR tube. p-tert-butyl H; H_A, and H_B = $ArCH_2Ar$.*

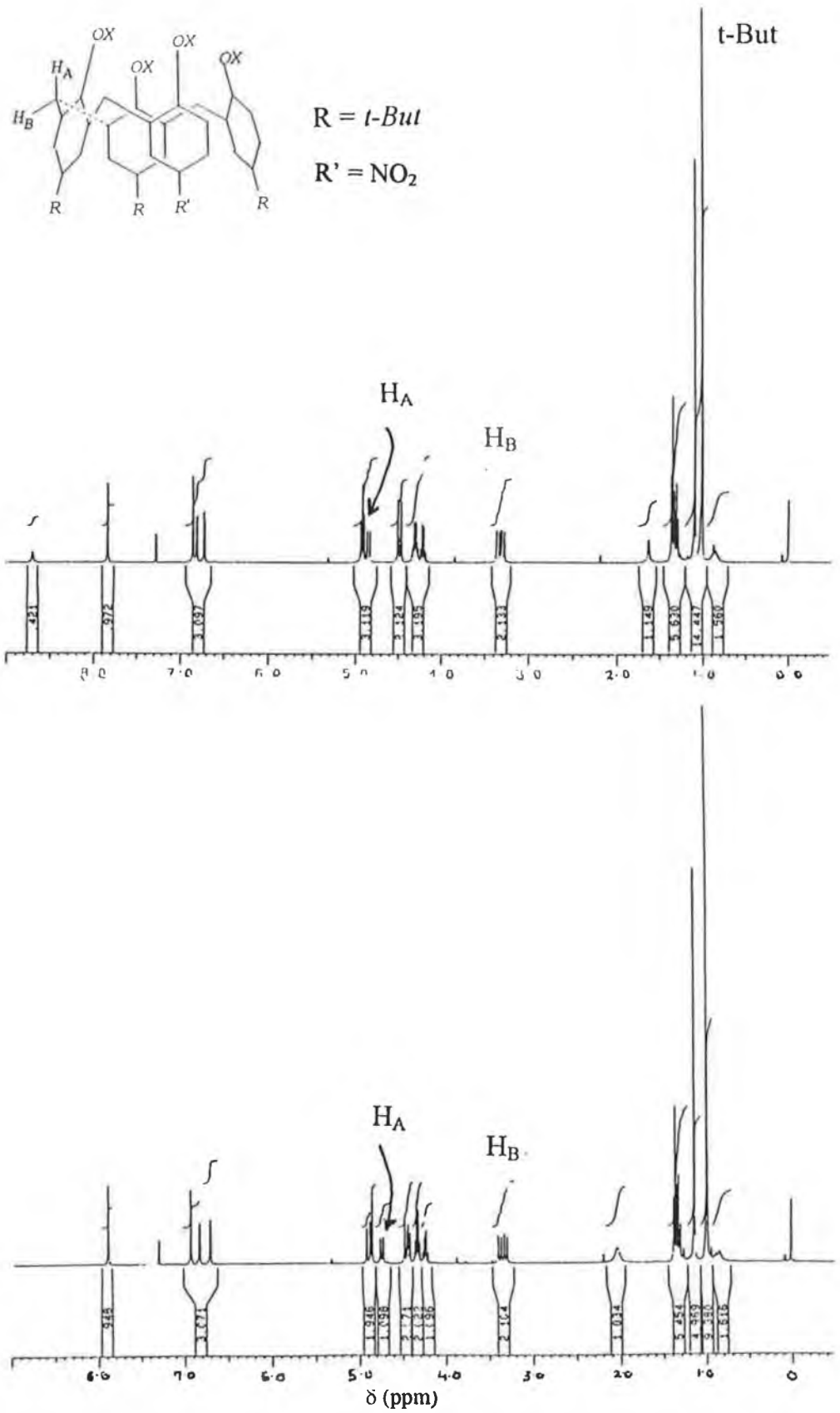

Figure 3.27:- *^1H NMR spectra of the free and complexed form of Ligand* ***4*** *in $CDCl_3$ at room temperature: (a) [KSCN]/[****4****] = 0: (b) [KSCN]/[****4****] = 1; where [****4****] = $5x10^{-3}$ M in $CDCl_3$. An aliquot from 1.0 M solution of KSCN in CD_3OD was added directly to a $CDCl_3$ solution of* ***4*** *in an NMR tube. p-tertbutyl H; H_A and H_b = $ArCH_2Ar$.*

Ligand 4 is capable of complexing both lithium and sodium, with a slightly more selective response for lithium, resulting in a colour change from colourless to yellow in the presence of a lipophilic base. It is more sensitive to both Li^+ and Na^+ than any of the previously examined ligands, Ligands 1 to 3. The λ_{max} for the two different complexes varies from 430 nm for sodium to 416 nm for lithium, which could be an indication of a direct interaction between Li^+ and the phenolate anion of the chromogenic nitrophenol which is making up part of calixarene ring. The presence of 4 mM potassium introduced in aqueous solution decreases the intensity of the colour produced in the presence of sodium indicating that the ligand is highly susceptible to variations in solvent character. At 10^{-4} M potassium there would appear to be no interference by the presence of K^+ on the ligands response to Na^+.

3.10 Discussion

The main features of the four calix[4]arene nitrophenol ligands obtained from the UV-Vis spectroscopy experiments are summarised in Table 3.1.

Table 3.1:- Comparison of the main features of Ligands 1 to 4 obtained by UV-Vis spectroscopy.

Ligand	Conc. (M)	Prot. λ_{max}	Deprot. Cplx. λ_{max}	Li^+ Linear Range (M)	Na^+ Linear Range (M)	Li^+ slope a.u./dec	K_{LiNa} at 10^{-2} M
1	$5x10^{-5}$	350 nm	424 nm	10^{-4}-$5x10^{-2}$	10^{-4}-10^{-2}	0.325	25.1
2	$7x10^{-5}$	350 nm	424 nm	10^{-4}-10^{-2}	—	0.250	34.7
3	$5x10^{-5}$	350 nm	424 nm	10^{-4}-$5x10^{-3}$	—	0.900	43.1
4	$5x10^{-5}$	330 nm	416 (Li^+) 430 (Na^+)	10^{-5}-$5x10^{-3}$	10^{-5}-10^{-3}	0.420	~ 10

From these results it can be seen that ligands 1 to 3 which have either one or four chromogenic nitrophenol moieties in which the ionisable phenolic group is ortho to the nitrogroup, all give similar spectral responses. No variations exist between protonated and deprotonated λ_{max} values between the monochromogenic Ligand 2 and the tetrachromogenic Ligands 1 and 3. They each have a protonated λ_{max} at 350 nm and a deprotonated complex λ_{max} at 424 nm.

Cause of Colour

The λ_{max} of both the protonated and deprotonated complex are synonomous with nitrophenol and subsequent nitrophenolate anion production under sufficiently basic conditions. Colour changes or bathochromic shifts in λ_{max} with nitrophenol chromogenic moieties were confirmed as long ago as 1949 by Coogeshall et al [20] to be due to the formation of the phenolate anion if the pH of the solution in which they were housed was increased sufficiently. A subsequent increase in acidity was found to result in a regeneration of the original colour (colourless). Similarly with all of the chromogenic ligands described here, an introduction of an acid such as HCl into the ligand-metal-base solution resulted in a return to a colourless solution. The yellow colour could be restored by subsequent addition of a base. Therefore the main cause of colour change with these calix[4]arenes, (Ligands 1 to 4) bearing nitrophenol chromogenic moieties is through proton exchange at the chromophoric group.

Mode of Complexation

The variation in intensity observed with the different cations for Ligands 1 to 3 seen in section 3.4, is most likely to be related both to cation size and to the effect each cation has on the chromogenic moieties. The processes described in equilibria **(3.1)** and **(3.3)** are responsible for colour generation. The equilibrium in equation **(3.1)** will proceed to the right i.e. formation of the complex, if the cation is capable of efficiently entering the calixarene, or simply if the ligand is a good ionophore. Therefore both equilibria combined give the observed stability constant of the system. The overall reaction from equations **(3.1)** and **(3.3)** is

constant of the system. The overall reaction from equations **(3.1)** and **(3.3)** is therefore the product of the stabilities of both the complexation and deprotonation reactions

$$L\text{-}COH + M^+ + B \rightleftharpoons LM^+CO^- + BH^+ \qquad \textbf{(3.8)}$$

$$K_{st} = \frac{[LM^+CO^-]\,[BH^+]}{[L\text{-}COH]\,[M^+]} \qquad \textbf{(3.9)}$$

This stability constant can be calculated using equation **(3.9)** assuming that the base concentration is effectively constant because it is present in a large excess. The pH of the system is of great importance since spontaneous phenolate anion production is undesirable. Under the conditions used in this research, the equilibrium in **(3.5)** is predominantly on the left i.e. prevention of phenolate anion production in the absence of metal, since no colour change or only a very slight colour change is observed upon addition of morpholine to the solutions in the absence of metal. The base on its own in the aprotic solvent THF is not strong enough to cause deprotonation.

Upon addition of a suitable metal-ion (e.g. Li^+), the value of β (Eqn. **3.2**) is sufficiently large to ensure that the equilibrium in **(3.1)** forced to the right encouraging metal ion inclusion in the calixarene cavity. Once the metal cation (Li^+ or Na^+) is introduced into the system deprotonation is seen almost instantaneously, indicating that the equilibrium in equation **(3.3)** is also forced to the right. This is indicative of the introduction of the positively charged metal ion into the ligand cavity effecting a lowering of the pK_a of the ionisable phenolic group which makes proton removal easier.

In the event that a cation, such as potassium, which is not efficiently taken up by the ligand, the population of complexes will be small and the equilibrium in **(3.1)** will not favour the right hand size, resulting in a very low β value. The lack of interaction or colour change with K^+ may be due to a size restriction of the hydrophilic cavity, which excludes complexation with this cation.

However, when the ionophore is capable of interacting with a cation (such as is the case with Li^+ and Na^+) the effect exerted by the cation on the chromophore becomes very important to the overall picture. The cation which effects the chromophore to the greatest extent should show an earlier response (i.e. at lower

concentrations). The pK_a of the dissociating protons of ionisable chromophores has previously been shown to be affected to different extents by the presence of different cations. Czech et al [21] found with chromogenic cryptaspherands, which had been prepared as their sodium bromide complexes, that a decrease in pK_a value of the compounds occurred on complexation with K^+ i.e. 8.27 to 6.58 $\pm$ 0.15, with values obtained in diethylene glycol monoethyl ether (DEGMEE). No values were obtained for uncomplexed molecules since sodium was present during synthesis, and the ligand was hence obtained as the Na^+ complex.

A difference in pK_a values was also observed for complexation with different cations [22] for chromogenic spherands. The pK_a of the phenolic proton of the dinitrophenylazophenol changed from 6.9 for the Na^+ complex to 5.9 for the Li^+ complex which displayed superior extraction ability. These measurements were carried out in 80% dioxane, 20% water at 30 $\pm$ 2° C. pK_a measurements were calculated using a pH titration. With Ligands **1** to **3**, the dissociating phenol is not actually making up part of the hydrophilic cavity but an interaction between the cation and the ionisable chromogenic moiety is possible (as will be discussed below) and a similar pK_a variation is attributed to the colour generation in this work. An example of an ionisable chromophore positioned more than a single bond away from the ionophoric part of the molecule is described by Takagi et al [23]. Alkali metal-ion selectivity in this system is dependent on two critical factors

i " size selectivity" by the crown ether macrocycle and

ii the coordination interaction or the ion-pair interaction of the anionic site of the deprotonated phenol with the crown ether-bound metal ion.

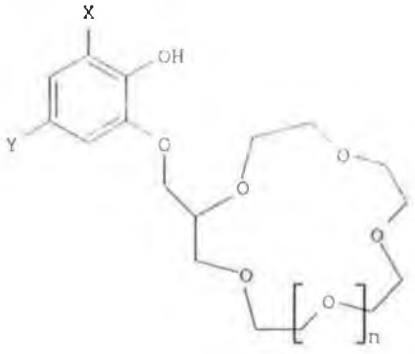

X = NO_2 Y =

3(xv)

Crown compound bearing ionisable chromoionophore [23].

So overall complexation occurs as follows

1. Compatible cation inclusion → pK_a change
2. Lowering of pK_a → phenolic proton exchange with suitable base.
3. Variation in pK_a change caused by different cations → Selectivity.

It is not clear as to whether one or more of the chromogenic moieties is being deprotonated in the two tetrachromogenic ligands examined, (Ligands 1 and 3). This will depend on the nature of the interaction between the Li^+ or Na^+ cations and the actual chromogenic ligands. The cations may not be within contact distance or may not interact to the same extent with all four of the chromogenic groups of the tetrachromogenic ligand. The higher initial absorbance of both of these compounds in the free protonated form compared to Ligand 2 is not surprising, since they each contain three extra chromogenic moieties which will add to the overall absorbance seen. The same overall spectral forms are observed for varying Li^+ concentrations for the tetra and monochromogenic ligands in terms of an approximate doubling of intensity or ε on going from the protonated absorbance maximum to the deprotonated absorbance maximum seen for the complex obtained when 0.1 M $LiClO_4$ had been added. This may be an indication that the presence of a similar deprotonation process for both types of ligand i.e. only one deprotonation is occurring. A second deprotonation, with delocalisations of the negative charges over the chromogenic π systems however, cannot be ruled out. The determination of the pK_a of each individual phenolic proton of the tetrachromogenic ligands may lead to more conclusive information on this point (eg. by non-aqueous titration).

Interaction of Cations with the Chromoionophores

Ligands 1 to 3 of the new chromogenic calix[4]arene tetraesters were found to exhibit a slight Li^+ over Na^+ selectivity with a much lower concentration of $LiClO_4$ required to see the response than for $NaClO_4$, whereas Ligand 4 exhibited a strong response to both Li^+ and Na^+ perchlorates between 10^{-5} and 10^{-3} M. Neither ligand showed any significant response to K^+.

The exact nature of the interaction, or the effect the Li^+ cation has on the chromogenic moiety is not known since no crystals of either the ligand or its complex could be obtained for x-ray crystal analysis. However, from preliminary molecular modelling, a model of Ligand 1 was obtained using Hyperchem,

structure **3(xiii)**. The distances between the carbonyl oxygens,(C=O) [see *(1) in* **3(xiii)**], which have previously been considered to make up part of the hydrophilic cavity capable of encapsulating cations [2], and the carbon (C) [see *(2) in* **3(xiii)**] of the chromogenic aromatic ring bonded directly to the ester groups of the calix backbone were estimated to be between 3.6 and 4.14 A. From these values it is conceivable that the inclusion of a positive charge in the cavity made up of the four phenolic oxygens of the calixarene and the four carbonyl oxygens will exert an effect on the π system of the chromogenic moiety which translates into an alteration of the pK_a of the labile phenolic protons. Atomic distances of this order of magnitude have previously been found to be sufficient for the inclusion of a cation by electrostatic interaction to occur. Arnaud-Neu et al found phenolate O---O intramolecular contacts to be between 3.03 and 5.16 A for a calix[4]arene tetraester molecule, and this was found to be sufficient for sodium cation inclusion [2].

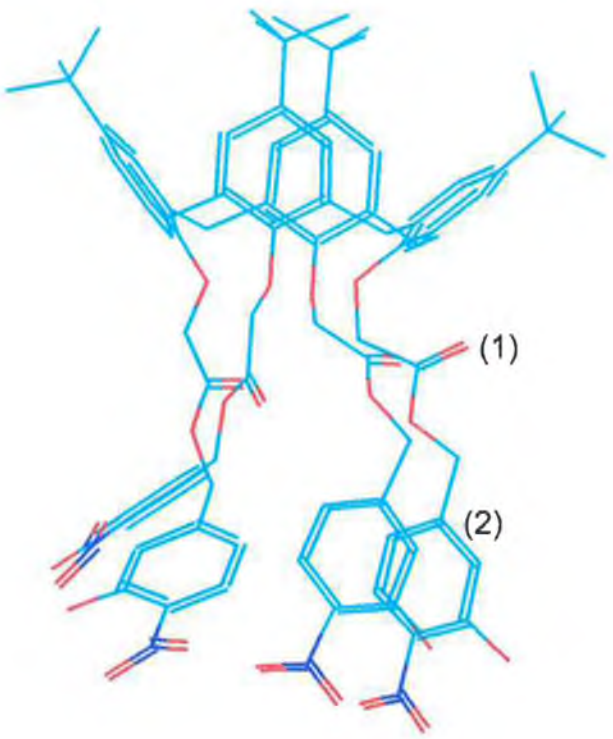

3(xiii)

Molecular model of Ligand 1 obtained using Hyperchem.,

Light Blue = C-C bonds

Red = Oxygen atoms

Dark Blue = Nitrogen atoms

Interaction between the cation and the chromogenic moiety may also occur via an interaction between the phenolic oxygen of the chromogenic moiety and the eight oxygens of the hydrophilic cavity or with the ethereal oxygens. An atomic distance of between 5.30 and 6.07 A was estimated from Hyperchem, to be between the ionisable phenolic oxygens of the chromogenic moiety (OH) [see *(3) in* **3(xiii)**] and the corresponding ethereal oxygens (O) [see *(4) in* **3(xiii)**]. These ethereal oxygens have previously been found to take up a position exo to the hydrophilic cavity made up of the carbonyl and aromatic oxygens of the pendent ester groups which has been found to encapsulate alkai metal cations on complexation [2, 17, 24]. The neutral uncomplexed ligand may show some electrostatic interaction between the hydrophilic cavity and the phenolic groups of the chromogenic nitrophenol. However, since we are dealing with essentially neutral molecular components and the energy of interaction of two neutral molecules due to Van Der Waals forces falls off as R^{-6} [25], (where R is their separation), any such interaction can be predicted to be insignficant. With the inclusion of a positive charge i.e. Li^+ or Na^+ cation, the possibility of an electrostatic interaction arises. Ions can interact over much longer distances than neutral atoms with electrostatic interactions falling off only as R^{-2}. Therefore, an electrostatic interaction between the positively charged cation and the phenolic group of the chromogenic moiety becomes possible. Rotation about the -O-CH_2-[C*-OH] bonds (where C*-OH symbolises the chromogenic nitrophenol), on Li^+ inclusion may reduce the distance between the ionisable phenolic oxygens and the hydrophilic cavity, with any such interaction having the effect of reducing the pK_a of the phenolic proton, through a direct interaction with the chromogenic π system. An interaction between the positively charged Li^+ almost certainly occurs with the π electron systems of the nitrophenol chromogenic moieties, (the distance estimated to be 3.6 and 4.14 A), and thereby stabilising the negatively charged phenolic oxygen of the chromophore by drawing charge density towards the positive charge. This effectively causes a delocalisation of the negative charge over the π system.

The overall energy of both the ligands and their deprotonated complexes can be described in terms of Gibbs free energy $-\Delta G^o$. The more negative the value of $-\Delta G^o$ the more stable the complex. Bohmer et al. [26] stated that in their work with structure **3(xvi)**, the pK_a values were a reflection of the difference in Gibbs free energy between the protonated molecule and the deprotonated monoanion of

the monochromogenic calix[4]arene. If both are stabilised to the same extent, no change in pK_a value occurs.

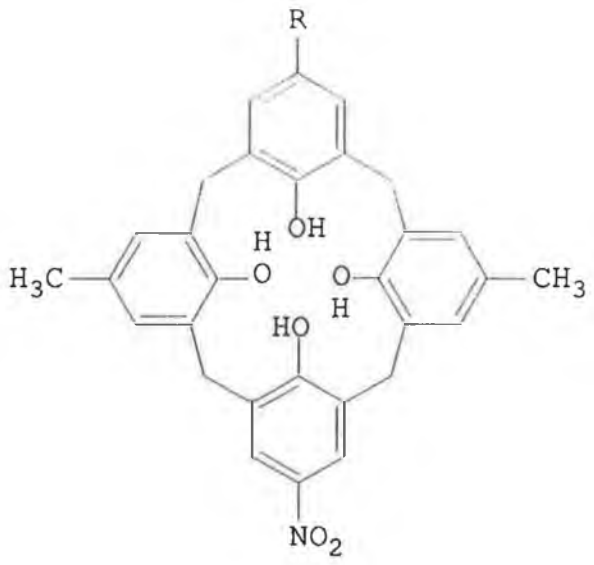

1 R = CH_3

2 R = $C(CH_3)_3$

(xvi)

Calix[4]arene mononitrophenol [26]

In Ligands **1** to **4**, the fact that phenolic dissociation does not occur in the presence of morpholine but does once a cation is included is indicative of an increase in the $-\Delta G^o$ value or a decrease of the energy of the whole system occurring with cation inclusion. The whole system favours a reduction in total energy or a stabilisation in energy occurs when the molecule returns to an overall a neutral state following metal-ion complexation, caused by the deprotonation of the chromophore.

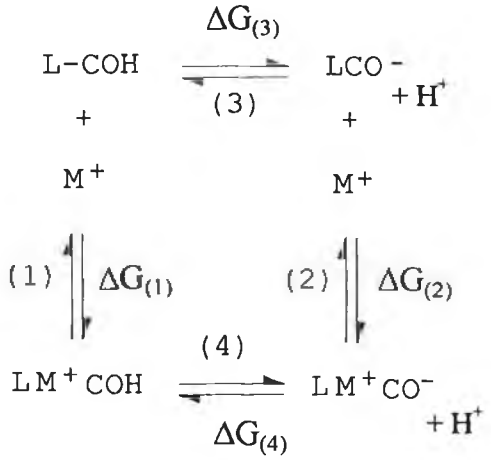

$\Delta G_{(2)}$ more negative than $\Delta G_{(1)}$

$\Delta G_{(4)}$ more negative than $\Delta G_{(3)}$

In energy terms, it would be predicted from the experimental evidence, that $\Delta G_{(4)}$ has the most negative value and that the production of the deprotonated complex is favoured in the presence of a suitable base.

Confirmation of Complexation

Equilibrium (**3.1**) i.e. where the ligand takes up the metal ion, must occur in order for a lowering of the pK_a of the chromogenic moiety to occur. The ability of the ligand to take up Li^+ or Na^+ cations in the absence of a base was demonstrated by 'H NMR spectroscopic experiments (Figure 3.13). The ^1H NMR complexation studies with NaSCN, revealed an ordering of the distorted cone conformation upon complexation with Na^+. Although the assignment of peaks in the NMR spectra was difficult due to their complex nature, it was clear that the introduction of Na^+ resulted in shifts in the position of a number of peaks. More ordered symmetry on complexation was confirmed by a simplification of the spectrum of the *t*-butyl hydrogens, which after complexation to exist in an equivalent environment, as shown by the singlet at 1.0 ppm. Molecular dynamics results along with x-ray crystal data for calix[4]arenes bearing both phenolic and carbonyl oxygens on the lower rim concur with the ^1H NMR results. Molecular dynamics work [24] with a calix[4]arene tetraamide suggested that the hydrophilic part of the molecule is not well preorganised for complexation in solution but rearrangement to a more rigid structure occurs on complexation at the lower rim.

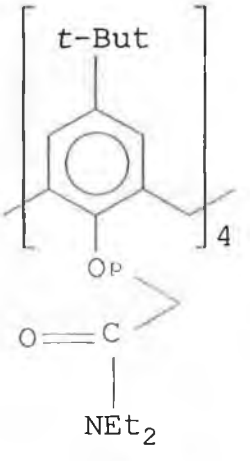

3(xi)

Top-bottom coupling i.e. between the upper hydrophobic part of the molecule and the lower hydrophillic portion, in the LLi^+ complex (where L is the ligand) was described. The rigidness of the hydrophillic part leads to the most asymmetrical cone, where two opposite *tert*-butyl groups are on average much closer (5.7) A than in the other LNa^+ and LK^+ complexes (9.5-9.7) A. This indicates that the whole molecule has become more ordered on complexation

with different cations conferring different degrees of order depending on how well it fits the cavity. It also indicates that the ordering or reduction in mobility of the hydrophilic part of the molecule caused by cation inclusion affects the whole structure. The ^{1}NMR spectra obtained for Ligand **4** with Li^+, Na^+, and K^+, concur with this explanation since the H_A and H_B protons along with some of the aromatic protons were found to shift by varying amounts, depending on the complexing cations. The smallest shifts were observed for K^+, which is generally considered to be too large to complex with the calix[4]arenes.

Calestani et al [17] reported the x-ray crystal structures of a calix [4]arene tetraacetamide in both its free and complexed states, **3(xii)** and **3(xvii)**.

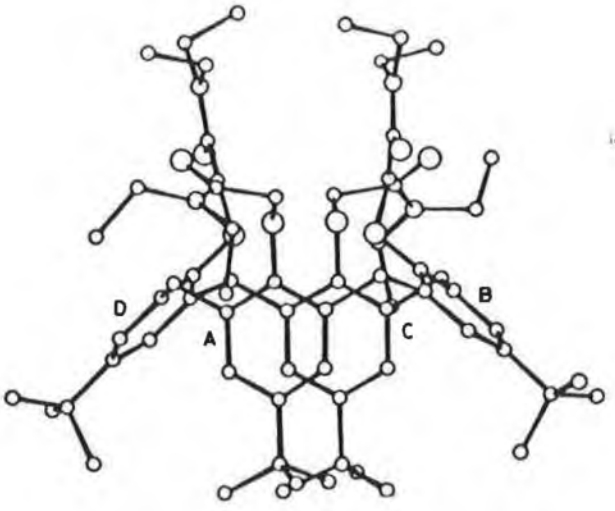

3(xii)

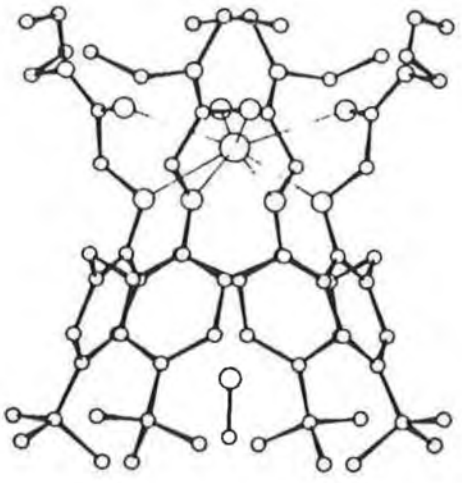

3(xvii)

The conformation of the four amide chains in the complex was found to be more symmetrical than that of the free ligand. In addition to this increase in symmetry of the hydrophilic part of the moiety upon complexation it was found that the aromatic hydrophobic part of the molecule was also affected. In the free ligand, as was previously stated, two opposite aromatic rings (A, C) are almost parallel to each other, and the other two (B, D) are almost perpendicular. After complexation, the dihedral angles between the aromatic rings and the plane of the methylene groups are all equivalent. This is again indicative of complexation conferring a more ordered structure on the calixarene molecule.

Effect of Solvent

The choice of solvent was found to be very important as the comparison of spectra between Ligand 1 in THF and MeOH illustrated (Figure 3.10). The effect a variation of solvent has on the acidity of solute molecules is well known. Methanol is an amphiprotic polar solvent with a dielectric constant of 32.63 [3] and a pK_a of 15.5 [27]. THF on the other hand has a much lower dielectric constant of 7.6 and would be classed as an aprotic protophillic solvent or in other words it has some basic properties but is a non-ionisable solvent [28].

Two parameters are important in assessing the cause of the substantial deprotonation of the ligand in methanol. Firstly the acid-base character of the methanol itself and secondly, its ability to facilitate deprotonation of the ligand by morpholine must be assessed. Morpholine is a stronger base than MeOH, and therefore methanol will not have the ability to deprotonate the ligand on its own. This is seen in spectrum (7) of Figure 3.10(b), where no deprotonation occurs when the ligand is dissolved in MeOH in the absence of a base.

Therefore we can conclude that the acidity of the solvent is not the property of methanol which is resulting in a much greater level of deprotonation in the presence of morpholine. The next property to look at is the polarity of the solvent where MeOH has a dielectric constant of 32.63. This value is much greater than the value of THF i.e. 7.6 and therefore methanol is much more capable of supporting the existence of ions than THF. The K_a in equation **(3.6)** will be enhanced as a result of this increased polarity and a colour change is seen even in the absence of metal-ions.

THF with its low dissociating abilities cannot sustain the presence of ions as well as methanol. The presence of morpholine in the Ligand-THF solution cannot force the equilibrium of equation **(3.5)** to the right sufficiently for a colour change to be observed in the absence of metals. So the THF-morpholine mixture is more discerning to changes in $LiClO_4$ concentrations.

The hypsochromic effect observed on going from THF to methanol is again an illustration of the effect a solvent variation has on the system, a point alluded to previously by Misumi et al [8]. This indicates that not only must the base be carefully chosen so as spontaneous deprotonation in the absence of the metal ion does not occur **(3.5)** but the medium in which all of the components are situated is also crucial to controlling the direction of this equilibrium. The effect of the

solvent on the basicity of the base used, or the ionising ability of the system cannot be neglected if a clear spectral difference is going to be obtained over the relatively large range of metal ion concentrations observed with the ligands in THF i.e 2 to 3 orders of magnitude. Further optimisation studies of both base and solvent are clearly needed in order to investigate whether the linear range, LOD or selectivity can be improved.

At an electronic level the hypsochromic λ_{max} shift on increasing the polarity of solvent from THF to methanol suggests that the peak produced for the deprotonated ligand is due to an $n \rightarrow \pi^*$ transition as there is electrostatic interaction between polar solvents and polar chromophores such as the nitrophenol groups. These solvents tend to stabilise both the non-bonding electronic states and the π^* excited states, causing the $n \rightarrow \pi^*$ transitions to move to higher energy [12]. However, the λ_{max} change is quite small i.e. 6 nm and therefore conclusive proof of one sort of transition over another i.e. $n \rightarrow \pi^*$ or $\pi \rightarrow \pi^*$, is not available. The high intensity or extinction coefficient of the peaks observed in this work is generally associated with $\pi \rightarrow \pi^*$ transitions which are allowed transitions compared to the $n \rightarrow \pi^*$ transitions which are considered to be forbidden and therefore exist as peaks of low intensity [29].

Two-Phase Experiments

The two phase experiments yielded some interesting results. Ligands **1** to **3** were all found to be capable of extracting metal cations from an aqueous phase into an organic phase (butan-1-ol) in which the ligand and the lipophilic base TDDA were dissolved. However, the zwitterionic nature of the deprotonated complex appeared to facilitate diffusion of this otherwise water insoluble ligand into the aqueous phase. The replacement of the *t-butyl* groups in the *para* position of the calixarene backbone by long chain C_{18} groups i.e. Ligand **3** was found to reduce this phenomenon considerably by making the ligand much more lipophilic overall. pH variations of the aqueous phase were found to affect the solubility of both the protonated and deprotonated complexes and further studies of switching solubility of the different components are warranted.

Ligand 4

In Ligand **4** the ionisable phenol is part of the calixarene cavity itself (see **3(xviii)**), and which is *para* to the electron withdrawing nitro group rather than *ortho* as with Ligands **1** to **3**. From work on simple *para* nitrophenols, it would be predicted that this chromogenic moiety would absorb at wavelengths of higher energy than the *ortho* nitrophenol [19]. The fact that the dissociating phenol is part of the hydrophillic cavity which is deemed to be responsible for cation uptake [2] is an initial indication that a different process is going to be involved for complexation. Bohmer et al. [26] found a phenomenon occurring with **3(xvi)** which was similar to that which was observed in this work. A hypsochromic shift in λ_{max} of approximately 20 nm is observed on going from complexation with Na^+ to Li^+ . Bohmer et al. attributed this to a possible Li^+ phenolate interaction occurring which they declare is not possible for the less charge dense Na^+ or K^+, although a response is observed for both. So with Na^+ an electrostatic interaction with the phenolic oxygen and the remaining carbonyl and aromatic oxygens is most likely to be the cause of the UV-Vis changes. With Li^+ a coulombic interaction occurs with the phenolate anion of the chromogenic nitrophenol, which makes up part of the calixarene backbone, accompanied by electrostatic interactions with the above mentioned oxygens, thus reducing the ease with which an electron can be moved from its π or n level up to a π^* level and this is seen as a hypsochromic shift. A similar phenolate interaction resulting in a hypsochromic shift was observed for the interaction between Ca^{2+} and a chromogenic crown ether [7]. Ca^{2+} like Li^+ has a high charge density and therefore interaction with these cations and a phenolate anion of a chromogenic moiety sited in the hydrophilic cavity is thought to be possible. Such an interaction with the phenoxy ion of Ligands **1** to **3** is not thought to be possible due to the remoteness of the ion from the central hydrophilic cavity into which the cation is likely to fit **3(xix)**.

This λ_{max} variation between different complexes offers the possibility of multi-wavelength analysis for determining the presence of either Na^+ or Li^+ in a sample. Figures 3.20 and 3.21 demonstrated that at 400 nm a selective response to Li^+ can be obtained with very little response to Na^+, whereas at 450 nm Na^+ can be determined with a little response to Li^+, and neglible response to K^+.

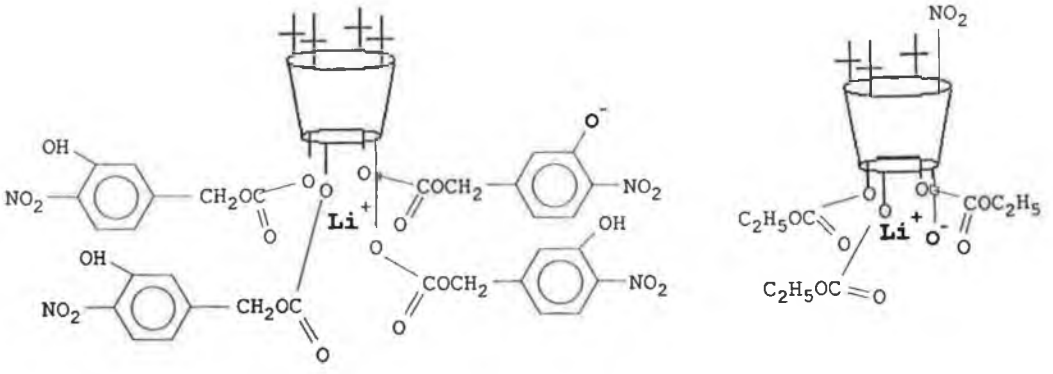

3(xviii) **3(xix).**

Representation of the relative positions of the cation and anion after complexation and deprotonation with Ligand 1, (3(xviii)), and Ligand 4, (3(xix)).

3.11 Conclusion

Four novel chromogenic calix[4]arenes have been examined and the following charcteristics have been found:

- A colour change from colourless to yellow occurs, upon complexation with Li^+, or Na^+, and to a lesser extent K^+, in the presence of a suitable base, with the intensity of the colour being cation concentration dependent.
- Ligands 1 to 3 display between a 10 and 50 fold Li^+ selectivity over Na^+, whereas Ligand 4 shows a similar response to both cations, but a variation in λ_{max} between the two complexes can be used as a means of indentifying the presence of either cation in a simple one cation solution.
- In the presence of a suitable base i.e. TDDA or morpholine, no colour change is seen in the absence of the complexing metal ion. Complexation has the effect of lowering the pK_a of the dissociating proton of the phenolic group of the chromogenic moiety.
- Complexation occurs in the absence of a base but no change in colour is produced. This was demonstrated by ^1H NMR spectroscopy which revealed shifts in the position of certain protons in the spectrum which have previously been determined to be synonomous with cation complexation.

- Ligands 1 to 3 were found to be capable of extracting Li^+ cations from an aqueous phase into an organic (butan-1-ol) phase. Subsequent leaching of the colour due to the complexed form into the aqueous phase was attributed to the zwitterionic nature of the deprotonated complex. This phenomenon was reduced in the case of Ligand 3 which had bulky C_{18} groups in the *para* position of the calixarene backbone which rendered the molecule more lipophilic and thus stabilised it in the lipophilic organic phase.

3.12 References

1. C.D. Gutsche, (edt.) "*Calixarenes*", Monographs in Supramolecular Chem.,Vol. 1, R.S.C, Cambridge, (1989).
2. F. Arnaud-Neu, E.M. Collins, M. Deasy, G. Ferguson, S.J. Harris, B. Kaitner, A.J. Lough, M.A. McKervey, M.J. Schwing-Weill and E.M. Seward, J. Am. Chem. Soc., 111 (1989) 8681.
3. R. Lide, (Ed.), "*Handbook of Chemistry and Physics*", 74th edition, CRC Press, Boca Raton, Florida, (1993)
4. A.F. Sholl, I. O. Sutherland, J. Chem. Soc., Chem. Commun., (1992) 1716.
5. D.J. Cram, R.A. Carmack, R.C. Helgeson, J.Am. Chem. Soc., 110 (1988) 571.
6. S. Misumi, T. Kaneda, J. of Inc. Phenom. and Molec. Rec. in Chem. 7, (1989) 83.
7. J. Van Gent, E.J.R. Sudholter, P.V. Lambeck, T.J.A. Popma, G.J. Gerritsma, D.N. Reinhoudt, J.Chem. Soc., Chem. Commun., (1988) 893.
8. T. Kaneda, K. Sugihara, H. Kamiya, S. Misumi, Tet. Lett., 22 (1981) 4407.
9. Y. Kubo, S. Hamaguchi, A. Niimi, K. Yoshida, S. Tokita, J. Chem. Soc., Chem. Commun., (1993) 305.
10. M.A. King, C.P. Moore, K.R.A. Samankumara Sandanayake, I.O Sutherland, J. Chem., Soc., Chem. Commun., (1992) 583.
11. H. Shimizu, K. Iwamoto, K. Fujimoto, S. Shinkai, Chem. Lett., (1991) 2147.
12. E.D. Olsen, "*Modern Optical Methods of Analysis*", McGraw-Hill, USA, (1975).
13. H.G. Lohr, and F. Vogtle, Acc. Chem. Res., 18 (1985) 65.
14. G. Barrett, V. Bohmer, G. Ferguson, J. F. Gallagher, S.J. Harris, R.G. Leonard, M.A. McKervey, M. Owens, M. Tabatabi, A. Vierengel, and W. Vogt, J. Chem. Soc., Perkin Trans 2, (1992) 1595.
15. R. Ungaro, and A. Pochini in *"Calixarenes: A Versatile Class of Macrocyclic Compounds"*. eds. J. Vicens and V. Böhmer (1991) Kluwer Academic Publishers, Dordrecht / Boston / London, p. 127-147
16. A. Arduini, A. Pochini, S. Reverberi, R. Ungaro, C.D. Andereetti, and F. Ugozzoli, *Tetrahedron* 42 (1986) 2089
17. G. Calestani, F. Ugozzoli, A. Arduini, E. Ghidini, and R. Ungaro, J. Chem. Soc., Chem. Commun., (1987) 345.
18. J. Wang, (Personal Communication)

19. C.N.R. Rao, "*Ultra-Violet and Visible Spectroscopy, Chemical Applications*" 3rd edition, Butterworths, London, (1975).

20. N.D. Coogeshall, and A.S. Glessner Jr., J. Am. Chem. Soc., 71 (1949) 3151.

21. B.P Czech, E. Chapoteau, W. Zazulak, C.R Gebauer, A. Kumar, Anal. Chim. Acta, 241 (1990) 127.

22. D.J. Cram, R.A. Carmack, R.C. Helgeson, J. Am. Chem. Soc., 110 (1988) 571.

23. M. Takagi, K.Ueno, Top. Curr. Chem., 121 (1984) 39.

24. P. Guilbaud, A. Varneck and G. Wipff, J. Am Chem. Soc., 115 (1993) 8298.

25. P.W. Atkins, "*Physical Chemistry*", Oxford University Press, (1978).

26. V. Bohmer, E. Schade, W. Vogt, Makromol.Chem., Rapid Commun. 5, (1984) 221.

27. "*Dictionary of Analytical Reagents*", Chapman and Hall, Chemical Database, Cambridge, (1993).

28. L. Safarik and Z. Stransky, Wilson and Wilson's Comprehensive Analytical Chemistry, Vol XXII. "*Titrimetric Analysis in Organic Solvents*" G. Svehla (Ed.), Elsevier, Amsterdam, (1986).

29. T. Nowicka-Janowska, K. Gorczynska, A. Michalik, E. Wieteska, Wilson and Wilson's Comprehensive Chemistry, Vol. XIX, "*Analytical Visible and Ultraviolet Spectrometry*" G. Svehla, Elsevier, Amsterdam, (1986).

Chapter 4

Nitrophenylazophenol Calix[4]arenes

4.1 Introduction

This chapter deals with another set of novel chromogenic calix[4]arenes, which possess the larger nitrophenylazophenol chromophores instead of the nitrophenol group discussed in Chapter 3. Five novel compounds, all synthesised by Dr Stephen J. Harris at D.C.U. are discussed. For synthetic details see references [1, 2].

This chromophore was chosen in an attempt to create compounds whose deprotonated form would have a longer wavelength absorbance maximum than the compounds containing the nitrophenol group. We have synthesised several tetrameric calix[4]arenes which incorporate a nitrophenylazophenol group as the chromogenic moiety in the ester portion of the molecule. Compounds with longer absorbance maxima such as these are more applicable from an optical sensor point of view due to the cheap availability of blue (λ_{max} 470 nm) or green (λ_{max} 565 nm) LEDs, which emit light in the range of the absorbance maxima of the azophenol group. Hence instrumentation development for these sensors would be much simpler than for shorter wavelength analogues as more complex excitation sources are required in the latter case.

The nitrophenylazophenol group has been used as the chromogenic moiety in many different cation binding systems. A crowned azophenol was shown to exhibit lithium specific colour changes in the presence of an amine [3], structure **4(i)**.

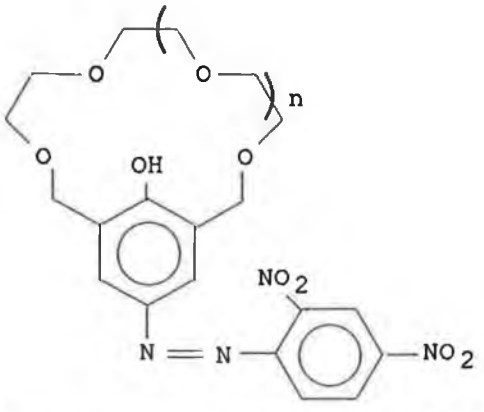

4(i) Crown nitrophenolazophenol [1], n=1.

Complexation with Li^+ is thought to occur as outlined in structure **4(ii)** [4]. The Li^+ complexation occurs by means of both the traditional electrostatic interaction

Complexation with Li^+ is thought to occur as outlined in structure 4(ii) [4]. The Li^+ complexation occurs by means of both the traditional electrostatic interaction between the positively charged cation and the δ^- of the oxygen atoms which make up the spherand ring but also a coulombic interaction with the phenolate anion is thought to be significant since no other cations were found to show any interaction.

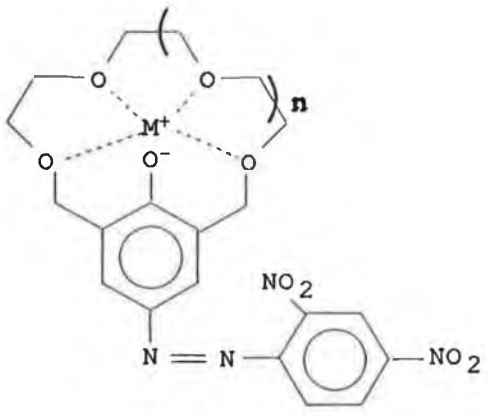

4(ii) Crown dinitrophenylazophenol complex, [4].

A number of amine selective azophenol crown ethers have also been described, with the nature of the amine (i.e. primary, secondary or tertiary) determining the wavelength of the absorbance maximum of the complex with some of the compounds [4]. Structure 4(iii) which is a nitrophenylazophenol crown compound incorporating an amine is one such compound. With this molecule there is utilisation of the phenolate anion and an electrostatic interaction between the oxygens of the spherand ring and the hydrogen atoms of the amine.

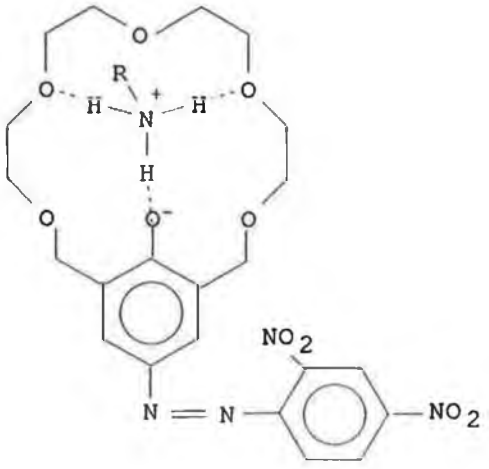

4(iii) Crown dinitrophenylazophenol amine complex [5].

A four membered spherand containing the *p*-nitrophenylazophenol chromogenic group has been shown to display lithium selectivity under hydrophobic conditions with no interaction with any other metals being observed [6]. The six-membered analogue of this spherand was found to respond to sodium and lithium ions with very little response to any other metal ions [7], (structure **4(iv)**). Molecular models (CPK) of the Li^+ and Na^+ complexes of structure **4(iv)** showed both of them to be capsular, an arrangement which would be very difficult to form with K^+ due to the larger size of the cation.

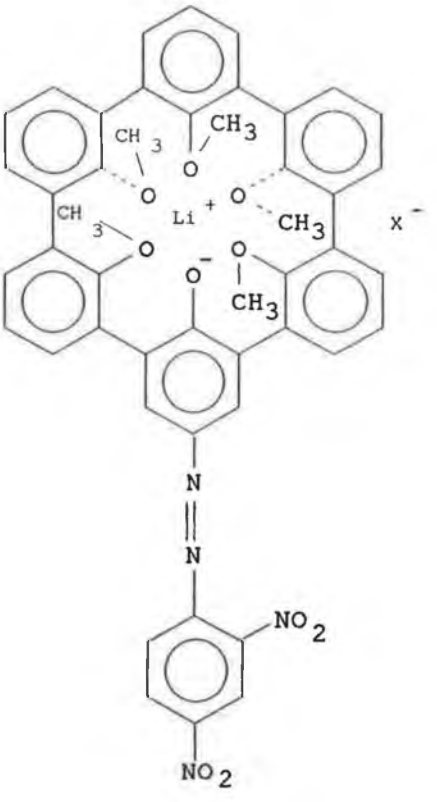

4(iv) Dinitrophenylazophenol spherand Li^+ complex [7]

Calixarene derivatives, another major class of macrocyclic receptor molecules, have recently evoked interest as a source of novel colorimetric sensors. Two calix[4]arenes bearing azophenol moieties as the chromogenic component have been recently described in the literature [8, 9], and one has been found to display lithium selectivity in a solid-liquid two phase extraction [8]. Shimizu et al. deduced from ^1H NMR experiments that Li^+ is bound to **4(v)** as a cation of the azophenolate anion and also interacts electrostatically with the three remaining phenolic oxygens. A dinitrophenylazophenol with a similar calixarene backbone was synthesised and found to respond to the lithium ion in the presence of a number of amines [9].

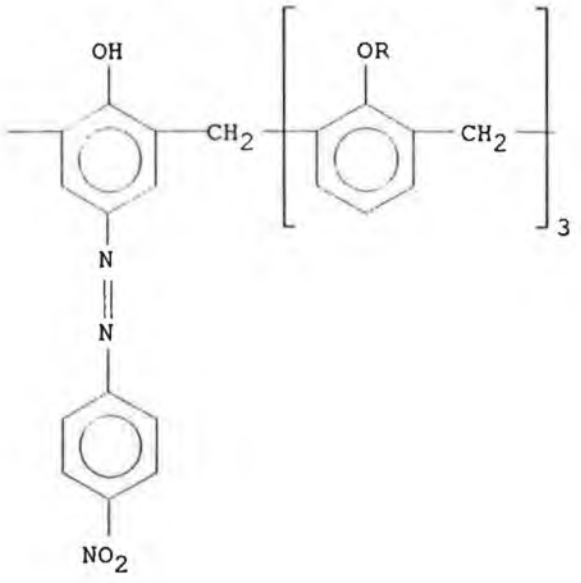

4(v), Nitrophenylazophenol Calix[4]arene, [8]

Another calixarene bearing the nitrophenylazophenol chromophore which showed excellent selectivity for potassium against sodium has also been described [10], structure 4(vi). In all three of these compounds, the phenol group (which is deprotonated to give the colour change upon complexation) is sited within the cavity into which the metal ion fits and complexation actually involves the phenolic oxygen atoms.

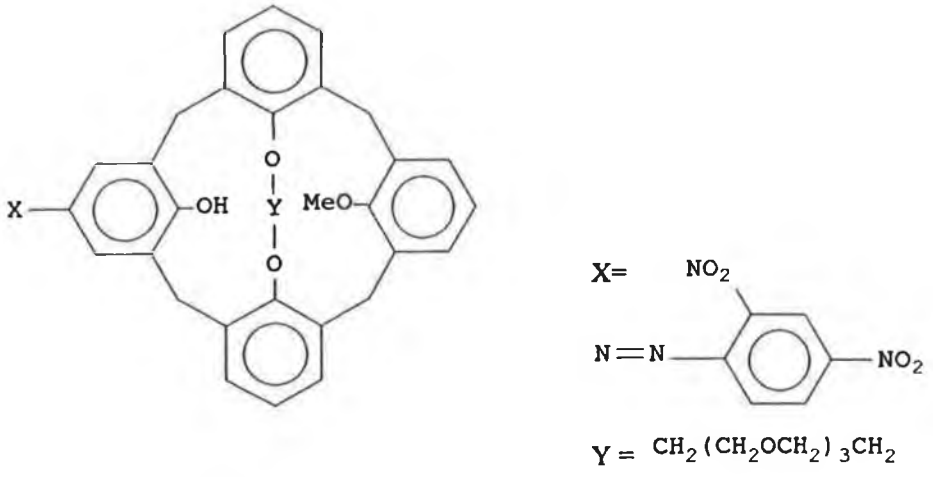

4(vi) Dinitrophenylazophenol bridged calix[4]arene, [10].

4.2 Structures of Compounds Under Examination

The five compounds examined in this work are as follows:-

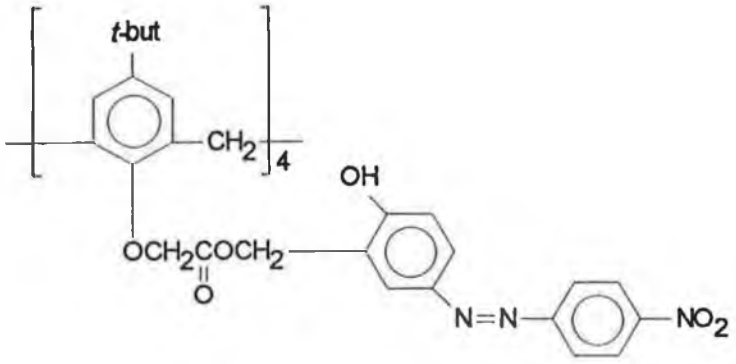

4 (vii) Ligand 5

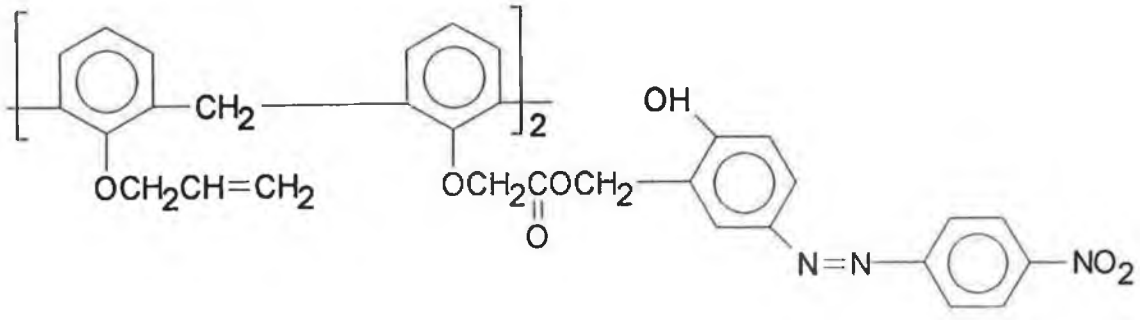

4 (viii) Ligand 6

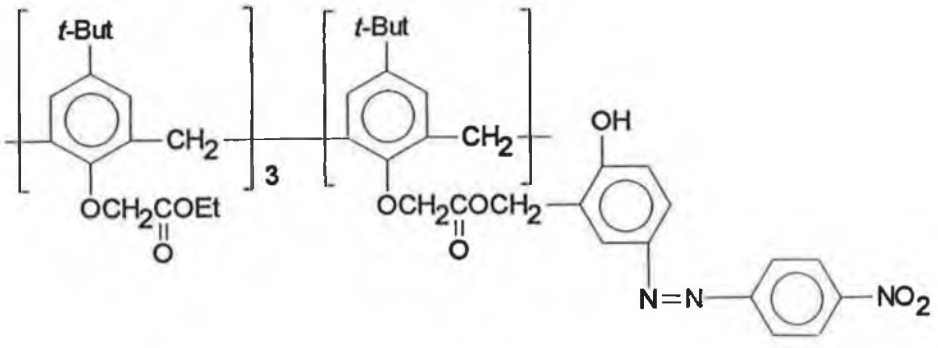

4 (ix) Ligand 7

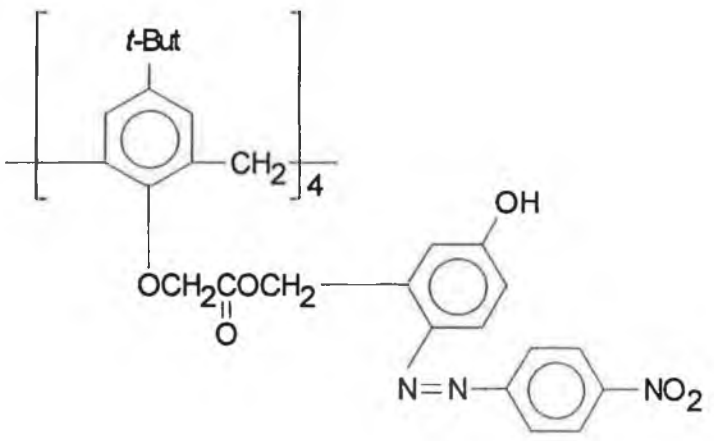

4 (x) Ligand 8

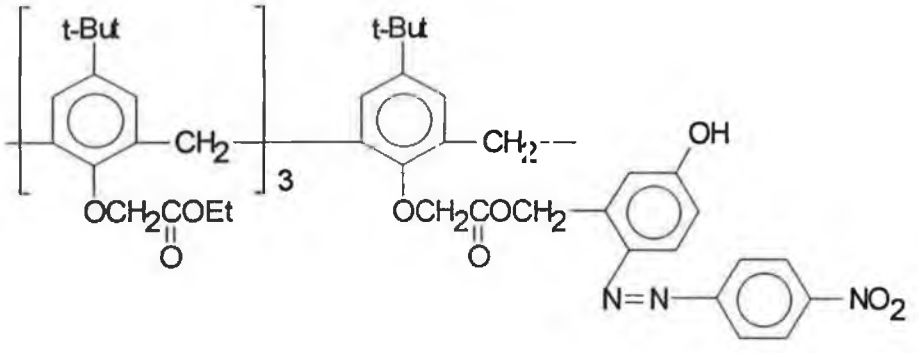

4 (xi) Ligand 9

All five ligands possess either one, two or four nitrophenylazophenol chromogenic moieties and as in the case of the nitrophenol moieties, these are classified as ionisable chromophores. In Ligands 5, 6, and 7 the methylene group of the ester portion of the calixarene is attached in the *ortho* position of the chromophore, whereas in ligands 8 and 9, the calixarene is attached in the *meta* position relative to the phenol group. All ligands except ligand 6, the dichromogenic ligand, have *tertiary* butyl groups in the *para* position of the calixarene backbone. Ligand 6 is peculiar to the other non-tetrachromogenic ligands 7 and 9 in that it has two allyl groups attached to the calixarene "arms" rather than ester groups which are seen in Ligands 7 and 9. It also has hydrogen atoms in place of *t*-butyl groups in the *para* position of the calix[4]arene backbone.

4.3 Mode of Action

Because all five ligands possess ionisable chromophores the mode of action described in Chapter 3 would be expected to also be applicable to these ligands. The nitrophenylazophenol chromogenic moiety again depends on deprotonation for a change in colour or an increase in absorbance at the λ_{max} of the deprotonated form. The phenolic group is part of a much larger conjugated π system with this moiety than it was in the nitrophenol chromogenic ligands. A larger π system bearing azo, phenolic and nitro chromophores attached to the aromatic rings would be expected to absorb radiation at longer wavelengths than the nitrophenol moieties [11]. The fundamental requirement of the presence of a base to cause a cation induced colour change was examined for Ligand **5**. No colour change is seen for 2.5 mL of a $5x10^{-5}$ M solution of Ligand **5** in THF upon the addition of 10^{-2} M $LiClO_4$. A colour change from yellow to red was noticed immediately upon the addition of TDDA. So again it can be seen that the presence of a base is required for the uptake of the phenolic proton.

4.4 Absorbance Spectra of Ligands 5-9

4.4.1 Introduction

Method 2.5.1 was used to assess changes in absorbance spectra upon interaction of the ligands with alkali metal cations. Solutions (5×10^{-5} M) of Ligand **5**, **7**, **8** and **9** and 6×10^{-5} M Ligand **6** were made up in THF. A 2.5 mL aliquot of each solution of ligand was taken and to this 100 µL of TDDA (tridodecylamine) were added to give a final TDDA concentration of $6x10^{-2}$ M. This volume of TDDA was found to be the optimum in studies similar to those described in Chapter 3. Incremental concentrations of aqueous lithium perchlorate were added to give final metal perchlorate concentrations of 10^{-6} M to 0.1 M in the sample. After gentle shaking, the clear yellow ligand solution changed colour to red immediately with the intensity of the resultant colour being dependent on the metal perchlorate concentration. This colour change was examined using UV-Vis spectroscopy in the range 300-800 nm.

A very slight colour change to barely orange is seen upon introduction of the TDDA to the free ligand and this is seen as a very slight increase in absorbance intensity at 520 nm. However the bulk of the ligand remains protonated until the

introduction of the metal perchlorate when the colour change to red occurs. This can be explained in terms of equations **3.4** and **3.6** where again $K_{a(L)} < K_{a(C)}$. The dissociation constant of the ligand appears to be reduced sufficiently in the presence of the metal to allow the base to cause deprotonation of the phenolic proton.

4.4.2 Ligand 5, Single-Phase Examination.

Figures 4.1(a) and 4.1(b) show the change in absorbance spectra of Ligand **5** at a concentration of $5x10^{-5}$ M with increasing concentrations of lithium perchlorate and sodium perchlorate respectively. No colour change was observed in the absence of base for any of the ligands on addition of $LiClO_4$ in control experiments where identical amounts of the metal perchlorates were added. This is indicative of the deprotonation of the azophenol group upon metal ion complexation being the cause of the colour change, as the presence of the base facilitates the removal of the phenolic proton. A slight colour change from yellow to bronze was noted upon addition of the TDDA, but this is barely discernible as an increase in intensity at the deprotonated λ_{max}.

The protonated form of Ligand **5** shows λ_{max} at 380 nm, with an ε value of $5x10^4$ L mol^{-1} cm^{-1}. As the concentration of $LiClO_4$ is increased in the presence of TDDA, the intensity of the absorbance at 380 nm decreases and simultaneously a new peak is observed at 520 nm which is attributed to the formation of the deprotonated complex. This peak increases in intensity with increasing $LiClO_4$ concentration. An isobestic point is observed at 424 nm indicating the presence of two absorbing species in equilibrium with each other. As well as the bathochromic λ_{max} shift seen on deprotonation, a hypochromic shift is also observed. A minimum ε value of $3.2x10^4$ L mol^{-1} cm^{-1} was estimated from the absorbance obtained for a 0.1 M solution of $LiClO_4$. From Figure 4.2 it can be seen that the absorbance is continuing to increase so a lower concentration of the deprotonated form of the ligand actually exists and therefore this value is an underestimation. A linear range from 10^{-4} to 10^{-1} M for $LiClO_4$ is obtained (Figure 4.2) with this ligand along with a L.O.D. of c. 5.8 x 10^{-5} M $LiClO_4$. A slope of 0.519 a.u./dec was found in this range.

A moderate response to $NaClO_4$ was observed for 10^{-3} and 10^{-2} M before a large increase in intensity was seen for 0.1 M. However the actual absorbance for 0.1 M $NaClO_4$ was approximately 0.65 a.u. less than that seen for 0.1 M $LiClO_4$.

This is an immediate indication that higher levels of sodium interferent will be tolerated by this ligand compared to the previously discussed nitrophenol ligands of Chapter 3, which showed comparable $LiClO_4$ and $NaClO_4$ absorbance at this highest level.

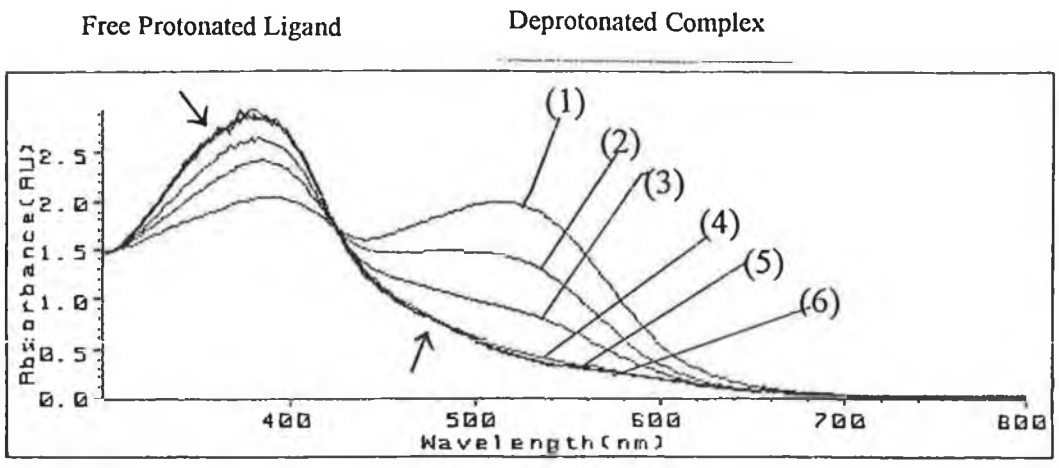

Figure 4.1(a):- Lithium Response, Ligand 5.

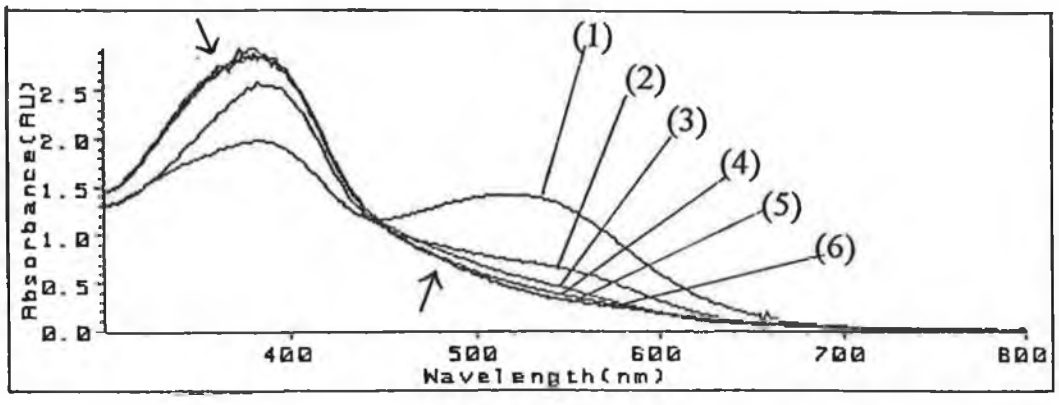

Figure 4.1 (b):- Sodium response, Ligand 5.

Figure 4.1:-*One-phase investigation of changes in the absorbance spectrum of 2.5 mL solutions of $5.0x10^{-5}M$ ligand 5, in THF with 100 μL TDDA, upon addition of aqueous (a) lithium perchlorate, and (b) sodium perchlorate with final metal perchlorate concentrations of; 0.1M (1), $10^{-2}M$ (2), $10^{-3}M$ (3), $10^{-4}M$ (4), $10^{-5}M$ (5), $10^{-6}M$ (6). See Table 2.1.*

Figure 4.2, a graph of absorbance at 520 nm versus the log of metal perchlorate concentration shows clearly the difference in response of the ligand to the two different cations.

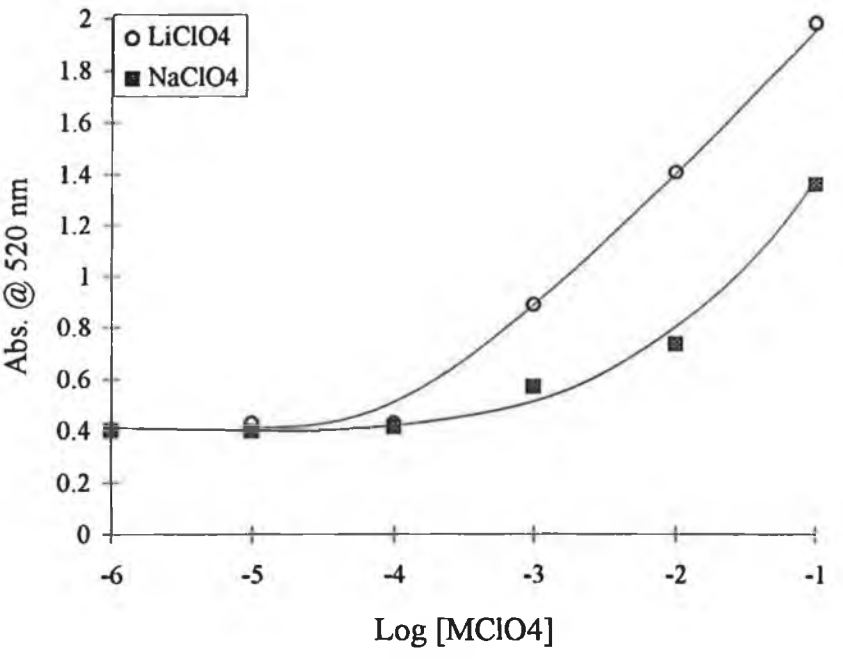

Figure 4.2:- *Comparison of absorbance at 520 nm of the lithium and sodium metal complexes of Ligand* ***5****.*

4.4.3 Ligand 6, Single-Phase Examination.

The absorbance spectra of Ligand 6, the dichromogenic ligand, with incremental increases in $LiClO_4$ and $NaClO_4$ in the presence of 100 μL of TDDA are shown in Figure 4.3(a) and 4.3(b) respectively.

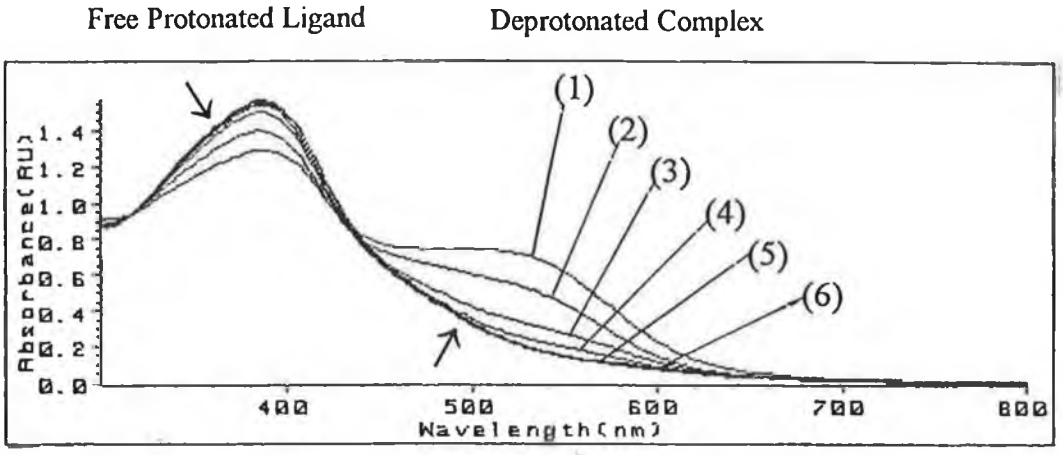

Figure 4.3 (a):- Lithium Response, Ligand 6.

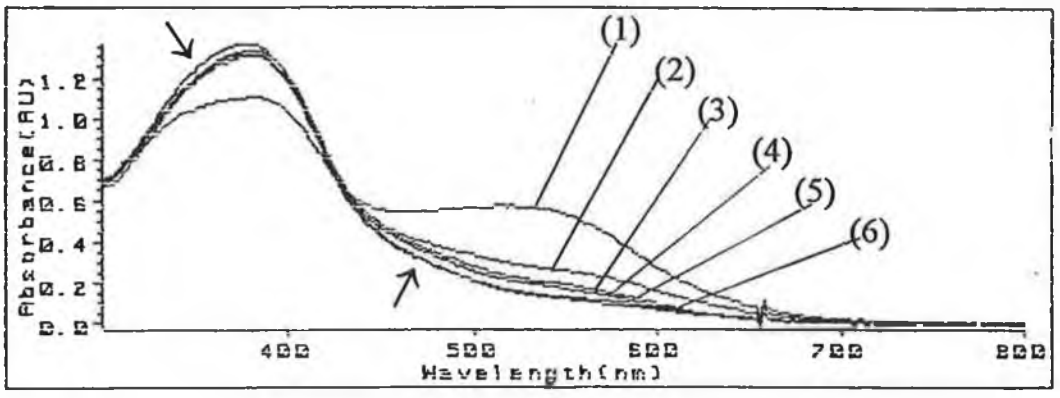

Figure 4.3 (b):- Sodium response, Ligand 6.

Figure 4.3:-One-phase investigation of changes in the absorbance spectrum of 2.5 mL solutions of $6.0x10^{-5}M$ ligand 6, in THF with 100 µL of TDDA, upon addition of aqueous (a) lithium perchlorate, and (b) sodium perchlorate with final metal perchlorate concentrations of; 0.1M (1), $10^{-2}M$ (2), $10^{-3}M$ (3), $10^{-4}M$ (4), $10^{-5}M$ (5), $10^{-6}M$ (6). See Table 2.1.

The protonated and deprotonated absorbance maxima for both complexes occur at 380 and 520 nm respectively, with an isobestic point at 420 nm. For the protonated form of the Ligand 380 nm ε was calculated to be $2.5x10^4$ L $mol^{-1}cm^{-1}$, which corresponds to an approximate halving of ε when the number of chromogenic groups is halved. An underestimation of ε for the deprotonated complex λ_{max} was carried out for the reasons outlined above to be approximately 10^4 L mol^{-1} cm^{-1}. The actual maximum intensity of the initial protonated ligand is approximately 1.4 a.u. compared to approximately 3.0 a.u. for the tetrachromogenic Ligand 5. This reduction in absorbance corresponds to the decrease in the number of chromogenic moieties in the two molecules and is comparable with the decrease in intensity observed on examining Ligands 1 and 2, the tetra and monochromogenic nitrophenol ligands respectively. The ligand responds to increases in $LiClO_4$ above a concentration of 10^{-4} M with a change in absorbance of 0.5 a.u. between this concentration and 0.1 M. Complexation with Na^+ exhibits an inferior response to that of $LiClO_4$ with very little change in absorbance seen prior to the addition of a final $NaClO_4$ concentration of 0.1 M. The absorbance of this highest $NaClO_4$ concentration once again is considerably lower than that observed for $LiClO_4$ and is seen clearly in Figure 4.4, a graph of absorbance at 520 nm versus the log of the metal perchlorate concentration.

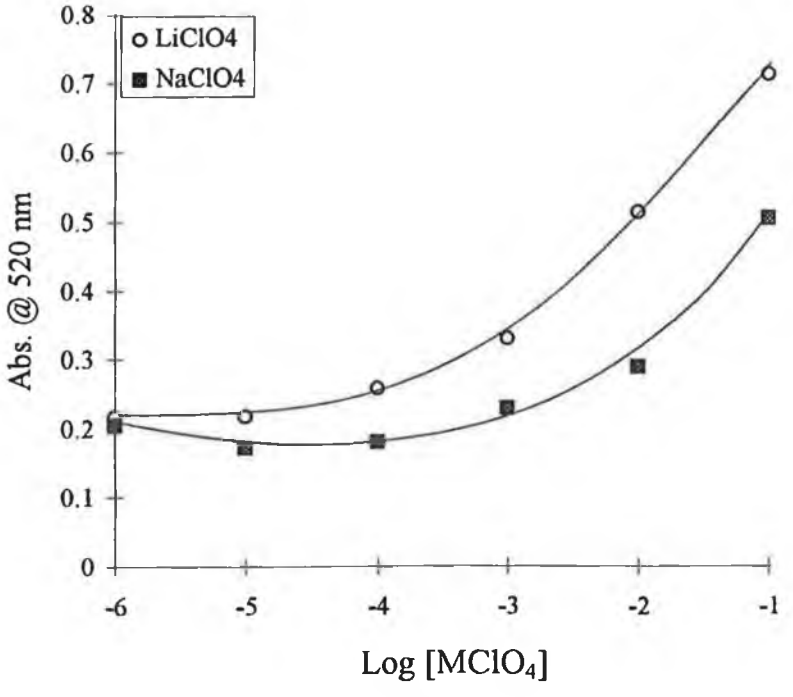

Figure 4.4:- *Comparison of absorbance at 520 nm of the lithium and sodium metal complexes of Ligand 6, with data obtained from the spectra in figure 4.3.*

4.4.4 Ligand 7, Single-Phase Examination

The monochromogenic ligand, Ligand 7, the final ligand of this series of ligands possessing the nitrophenylazophenol chromophore with the calixarene attached *ortho* to the chromogenic phenolic group produced the following spectra. Figures 4.5 (a) and 4.5 (b) show the spectral changes of Ligand 7 in the presence of TDDA, to increases in $LiClO_4$ and $NaClO_4$ respectively.

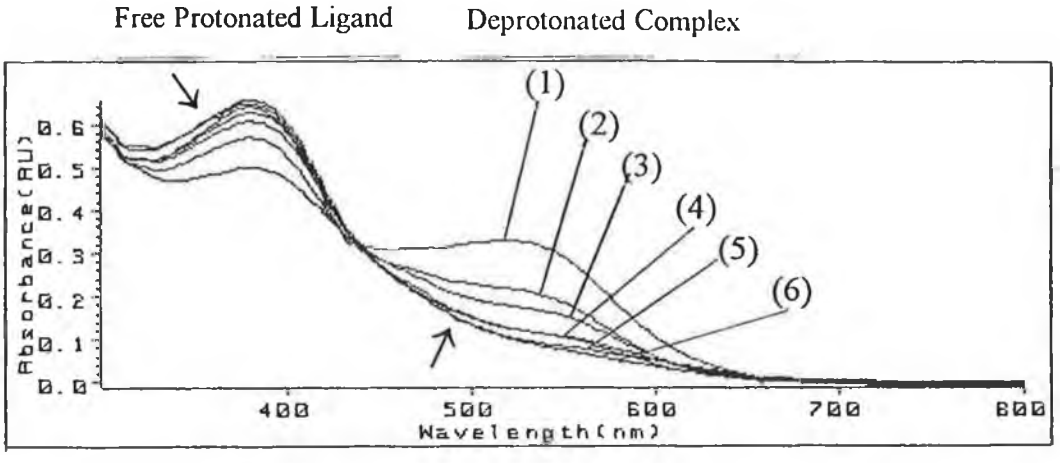

Figure 4.5 (a):-Lithium response, Ligand 7.

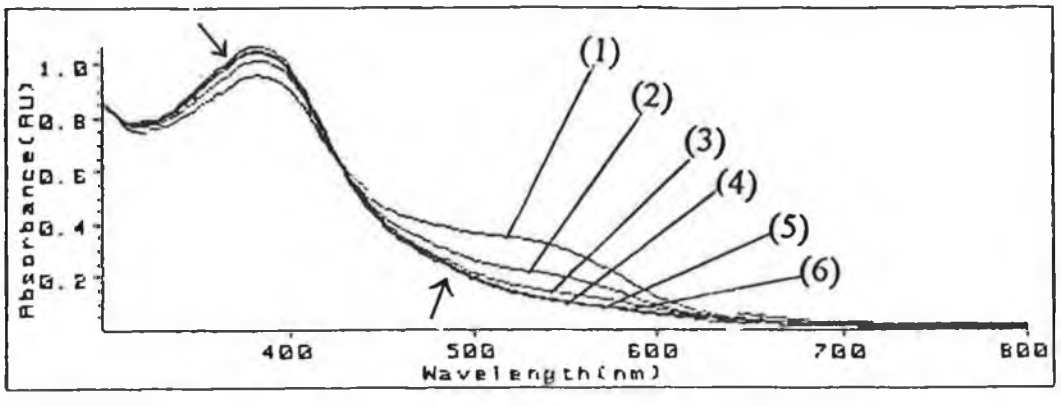

Figure 4.5 (b):- Sodium response, Ligand 7.

Figure 4.5:-One phase investigation of changes in the absorbance spectrum of 2.5 mL solutions of $5.0x10^{-5}$M ligand 7, in THF with 100 μL of TDDA, upon addition of aqueous (a) lithium perchlorate, and (b) sodium perchlorate with final metal perchlorate concentrations of; 0.1M (1), 10^{-2}M (2), 10^{-3}M (3), 10^{-4}M (4), 10^{-5}M (5), 10^{-6}M (6)

The protonated λ_{max} again occurs at 380 nm, ε ($1.32x10^4$ L mol^{-1} cm^{-1}). This again corresponds to a halving of ε as the number of chromogenic groups is halved. The same λ_{max} is observed for both the lithium and sodium complexes at 520 nm, (ε_{min} $4x10^3$ L mol^{-1} cm^{-1}). Isobestic points are observed at 430 nm. The superior response of Ligand 7 to lithium over sodium is illustrated in Figure 4.6. A linear range for $LiClO_4$ is seen from 10^{-4} to 0.1 M compared to a range of 10^{-3} to 0.1 M seen for $NaClO_4$. A slope of 0.107 a.u./dec is seen in the range 10^{-4} to 10^{-1} M for $LiClO_4$. No real response is observed for $NaClO_4$ until after 10^{-3} M $NaClO_4$ has been added and maximum absorbance reached at 0.1 M $NaClO_4$, the highest concentration is a mere 0.2 a.u. The reduction in intensity of the protonated form of this ligand compared to that of Ligand 6 is again due to the fact that the number of chromogenic moieties has been reduced to one and therefore a reduction in intensity is expected. The absorbance due to a number of separate chromogenic groups which are not conjugated on a molecule is additive and therefore a reduction in the number of chromogenic moieties avaliable for absorption will decrease the observed absorbance [12].

A slope of 0.059 a.u./dec is seen for the three points in the range 10^{-2} M, $5x10^{-2}$ M and 0.1 M $NaClO_4$. This signifies a slight departure from the behaviour of Ligands 5 and 6 towards $LiClO_4$, where there was no significant response until a final $NaClO_4$ concentration of 10^{-2} M had been added. However, the actual total absorbance change in the concentration range in which the ligand appears to be responding to the presence of $NaClO_4$ is only 0.1 a.u., which would be a major limiting factor for its application as a Na^+ sensing material in the absence of Li^+.

Figure 4.7 shows the large increase in intensity observed as the number of chromogenic groups on the molecule is increased. The large absorbance change of Ligand 5 with increasing $LiClO_4$ would render it more useful as a visual indicator than the more subtle colour changes exhibited by Ligands 6 and 7.

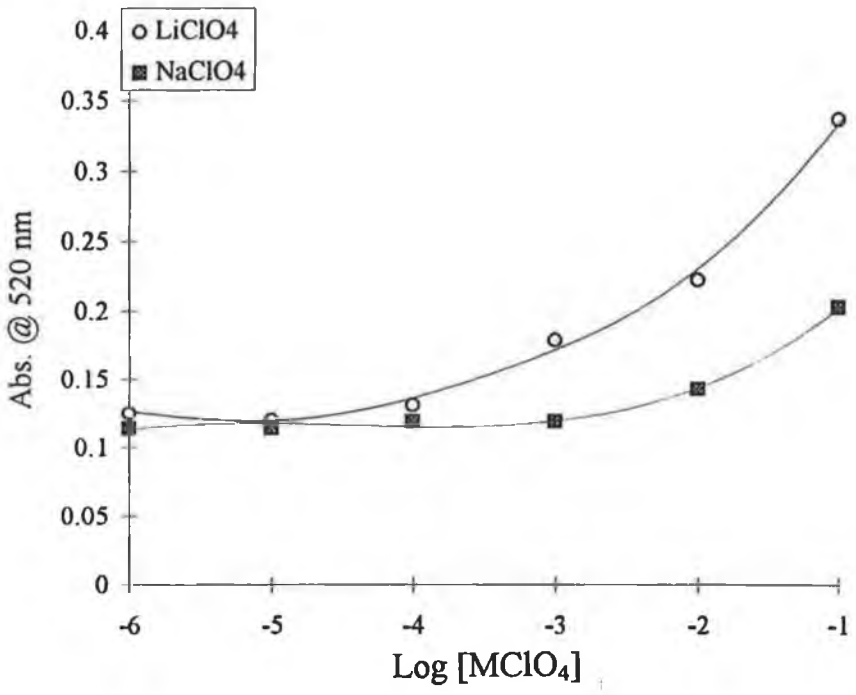

Figure 4.6:- *Comparison of absorbance at 520 nm of the lithium and sodium metal complexes of Ligand 7, with data obtained from spectra in figure 4.5.*

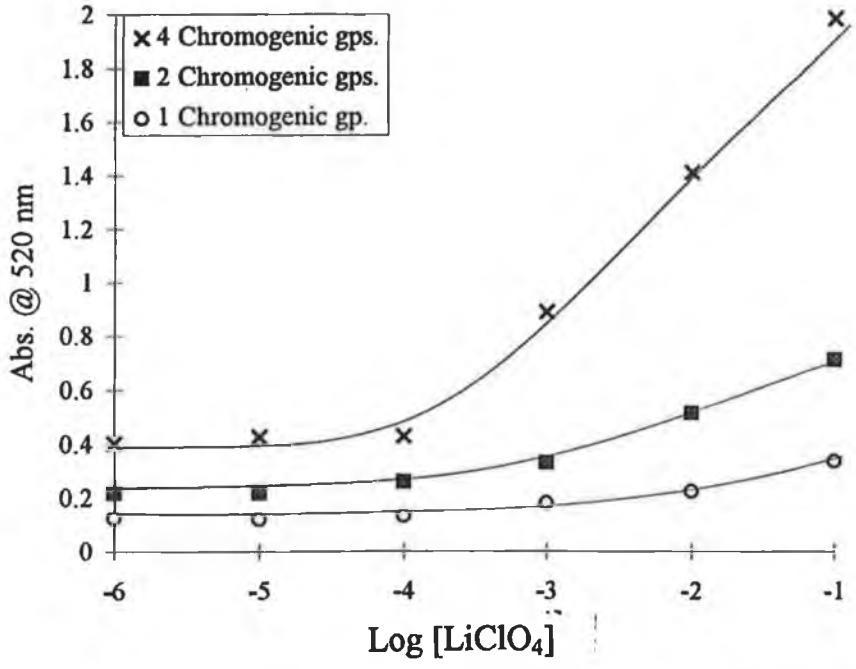

Figure 4.7:-*Comparison of the response of Ligand 5, 6, and 7 to the presence of varying concentrations of* $LiClO_4$.

4.4.5 Ligand 8 and 9, Single-Phase Examination.

Ligands 8 and 9 are the tetrachromogenic and monochromogenic ligands of another class of chromoionophore. The chromogenic moiety is attached to the calixarene backbone *meta* to the phenolic group of the nitrophenylazophenol. Figure 4.8 shows the absorbance spectrum for Ligand 8 in the presence of 100 μL of TDDA with increasing concentration of $LiClO_4$ from 10^{-6} to 10^{-1} M. Ligand 8 does not have a clear protonated λ_{max} in the visible region because the absorbance continues to increase as it approaches the ultraviolet region of the spectrum. There is very little difference in intensity between the peaks in the region below 400 nm where absorbance of the protonated form would be expected. The deprotonated complex λ_{max} occurs at approximately 540 nm with broad flat peaks being visible, making an exact λ_{max} determination difficult.

Figure 4.9 shows the response of this ligand to $LiClO_4$. A linear range of three orders of magnitude from 10^{-3} M to 0.1 M is again evident with an increase in absorbance above 10^{-4} M, indicating an LOD between 10^{-3} and 10^{-4} M $LiClO_4$. The absorbance response range of 0.2 a.u. obtained is however very small compared to the range of 1.6 a.u. seen for the other tetrachromogenic ligand, Ligand 5, over a similar concentration range The slope of the response from 10^{-3} to 10^{-1} M is 0.096 a.u./dec.

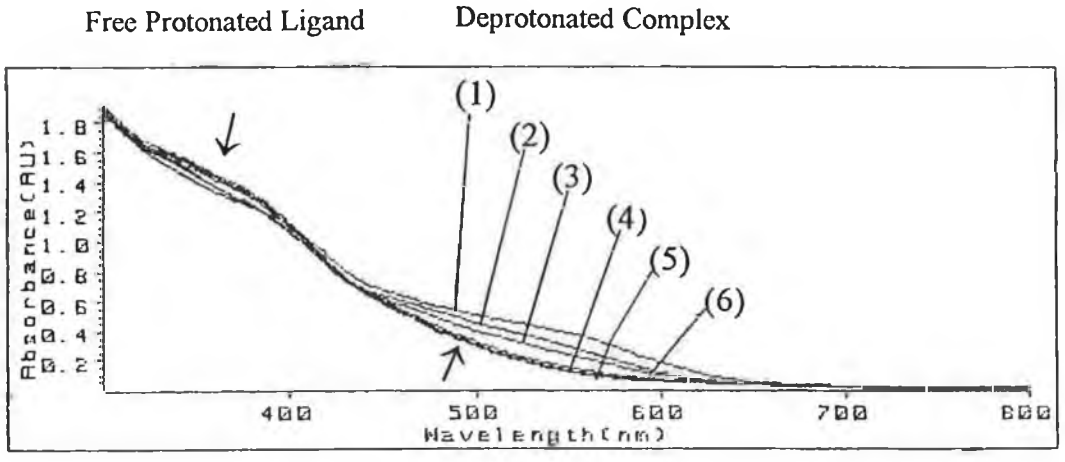

Figure 4.8:- *One-phase investigation of changes in the absorbance spectrum of 2.5 mL solutions of $5.0x10^{-5}M$ ligand* ***8****, in THF with 100 μL of TDDA, upon addition of aqueous lithium perchlorate with final metal perchlorate concentrations of; 0.1M (1), $10^{-2}M$ (2), $10^{-3}M$ (3), $10^{-4}M$ (4), $10^{-5}M$ (5), $10^{-6}M$ (6). See Table 2.1.*

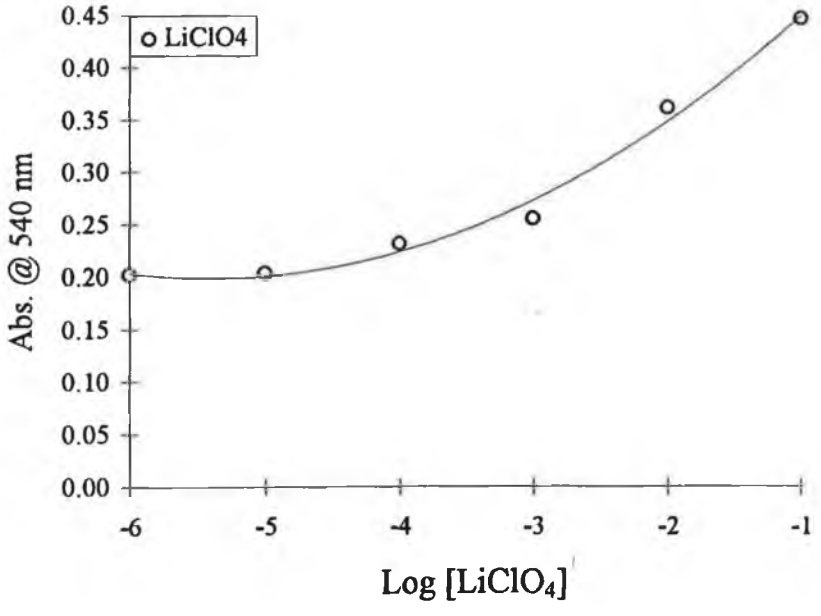

Figure 4.9:- *Graph of absorbance at 540 nm versus log $[LiClO_4]$ for the deprotonated Li^+ complex of Ligand* ***8****.*

The spectra obtained for the $LiClO_4$ interaction with Ligand 9, the monochromogenic ligand of this series are shown in Figure 4.10. Ligand 9 shows a clearer protonated λ_{max} at 380 nm than that seen with Ligand 8. The deprotonated Li^+ complex has a λ_{max} of 540 nm in the presence of TDDA. The response curve for this ligand is seen in Figure 4.11.

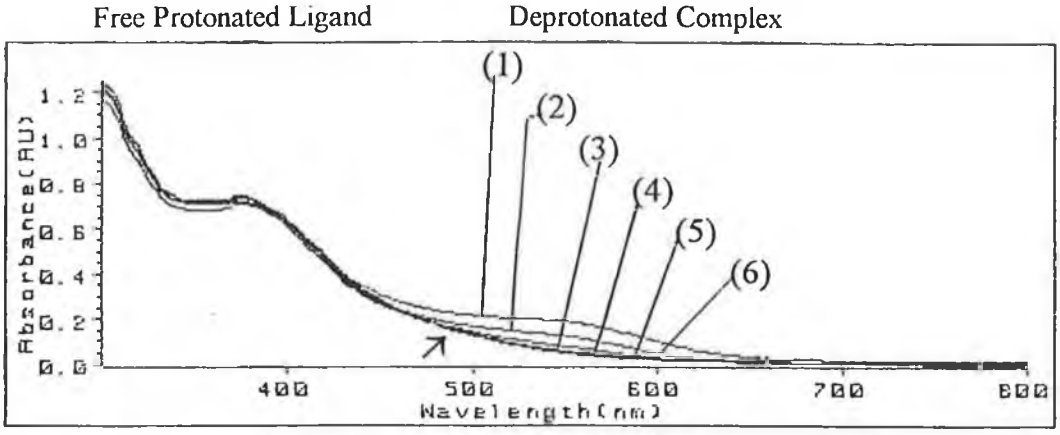

Figure 4.10:- *One-phase investigation of changes in the absorbance spectrum of 2.5 mL solutions of $5.0x10^{-5}M$ ligand 9, in THF with 100 µL of TDDA, upon addition of aqueous lithium perchlorate with final metal perchlorate concentrations of; 0.1M (1), $10^{-2}M$ (2), $10^{-3}M$ (3), $10^{-4}M$ (4), $10^{-5}M$ (5), $10^{-6}M$ (6). See Table 2.1.*

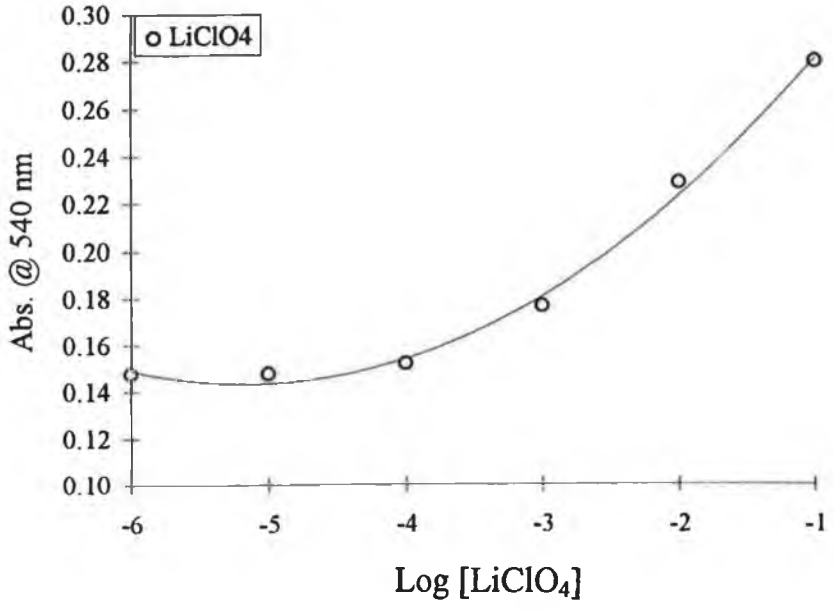

Figure 4.11:- *Graph of absorbance at 540 nm versus log $[LiClO_4]$ for the deprotonated Li^+ complex of Ligand 9.*

The absorbance change with this ligand is the poorest observed extending from 0.15 to 0.28 a.u. but inspite of this a discernable linear range from 10^{-3} M to 0.1 M is again observed with practically no change in absorbance seen, prior to the addition of 10^{-4} M $LiClO_4$.

4.5 Selectivity Determination

Selectivity coefficients were determined using Method 2.5.2 described in Chapter 2, with fixed background interferents of 0.05 and 0.1 M $NaClO_4$. These higher interferent levels were used with this set of ligands compared to those used with the nitrophenol ligands because of the poorer response observed in the presence of $NaClO_4$ for the nitrophenylazophenol ligands seen in section 4.4. Spectra were obtained from 300-800 nm and graphs of absorbance at 520 nm for Ligands 5, 6 and 7, and 540 nm for Ligands 8 and 9 versus the log of the concentration of lithium perchlorate drawn. At high concentrations, the sodium ion has the effect of reducing the response of the ligand to the lower concentrations of $LiClO_4$ as it dominates the complexation process with the ligand and swamps any lithium ion effects. However, at higher lithium ion concentrations, a response will be observed because of greater affinity of the ligand for lithium ions. From these graphs, selectivity coefficients can be estimated from the ratio of the sodium and lithium ion concentrations at the intersection of the sodium and lithium dominant response regions of the curves.

Figure 4.12 (a), (b) and (c) shows the absorbance at 520 nm versus the log of the lithium perchlorate concentration for Ligands 5, 6 and 7 respectively at each level of sodium perchlorate interferent.

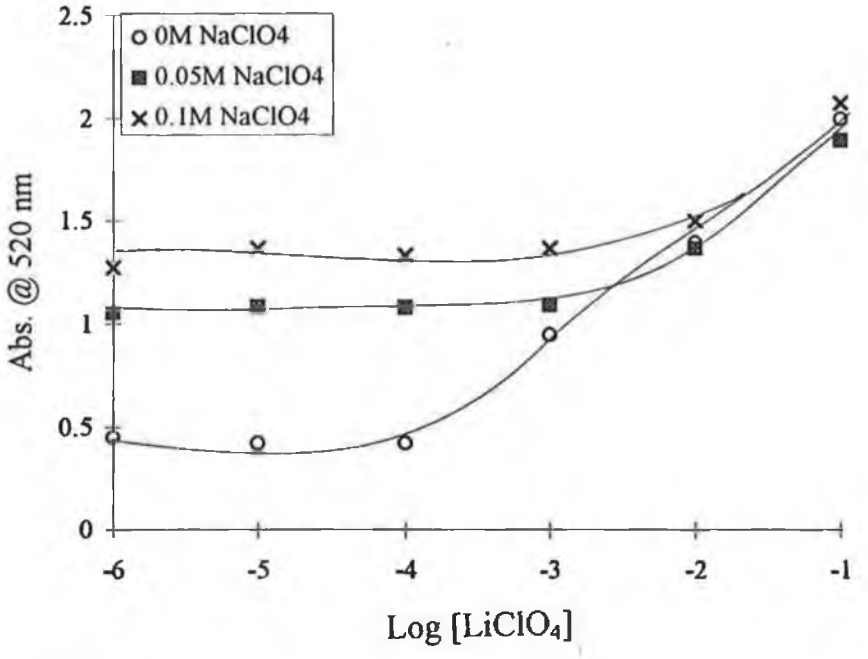

Figure 4.12 (a):- Selectivity, Ligand 5.

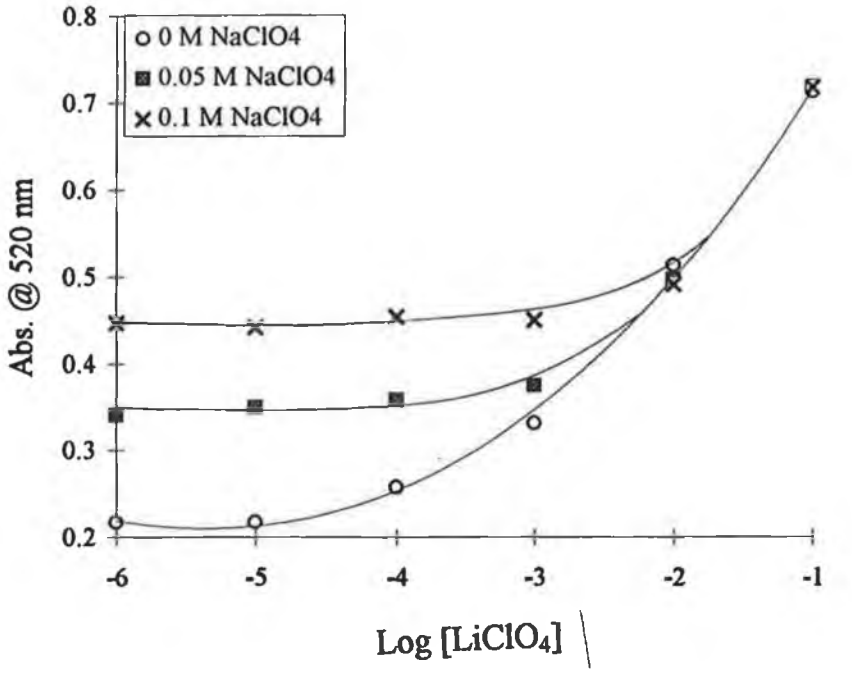

Figure 4.12 (b):- Selectivity, Ligand 6.

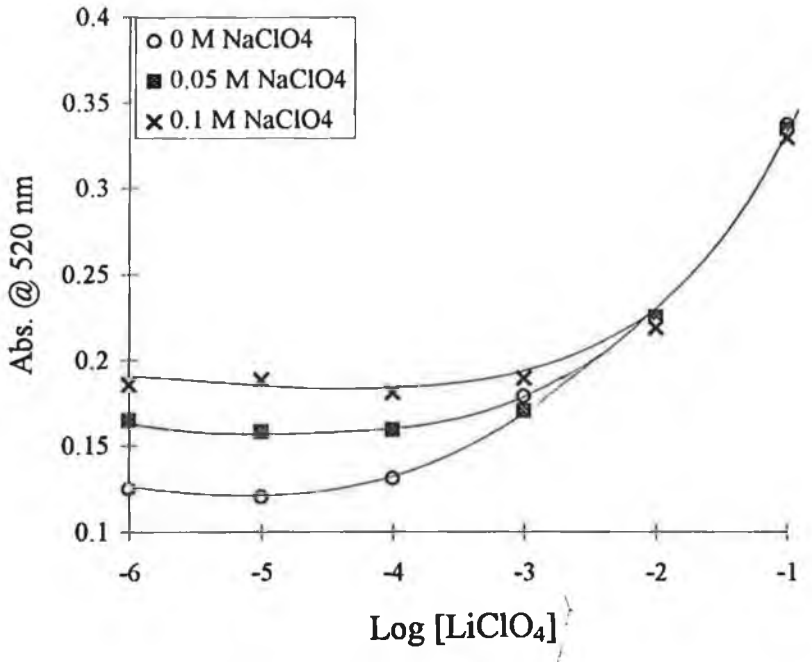

Figure 4.12 (c):-Selectivity, Ligand 7.

Figure 4.12:- *One-phase studies of the optical response of solutions at 520 nm of (a) $5x10^{-5}$ M Ligand 5 , (b) $5x10^{-5}$ M Ligand 6, and (c) $6x10^{-5}$ M Ligand 7, in THF with 100 μL TDDA, with varying concentrations of lithium perchlorate in the presence of fixed concentrations of sodium perchlorate (0.1 and $5x10^{-2}$ M)*

The monochromogenic ligand, Ligand 7, displayed the best lithium against sodium selectivity. Selectivity coefficients of 73.5, 50.0 and 31.6 against 0.05 M sodium and 73.3, 36.8 and 31.5 against 0.1 M sodium for Ligand 7, 6 and 5 respectively were estimated. These values are an improvement on those obtained previously with the nitrophenol ligands [Chapter 3], but since different interfering ion concentrations were used, and as can be observed from the results obtained, selectivity is a function of the concentration of the interfering ion, the values cannot be compared directly.

Figure 4.13 (a) and (b) show the selectivity diagrams at 540 nm for Ligands 8 and 9. Inspite of the narrow absorbance change seen over the $LiClO_4$ concentration range for both ligands it was still possible to observe the effect of fixed $NaClO_4$ concentration of 10^{-2} M and 0.5 M on the $LiClO_4$ response curve and thereby calculate selectivity coefficients. Again the monochromogenic ligand of the series, Ligand 9, demonstrated slightly superior selectivity over its tetra chromogenic counterpart. The selectivity coefficients K_{LiNa} of 50 and 12.5 were

obtained for Ligands 9 and 8 respectively with a fixed background interference of 5 x 10^{-2} M $NaClO_4$.

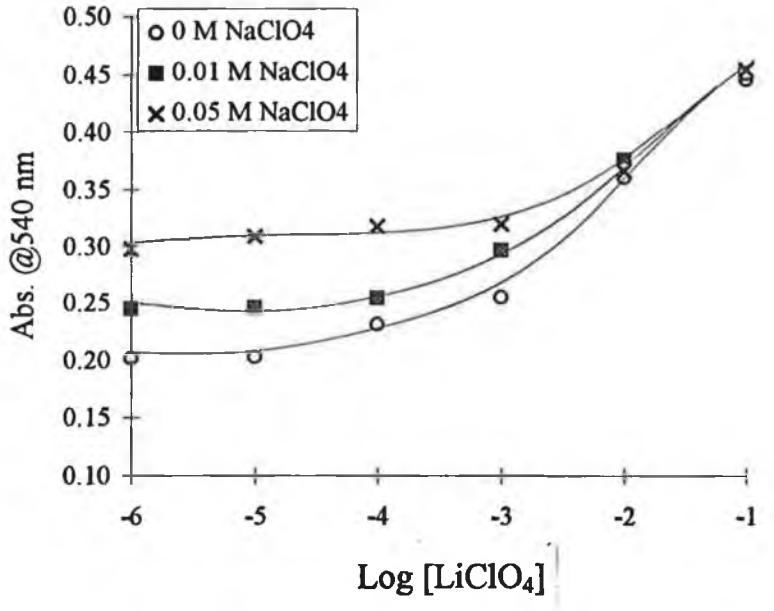

Figure 4.13(a):-Selectivity, Ligand 8.

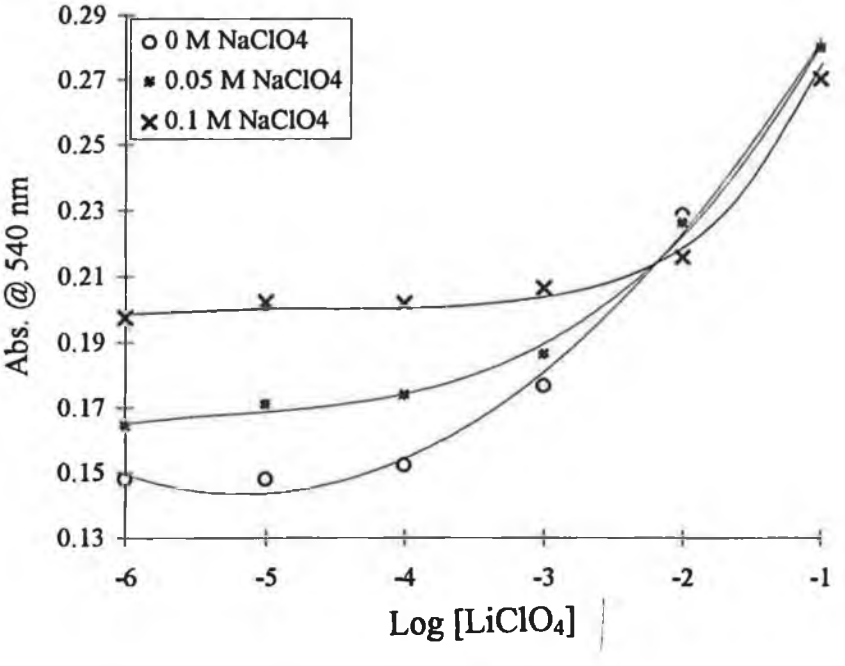

Figure 4.13 (b):- Selectivity, Ligand 9.

Figure 4.13:- *One-phase studies of the optical response at 540 nm of solutions of $5x10^{-5}$ M solutions of (a) Ligand 8 , and (b) Ligand 9, in THF with 100 μL TDDA, with varying concentrations of lithium perchlorate in the presence of fixed concentrations of sodium perchlorate (a) 0.01& 0.05 M, (b) 0.05 & 0.1M.*

A comparison of K_{LiNa} selectivity coefficients for all of the nitrophenylazophenol ligands is shown in table 4.1.

Table 4.1:-Selectivity Coefficients for Ligands 5-9.

Ligand	$[Na^+]$ / M	K_{LiNa}
5	0.1	31.5
5	0.05	31.6
6	0.1	36.8
6	0.05	50.0
7	0.1	73.3
7	0.05	73.5
8	0.05	12.5
8	0.01	10.0
9	0.1	23.4
9	0.05	50.0

4.6 Two Phase Analysis of Nitrophenylazophenol Ligands 5 to 9

4.6.1 Choice of Water Immiscible Solvent

Prior to the examination of the ability of the nitrophenylazophenol ligands to extract cations from an aqueous layer into an immiscible organic layer, a suitable organic solvent had to be found. A suitable organic phase is one which can maintain both the complexed and uncomplexed form of the ligand in it, and prevent any leaching of either form of the ligand into the aqueous phase.

A number of solvents were examined by making up $5x10^{-5}$ M solutions of Ligand 5 in each of a range of solvents. 20 μL of triethylamine (TEA) was added followed by 10 μL of 1 M $LiClO_4$ to give a final $LiClO_4$ concentration of $4x10^{-3}$ M. Finally 2.5 mL of water was added. Any colour changes upon each addition were noted as was the ability of any colour generated to remain in the organic layer. Blank experiments were carried out for each solvent containing everything except the lithium perchlorate for comparison purposes. The colorimetric response observed for each solvent is summarised in Table 4.2.

Table 4.2:- Examination of water immiscible solvents for two phase experiments.

Solvent	*Colour upon addition of TEA*	*Colour upon addition of $LiClO_4$*	*Colour upon addition of water*
1.Dichloromethane	Yellow -> orange	Increase in orange colour	*Org.* Increase in orange *Aq.* Orange and cloudy
2. Butan-1-ol	Yellow -> orange	Slight increase in orange	*Org.* Red *Aq.* Colourless,
3. Butanone	Yellow -> bronze	Red/ Purple	*Org.* No change in colour. Cloudy *Aq.* Red/purple
41,1,1Trichloroethane	Remained yellow	Orange	*Org.* No change in colour. Cloudy. *Aq.* Orange
5. Butan-2-ol	Yellow -> orange	Red/purple	*Org.* Red *Aq.* Clear colourless

Due to the fact that butan-1-ol was capable of retaining all of the colour produced by the ligand-metal-base reaction, it was chosen as the solvent to further examine all three ligands. Butan-2-ol was also tested and although it gave similar results it was found to take up to 30 minutes for it to settle out from the aqueous phase after the two phases had been mixed. Butan-1-ol took approximately 15 minutes to separate from water after the two phases had been mixed. It was found that by using TEA, a large increase in colour intensity which was independent of metal perchlorate concentration was noticed upon addition of water to the system. It was therefore decided to use a weaker and more hydrophobic base. TDDA was examined as an alternative base. The pK_a of TEA in water is 11.01 [13] whereas TDDA has a lower value of 10.6 [14]. Although a different, less polar solvent i.e. butan-1-ol, is being used, it would appear that relative to each other TEA is also a stronger base than TDDA in this solvent.

Upon addition of TDDA a colour change from yellow to barely orange was noted. This colour was stronger than that observed when TDDA was added to solutions of the ligand in THF.

Figure 4.14 shows the change in the single-phase UV-Vis absorbance spectra of Ligand 5 dissolved in butan-1-ol in the presence of TDDA, produced by varying concentrations of $LiClO_4$ using Method 2.5.4 In butanol the maximum absorbance wavelengths were observed at 500 nm for Ligands 5, 6 and 7 with isobestic points at 425 nm. Upon addition of water to the system no colour transfer to the aqueous phase was noted even after a number of days.

Ligand **5** demonstrated the ability to extract $LiClO_4$ from an aqueous phase into the butan-1-ol phase which contained the ligand and the lipophilic base TDDA. The following spectra, shown in Figure 4.15, were obtained when the concentration of $LiClO_4$ was incrementaly increased from 10^{-6} to 10^{-1} M in the aqueous phase using Method 2.5.4.

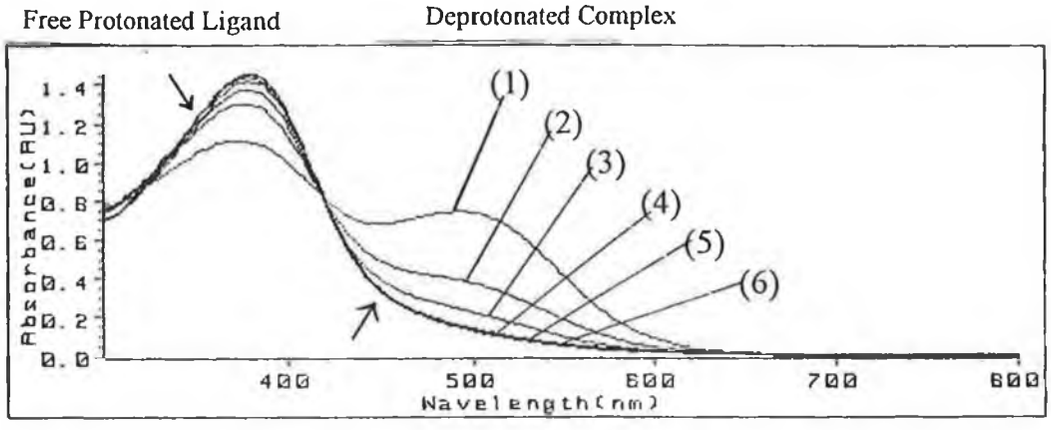

Figure 4.14:- *One-phase investigation of changes in the absorbance spectrum of 2.5 mL of a $5x10^{-5}$ M solution of Ligand **5** in butan-1-ol with 100 μL of TDDA, upon addition of lithium perchlorate, to give final concentrations of (1) 0.1 M, (2) 10^{-2} M, (3) 10^{-3} M, (4) 10^{-4} M, (5) 10^{-5} M, (6) 10^{-6} M. See Table 2.1.*

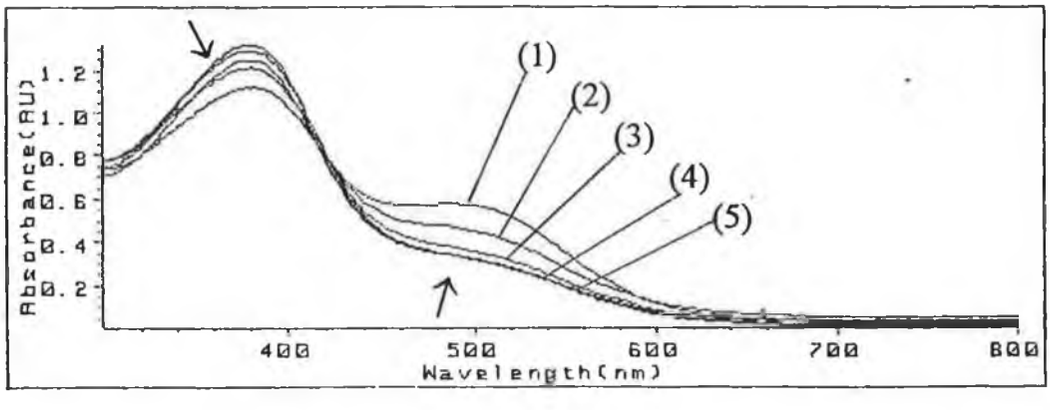

Figure 4.15:- *Two phase study showing changes in the absorbance spectrum of the organic (butan-1-ol) phase for 5 $x10^{-5}$ M Ligand **5** , with 20 μL of TDDA, when lithium perchlorate was added to the aqueous phase of the two phase system to give the following aqueous phase concentrations (1) 0.1 M, (2) 10^{-2} M, (3) 10^{-4} M, (4) 10^{-5} M, (5) 10^{-6} M.*

Although the same absorbance changes observed in the one phase work are not achieved, a discernable difference in absorbance is observed above 10^{-4} M $LiClO_4$. A higher initial absorbance is seen for the ligand-TDDA mixture in the two-phase system compared to that of the one-phase system in butanol. Visually there is an increase in the colour seen when TDDA is added to the two phase system compared to when it is added to the one phase system. This could be attributed to a greater degree of hydration of the ligand-base-solvent mixture which would make the overall medium more polar resulting in an easier deprotonation of the phenolic hydrogen in the presence of the base.

For Ligands **6** and **7**, no colour transfer into the aqueous phase was observed after complexation, however the ability to distinguish between the different levels of $LiClO_4$ has been lost with an even more intense initial TDDA-ligand peak at 500 nm (see Figure 4.16 and 4.17) being observed. None of the ligands was found to undergo significant deprotonation in just the presence of TDDA. However, the lack of transfer of the deprotonated complex to the aqueous phase is significant from a sensor point of view. Ligand **5** has the ability as was mentioned to extract Li^+ from the aqueous phase and further modifications of the properties i.e. basicity of both phases, could result in larger spectral variations beteween the different $LiClO_4$ concentrations.

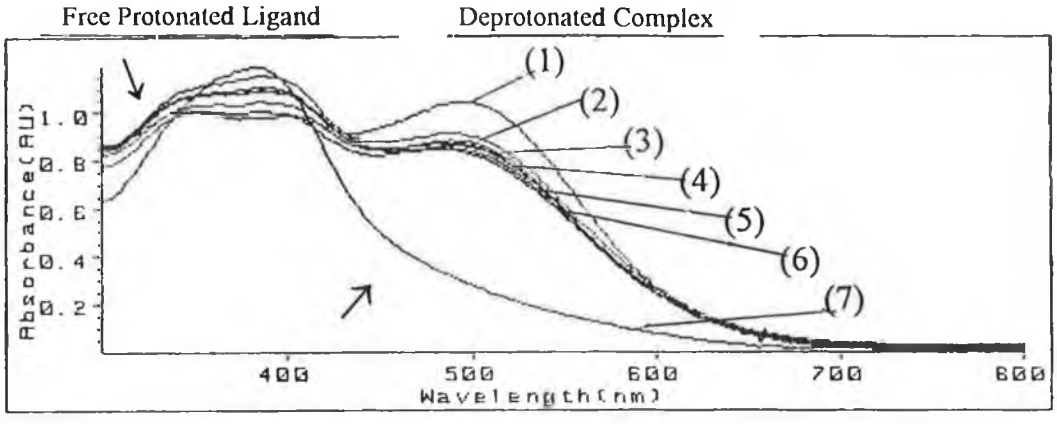

Figure 4.16:- *Two-phase study showing changes in the absorbance spectrum of the organic (butan-1-ol) phase for 5 x10^{-5} M Ligand* **6** *, with 20 μL of TDDA, when lithium perchlorate was added to the aqueous phase of the two phase system to give the following aqueous phase concentrations (1) 0.1 M, (2) 10^{-2} M, (3) 10^{-3} M, (4) 10^{-4} M, (5) 10^{-5} M, (6) 0 M, (7) 0 M, 0 M TDDA.*

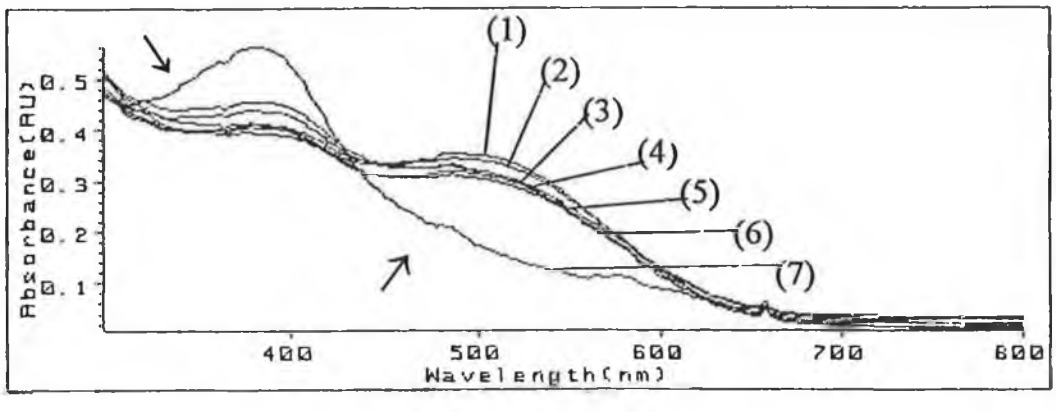

Figure 4.17:- *Two-phase study showing changes in the absorbance spectrum of the organic (butan-1-ol) phase for 5 x10^{-5} M Ligand* **7** *, with 20 μL of TDDA, when lithium perchlorate was added to the aqueous phase of the two phase system to give the following aqueous phase concentrations (1) 0.1 M, (2) 10^{-2} M, (3) 10^{-3} M, (4) 10^{-4} M, (5) 10^{-5} M, (6) 10^{-6} M,) 0 M, 0 M TDDA (7), .*

4.7 NMR Complexation Studies

^{1}H-NMR experiments were carried out using Method 2.5.5. The ^{1}H-NMR spectrum (Figure 4.18(a)) of the ligand between 0 and 0.5 ppm, is not as complicated in this region as the spectrum obtained for Ligand **1** (Figure 3.13(a)). It shows the typical tetrameric calixarene single AB system at 3.2 and 4.75 ppm arising from the non-equivalence of the protons in the Ar-CH_2-Ar methylene bridging groups forming the calixarene annulus, and the strong resonance of the *para-t*-butyl groups at 1.1-1.2 ppm [15]. The high-field doublet at 3.2 ppm as was stated in Chapter 3 was previously assigned to the equatorial protons H_B and the low-field doublet at 4.75 ppm has been assigned to the axial protons H_A (**4(xiv)**) [16]. The complex features around 1.0-1.5 ppm are thought to arise from a distorted cone structure in the calixarene, i.e. the annulus is twisted possibly by intra molecular hydrogen bonding which render the *para*-t-butyl groups non-equivalent [17].

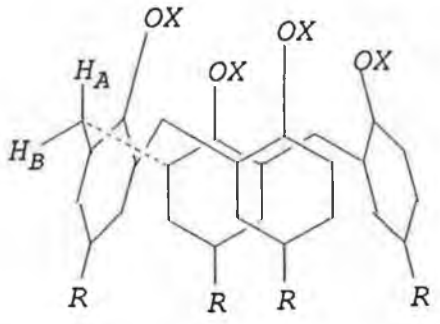

R = *p-t*-butyl

4(xii) *Cone shaped Calix[4]arene Showing the Bridging Methylene Protons, (the double bonds of the aromatic rings have been omitted to aid clarity).*

^{1}H-NMR spectra (Figure 4.18a-c) of different molar ratios of NaSCN to **5** (both in CD_3OD) strongly suggest that the molecular conformation of the ligand becomes much more ordered on complexation. Figure 4.18 (b) shows the effect of adding 0.5 mole equivalent of sodium thiocyanate to the ligand (where $[Na^+]/[ligand] = 0.5$). Two new doublets associated with the AB system have appeared at 3.4 and 4.3 ppm. The reduction in separation of these doublets is caused by changes in the environment of the bridging methylene protons brought about by the presence of M^+ which has the effect of changing the angle of the CH_2 protons. The upfield shift of the H_A protons to 4.3 ppm indicates that these protons are very sensitive to small variations in the polar environment of the aromatic ether and ester oxygens which are in close proximity and that they have become more shielded from the effects of this hydrophilic cavity made up of the

oxygen heteroatoms. The H_B protons experience a down-field shift to 3.4 ppm as they become less shielded from the effects of the hydrophilic cavity. This is due to a slight change in the angle of the H_B protons upon metal ion inclusion. The convergence of the H_A and H_B protons is indicative of the occurrence of complexation with the cation [15-17].

Another important spectral change occurs at this level of NaSCN. A simplification of the signals due to the *t*-butyl protons is evident and is indicative of a more ordered structure being conferred on the whole molecule with complexation [15-17]. Such an interpretation is consistent with both x-ray crystal studies of calixarenes and their complexes [18] and with molecular dynamics studies [19] which were discussed in Chapter 3.

Addition of a 1.0 mol equivalent of sodium (**R**=1.0, Figure 4.18(c)) leads to the complete disappearance of the complex feature at 1.0-1.5 ppm, replaced by a single, strong resonance at 1.2 ppm, and the full development of the new doublets of the AB system at 3.4 and 4.3 ppm. Further change in the metal-to-ligand ratio has no effect on the ^{1}H-NMR spectrum. No colour change was noted during any of the above experiments in contrast to the experiments performed in the presence of a base discussed earlier (section 4.2.2). Above a concentration of 1 mole equivalent, any subsequent addition of NaSCN resulted in no further positional shifts in the ^{1}H NMR spectrum. This is indicative of a 1:1 metal-ligand stoichiometry.

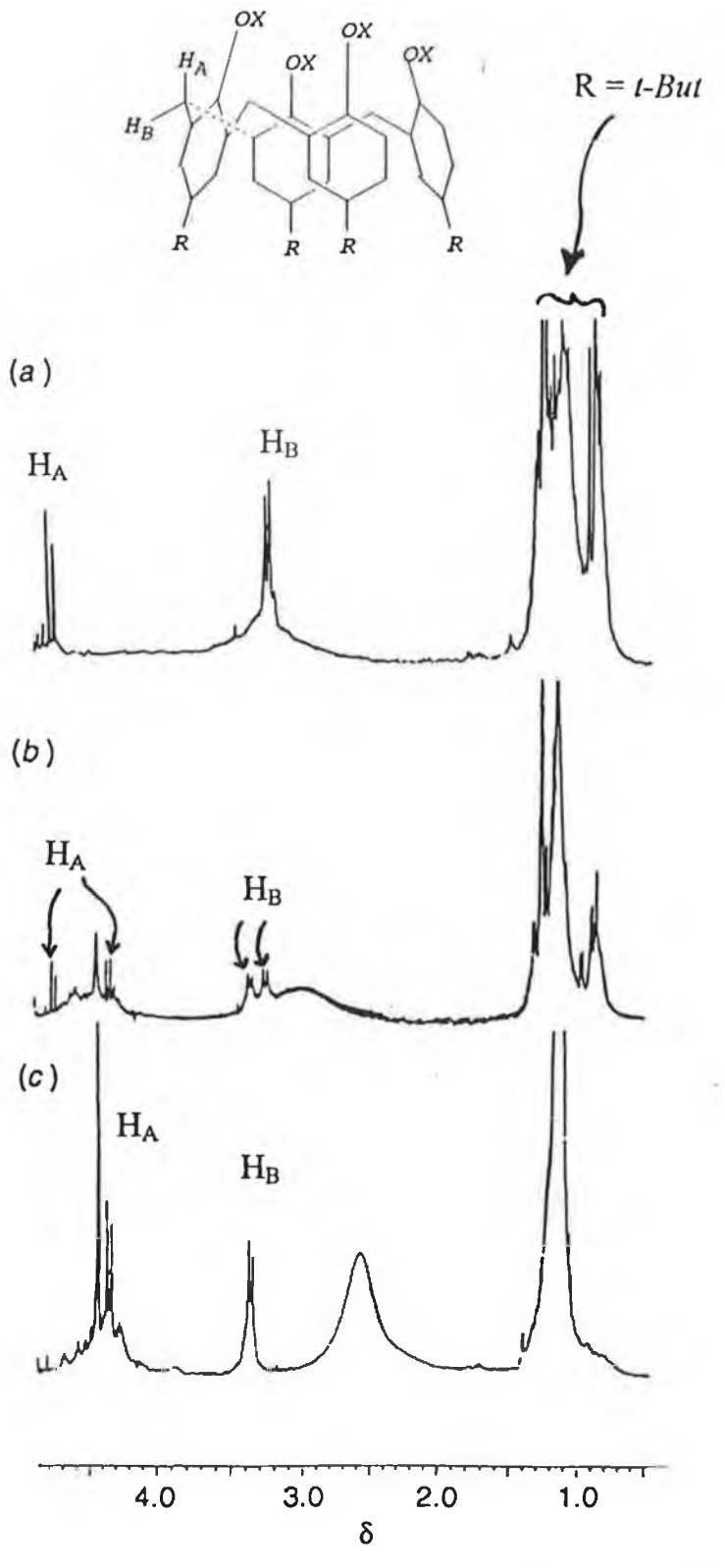

Figure 4.18:-The effect of complexation with Na^+ on the ^{1}NMR spectrum of 5. Aliquots from a CD_3OD solution of 1.0 M NASCN were added directly to a 2.3 mM solution of 5 in $CDCl_3$ in an NMR tube. p-tert-butyl H; H_A, H_B =$ArCH_2Ar$. Conditions: (a) [NaSCN]/[5] = 0 (no metal added); (b) [NaSCN]/[5] =0.50; (c) [NaSCN]/[5] = 1.00. See Method 2.5.5.

4.8 Discussion

Five novel chromogenic calix[4]arenes bearing nitrophenylazophenol groups have been examined and (like three of their nitrophenol counterparts, see Chapter 3) they all displayed lithium selectivity over sodium.

Table 4.3:- Comparison of Data obtained for Ligands 1 to 9 obtained from UV-Vis experiments

Ligand	[Ligand]	Prot. λ_{max}	Deprot. Li^+ λ_{max}	Li^+ Lin. range	Li^+ Slope a.u./dec	L.O.D. (M)	$K_{Li,Na}$
1	$5x10^{-5}$	350	424	10^{-4} - $5x10^{-2}$	0.325	$< 10^{-4}$	25.1 *a*
2	$7x10^{-5}$	350	424	10^{-4}-10^{-3}	0.250	$< 10^{-4}$	34.7 *a*
3	$5x10^{-5}$	350	424	10^{-4}-$5x10^{-3}$	0.900	$< 10^{-4}$	43 1 *a*
4	$5x10^{-5}$	330	416	10^{-5}-10^{-3}	w.o.	$< 10^{-5}$	~ 10 *a*
5	$5x10^{-5}$	380	520	10^{-4}-10^{-1}	0.519	$< 10^{-4}$	31.6 *b*
6	$6x10^{-5}$	380	520	10^{-4}-$5x10^{-2}$	0.66	$< 10^{-4}$	50.0 *b*
7	$5x10^{-5}$	380	520	10^{-4}-10^{-1}	0.059	$< 10^{-4}$	73.5 *b*
8	$5x10^{-5}$	n.d *	540	10^{-3}-10^{-1}	0.096	$< 10^{-3}$	12.5 *b*
9	$5x10^{-5}$	n.d.*	540	$5x10^{-3}$-10^{-1}	0.039	$< 10^{-3}$	50.0 *b*

* n.d. = not determinable

a Selectivity determined with a $NaClO_4$ interferent concentration of 10^{-2} M

b Selectivity determined with a $NaClO_4$ interferent concentration of $5x10^{-2}$ M

The absorbance maximum for both the Li^+ and Na^+ complexes appears at the same wavelength, for all of the ligands i.e. 520 nm for Ligands 5 to 7 and 540 nm for Ligand 8 and 9, suggesting the existence of a similar mode of complexation for both cations. A variation in λ_{max} with the complexation of different cations is seen in the case of neutral chromoionophores in which the chromogenic moiety is sited either within or in close proximity to the ionophoric cavity [20], structure 4(xiii) . For example, inclusion of a cation into the cavity of this structure, (part of which was made up of the neutral chromogenic moiety), resulted in an electronic disturbance which propagated through the whole n and π system. Thus variations in the extent of interaction between the chromogenic moiety and the various cations, resulted in variations in the resulting λ_{max} of the complexes formed. A similar situation was described in Chapter 3 for Ligand 4, in which the ionisable phenolic chromophore was housed within the calixarene cavity.

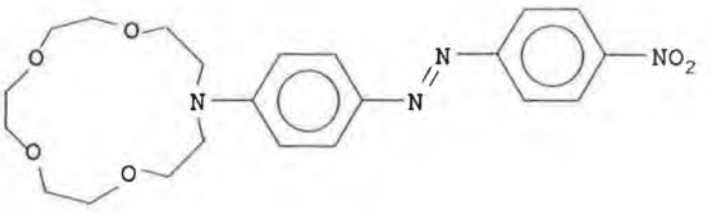

4(xii)
Neutral Chromoionophore [20].

Ligands 8 and 9 showed two main differences to Ligand 5 to 7.

- Firstly they displayed a deprotonated complex λ_{max} at longer wavelengths i.e 540 nm vs. 520 nm.
- Secondly, the actual intensity produced upon metal-ion complexation was much lower than for Ligands 5 to 7 i.e. for the two tetrachromogenic Ligands 8 and 5, maximum absorbances of 0.45 a.u. and 2 a.u. respectively were obtained.

In both of these the calixarene backbone is attached in the *meta* position relative to the ionisable phenolic group of the chromogenic moiety whereas in Ligands 5 to 7 it is attached in the *ortho* position. This change in positions of the phenolic group may result in it being too remote from the hydrophilic cavity to allow significant interaction between the deprotonated chromophore and the cavity housing the metal cation. Therefore, the electronic transitions responsible for generating the deprotonated complex spectrum are not as favourable as before. This emphasises the difficulty in producing a successful "designer" molecule, since the interactions involved in generating the colour change are very subtle and impossible to predict.

The spectral peaks observed with these ligands were found to be much broader than those seen for the nitrophenol ligands (Ligands 1 to 4), This is possibly due to a more complex intramolecular energy being involved with these larger, more complex chromogenic groups [12].

Cause of Colour

The principle on which these molecules change colour on complexation in the presence of a base, is the same as that described for Ligands 1 to 3, since again we are dealing with ionisable chromoionophores. These ligands also depend on the dissociation of the phenolic hydrogen of the chromogenic moiety (in this case a nitrophenylazophenol) for colour generation.

Mode of Complexation

The equations and equilibria outlined in Chapter 3 (**3.1** to **3.9**) are again fundamental to understanding the role played by the ligands, the base and the metal cations. No real colour change is observed with the addition of the base prior to the addition of $LiClO_4$ or $NaClO_4$. This again signals that the inclusion of a metal cation into the calixarene cavity is exerting an effect on the ionisable chromophore, thereby lowering its pK_a and facilitating proton uptake by the base. The UV-Vis experiments in section 4.4 clearly indicate a spectral response to Li^+ at lower concentrations than Na^+, with the inclusion of the cations causing an increase in the absorbance of the deprotonated complex λ_{max}.

The variation in response to different cations, as was stated in Chapter 3, is a function of both the stability constant β of the complex, and of the effect the inclusion of a cation has on the pK_a of the dissociating phenolic proton. Cavity size and level of preorganisation for cation inclusion is important in determining the magnitude of β as is the number of heteroatoms (in this case oxygen atoms) available for electrostatic interaction with the incoming cation by formation of the hydrophilic cavity [21]. Since calix[4]arenes tetraesters make up the ionophoric part of the molecule with Ligands **5**, and **7** to **9** from the outset it would be expected that they would show optimum uptake of smaller cations i.e. Na^+ and K^+ as opposed to the larger Cs^+ and Rb^+ which have been found to be more likely to be complexed by the calix[6]arenes which have a much larger cavity available [25]. In previous studies where calix[4]arene tetraesters [23, 24] and ketones [25] were incorporated into PVC membranes and used for potentiometric measurements selectivity was observed for Na^+ over K^+ with very little or no response to Li^+. Similarly in extraction studies using similar calix[4]arenes [22], sodium selectivity over K^+ and Li^+ was again observed. Therefore as with the nitrophenol ligands of Chapter 3, the Li^+ selectivity was quite surprising. Potentiometric studies with Ligand **4** were attempted but due to to solubility problems of the membrane components no conclusive results were obtained. The reduced spectral response observed with the introduction of $NaClO_4$ is likely to be associated more with the effect Na^+ has on the pK_a of the ionisable phenol compared to Li^+ than it has to do with the stability constant β of its complex. Undoubtedly complexation occurs with Na^+ (as shown by ^1H NMR experiments to be discussed below) and Li^+, but the less densely charged Na^+ cation cannot quite exert the same effect on the pK_a of the phenolic proton of the chromophore a phenomenon which has been reported by other workers [26, 27].

Therefore complexation with Li^+ occurs at lower concentrations than Na^+, although the Na^+ cation may possibly be more suited to the size of the calix cavity, but the possibility that Li^+ enters the cavity in its hydrated form, thus increasing its ionic radius may not be ruled out.

Therefore, both the pK_a and stability constants of the complexes are both interrelated and interdependent when it comes to determining which cation will cause the greatest spectral change. Once complexation occurs, the relinquishing of the proton by the chromogenic moiety to give effectively a molecule which is overall neutral, is energetically more favourable than it would be for the molecule to remain with a single positive charge.

On examining the structures of the ligands 5 to 7 it can be seen that the deprotonating phenol group is potentially much closer to the ester groups directly attached to the calix[4]arene backbone than was the case with Ligands 1 to 3 and therefore there is greater potential for the inclusion of a cation in the hydrophilic cavity to exert an effect on the chromogenic moieties. A greater degree of preorganisation may even be afforded by the chromogenic phenolic oxygens. The lack of suitable crystals for the x-ray analysis of either the ligands or their complexes again precludes a definitive explanation of the exact interaction of the hydrophilic cavity containing the cation and the chromogenic moiety.

Selectivity

A slight improvement in K_{LiNa} was observed with these nitrophenylazophenol ligands compared to the nitrophenol ligands of Chapter 3, with a maximum of a 75-fold selectivity being seen for the monochromogenic ligand, Ligand 7. The reasons for Li^+ selectivity were outlined above. Higher concentrations of sodium were tolerated with these ligands in the presence of lithium, which is a reflection on the difference in the shape of the response curves observed by the nitrophenylazophenol ligands compared to those observed for the nitrophenol ligands, see Figure 4.19 for comparison. With the nitrophenol ligands, although no significant response was observed before a final concentration of 10^{-3} M $NaClO_4$ had been added, the highest concentration of 0.1 M $NaClO_4$ exhibited an absorbance at the deprotonated λ_{max} at approximately the same level as that exhibited by the 0.1 M $LiClO_4$ solutions. In contrast the response to 0.1 M $NaClO_4$ for the nitrophenylazophenol ligands was seen at much lower levels to that of 0.1 M $LiClO_4$.

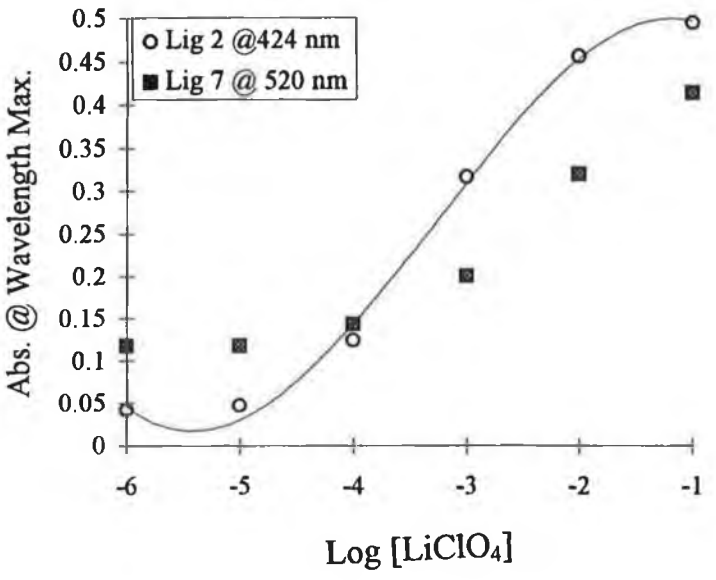

Figure 4.19:-Comparison of Li^+ response for monochromogenic (1) Nitrophenol Ligand 2 and (2) nitrophenylazophenol Ligand 7.

In terms of chromogenic determination of Li^+, an approximate 75 fold selectivity is a slight improvement on the nitrophenol ligands described in Chapter 3 but is still a good deal away from the ideal situation where a 1000 fold selectivity for Li^+ over Na^+ is the optimum.

The use of the nitrophenylazophenol ligands accomplished one of the aims set out at the start of this chapter, to achieve larger λ_{max} shifts and therefore move the deprotonated λ_{max} into a more useful region of the spectrum in terms of instrumentaion development. A bathochromic shift on deprotonation from 380-520 nm is observed for these ligands compared to a shift from 350-426 nm for the nitrophenol ligands, with the molar extiction coefficient values (ε) being large enough (i.e 5×10^3 - 10^5 L mol^{-1} cm^{-1}) for use as the indicator components in optical sensors.

Solvent Effects

On changing the solvent from THF to Butan-1-ol, a hypsochromic λ_{max} shift of 20 nm was observed. Butanol is a slightly more polar solvent than THF i.e. dielectric constant $_{(butanol)}$ =17.8, dielectric constant $_{(THF)}$ = 7.6 [13]. The greater ionising ability of butan-1-ol would be expected to result in a greater degree of phenolic dissociation in the presence of TDDA. Effectively the whole medium is slightly more polar than was the case with THF. This increased colour is indicative of a solvent dependency on coloration with (in this instance) butan-1-ol being a more polar solvent than THF and therefore a variation in λ_{max} would be predicted in this new medium.

This decrease in λ_{max} concurs with the behaviour seen for Ligands 1 to 3 on changing solvent from THF to either methanol or butan-1-ol. A hypsochromic shift like that observed here on going to a more polar solvent has been associated with $n \rightarrow \pi^*$ transitions [28]. Polar solvents tend to stabilise both the non-bonding electronic states and π^* excited states of polar chromophores like those in Ligands 5 to 7 causing the transitions to move to higher energies. However, as with the Ligands 1 to 3 the intensity of these ligands is quite large i.e. protonated ligand at 5×10^{-5} M has an extinction coefficient of 2.8×10^4 $M^{-1}cm^{-1}$. Such a strong absorbance is generally associated with the "allowed" π to π^* transition.

Confirmation of Complexation

Confirmation of metal ion complexation was again demonstrated in the absence of colour generation by ^1H NMR spectroscopy experiments in which characteristic peak shifts were observed upon addition of NaSCN to Ligand 5.
A number of conclusions can be drawn from these experiments:-

- Complexation was judged to have occurred, as the signals for the H_A and H_B protons were seen to move towards each other on metal-ion inclusion.
- On formation of the complex, the ligand adopts a much more symmetrical conformation. This was seen in the simplification of the signals due to the *t*-butyl peaks into a singlet.
- No further spectral shifts were observed after a 1:1 metal:ligand ratio had been reached and therefore the metal-ligand complex was concluded to have a 1:1 stoichiometry, with the equilibrium favouring the formation of the complex.

- No deprotonation of the ligand occurs on complexation since no base was present. This again highlights the point that for colour generation two processes have to occur, namely

1. Cation inclusion depending on β
2. Effect on $pK_a \rightarrow$ phenolic proton exchange with suitable base,
   and that in the absence of either of these, a colour change will not occur. (See discussion earlier for processes).

Two-Phase Studies

The two phase results for Ligand **5** were the best seen for all of the ligands examined in terms of combining two important properties i.e ability to extract Li^+ from an aqueous phase causing a colour change in the organic phase, and also ability to maintain the deprotonated complexed form in the organic phase. Ligand **5** demonstrated the ability to extract Li^+ from an aqueous phase causing a colour change, (Figure 4.15) with the intensity of the colour produced being dependent on the $LiClO_4$ concentration in the aqueous phase. Above 10^{-4} M $LiClO_4$ (spectrum 4 of Figure 4.15) a discernible increase in absorbance at the deprotonated λ_{max} was seen with increasing $LiClO_4$. No colour transfer due to the deprotonated complex transferred into the aqueous phase. Neither Ligand **6** nor Ligand **7** exhibited a transfer of colour into the aqueous phase, but the ability to distinguish between different concentrations of $LiClO_4$ had been lost. The lack of colour transfer with the nitrophenylazophenol ligands compared to the nitrophenol ligands is due to the much more lipophilic nature of this chromogenic moiety. The effect of a second aromatic ring seems to outweigh the effect of the hydrophilic nitro and phenolic chromophores and stabilises the molecule in the organic phase.

The increased absorbance seen for the deprotonated form of Ligands **6** and **7** in butanol compared to THF, (compare 4.16 with 4.3 (a) and 4.17 with 4.5 (a)) in the presence of only the base is indicative of the effect a change in solvent has on the pK_a of the ionisable phenilic group. The higher dielectric constant of butan-1-ol compared to THF seems to effect the pK_a of the Ligands **6** and **7** to a greater extent than Ligand **5** where only a slight change in absorbance was seen in the absence of Li^+. Another factor which could be causing the high absorbance of Ligands **6** and **7**, (Figure 4.16 and 4.17) in the two phase system is the influence the amphiprotic solvent, water, has on the polarity of the organic phase. Although two separate layers form when butan-1-ol and water are mixed, a

ceratin percentage of water is soluble in butan-1-ol i.e. 20.5% w/w, [29]. Therefore after mixing there will be a considerable water content in the organic phase. This will have the immediate effect of increasing the overall polarity of the solvent, thereby facilitating the existence of ions, and from the two-phase spectra of Ligand 6 and 7 it would appear that it is altered sufficiently to effect the dissociating phenolic proton of both of these molecules. Ligand 5 does not appear to be quite as susceptible to this potential effect and may be indicative of the four chromogenic moieties of this molecule taking up a conformation which reduces the effect of subtle solvent changes on the phenolic protons.

The higher intensity of the Ligand-TDDA peaks for both Ligand 6 and 7 may be a possible indication of a difference in initial pK_a of the phenolic protons of both of these compared to Ligand 5. In Ligand 5, which has four chromogenic nitrophenylazophenol groups, there is a possibility of intramolecular H bonding between adjacent phenolic groups of the chromogenic groups, since rotation of these groups about the OCH_2-(C*OH), (where C* represents the chromogenic moiety) bonds would be possible. With Ligands 6 and 7 this would not be possible as these ligands contain only one or two chromogenic moieties respectively, and the introduction of water may result in H bonding with the phenolic oxygens of the chromogenic moieties which could facilitate phenolic proton transfer to TDDA as the immediate environment around the phenols would be more polar leading to an increase in ionising ability. The degree of solvation of the ligands and their susceptibility to slight modifications in the polarity of the medium in which they are housed, by the introduction of small quantities of water, is not necessarily the same for all of the ligands. However no evidence was found during the one-phase experiments for the existence of a substantial difference in pK_a values between the Ligands 5, 6 and 7.

No colour transfer of the deprotonated complex of Ligands 5 to 7 was observed from butanol into an aqueous phase, possibly due to the hydrophobic nature of the much bulkier chromogenic moieties on these compounds compared to those of Ligands 1 and 3. However only Ligand 5 displayed the ability to extract $LiClO_4$ from such an aqueous phase into the organic phase housing the ligand (Figure 4.15) and the base but the intensity of the response to each individual concentration was greatly diminished. This caused a bunching of the peaks for the various $LiClO_4$ concentrations although it is possible to distinguish between the peaks at concentrations above 10^{-3} M. This is due to the fact that in the two phase experiments, the Li^+ cation has to be extracted from the aqueous phase and

therefore the concentration of Li^+ in the organic phase will be lower than when the salt was added directly to the organic phase as it was in Figure 4.14.

The Future

Further work on all of these compounds could include

- Optimisation of the organic solvent and reaction conditions used.
  The work described here displayed a large solvent dependency due to the varying ionising abilities of different solvents, which resulted in a variation in the ease with which the phenolic proton of the chromogenic moiety is removed.
- Measure accurately the fundamental properties of some of these materials (i.e pK_a, β values, effect of pH on the compounds,)
  The results obtained demonstrated that different cations effect the chromogenic calix[4]arenes in different ways. A comparison of these values, for all of the ligands studied may lead to a clearer picture of the importance that subtle differences in ligand substituents have on the whole molecule.
- Fabrication/immobilisation of materials on substrates to produce an optical sensor.
  The ultimate application of this type of chromogenic ionophore is the development of an optical sensor for cation analysis. A suitable immobilisation technique for these materials on a substrate such as an optical fibre will be of primary importance if these compounds are to be utilised fully.

4.9 Gaseous Amine Detection

Introduction

The vital role played by a suitable base in the ionisable chromogenic system has been highlighted in both Chapters 3 and 4. The actual nature of the base is also very important, with different bases conferring slightly different properties, in terms of intensity, on the systems. A clear example of this was seen in section 4.6.1 where a strong base such as TEA caused a colour change to red in the absence of metal perchlorate, but the slightly weaker base TDDA could not produce this clear change until metal perchlorate had been added. The equations outlined in Chapter 3 have been shown to hold true both in UV-Vis and NMR experiments and it is equation 3.5 which evoked the investigation of the potential of the Ligand-metal complex to produce a colour change upon reaction with gaseous amines.

$$L\text{-}COH + M^+ \overset{\beta}{\rightleftharpoons} LM^+\text{-}COH \qquad \textbf{(3.3)}$$

$$LM^+\text{-}COH + B \overset{K_{a(C)}}{\rightleftharpoons} LM^+\text{-}CO^- + BH^+ \qquad \textbf{(3.5)}$$

$$L\text{-}COH + B \overset{K_{a(L)}}{\rightleftharpoons} L\text{-}CO^- + BH^+ \qquad \textbf{(3.1)}$$

As was previously stated a very strong base is required to cause phenolic-proton dissociation on its own, whereas the presence of a metal cation had the effect of rendering the chromophore phenolic proton more labile and thereby lowering the pK_a value.

In this section Ligand **5**, the tetra-nitrophenylazophenol ligand capable of producing the largest absorbance change (1.7 a.u. from 10^{-4} to 10^{-1} M $LiClO_4$) upon interaction with $LiClO_4$ is assessed for its potential as a gaseous amine indicator system. Since the actual colour, rather than the intensity, produced in the one phase experiments with Ligand **5** did not vary from metal to metal or from base to base, it was envisaged that this new system would produce an indicator capable of detecting gaseous amines in a non-selective manner. Trimethylamine (TMA) concentrations in the range 0.05 to 5 ppm are currently

often measured using commercial Gastec amine indicator tubes [30]. As was discussed in Chapter 1, certain gaseous amines such as TMA and DMA are produced as sea fish spoil [31]. The development of a rapid indicator system to monitor the freshness of fish by the monitoring of gaseous amines produced could be of major benefit to the food industry.

So in this section the ligand-metal-base system previously used to detect the presence of metal ion (M^+) is being reversed i.e. using the complex to detect the base (B). As the sample would not normally contain volatile bases selectivity is not a prerequisite for the application envisaged.

4.10 Liquid Phase Experiments

For any visual indicator system to be effective, a large colour/spectral difference must exist between the indicator prior to interaction with the species of interest and after interaction. As was seen in section 4.2.2 , the higher the concentration of $LiClO_4$ added to the ligand base mixture, the more intense the colour obtained. A number of $LiClO_4$ concentrations were examined in order to optimise the analytical range of the method. Butanol was chosen as the solvent for the dissolution of the ligand in the liquid phase experiments due to its high boiling point which rendered heating of the gas tight vessel to enhance the release of TMA from aqueous solution possible.

Method 2.6.1 was followed for the liquid phase experiments. A 2.5 mL solution containing $5x10^{-5}$ M of Ligand **5** of 0.5 M $LiClO_4$ in butanol was placed in a test tube in a gas tight vessel. Fixed volumes between 0.2 and 50 μL of a 25% aqueous TMA solution were injected into a 550 mL capacity vessel through a supa-seal cap, ensuring that none of the liquid entered the test tube containing the indicator solution. This gave final TMA concentration in the approximate range 0.1 to 25.0 ppm, assuming all TMA passes into the gas phase. A schematic of this experimental setup is shown in Figure 4.19. The vessel was heated gently in a 50°C oven to aid the evolution of TMA (b.p.2.9° C) from the aqueous form. After reaction samples of the solution were removed in order to obtain the UV-Vis spectra between 300 and 800 nm.

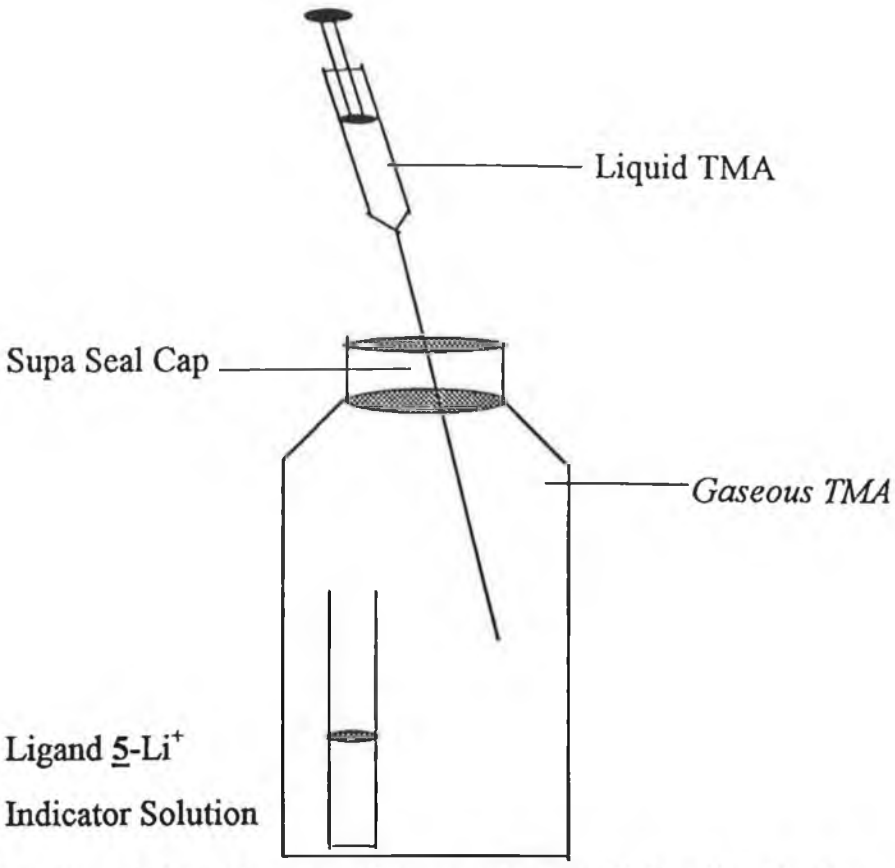

Figure 4.20:- *Figure of apparatus used for liquid-phase gaseous amine detection.*

On release of the TMA inside the gas tight vessel, the colour of the indicator solution changed from yellow to red. This colour change occurred instantaneously at the butan-1-ol gas interface and spread throughout the whole solution after the vessel was shaken. Since no base was added to the indicator solution prior to the introduction of the gaseous TMA, the initial colour of the ligand-metal complex was yellow rather than the bronze colour seen in section 4.2.2. The colour change was simply due to the deprotonation of the complex. Figure 4.20 shows the spectra obtained for the above experiments. A λ_{max} of 500 nm is seen for the deprotonated Li^+ complex of Ligand **5** in butanol with the λ_{max} of the protonated complex occurring at 376 nm and an isobestic point is visible at 420 nm

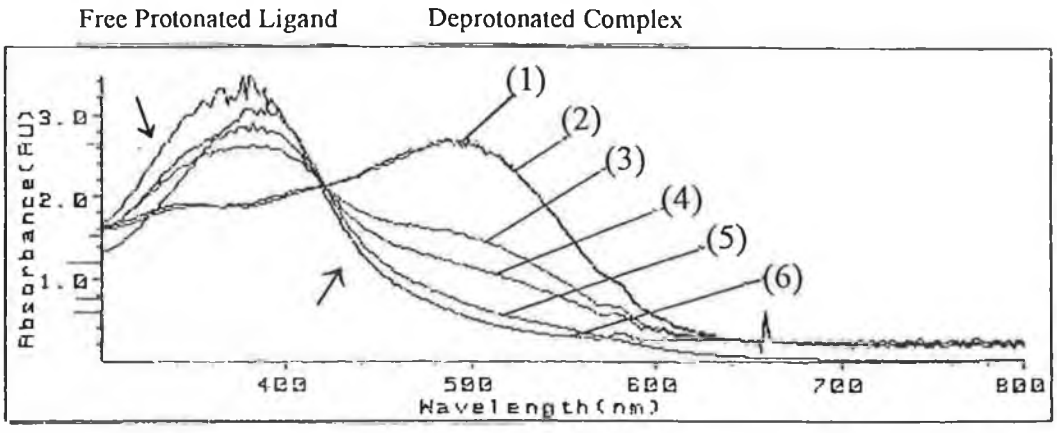

Figure 4.21:- *UV-Vis spectra showing the effect of TMA on the UV-Vis spectrum of the complex. Changes in the absorbance spectrum of a 2.5 mL solution of* $5x10^{-5}$ *M Ligand* **5** *with 0.5 M* $LiClO_4$ *in butanol, upon exposure to gaseous TMA in the following concentations: (1) 45.00 ppm , (2) 22.50 ppm, (3) 4.88 ppm, (4) 2.25, (5) 0.45 ppm, (6) 0 ppm.*

Figure 4.22 shows a graph of the absorbance at 500 nm versus the concentration of TMA. A change in absorbance is observed even at the lowest concentration level of 0.45 ppm, and rises rapidly between this value and 4.88 ppm. A further increase is observed up to 22.5 ppm but the curve is no longer linear and no further increase in absorbance is seen above this level. The time taken for colour development ranged from under 10 seconds for concentrations above 4.5 ppm to 3 hrs for 0.45 ppm. However, these times are diffusion limited rather than a reflection of the reaction rate, as the TMA has to partition from the gas into the butanol phase, react with the ligand, and the coloured deprotonated complex, then has to diffuse throughout the bulk butanol phase. Reproducibility at sub ppm levels was difficult due to the very slight colour change which was involved and the time which it took for colour evolution. The high viscosity of butanol, 2.95 mN sec m^{-2} [11], may have contributed to the time delay between injection of the TMA sample and colour evolution at the lower concentration levels.

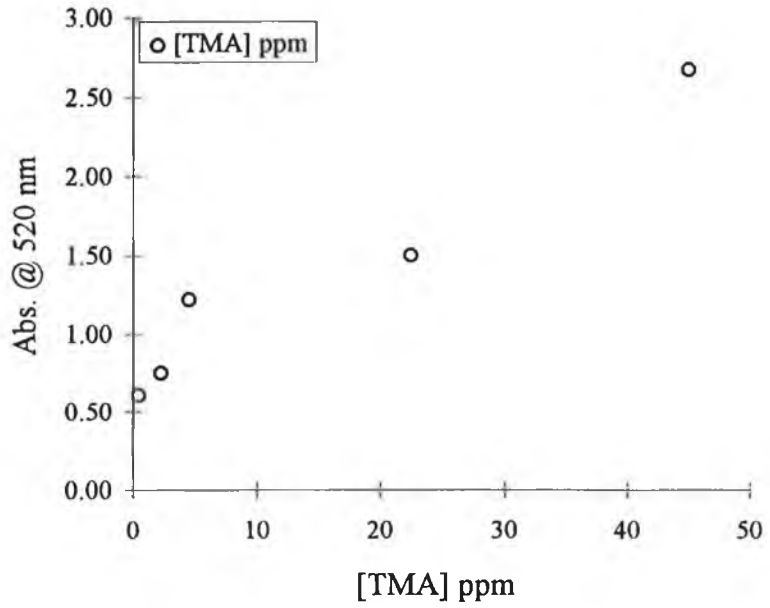

Figure 4.22:- *Graph of absorbance of Ligand* **5** *lithium complex at 500 nm versus [TMA].*

Similar experiments were carried out in which either the ligand or $LiClO_4$ concentration was varied. Above a concentration of $5x10^{-5}$ M Ligand **5** the absorbance of the protonated form of the ligand was above the range of the instrument i.e > 3 a.u. Sample dilution could have been carried out to bring the absorbance of the sample on to the scale of the instrument. In this system an equilibrium between the gaseous amine and the protonated complex is set up in the gas tight environment. Upon removal of the indicator solution from this environment the concentration of base in contact with the indicator solution is drastically reduced and in order to reestablish equilibrium some of the gaseous base will diffuse into the surrounding environment which resulted in a colour change back to the original yellow.

Variations in $LiClO_4$ concentration in the ligand solution, would be expected to result in different deprotonated spectra in the presence of the same concentration of TMA. This was seen in section 4.4 where with increasing $LiClO_4$ concentration an increase in absorbance at the deprotonated complex λ_{max} was seen in the presence of fixed concentrations of TDDA. Such a variation could be

used to vary the concentration range for which the complexed ligand could respond. Figure 4.23 shows the change in spectrum for $5x10^{-5}$ M Ligand **5** , 2.5 M $LiClO_4$ added directly to the solution as a solid, to the presence of 2.25 ppm TMA. Comparing the response of the indicator solutions which had been made up with different $LiClO_4$ concentrations to the presence of 2.25 ppm in Figures 4.21 and 4.23 illustrates the point that the intensity of the colour change observed upon interaction with certain TMA concentrations can be controlled by the concentration of $LiClO_4$ in the indicator solution. This point is reiterated in Figure 4.24 where a 0.1 M $LiClO_4$ concentration, with $LiClO_4$ introduced into 2.5 mL indicator samples as 20 μL of 3.3 M $LiClO_4$ (aq.), similar spectral shifts to that seen in Figure 4.21 is produced only after a final gaseous TMA concentration of 50 ppm is present.

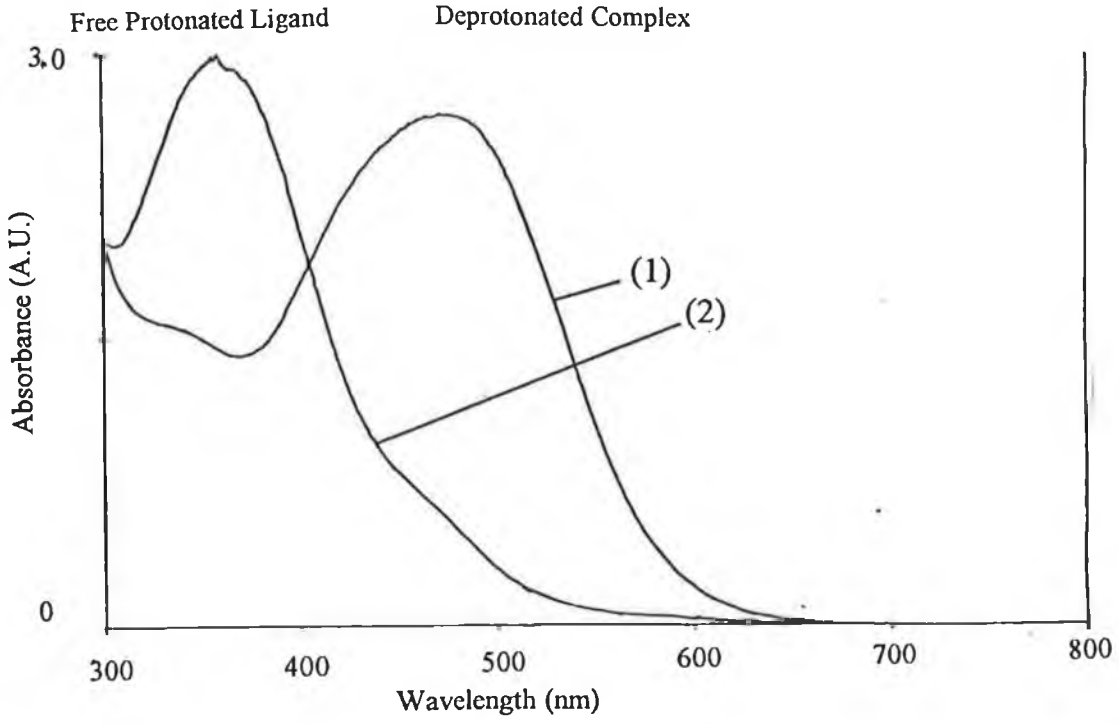

Figure 4.23:-Spectra of $5x10^{-5}$ M Ligand 5 with 2.5 M $LiClO_4$ in the presence of TMA concentrations of (1) 2.27 ppm and (2) 0 ppm.

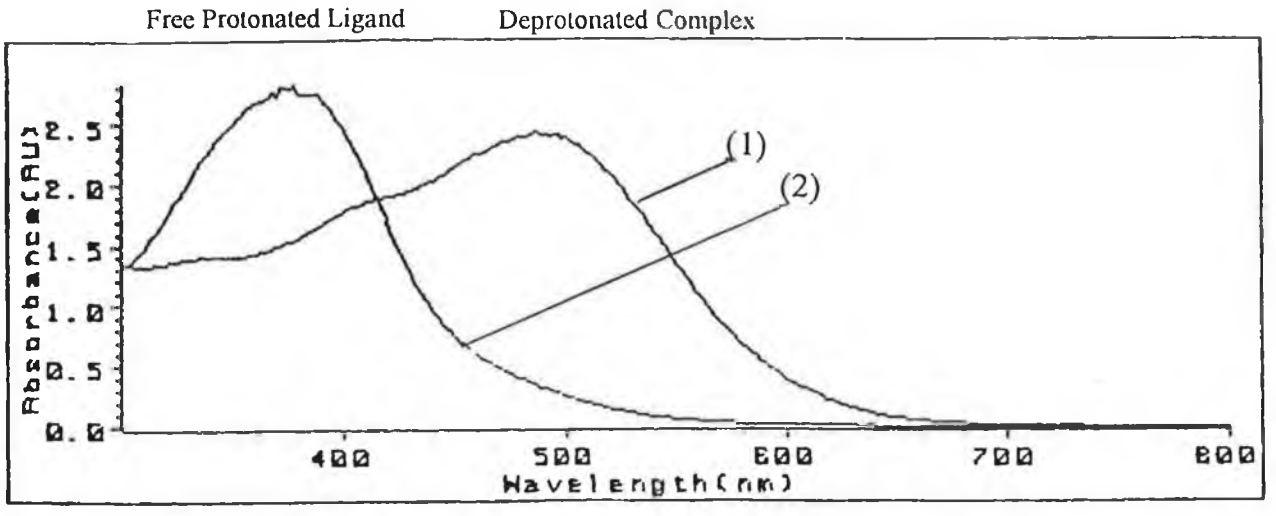

Figure 4.24:-Spectra of $5x10^{-5}$ M Ligand 5 with 0.1 M $LiClO_4$ in the presence of TMA conentrations of (1) 50 ppm and (2) 0 ppm.

From the liquid phase experiments it can be concluded that the Ligand 5-Li^+ complex is capable of detecting TMA, with the concentration of $LiClO_4$ having a large bearing on the concentration range of TMA concentrations which can be determined.

4.11 Test Strip Results

The above initial screening experiments established that the principle of using the ligand complex to determine gaseous amines was possible. The goal of the work was to develop a workable, quick test for such gases. One of the problems quoted in the last section for this system was that of reaction time especially at lower concentrations. One solution to the limitation induced by the necessary diffusion of the TMA throughout the butan-1-ol phase would be to increase the surface area of the ligand-complex exposed to the gaseous environment.

Ideally a solid support on which the chromogenic complex could be immobilised was sought. The support chosen was Whatman no. 1 filter paper, 4.25 cm diameter disc. Initial experiments were carried out by carefully adding 2.5 mL of a $5x10^{-5}$ M solution of Ligand **5** which was also 0.1 M in $LiClO_4$ to a filter paper disc and allowing solvent evaporation before the next addition was made. The reduction in $LiClO_4$ concentration occurred due to the reduced solubility of this solute in THF compared to in butanol. This process resulted in a yellowish tinge being visible on the support. 2.5 mL of a $5x10^{-5}$ M solution was chosen in order to keep the total weight of ligand constant between the liquid-phase and solid support work constant.

The disc was placed on a wire mesh which rested midway inside a 2.71 L capacity gas tight vessel. Upon introduction of 10.7 μL TMA, which is equivalent to 1.0 ppm TMA, into the vessel, ensuring none of the liquid TMA came in contact with the disc, an instantaneous colour change to pink/red was noticed. This indicated that the solid support system was capable of operating as a gaseous TMA indicator and with the complete surface area of the indicator being in contact with the gaseous environment a reduced analysis time was already evident.

A series of experiments was set up to determine the analytically useful range of the method and the LOD possible with this method. The experiments were set up as above except that a 0.5 mL solution which contained 0.235mg of ligand **5** was used. The solution remained 0.1 M with respect to $LiClO_4$. The final TMA concentration was varied from 0 to 50 ppm. The lowest TMA concentration for which a change in colour was noted was 0.04 ppm TMA, where a colour change from yellow to orange was observed. Above this concentration the colour intensity increased discernibly to red. The test discs were then immersed in 5 mL acetonitrile to extract the complex for UV-Vis analysis. The spectra obtained are shown in Figure 4.24. These extractions were carried out to demonstrate that the same processs of deprotonation of the complex was occurring in these stationary phase experiments.

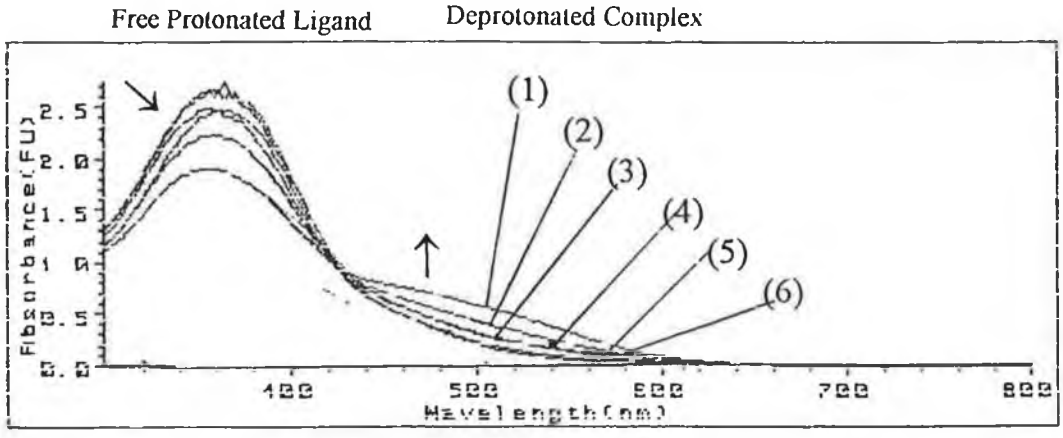

Figure 4.25:- *UV-Vis spectra showing the effect of TMA on the UV-Vis spectrum of the immobilised complex. Changes in the absorbance spectrum of a 5.0 mL acetonitrile extract of indicator discs coated with 0.5 mL of a $2.7x10^{-4}$ M Ligand 5 and 0.1 M $LiClO_4$ solution in THF, upon exposure to gaseous TMA in the following concentations: (1) 50.00 ppm , (2) 10.00 ppm, (3) 1.00 ppm, (4) 0.1 ppm, (5) 0.05 ppm, (6) 0 ppm.*

The intensity of the extract was less than that observed when the complex was in the immobilised state. This was partly due to the dilution factor imposed on the system by using 5 mL of acetonitrile but also due to the fact that all of the extracted discs still had a slight yellow tinge after extraction and drying. However, although the change in intensity at 500 nm is not that large it proves that essentially the same process which existed in the liquid phase experiments was occuring.

Disc coating conditions were optimised and are described in Method 2.6.2. With this system, striking colour changes from yellow to red were noted on the test discs for concentrations above 0.02 ppm, with a detectable difference in colour observed for TMA concentrations in the range 0.02 to 30 ppm. Plate 4.1 shows the colour change observed with 1 ppm TMA. Above 30 ppm no further change in colour density was visually discernible. Full colour development occurred very quickly after the introduction of TMA into the gas-tight system, with the lowest concentrations producing colour change in under 2 minutes, and shorter times being observed for higher concentrations. The process is completely

reversible, and test strips left in air returned to their original form within several minutes.

Plate 4.1:-*Colour change obtained in the presence of 1.0 ppm TMA using test strips made by carefully adding 0.2 mL of a THF solution which was $6x10^{-4}$ M in Ligand 5 amd 0.1 M in $LiClO_4$ onto a Whatman No. 1 filter paper disc (4.25 cm radius) and allowing to dry. On the left is a control strip which was subjected to exactly the same conditions as the experimental strip but without exposure to TMA. A clear change in colour from yellow to red is evident.*

4.12 Covered Test Strips

As we were intrested ultimately in the application of this indicator in the food industry, and most likely as a component of food packaging, experiments were subsequently carried out to determine whether the test strips could react to the presence of gaseous TMA when enclosed in a gas-permeable membrane such as low density polyethylene (LDPE). LDPE exhibits good barrier properties to water vapour but has high gas transmission capabilities [31]. The test strips were prepared as before except that they were wrapped in LDPE before being placed in a gas-tight vessel. Visually, no colour change was observed below 0.4 ppm TMA for exposure times of up to 8 hours. The development time decreased with increasing TMA concentration with full colour changes being observed after 20 minutes for 2.5 ppm TMA and almost instantaneous colour changes being observed above 10 ppm TMA.

4.13 Discussion

As outlined in Chapter 1, a simple sensitive colorimetric indicator for TMA would be of great potential use in the food industry for the detection of spoilage in fish products. The ligand investigated in this research can provide such an indication, and can be used while separated from the foodstuff by a gas permeable membrane. Obviously, for applications of this system the conditions of storage should be such that the amine is available in gaseous form. Refrigeration is usually carried out at 4° C, a temperature above the boiling point of TMA, so under these conditions some evolution of TMA would be expected if the fish sample had begun to spoil. The method has attracted industrial interest and has been patented [33].

Interestingly, the colour density is much greater and reaction times are much shorter for the test strips compared to the liquid-phase experiments, despite a lower concentration of metal ions being available in the case of the former. This arises because in the liquid-phase experiments, the experimental design is such that the amine must partition into the butanol phase and diffuse throughout it in order to generate the colour; whereas with the test strip, only the coated surface of the paper is involved and its entire surface area is in contact with the gaseous environment. Hence in the absence of any bulk diffusion processes, colour generation is much faster. In addition, as the ligand-metal mixture is not dispersed throughout a bulk liquid phase in the case of the test strips, but rather concentrated into a thin layer adhering to the paper surface, the density of the colour observed is much greater than for equivalent concentrations of TMA in the liquid phase experiments. The experiments with the LDPE coated test strips suggest that a sealed test strip of this type could be used on the outside of packaged foods to indicate the onset of spoilage. However, much work remains to be done before anything of this nature could be realised in practice.

In conclusion, an extremely rapid and sensitive visual method for the detection of TMA has been developed. The range of detection possible so far is between 0.02 and 30 ppm (maximum values assuming total transfer of the TMA injected into the gas phase), although this may be further reduced through variation of the reaction conditions or the development of related chromoionophores with larger molar absorptivities. Although the deprotonation process is relatively non-selective, some degree of selectivity may be achieved on the basis of the K_b value

of the base through variations of the K_a of the ligand produced on complexation with different metal ions co-immobilised with the ligand on the test discs. However, as a variety of volatile amines are evolved during fish spoilage, a broad-band indicator such as the indicator described above is more appropriate.

4.14 Overall Conclusion

Five novel calix[4]arenes bearing nitrophenylazophenol chromogenic moieties have been examined and their main features are summarised below:-

- A colour change from yellow to red is seen upon complexation with Li^+ or Na^+ in the presence of a suitable base. The intensity of the colour produced is dependent on the concentration of metal-cation added and a greater colour change is seen upon complexation with Li^+ than Na^+ at each concentration level.
- The positioning of the ionisable phenolic group relative to the hydrophilic cavity was found to be important with relation to the absorbance produced on complexation. Ligands 5 to 7 in which the hydrophilic cavity was attached in the *ortho* position relative to the ionisable phenol, produced much stronger absorbances than Ligands 8 and 9 in which the hydrophilic cavity was attached at the *meta* position.
- In the presence of a suitable base i.e TDDA, no colour change is observed in the absence of the complexing ion. This is again indicative of complexation effecting a lowering of the pK_a of the dissociating proton.
- Complexation occurs in the absence of a base, but no colour change is produced. This was demonstrated by ^1H NMR spectroscopy.
- Ligand 5 displayed the ability to extract Li^+ cations from an aqueous to an organic phase producing a spectral change in the organic phase, which was dependent on metal-ion concentration. No subsequent leaching of the deprotonated complex to the aqueous phase occurred.
- Ligand 4 was used in the development of a solid-phase gaseous TMA detector. The Ligand-Li^+ complex coated test strips showed rapid colour changes from yellow to red when it was exposed to gaseous TMA in a concentration range of 0.02 to 30 ppm.

4.15 References

1. M. McCarrick, S.J. Harris, and D. Diamond, Analyst, 118 (1993) 1127.
2. M. McCarrick, S.J. Harris, and D. Diamond, J. Mater. Science, 4, 2 (1994) 217.
3. T. Kaneda, K. Sugihara, H. Kamiya, S. Misumi, Tet. Lett., 22 (1981) 4407.
4. R.E. Moss, I.O. Sutherland, Anal.Proc., 25 (1988), 272.
5. S. Misumi, T. Kaneda, Journal of Inclusion Phenomena and Molecular Recognition in Chemistry 7 (1989), 83.
6. D.J. Cram, Angew. Chem., Int. Ed. Engl. 25 (1986) 1039.
7. D.J. Cram, R.A. Carmack, R.C. Helgeson, J. Am. Chem. Soc., 110 (1988), 571.
8. H. Shimizu, K. Iwamato, K. Fujimoto, S. Shinkai, The Chemical Society of Japan, Chemistry Letters, (1991) 2147.
9. Y. Nakamoto, T. Nakayama, T. Yamagishi, S. Ishida, "Workshop on Calixarenes and Related Compounds", Johannes Gutenberg-Universität, Mainz, Germany. August 28-30 (1991) Poster 1.
10. A.M. King, C.P. Moore, K.R.A. Samankumara Sandanayake, I.O. Sutherland, J. Chem. Soc., Chem. Commun., (1992) 582.
11. C.N.R. Rao, *"Ultraviolet and Visible Spectroscopy , Chemical Applications"* 3rd Edition, Buttersworths, London, (1975).
12. T. Nowicka-Jankowska, K. Gorczynska, A. Michalik, E. Wieteska, *"Wilson and Wilson's Comprehensive Analytical Chemistry, Vol XIX, Analytical Visible and Ultraviolet Spectrometry"*, G. Svehla (ed.), Elsevier, Amsterdam, (1986).
13. *"CRC Handbookof Chemistry and Physics"*, David R. Lide (Edt.), CRC Press, Boca Raton, Florida, (1993).
14. U. Oesch, Z. Brzozka, A. Xu, B. Rusterholz, G. Suter, H.V. Pham, D.H. Welti, D. Ammann, E. Pretsch, and W. Simon, Anal. Chem., 58 (1986) 2285.
15. A. Arduini, A. Pochini, S. Reverberi, R.Ungaro, C.D. Anderetti and F. Ugozzoli, Tetrahedron, 42 (1986) 2089.
16. R. Ungaro and A. Pochini in *"Calixarenes: A Versatile Class of Macrcyclic Compounds"*, (edts.) J. Vicens, and V. Bohmer, Kluwer Academic Publishers, Dordrecht, (1991) 127-147.
17. G. Barrett, V. Bohmer, G. Ferguson, J.F. Gallagher, S.J. Harris, R.G. Leonard, M.A. McKervey, M. Owens, M. Tabatabi, A. Vierengel, and W. Vogt, J. Chem. Soc., Perkin Trans. 2, (1992) 1595.

18. G. Calestani, F. Ugozzoli, A. Arduini, E. Ghidini, and R. Ungaro, J. Chem. Soc., Chem. Commun., (1987) 345.

19. P. Guilbaud, A. Verneck, and G. Wipff, J. Am Chem. Soc., 115 (1993) 8298.

20. H.G. Lohr and F. Vogtle, Acc. Chem., Res., 18 (1985) 65.

21. D.J. Cram, G.M. Lein, J. Am.Chem. Soc., 107 (1985) 3657.

22. F. Arnaud-Neu, E.M. Collins, B. Laitner, M. Deasy, G. Ferguson, S.J. Harris, A.J. Lough, M.A. Mc Kervey, E. Marques, B.L Ruhl, M.J. Schwing-Weill, and E.M. Seward, J. Am Chem. Soc., 111 (1989).

23. A. Cadogan, D. Diamond, M.R. Smyth, M. Deasy, M.A. McKervey, and S.J. Harris, Analyst, 114 (1989) 1551.

24. D. Diamond, G. Svehla, E. Seward, and M.A. McKervey, Anal. Chim. Acta., 204 (1988) 223.

25. M. Telting-Diaz, D. Diamond, M.R. Smyth, E.M. Seward, and M.A. McKervey, Electroanalysis, 3 (1991) 371.

26. B.P.Czech, E. Chapoteau, W. Zazulak, C.R. Gebauer, A. Kumar, Anal. Chim. Acta, 241 (1990) 127.

27. D.J. Cram, R.A. Carmack, and R.C. Helgeson, J, Am. Chem. Soc., 110 (1988) 571.

28. E.D Olsen, "*Modern Optical Methods of Analysis*", McGraw-Hill, USA, (1975).

29. L. Safarik, Z. Stransky, "*Wilson and Wilson's Comprehensive Analytical Chemistry, Volume XXII, Titrimetric Analysis in Organic Solvents*", (edt.) G. Svehla, Elsevier, Amsterdam, (1986).

30. N.J.C. Strachan, F.J. Nicholson, Int. J. Food Sc. and Tech., 27 (1992) 261.

31. C.K. Simmonds, E.C. Lamprecht, in "*Microbiology of Frozen Foods*" (edt.) R.K. Robinson, Elsevier, London, (1985) 169-208.

32. N.T. Crosby, "*Food Packaging Materials*", Applied Science Publishers Ltd., London, (1981).

33. Chromogenic Ligands and Use Thereof in Optical Sensors, S.J. Harris, M.A. McKervey, and D. Diamond, European Patent Application, lodged 6th August 1993, No. S922577.

Chapter 5

The Development of Novel Solid Contact Ion-Selective Electrodes

5.1 Project Aim

The aim of the work discussed in this chapter was to develop novel all solid-state ion-selective electrodes. This was a continuation of work carried out by Cadogan et al [1] where an intermediate layer of the conducting polymer, polypyrrole, which has both ionic and electronic conducting properties, is placed between an electronically conducting substrate such as platinum, and an ion-selective membrane. By using an alternative conducting polymer, polythiophene (PT) or polyoctylthiophene (POT), it was hoped that novel Li^+ and Cl^- detection systems could be fabricated and that the charge transfer mechanism previously proposed could be confirmed and further elucidated.

5.2 Theory and Literature

5.2.1 Introduction

This chapter deals with another means of transduction of ions, that of potentiometry. An introduction into the different components used in potentiometry, i.e. membrane with internal filling solution, coated wire and solid contact electrodes, and to conducting polymers and their applications in potentiometric sensors is given. This is followed by a section outlining all of the experimental procedures used in this work. Finally the results of the work carried out on the characterisation of a novel ISE system incorporating the semiconducting polymers polythiophene and polyoctylthiophene as a solid contact between a metallic substrate and a lipophilic neutral carrier are presented.

5.2.2 Potentiometry

Potentiometry is one of the most widely used electroanalytical methods. The term potentiometry pertains to the technique of measuring the potential of a galvanic cell or electromotive forces (emf). The simplest electrochemical cell, consists of two electrical conductors or electrodes immersed in a conducting electrolyte solution.

In potentiometry the voltage source is a form of galvanic cell in which electrochemical reactions occur spontaneously at the electrolyte/electrode interface when the electrodes are connected by a conductor. The two electrodes are known as the measuring and reference electrodes respectively. The overall cell potential is measured when the reversible electrode reactions have reached thermodynamic equilibrium. The true values of this potential can only be measured under zero current conditions. The main task in analytical potentiometry is to relate changes in cell potential to shifts in a particular ion activity arising from its reversible exchange at the ISE membrane/sample interface boundary. This can only be achieved if all other potentials arising in the cell are independent of the solution composition.

5.2.3 Conventional Ion-Selective Electrodes

The conventional cell arrangement for potentiometric measurements using an ion-selective electrode is [2]

internal reference element	internal aqueous ref. solution	ion-selective membrane	external reference electrode

and is shown in diagrammatic form in Figure 5.1 [3]

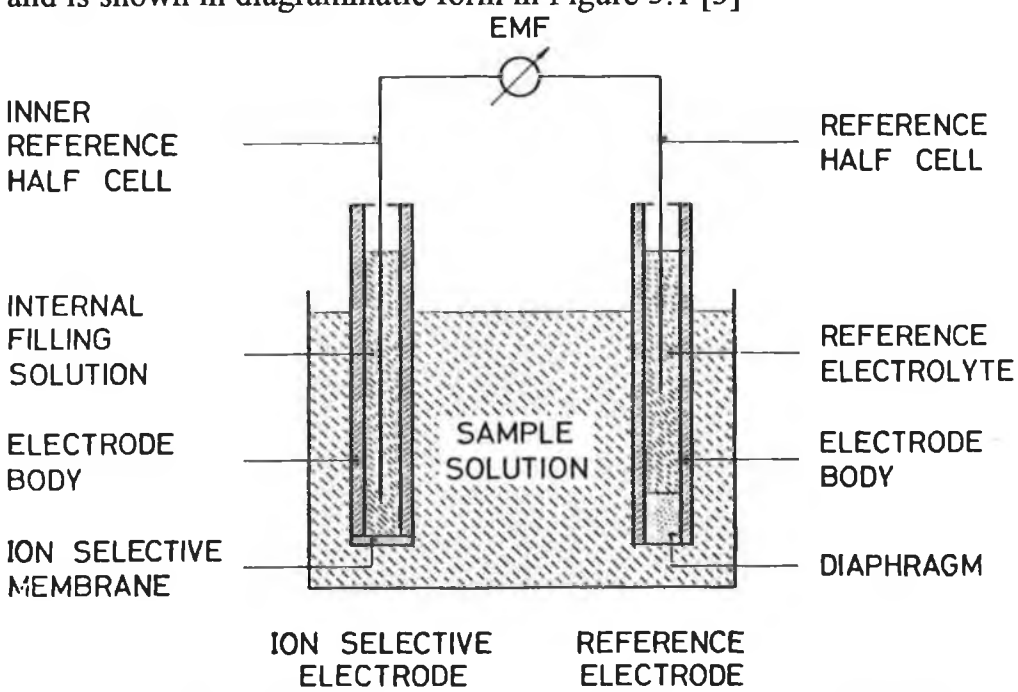

Figure 5.1:-Schematic diagram of a membrane electrode measuring circuit and cell assembly [3].

The working electrode in this arrangement utilises an internal filling solution to make contact between the internal reference electrode and the permselective membrane in contact with the sample solution. This is in contrast to solid contact electrodes, which will be discussed later, where contact between the membrane and the internal electrode is made by a solid-state material. In the conventional configuration the internal aqueous reference solution, which contains the ions necessary to maintain constant potentials at both the reference element and the inner surface of the ion-selective membrane is held at a constant composition. In a simple system where the reference electrode does not have a liquid junction such as an Ag/AgCl reference electrode, the overall cell potential (E_{cell}) would be given by

$$E_{cell} = E_{ISE} - E_{Ref} \qquad (5.1)$$

where E_{ISE} is the ion selective electrode potential and E_{ref} is the reference electrode potential. If the sensing electrode responds in a Nernstian fashion to the analyte ion (i^{z+}) then

$$E_{ISE} = E^{\circ} + 2.303\frac{RT}{z_i F}\log a_i \qquad (5.2)$$

where i is the analyte of interest, of charge z_i and activity a_i; R, T and F are the gas constant, the absolute temperature and the Faraday constant respectively and E^o is the standard electrode potential, which is ideally constant under the conditions of use. If E_{ref} is independent of the sample composition (i.e. constant) then by combining equation **(5.1)** and **(5.2)** the following equation can be written

$$E_{cell} = constant + 2.303\frac{RT}{z_i F}\log a_i \qquad (5.3)$$

Hence the cell will respond in a Nernstian manner to changes in a_i.

However the reference electrode must often be separated from the sample solution because the reference electrode potential is affected by the sample composition or because of cell design considerations. This is the arrangement illustrated in Figure 5.1 where the electrical contact between the reference half-cell and the sample solution is achieved by means of a salt bridge. Such a bridge/solution boundary gives rise to the possibility of ionic diffussion which introduces a liquid-junction potential into the system (E_{jn}), thereby changing the overall cell-potential to:-

$$E_{cell} = constant + S\log a_i + E_{jn} \qquad (5.4)$$

where E_{jn} is the junction potential and $S = 2.303\frac{RT}{z_i F}$.

Liquid junction potentials are a direct result of the differences in ionic mobilities of the positive and negative ions constituting the bridge electrolyte resulting in a charge separation. For example if the postitive ions migrate faster into the sample solution than the negative ions, a charge separation soon develops at the sample/bridge junction. The magnitude of the resulting potential difference is dependent on a number of factors, such as the identity of the bridge ions, the composition of the sample solution, the geometry of the junction and the temperature.

As the junction potential contributes to the overall cell potential, it is important that it be as small as possible, or at least invariant during use. Due to the similar mobilities of K^+ and Cl^-, saturated KCl solutions are frequently used in the preparation of bridges as only relatively small junction potentials will arise [4]. A mathematical description of the junction potential is given by the Henderson Equation **(5.5)** [5]

$$E_D = \left(\frac{\sum z_i u_i a_i(0) - \sum z_i u_i a_i(d)}{\sum z_i^2 u_i a_i(0) - \sum z_i^2 u_i a_i(d)}\right) x 2.303\frac{RT}{F}\log\left(\frac{\sum z_i^2 u_i a_i(0)}{\sum z_i^2 u_i a_i(d)}\right) \qquad (5.5)$$

The summation terms include contributions by all the ionic species (i) that are present within the membrane, the absolute value of the charge numbers z_i, mobilities u_i and activities a_i and assumes a linear diffusion gradient, and (d) and (o) are due to the diffusion layer between the internal reference solution and the external sample respectively.

5.2.4 Activity Coefficients

From the Nernst equation (equation **5.2**) it can be seen that the electrode response is related to the activity of the ion of interest a_i. Due to deviations from ideal behaviour, the activity of an ion in solution is not identical to its concentration but can be related to it by the equation

$$a_i = f_i c_i \qquad (5.6)$$

where for an ion (i), a_i is the activity, (c_i) is the concentration and (f_i) is an activity coefficient. As $c_i \rightarrow 0$, $f_i \rightarrow 1$, and activity and concentration become

identical in infinitely dilute solutions. The activity coefficient (f_i) quantifies the degree of deviation of an ideal solution from the ideal situation. Its value depends on the ionic strength of the solution.

$$I = \frac{1}{2}\sum c_i z_i^2 \qquad (5.6)$$

where c_i = molar concentration of i.

One of the simplest methods for the calculation of activity coefficients is the Davies model [6],

$$\log f_i = -Az_i^2\left(\frac{\sqrt{I}}{1+\sqrt{I}} - 0.2I\right) \qquad (5.7)$$

where A is a solvent dependency constant (0.512 for water). This equation can only be used for solutions up to approximately I = 0.1 M.

5.2.5 Membrane Potentials

In an ideal potentiometric cell, where effectively the contributions from the reference electrode, and the junction potential are constant, changes in the membrane potential E_m can be monitored as changes in overall cell potential. The membrane potential is determined by the boundary potentials at the two membrane/solution interfaces and any diffusion potential which arises as a result of variation in the ion composition through the membrane. This is shown diagramatically in Figure 5.2

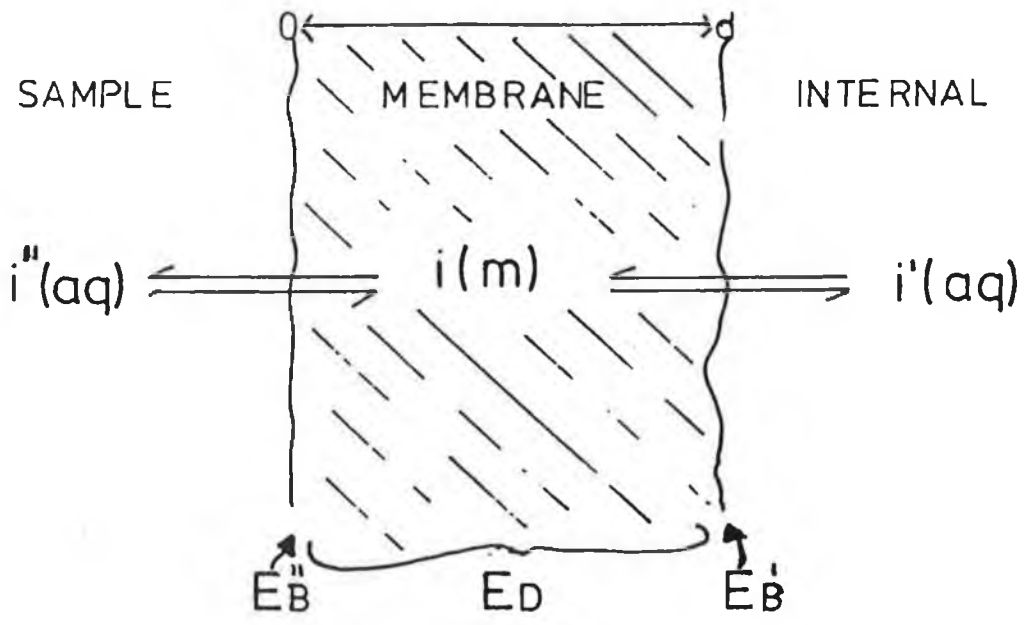

Figure 5.2:-Boundary and diffusion potentials of ion-selective liquid-membranes.

where E'_B is the potential at the internal solution boundary, E''_B the potential at the sample boundary and E_D is the diffusion potential which arises from the spontaneous transport of charged species across the membrane so that a potential gradient is formed. The full membrane potential is then given by

$$E_m = E''_B - E'_B + E_D \qquad (5.9)$$

5.2.5.1 Boundary Potential

The phase boundary potential arises from the non-uniform distribution of electrically charged species between the two phases. Both chemical and electrical potential contributions must be taken into account in descriptions of ion transport or ion distribution. For an ion i of charge z_i exchanging reversibly across an aquo-liquid membrane boundary, the work done in establishing equilibrium can be described by

$$-\Delta G = z_i F E_B \qquad (5.10)$$

where ΔG is the change in Gibb's free energy, F is the Faraday constant and E_B is the electrical potential established over the boundary. The decrease in Gibb's free energy is given by the difference in the partial molar Gibb's free energy (μ) for the ion i in the membrane (m) and the aqueous (aq) phases

$$-\Delta G = \mu_{i(aq)} - \mu_{i(m)} \qquad (5.11)$$

While measurements are usually carried out under a wide variety of conditions, these are conventionally related to the work done to bring about the same charge under standard conditions by

$$-\Delta G^{\circ} = \mu^{\circ}_{i(aq)} - \mu^{\circ}_{i(m)} = z_i F E^{\circ}_B \qquad (5.12)$$

and the standard state $^{\circ}$ is related to other states by

$$\mu_i = \mu_i^{\circ} + RT \ln a_i \qquad (5.13)$$

So substituting into equation **5.11** above

$$-\Delta G = \mu^{\circ}_{i(aq)} - \mu^{\circ}_{i(m)} + RT \ln \frac{a_{i(aq)}}{a_{i(m)}} \qquad (5.14)$$

The electrical potential at the interface is thus

$$E_B = \left(\frac{\mu^{\circ}_{i(aq)} - \mu^{\circ}_{i(m)}}{z_i F} \right) + \frac{RT}{z_i F} \ln \left(\frac{a_{i(aq)}}{a_{i(m)}} \right) \qquad (5.15)$$

If E°_B the standard potential $= \frac{\left[\mu^{\circ}_{i(aq)} - \mu^{\circ}_{i(m)}\right]}{z_i F}$. Then the boundary potential at any particular membrane interface is

$$E_B = E^{\circ}_B + \frac{RT}{z_i F} \ln \left(\frac{a_{i(aq)}}{a_{i(m)}} \right) \qquad (5.16)$$

As there are two membrane interfaces, (') the internal interface and (") the external interface. Two equations can be written for the boundary potentials E'_B and E''_B from **(5.16)** above.

$$E_B' = E_B^o + \frac{RT}{z_i F} \ln\left(\frac{a_{i(aq)}'}{a_{i(m)}'}\right) \qquad (5.17)$$

$$E_B'' = E_B^o + \frac{RT}{z_i F} \ln\left(\frac{a_{i(aq)}''}{a_{i(m)}''}\right) \qquad (5.18)$$

Combining **(5.17)** and **(5.18)** the net boundary potential across the membrane is

$$E_B'' - E_b' = E_B^{o''} - E_B^{o'} + \frac{RT}{z_i F} \ln\left(\frac{a_{i(aq)}'' a_{i(m)}''}{a_{i(aq)}' a_{i(m)}'}\right) \qquad (5.19)$$

Assuming the activity of the ion a_i is the same at both interfaces in the membrane i.e $a_{i(m)}' = a_{i(m)}''$ then

$$E_B'' - E_B' = E_B^{o''} - E_B^{o'} + \frac{RT}{z_i F} \ln\left(\frac{a_{i(aq)}''}{a_{i(aq)}'}\right) \qquad (5.20)$$

5.2.5.2. Diffusion Potential

Although the membrane is considered to be a uniform phase, the free energies of the membrane components undergo variation with time and this gives rise to diffusional fluxes of ions within the membrane. Although more commonly used for the estimation of junction potentials, the Henderson approximation can be used to describe the diffusion potential across the membrane. This allows easy and rather close characterisation of the diffusion potential in terms of boundary concentrations and mobilities of diffusing ions, (see equation **(5.5)**).

Relating this equtaion to Figure 5.2, x = 0 for the sample boundary ("), x = d at the internal boundary (') and the thickness of the membrane is d. If we assume there is a negligible drop in primary ion activity across the membrane i.e.

$$a_{i(o)} \approx a_{i(d)} \qquad (5.21)$$

and that there is virtually no penetration of the membrane by interfering ions (j)

$$a_j \sim a_{j(d)} \sim 0 \qquad (5.22)$$

then the substitution into the Henderson equation leads to the approximation

$$E_D \sim 0 \qquad (5.23)$$

5.2.5.3 The Complete Membrane Potential

Since E_D can be approximated to zero or is at least constant, variations in the overall membrane potential will be determined by the values of the boundary potentials. As the internal electrolyte activity a'_i is constant, substitution of equation (5.23) into equations (5.9) and (5.20) gives an expression for the overall membrane potential:

$$E_M = E_M^{\circ} + \left(\frac{RT}{z_i F}\right) \ln a_i'' \qquad (5.24)$$

where E_M° is a standard membrane potential and includes contributions from E_D, $E_B^{\circ''}$ and E_B'. Provided that the junction potential (E_{jn}) and the reference potential (E_{ref}) remain constant the overall cell potential will depend on the activity of the primary ion a_i"in solution and can be defined by

$$E_{cell} = \text{constant} + S \log a_i'' \qquad (5.25)$$

For a ten-fold change in primary ion activity (a_i) the ideal slope (S) is 2.303 $\frac{RT}{z_i F}$. This is 59.2 mV for a monovalent ion and 29.6 mV for a divalent ion at 25°C. Hence overall changes in cell potential will be ideally determined by changes in E''_B

5.2.6 Ion-Selective Membrane Components

Two main types of ion-selective compounds are used as dissolved components in liquid membrane sensors:

(i) Organic ion-exchangers such as organophosphates or tetraphenylborate (cation exchanger) and tetraalkylammonium ions (anion exchangers).

(ii) Uncharged molecules (neutral carriers) capable of complexing metal ions and drawing them into the membrane. Various classes of neutral carrier ionophores have been used in potentiometric ISE work such as crown ethers, spherands,

calixarenes and the naturally occuring macrotetrolides, all of which were discussed in Chapter1. The mode of action of these macromolecules with cations discussed there remains applicable to the present discussion. The electrodes described in this chapter are neutral carrier ionophores, containing exchangers to improve response characteristics, and discussion here will be confined to this class of selective membrane component.

5.2.7 Cation Selectivity

In section 5.2.5 it was stated that the generation of a boundary potential at the membrane electrolyte interface requires the selective inclusion of ions of the same charge into the membrane phase and the simultaneous rejection of counterion. Therefore, a cation selective membrane selectively exchanges cations and vise versa. Thus far the change in electrode potential has been discussed in terms of the ideal situation where the electrode responds solely to the presence of the analyte ion. In reality all electrodes are exposed to interfering ions, both cationic and anionic in nature. The response of the electrode must also be considered in terms of these interfering ions, which will intract with the electrode to varying degrees. The Nikolskii equation [6] introduces a term for the presence of interfering ions into the Nernst equation:-

$$E_M = E_M^\circ + 2.303\frac{RT}{z_i F}\log\left[a_i + \sum k_{ij}^{pot}\left(a_j\right)^{z_i/z_j}\right] \qquad (5.26)$$

where a_i = activity of the primary ion (i) in the sample solution, a_j = the activity of the various interfering ions (j) in the sample solution, E_M° = a standard boundary potential of the membrane, incorporating other potentials besides the external boundary potential, k_{ij}^{pot} (the selectivity coefficient) is a weighting factor to include contributions from interfering ions (j) to the total membrane potential (E_M). In the absence of other ions ($a_j = 0$) or an ideal electrode ($k_{ij}^{pot} = 0$, for all interferents j) the equation reduces to a Nernstian form for the primary ion.

5.2.8 Neutral Carrier ISEs

The traditional barrel configuration ISEs shown in Figure 5.1 containing neutral carrier ionophores as the membrane recognition components have been used in

numerous analytical situations over the last 30 years or so. The huge developments in ISE research over this period has been driven in part by the speed and ease of ISE use, the wide dynamic range possible and the relatively low cost of the devices.

Many of the compounds described in chapter 1 sections 1.2 and 1.3 were incorporated into potentiometric ion selective electrode. For an extensive list of neutral carrier based ISEs and their current applications one should look to the excellent reviews [7-15].

5.2.9 Coated Wire Electrodes (CWE)

The cumbersome nature of the traditional barrel configuration has proven to be problematic for some applications and attempts at miniaturisation brought about new sensing systems namely solid contact (SC) electrodes such as solid crystal membranes, conducting filled polymer electrodes and coated wire electrodes (CWE). In the context of the work to be described in this chapter where a novel solid-contact electrode incorporating a conducting polymer between the ion sensing membrane and the electronic contact, is compared to a CWE of the same ion sensing membrane, it is pertinent at this point to review the work previously done on CWEs.

In a CWE an electroactive species is incorporated in a thin polymeric film [2], usually poly(vinylchloride) (PVC) [although poly(methylmethacrylate) is often used], and subsequently dip-coated directly onto a conducting substrate. This electrode configuration results in the elimination of the conventional aqueous internal reference system found in conventional arrangements as depicted in Figure 5.1. This attribute provides new advantages of simplicity of design, lower costs, mechanical flexibility in terms of being able to use the electrode horizontally, vertically or inverted and the possibility of miniaturisation and microfabrication have widened the potential applications of CWEs. The basis of such solid contact electrodes is shown diagramatically in Figure 5.3

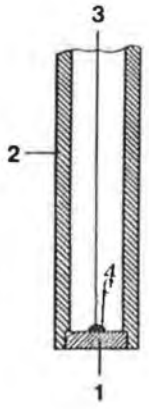

Figure 5.3 :-Solid contact electrode configuration.1, membrane, 2, electrode body, 3, cable connection to amplifier, 4, solid contact.

The first CWE described in the literature was in 1970 by Hirata and Date[16] but the name was not coined until 1971 by Cattrall and Freiser [17]. The electrode described by Hirata and Date was a Cu-responsive electrode made by attaching Cu_2S- impregnated silicone rubber or epoxy resin film to either a copper foil or platinum. This electrode exhibited a Nernstian response to Cu(II). Subsequently this group developed an electrode sensitive to Pb with lead sulphide impregnated silicone rubber membrane coated onto platinum wire or plate [18].

In 1971 Cattrall and Freiser [17] entered the field referring to their calcium selective electrode as a CWE. The electrode they described was made by dipping a platinum wire a number of times in a 6:1 mixture of 5% polyvinylchloride (PVC) dissolved in hexanone and 0.1 M calcium didecylphosphate in dioctylphosphonate. After the coating had been allowed to set overnight the remainder of the exposed wire was covered by wrapping it tightly with a parafilm to prevent direct contact of the metal surface with the test solution. This method of "dip coating" of the electroactive components which are usually imbedded in some polymer material, until a bead is formed on the substrate wire has subsequently been used in many CWE electrodes [2]

Ion sensors for calcium [19, 20] nitrate [21], potassium [22, 23] and halides [24] have been developed and a substantial review is offered by Cattrall and Hamilton on CWE not just for cations but also for anions and organic ions [2].

Even from the earliest reports of ion-selective CWEs it became apparent that certain factors in the treatment of these electrodes had to be very carefully considered due to the unknown nature of the conduction mechanism at the internal boundary. The effect of various conditioning parameters were highlighted by Hirata and Date [16, 18] who concluded that the swelling of the polymer bed by an aqueous salt solution of the cation of interest was necessary to establish a stable potential. This swelling was considered to enhance the conduction process. Although equal and even superior selectivities have been claimed for the devices compared to their conventional counterparts [25], comparisons of selectivity coefficient data for different electrodes can be unreliable due to a number of different methods being employed for their determination and due to variations in electrode treatment prior to use [2]. The standard potential of CWEs is often unstable varying for one electrode during its lifetime as well as differing between electrodes of the same type, and hence they require frequent recalibration.

In spite of the observed success of CWEs such problems raised fundamental questions concerning the charge conduction mechanism occuring in the membrane phase and at the polymer-substrate interface. As described earlier (section 5.2.3) in a conventional ISE the reversibility and equilibrium of transition from ionic to electronic conductivity is ensured by the reversible half cell at the silver-silver chloride wire in the internal filling solution. Such a mechanism would appear to be absent in CWEs since the ionically conducting polymer is in direct contact with the electronically conducting metallic substrate with no intermediary phase to bridge the gap.

The term 'blocked interface" was introduced by Buck [26] who classified coated wire electrodes as being "completely blocked" because the membrane/substrate interface is blocked to a reversible electron or ion transfer. The lack of reproducible potentials can be justified if the coupling between the metal substrate and the membrane in CWEs is seen as capacitive which would by its sensitive nature be affected greatly by external substances penetrating between the two layers.

Cattrall and Hamilton in their review [2] state that in the absence of an internal reference solution, the composition of the sample solution and the extraction behaviour of any interfering ions will be the determining factor for the equilibrium composition of the membrane. No diffusion potential will occur

within the membrane because no ionic gradient will be set up across it, due to the absence of the internal filling solution, and therefore selectivity will be determined by the relevent distribution constants, and with the mole fraction of the lipophilic ion in the membrane also playing an important role.

However, this is only true when the diffusion layer reaches the inner surface region of the membrane; or in other words when the membrane has been conditioned sufficiently for its equilibrium composition throughout the membrane thickness to have been established. Before this equilibrium has been obtained an ionic gradient will occur as the ions establish themselves throughout the membrane and the ionic mobilities of the different ions must be considered. After equilibrium has been attained it may be envisaged that the CWEs would exhibit superior selectivity to their conventional counterparts since the selectivity with the CWEs depends solely on extraction constants. However, on a less positive note, the equilibrium time is crucial and is dependent on membrane thickness. This problem could be a cause of the inherent reproducibility problems. The response of the CWE, unlike conventional ISE's, is also affected by the mole fraction of lipophilic ion in the membrane and thus CWEs are susceptible to drift problems due to leaching of reagent.

Returning to the problem of the "blocked" interface, a number of authors have carried out studies and suggested theories as to how the conversion from ionic to electronic conduction is occuring. Cattrall et al [19] first proposed the theory that fortuitously the coated wire electrodes contained a thermodynamically feasible process at the PVC-platinum interface in the form of an oxygen electrode. This theory stemmed from the fact that both oxygen and water can penetrate through PVC. Other factors have also been considered to be important in establishing an inner reference electrode such as oxidizable impurities from the membrane, such as hydroquinone which is present as a stabiliser in THF, the solvent used for the dissolution of the membrane components.

In principle there are many processes which are capable of explaining the relatively stable potentials at the metal/membrane interface implied by the successful construction and application of CWEs. However no one definitive mechanism has been proven to be responsible for their maintenance.

5.2.10 Solid Contact ISEs

Another route to producing electrodes which eliminate the internal liquid junction is to coat conducting substrates with a combination of both electronically and ionically conducting materials. The basic idea is illustrated in Figure 5.4.

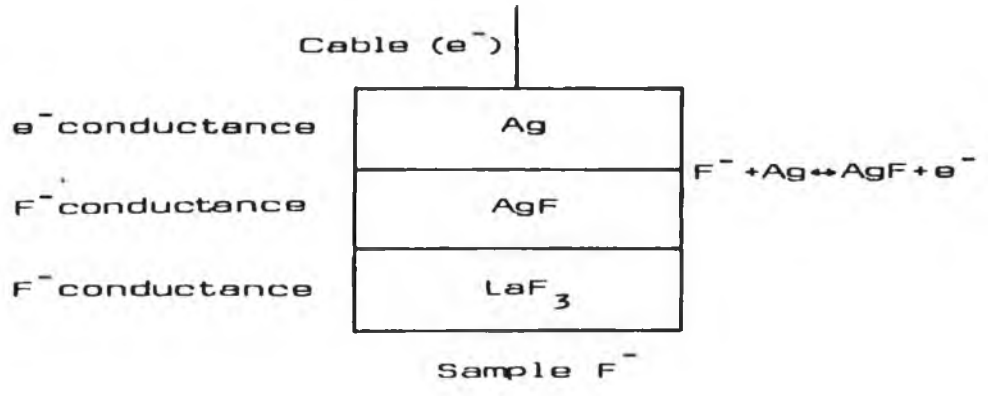

Figure 5.4:- Solid-state connection of ion-selective membranes. The kind of conductivity is indicated on the left and the reaction at the critical interface on the right. "Ag" indicates a silver-filled epoxy glue which is mainly used for making the contact [27].

In this F^- sensor the ion-selective component of the membrane is LaF_3. In order to provide a reversible interface, something which is not immediately apparent in the CWEs, an electron conducting silver and additional layer of AgF is provided. This system in the absence of a liquid junction provides a direct means of transmission of "ionic" information to the electronically conducting cable, via the equilibrium which is set up at the AgF/Ag boundary in a manner analogous to the well-known Ag/AgCl system i.e. $F^- + Ag \leftrightarrow AgF + e^-$.

Many solid internal contact ISEs have been designed and characterised. A number of different categories have emerged in this field, namely:

1. Electrodes with solid crystal membranes,
2. Glass electrodes with solid internal contact

3. PVC matrix electrodes with solid contact, and a substantial review is provided by Nikolskii and Materova [25].

5.2.11 Conducting Polymers

5.2.11.1 Introduction

Conducting polymers constitute a unique class of materials which combine the electrical and optical properties of metals and semiconductors with the good mechanical properties and processing advantages of polymers. This broad definition of the term is an immediate indication of the multidisciplinary nature of the field which has attracted the attention of a range of scientists, including physicists, chemists and materials scientists.

Three main categories exist in polymeric systems capable of conducting charge. These are ionically conducting polymers, redox polymers and electronically conducting polymers. In ionically conducting polymers the movement of ions through the polymer network is responsible for charge transport [28]. Redox polymers comprise an electrically insulating polymer backbone to which individual electroactive groups are covalently attached [29], such as $[Os(bipy)_2(PVP)_nCl]Cl$, [30]. Charge transport occurs by hopping of the charge carriers from one redox centre to another, while the backbone remains unaltered in the process. Both of these categories of polymers are outside the scope of this chapter and will not be discussed further.

The term "conducting polymer" is reserved here for conjugated organic polymers that can be made electrically conducting by a process called "doping". They have an anisotropic, quasi one-dimensional structure consisting of long conjugated chains and charge transport or electrical conductivity, is connected to electrical excitations within this backbone itself. Therefore they are sometimes referred to as "intrinsically conducting polymers" or synthetic metals [31].

The tremendous expansion in the field of conducting polymers since the late 1970's stems from the discovery in 1977 by Heeger and Mac Diarmid that doping polyacetylene (PA) with iodine endowed the polymer with metallic properties including an increase in conductivity of 10 orders of magnitude [32, 33]. B.A.S.F. have reported a conductivity of 147,000 S cm^{-1} (siemens per centimeter)

for polyacetylene [34]. Good insulators such as teflon and polystyrene have conductivity close to 10^{-18} S cm^{-1} and good conductors such as copper and silver have conductivities close to 10^{6} S cm^{-1}. Since their encouraging properties were discovered in 1977, a number of other organic polymers have been prepared and examined for the conducting ability. They all possess the structural characteristic which is synonomous with conducting polymers, namely conjugation of the chain linked electroactive monomeric units. Figure 5.5 shows a selection of the most frequently examined polymers.

polyacetylene (PA)

polyphenylene (PPP)

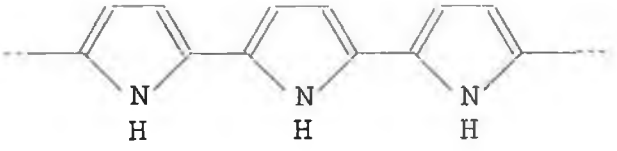

polypyrrole (PPy)

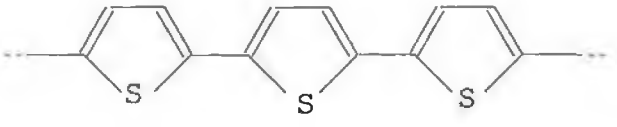

polythiophene (PT)

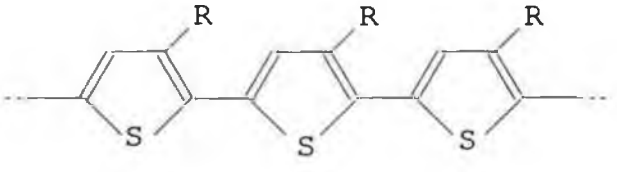

poly(3-alkylthiophene)
R = alkyl side-chain
(PAT)

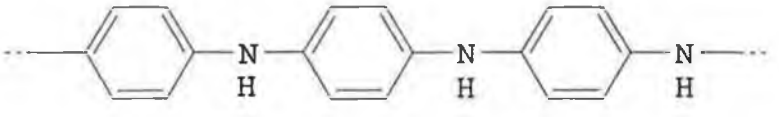

polyaniline (PANI)

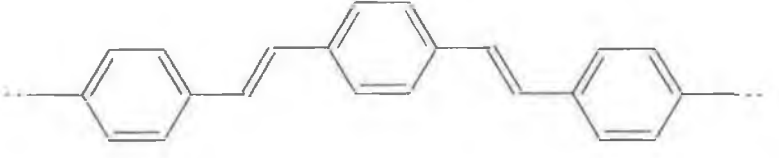

poly(phenylene-
vinylene) (PPV)

Figure 5.5:-Chemical structure of some common conducting polymers, with the names and abbreviations that are in general use in the literature.

5.2.11.2 Charge Conduction in Metals and Semiconductors

According to the band theory of solids the highest occupied band in a material is called the valence band and the empty band above it is called the conduction band. In metals a half filled valence band facilitates the free movement of electrons resulting in conduction. Insulators and semiconductors are materials whose conduction band is completely or almost completely empty respectively. An energy gap exists between these filled valence bands and the conduction band with the size of the gap being the determining factor in whether any electrons will be able to leave this level to the conduction band and thereby result in conduction. Semiconductors have a narrow forbidden gap above the top filled valence band (VB). At normal temperature and pressure only a small percentage of electrons can cross the energy gap and populate the conduction band (CB). Insulators have a wide energy gap which is a barrier to the electrons and therefore excitation of carriers in insulators is impossible. The band structures are shown in diagramatic form in Figure 5.6 [35].

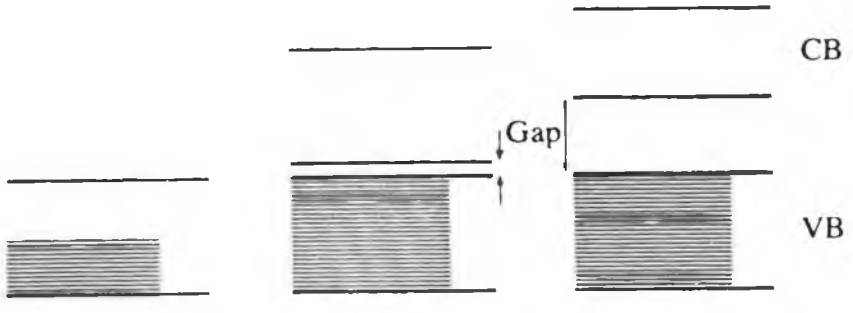

(a) Metal (b) Semiconductor (c) Insulator

Figure 5.6:-*Band structures of (a) metal, (b) semiconductors, and (c) insulators [35].*

An ordinary conjugated polymer is similar to an insulator or a semiconductor, in that there is an energy gap between the full valence band and the conduction band. In order to have a high electrical conductivity they have to be doped.

5.2.11.3 Doping

The term "doping" when applied to the field of conjugated polymers means to oxidise (p-doping) or reduce (n-doping) the conjugated polymer backbone with simultaneous incorporation of charge compensating ions (doping ions). Doping can be carried out either chemically or electrochemically and this is shown schematically by the following reactions:-

Chemical

p-doping $P + A \rightarrow P^+A^-$ **(5.27)**

n-doping $P + D \rightarrow P^-D^+$ **(5.28)**

Electrochemical

p-doping $P + X^- \rightarrow P^+X^- + e^-$ **(5.29)**

n-doping $P + N^- \rightarrow P^-N^+ - e^-$ **(5.30)**

In chemical doping the conjugated polymer (P) is oxidised by an electron acceptor (A) or reduced by an electron donor (D). In electrochemical doping the conjugated polymer is oxidised or reduced by the applied electrical potential with simultaneous incorporation of an anion (X^-) or a cation (N^+) respectively. The inclusion of the doping ions (X^- and N^+) in electrochemical polymerisation is a means of charge compensation on the polymer. Therefore the doping reactions (**5.29** to **5.32**) result in the polymer becoming electrically conducting by the inducement of positive or negative charges that can move along between the polymer chains. Returning to the band theory of solids this means that the doping reaction induces new energy bands in the band gap, making it possible for electons to traverse this gap and move into the new bands, increasing the conductivity of these materials. High electrical conductivity can be obtained at high doping levels where the band structure of conjugated polymers approaches that of metals.

5.2.11.4 Synthesis of Conducting Polymers

Conducting polymers may be prepared either by chemical or electrochemical polymerisation from a monomer solution. A chemically synthesised polymer is produced in its undoped state. It can be subsequently doped chemically, by treating with a reducing or oxidising agent eg. iodine, bromine, ferric chloride or

arsenic pentafluoride (p-doped) or alkali metals e.g. sodium (n-doped), or electrochemically to its conducting state.

With the exception of polyacetylene (PA) it was observed that all important conducting polymers can be electrochemically produced by anodic oxidation [36]. This method offers an immediate advantage over chemical methods in that the conducting films are formed directly on the electrode. Also, electrochemical polymerisation offers a versatile and easily controlled method of producing thin films of conductive polymers which can be characterised in situ both during and after polymerisation. In electrochemical polymerisation both polymer formation and doping occur simultaneously. The polymer can be returned to its neutral (undoped) state after polymerisation by electrochemical reduction. The polymer layer can then be redoped either chemically or electrochemically.

Three different methods exist for electrochemical polymerisation - potentiostatic, galvanostatic or potentiodynamic. A three electrode voltametric cell is used. The working electrode on which the polymer is formed is usually made of platinum, glassy carbon, gold or ITO glass (indium tin oxide). In galvanostatic methods a certain amount of curent is drawn through the cell and the polymer is formed as a film on the working electrode. In potentiostatic methods the electrode is kept at a constant potential at which the polymerisation reaction takes place. In the last method, potentiodynamic polymerisation, the potential is continuously swept in and out of the range where polymerisation takes place. New material is formed during each scan. During the reverse scan the new material formed will be reduced, and on the next scan the earlier layers will be reoxidised simultaneously with the formation of new polymer layers.

Anodic electropolymerisation of heterocyclic monomers has been widely used to synthesise conjugated polymers on electrode surfaces [31, 36]. The mechanisms of the polymerisation reaction, nucleation and film growth are not fully understood. The following general mechanism gives an indication of how the polymerisation reaction is expected to proceed [36] and is shown in diagrammatic form in Figure 5.7.

i Oxidation of the monomer to form a radical cation, by maintaining the potential above the oxidation potential of the monomer [36, 37],

ii Coupling of the two radical cations to form an α, α linkage,

iii deprotonation giving the neutral dimer,

iv oxidation of the dimer, (dimers and higher oligomers generally have lower oxidation potentials than the corresponding monomers, resulting in immediate reoxidation [38], i.e. for thiophene E_{ox}^{mon} = 1.65 V vs. SCE, and E_{ox}^{poly} = 1.1 V).

As the reaction continues, the average chain length of the oligomers increase, their solubility decreases and gradually a film of conjugated polymer is formed on the electrode surface. In order to maintain electrical neutrality in the material, negative ions, (so-called doping ions) enter the polymer membrane to counterbalance the positive charge of the polymer backbone. The occurence of side reactions in parallel with the polymerisation reaction can however complicate the picture, and possible side reactions must therefore be considered and measures to eliminate them taken.

Since the polymerisation reaction proceeds by a radical cation intermediate, it is clear that the reaction will be sensitive to the nucleophilicity of the environment in the region near the electrode surface. This necessitates the use of solvents which are poor nucleophiles i.e. aprotic solvents [31].

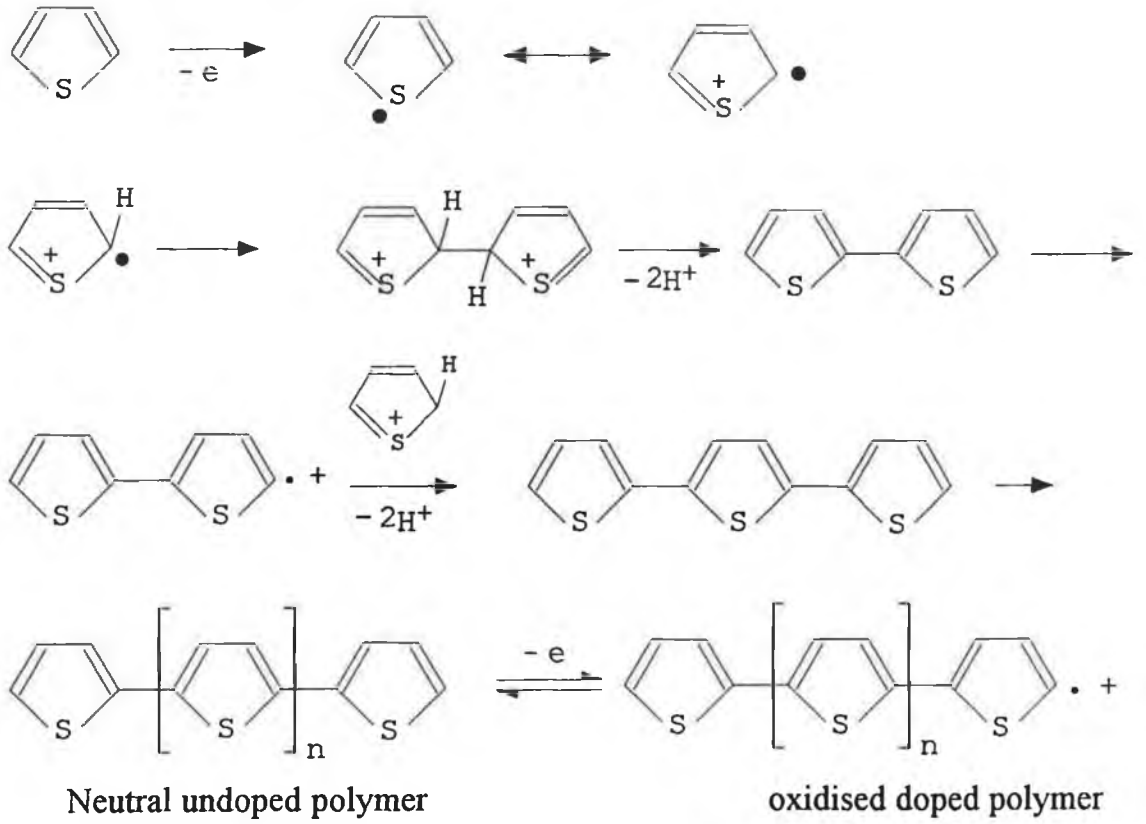

Figure 5.7:- *General scheme for the electrochemical polymerisation of heterocycles such as polythiophene[31].*

From microanalytical studies [39], of a number of electrochemically synthesised polymers a polymeric structure containing 4 monomer units per counterion for polypyrrole, polythiophene and polyfuran and 2 monomeric units for polyindole, making the whole film electroactive.

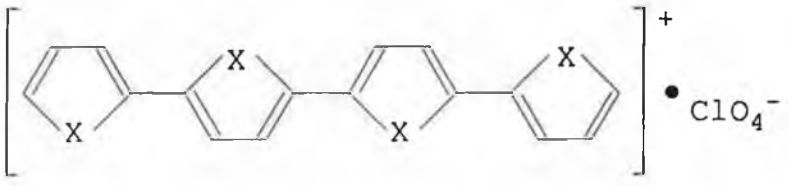

X = N, S, O

From this it is clear that anions must be present in the oxidised polymer film inorder to satisfy the electroneutrality condition [31]. When the polymer is reduced to its undoped state, anions may be expelled from the film, cations may enter the film or both processes may occur together [40-44].

5.2.12 Analytical Applications of Conducting Polymers

The charge storage properties and spectral variation upon oxidation and reduction of conducting polymers have attracted many authors to their potential uses in rechargeable batteries and electrochromic devices, [31, 36]. However, the ability to apply an electrically conductive layer onto a substrate surface by electropolymerisation and to subsequently control the level of conduction by doping or undoping has led to the widespread investigation of the analytical applications for these new materials. The most widely used conducting polymers to date in these applications are polypyrrole, polythiophene, poly-3-alkylthiophenes and polyaniline.

Conducting polymers are potentially extremely versatile molecular recognition systems. Their versatility stems from the fact that they have both inherent recognition properties and such properties can be built into them. These include

i ability to exchange doping ions

ii incorporation of further recognition/complexing molecules such as ethylenediamine tetraacetic acid (EDTA) [45] or biorecognition molecules such as enzymes [46].

iii changes in electrical conductivity at the polymer membrane arising from the fact that ceratin vapours such as methanol cause a swelling of conducting polymers such as PPy, [47].

A number of general articles encompassing the wide range of applications and sensing techniques which have been used with conducting polymers have been published recently, [48-51]. In the work presented here, the polymers PT and POT are used in potentiometric electrodes for the determination of both cations and anions. Compared with voltammetric applications, the use of conducting polymers for fabrication of potentiometric sensors is relatively rare.

Polypyrrole has been examined as an ion-sensing material by a number of authors [52-57]. Dong et al. [52-54] have shown that there is a correlation between the open-circuit potential of doped polypyrrole and the concentration of inorganic anions such as Cl^-, Br^-, NO_3^- and ClO_4^- in solution. Fast and stable potentiometric responses were given by all of these polypyrrole electrodes to their dopant anion. A response was also seen to other anions resulting in poor selectivity [53-55, 57]. However, the selectivity order could be altered by the use of different dopant ions and another feature of these electrodes was their ability to perform in some non-aqueous solvents, a feature which is not possible with conventional PVC ISE's. Low resistance and relatively fast response times were also quoted as encouraging characteristics in some of these electrodes [53].

Bobacka et al. [57] found that the conditions of electropolymerisation and in particular the nature of the dopant ion had a substantial effect on selectivity and electrode response. They doped polypyrrole with four different salts i.e sodium p-toluene sulphonate (NaTOS), $NaBF_4$, sodium dodecylsulphate (NADS), and indigo carmine, and obtained a response to NaCl that went from anionic for NaTOS and $NaBF_4^-$ to cationic for indigo carmine, with a very small anionic response when doped with DS^-. These results bear a relationship with the mechanism of ionic and redox sensitivity of p-type conducting polymers offered by Lewenstam et al. [58].

The diversity in PPy response with different anions was seen in terms of the variation in dopant ion mobilities. TOS^- and BF_4^- were found to be mobile in PPy allowing complete exchange with similarly mobile Cl^-, and therefore an anionic response ensued.

Indigo carmine is practically immobile in PPy and as a result may act as a cation exchanger. Analogy was made with the cation sensitivity outlined by Okada et al. [59]. In this work, napthalene sulphonates were used as the doping ions of PPy. Improved cation response was observed as the concentration of sulphonate

groups increased. They also suggested that not all of the sulphonate groups of the divalent and trivalent anions in PPy were required for charge compensation with the imino groups of the polymer backbone and that the excess sulphonate groups may act as cation exchange sites causing the cationic response. Bobacka et al. [57] suggested a similar explanation for this behaviour, that the amount of negative charges incorporated by indigo carmine during electropolymerisation of PPy exceeds the amount of positive charges on oxidised PPy, and the excess negative sites function as a cation exchanger.

The explanation given for the barely anionic response of the electrode doped with DS^- is that this anion diffuses at a very slow rate but after prolonged immersion in a solution of chloride salt, a certain degree of exchange with Cl^- occurs.

Polythiophene and substituted polythiophenes have also been examined [60, 61], as potentiometric ion sensors. Karagozler et al. [60] produced a potentiometric iodide ion sensor using the conducting poly(3-methylthiophene). After electropolymerisation in the presence of the monomer and 100 mM Bu_4NBF_4, the electrode was transferred to an aqueous solution of KI, where the electrode was redoped by repeated potential cycles. Such electrodes were found to give a selective iodide response in the presence of a range of cations including Cl^-, Br^-, NO_3^- and ClO_4^- but suffer from interference by iodine reducing species such as CN^-.

Bobacka et al. [60] described cation sensitivity by PT and some of its 3' substituted derivatives i.e POT, when they were used in their undoped neutral state. The cation sensitivity was attributed to a possible interaction between the cations and the potentially electron donating sulphur atoms of the thiophene backbone. The cation response was non-selective and sub-Nernstian i.e slopes of approximately 45 mV/dec for POT, indicating a mixed ionic response [57, 58]. The lack of clear anion or cation selectivity demonstrated by a number of authors in the form of sub-Nernstian slopes has been explained recently [58]. They say that the open circuit potential of their PPy electrode systems is determined by anions, cations and/or redox couples in solution, giving rise to the so called mixed response. Because both electron and ion-transfer frequently occur simultaneously in these conducting polymer systems they suggest that the use of PPy or analogous conducting polymers as an ion-selective electrode sensing materials may be limited.

However, conducting polymers may prove useful as intermediate layers in solid-state ion-selective electrodes. Cadogan et al. [1] have described an example of an application based on the mixed ionic and electronic conductivity of conjugated polymers. Polypyrrole is used as the solid contact between the metal substrate and the ion-selective membrane. It was suggested that the ionically and electronically conducting polypyrrole acts as a bridge between the electronically conducting metal and the ionically conducting membrane, and therefore the contact will not be blocked as is the case in CWEs which were discussed earlier.

In this work it was hoped that an analogous solid contact electrode, this time incorporating undoped polythiophene or polyoctylthiophene as the electronically conducting material could be used in conjunction with previously examined ionophores and thereby further elucidate the mechanism of action of these all solid state electrodes. As was previously mentioned PT and POT in their undoped state have been shown to exhibit non-selective cation responses [61].

5.3 Experimental

5.3.1 Reagents

Thiophene and anhydrous propylene carbonate (PC) were used as obtained from the Aldrich Chemical Company. 3-octylthiophene was used as received from Neste Oy (Research Centre, SF-06850 Kulloo, Finland). Analytical grade reagent salts were obtained from Merck or Fluka and were used without further purification by dissolution in distilled deionized (millipore grade) water. Lithium tetra-fluoroborate ($LiBF_4$) and tetrahydrofuran (THF) were obtained from Fluka. Both the lithium and chloride selective ion selective cocktails were obtained from KONE Corporation and contained ion-exchanger, plasticiser and PVC dissolved in THF. The names of the ionophores used were not disclosed due to company policy restrictions, but for lithium-selective electrodes, a lithium-selective neutral carrier ionophore was used, (see Chapter 1 for a general description). An anion exchanger was used as the chloride-selective component in the chloride-selective cocktail. Chemically synthesised polyoctylthiophene (POT)c received from Neste Oy, was placed in THF. A proportion of the (POT)c was dissolved in the THF. The solution was filtered and the THF allowed to evaporate giving POTc which was completely THF soluble.

5.3.2 Electrode Nomenclature

Table 5.1 outlines the acronyms and their meanings for all of the electrodes which were examined.

Table 5.1:- *Table of acronyms for electodes to be described.*

Acronym	Full Name and Meaning
(CPE)	Conducting polymer electrodes which have only conducting polymer added/electropolymerised onto platinum (Pt) or Glassy Carbon (GC) substrate.
(CWE)	Coated wire electrodes which have PVC ionophore layer directly in contact with Pt or GC substrate.
(SC)	Solid-contact electrodes which have an intermediary conducting polymer layer i.e PT or POT, between the substrate and the PVC ionophore layer
(HFE)	Hybrid film electrodes are prepared by mixing various quantities of $(POT)_c$ and PVC ionophore cocktail, and pipetting the mixture onto the substrate.

The following is an example of an electrode name:-

$$(SC)Pt/PT/PVC(Li^{+})$$

The first term in this name (SC) reveals the type of electrode i.e. solid-contact. The next term (Pt) indicates what substrate is used i.e. platinum. The third term (PT) describes what conducting polymer is producing the solid contact and finally the last term indicates what cation the ionophore in the PVC cocktail is selective for i.e. PVC(Li^{+}) contains a lithium selective ionophore.

5.3.3 Electrode Fabrication and Measurements:-

5.3.3.1 Electropolymerisation of PT and POT

The galvanostatic electropolymerisations were carried out using a Metrohm AG Herisau Coulometer, Type E211, with a Princeton Applied Research Model 174A Polarographic Analyzer being used to undope the polymer immediately after synthesis. The electrochemical cell was a conventional three-electrode system mounted on a Metrohm 663 VA Stand. The working electrode was a platinum (Pt) disk (Metrohm) (diameter 3 mm) set in teflon (overall diameter 7 mm) with a glassy carbon rod counter electrode (Metrohm). The reference electrode was a Ag/AgCl/KCl (3M) reference electrode (Metrohm) that was connected to the cell via a bridge filled with 0.1M $LiBF_4$-PC. All solutions were degassed by bubbling with high purity nitrogen. Electrodes were polished to a mirror finish with 0.3 μm of Al_2O_3 paste and rinsed with water and chloroform.

Polythiophene (PT) and polyoctylthiophene (POT) were deposited by galvanostatic polymerisation of thiophene (0.1M) and 3-octylthiophene (0.1M) respectively in 0.1M $LiBF_4$-PC by passing a constant current of 0.1 mA (1.43 mA/cm2) through the system for 80 s. The amount of charge passed during polymerisation of PT and POT was previously found to be 8 mC [61]. The film thickness for POT prepared under these conditions has been estimated to be 0.25±0.1 μm by using a Sloan Dektak II Profilometer [62]. The electropolymerisation was performed at room temperature (23 ± 2°C) and the working electrode was rotated at about 1500 rpm during polymerisation.

The potential of the polymer electrodes was brought to 0 V and kept there for between 1 and 5 minutes immediately after polymerisation in order to reduce

(undope) the polymer films. After undoping, the electrodes were rinsed with PC and water and stored in aqueous solutions (10^{-1} M LiCl) for 1 day for POT and for up to 4 days for PT prior to potentiometric measurements.

5.3.3.2 Application of ISE Cocktail to the Solid Contact

After checking that the polymers were giving a potentiometric cationic response similar to that previously obtained [61], the ion-selective cocktail was added. The electrode to be coated was clamped in an upright position and a 100 μL portion of the PVC cocktail containing the ionophore was pipetted on top. The electrode was protected from particulate contamination and allowed to dry for at least 10 hours resulting in an ion-selective membrane (ISM) on top of the PT or POT electrode. The resulting solid-contact ion selective electrode (SCISE) was conditioned for at least 12 hours in 0.1 M LiCl prior to being used for potentiometric measurements. Construction of the SCISE is shown schematically in Figure 5.8.

It has been shown that unlike PT or PPy, 3-alkyl substituted polythiophenes display solubility properties in a number of organic solvents [63]. Therefore it must be noted here that POT is slightly soluble in THF, the PVC cocktail solvent, and that a merger of the two polymeric layers inevitably occurred. After use the PVC layer was removed from the electrode and a complete coating of POT was still evident on the Pt surface, so it can be concluded that the interface between Pt and the rest of the electrode was entirely composed of POT.

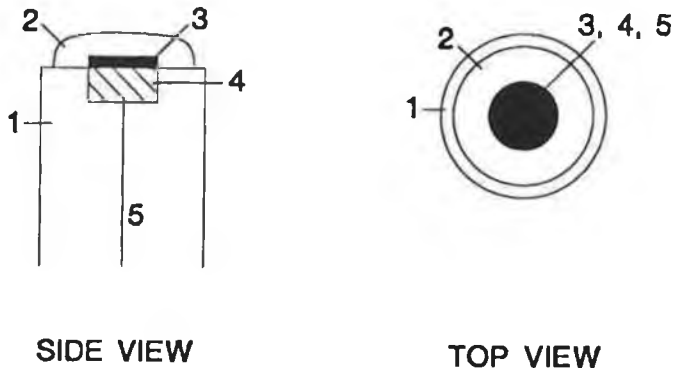

Figure 5.8 :- Schematic description of the active part (top) of the solid contact ion-selective electrode (SCISE), with 1. teflon body, 2. ion-selective PVC based membrane, 3. POT or PT solid contact, 4. Pt or GC substrate 5. electrical contact.

5.3.3.3 Preparation of Coated Wire Electrodes

The substrates used for the CWE i.e. platinum (Pt) and glassy carbon (GC), were polished and rinsed in the same way as for the SCISE. Thereafter 100 μL of ion-selective cocktail was applied on top of the bare electrode which was then allowed to dry overnight before being conditioned in 0.1 M LiCl.

5.3.3.4 Preparation of Hybrid-Film Ion-Selective Electrodes

The working electrode was a glassy carbon (GC) disc, (Metrohm), diameter 3 mm set in Teflon with an overall diameter of 10 mm. Electrodes were polished with 0.3 μm alumina and rinsed with water and chloroform. A number of mixtures of chemically prepared polyoctylthiophene $(POT)_c$ and the ionophore PVC cocktail were prepared in 2 mL vials for application to the electrode (See Table 5.2). The total dry weight was kept constant at 12.27 mg, which is equivalent to the weight of 100 μL of the lithium ionophore PVC cocktail, after the THF had been allowed to evaporate. The (POT)c was dissolved in the ionophoric cocktail and THF was added to bring the volume to 120 μL.

Table 5.2 Hybrid Film Electrode (HFE) Compositions.

Electrode Name	% POT	Wt. of POT$_c$ (mg)	Vol. Cocktail (μL)
(a)	0	0	100
(b)	5	0.61	95
(c)	10	1.23	90
(d)	15	1.84	85
(e)	20	2.45	80
(f)	25	3.07	75
(g)	50	6.14	50
(h)	75	9.20	25
(i)	100	12.27	0

The electrode to be coated was clamped in an upright position and the PVC/POT solution was pipetted on top. The electrode was then protected from particulate contamination and allowed to dry for at least 7 hours. This left a black film (approximately 100-150 μm thick) on the glassy carbon substrate contact for all electrodes containing (POT)c. The electrode was then conditioned in a 0.1 M solution of LiCl for 12 hours before being examined for potentiometric cationic response.

5.3.4 Potentiometric Measurements

5.3.4.1 Potentiometric Measurements of Polymer Electrodes

All potentiometric measurements were carried out using a Metrohm 663VA Stand, connected to a Metrohm 632 pH Meter. The potentiometric response of the polymer electrodes, used as indicator electrodes, was obtained in conjunction with the Ag/AgCl/KCl (3M) reference electrode, connected to the cell via a bridge filled with the test solution (0.1M LiCl). No background salt was used since cationic sensitivity, not selectivity, is a feature of these polymer electrodes. The liquid junction potential arising from the concentration difference between the reference bridge (10^{-1}M) and the test solution (10^{-1} - 10^{-6} M) was taken into account and the potential values reported for the polymer electrodes have been corrected using the Henderson Equation [5] (equation 5.5). The polymer electrodes were equilibrated in each new solution for two minutes before a

reading was taken. The working electrode was rotated at 500 rpm during the first minute to enhance speed of equilibration and a value was taken 1 minute after the end of rotation. Film conditioning and potentiometric measurements were performed at room temperature in open air. The slope values quoted here have been calculated by linear regression using the three points spanning a concentration range of two decades (usually 10^{-1} and 10^{-3} M LiCl).

5.3.4.2 Potentiometric Measurements of PVC Coated Electrodes

The potentiometric measurements of the SC polymer electrodes coated with PVC(Li^+) and the lithium CWEs i.e (CWE)Pt/PVC(Li^+)) were obtained in a similar manner to the polymer electrodes except that a background salt of KNO_3 (0.1M) was used as the bridge solution and was also included in all of the LiCl standards from 10^{-1} -10^{-6} M. For the chloride selective CWE, i.e. (CWE)Pt/PVC(Cl^-) electrode no background salt was used in any of the measurements since NO_3^- and SO_4^- were both found to interfere significantly with the chloride response. Therefore all values quoted are corrected for liquid junction potential using the Henderson equation (**5.5**). All slopes are calculated over the three decades from 10^{-1} to 10^{-4} M LiCl.

5.3.4.3 Hybrid Film Ion-Selective Electrodes

The hybrid-film polymer electrodes were used as the working electrodes and the reference electrode was an Ag/AgCl/KCl (3 M) electrode that was connected to the cell via a bridge containing 0.1 M KNO_3 or 0.1 M LiCl depending on whether a background salt was present in the analyte solution.

For cationic response to LiCl measurements for electrodes 1-6 all LiCl solutions between 10^{-1} and 10^{-6} M also contained a background salt of 0.1 M KNO_3. With electrodes 7 and 8 no background salt was used, since no cationic selectivity was being exhibited. Therefore the potentials shown have been corrected for liquid junction potential arising from the concentration difference between the reference bridge (10^{-1}M) and the test solutions (10^{-1} to 10^{-6} M) by the Henderson Equation. The electrodes were equilibrated for two minutes in each cation solution prior to taking a reading. The solution was stirred with a magnetic stirrer for the first minute to increase speed of equilibration, and was then

allowed to rest for the second minute before a mV reading was taken. Film conditioning and potentiometric measurements were carried out at room temperature (23 $\pm$ 2°C) in open air. The slopes presented have been calculated by linear regression using three points spanning a concentration of 2 decades from 10^{-1} to 10^{-3} M.

The limit of detection (LOD) was calculated as the concentration at which the response curve deviated from linearity by 18 mV. The response time is defined here as the time needed for the electrode to reach a stable potential value (within 1 mV of the steady state value) after a concentration step from 10^{-4} to 10^{-3} M of the primary ion [64].

The stability of all of the electrodes was determined by examining the potential of each electrode in a solution of 10^{-1} M LiCl over a 5-7 day period. The effect of nitrogen on the rest potential of all of the electrodes was examined. The electrodes were kept in open stirred solutions of 10^{-1} M LiCl until a steady potential had been attained, and then purged with N_2 for 2 hours, with the potential being monitored continuously. The nitrogen was then removed and the potential once again monitored.

5.3.5 Estimation of Selectivity Coefficients

A selectivity constant or coefficient is used to indicate the extent to which an interfering ion (j), interferes with the response of an electrode to its primary ion (i) and has already been defined by the Nikolskii Equation (**5.26**)

$$E_M = E_M^o + \frac{2.303RT}{z_i F} \log \left[a_i + \sum k_{ij}^{pot} a_j^{zi/zj} \right] \qquad (5.26)$$

where z_i and z_j are the charges on the ion **i** and **j** respectively and E^o is the standard potential of the electrode or a constant. The term selectivity coefficient can be misleading in several ways which are outlined below. This may result in coefficients that are not highly reproducible or precise being quoted

a The selectivity coefficients for any interfering ions are dependent on the ionic strength of the solution and the activity level at which the primary and interfering ions are measured,

b They depend on whether potentials are taken in mixed or separate solutions containing the two ions,

c The actual method/equation used to obtain the final result has an effect on the calculated selectivity coefficient value.

d The membrane composition of the electrode e.g. the amount and type of ionophore, plasticiser and additives which is mainly determined by the membrane manufacturer, will affect the selectivity characteristics of a particular electrode.

Therefore it is crucial when quoting selectivity coefficient values that the composition of the electrode, the conditions under which the measurements were made and the methods used in the calculations are stated A number of methods have been outlined for obtaining estimates of k_{ij}^{Pot}, with the most frequently used methods being the separate and mixed solution methods which have been described in full by Moody and Thomas [6].

5.3.5.1 Separate Solution Method

A calibration curve is obtained for the primary ion (i) over the concentration range usually from 10^{-1} to 10^{-5} M. A similar curve is prepared for the interfering ion (j),
see Figure 5.9, The selectivity coefficient can then be calculated by either of two methods (a) equal activities or (b) equal potentials.

(a) Equal Activities

The electrode potential, Ei, to the primary cation (i) only , is given by the Nernst equation

$$E_1 = E^o + S \log a_i \qquad (5.2)$$

where S = 2.303 RT/nF
The electrode response to a mixture of cations is given by the Nikolskii equation (5.25) above. If the electrode is placed in a solution containing the interfering cation (j) only then can the potential (E_2) to cation (j) be obtained from equation (5.25) by letting $a_i = 0$, and

$$E_2 = E^o + S \log k_{ij}^{pot} a_j \qquad (5.31).$$

When $a_i = a_j$ and provided the valency of the cations is the same i.e. $z_i = z_j$ then k_{ij}^{pot} can be calculated from

$$\log k_{ij}^{pot} = \frac{(E_2 - E_1)}{S} \qquad (5.32)$$

when the potentials E_1 and E_2 have been measured. Since the selectivity coefficients are activity dependent, for comparison purposes the chosen activity should always be reported (usually 10^{-2} or 10^{-1} M).

(b) Equal Potentials.

Alternatively a method of equal potentials may be used. When $E_1 = E_2$ equations (5.2) and (5.33) may be combined to give

$$k_{ij}^{pot} = \frac{a_i}{a_j} \qquad (5.33)$$

The activities a_i and a_j can be read from the calibration curve (Figure 5.9), where the potentials E_1 and E_2 are equal. If the primary and interfering ions have different charges, the equation may be modified to

$$k_{ij}^{pot} = \frac{a_i}{a_j^{zi/zj}} \qquad (5.34)$$

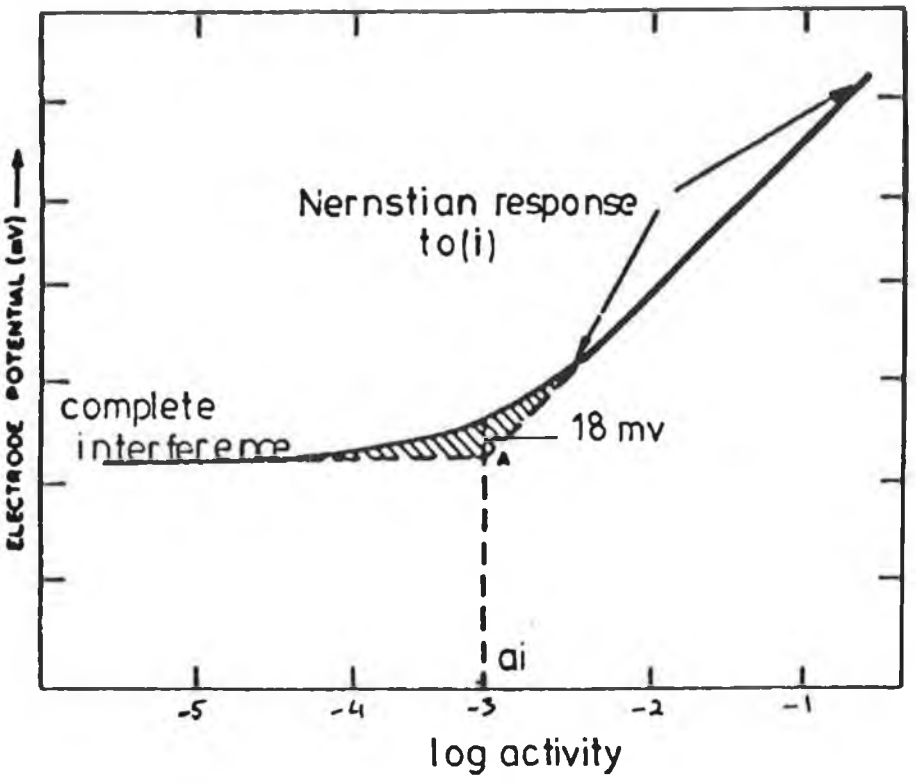

Figure 5.9:- *Estimation of the selectivity coefficient k_{ij}^{Pot} using separate solution method. (A) Response to primary ion (i) only; (B) response to interfering ion (j) only [6].*

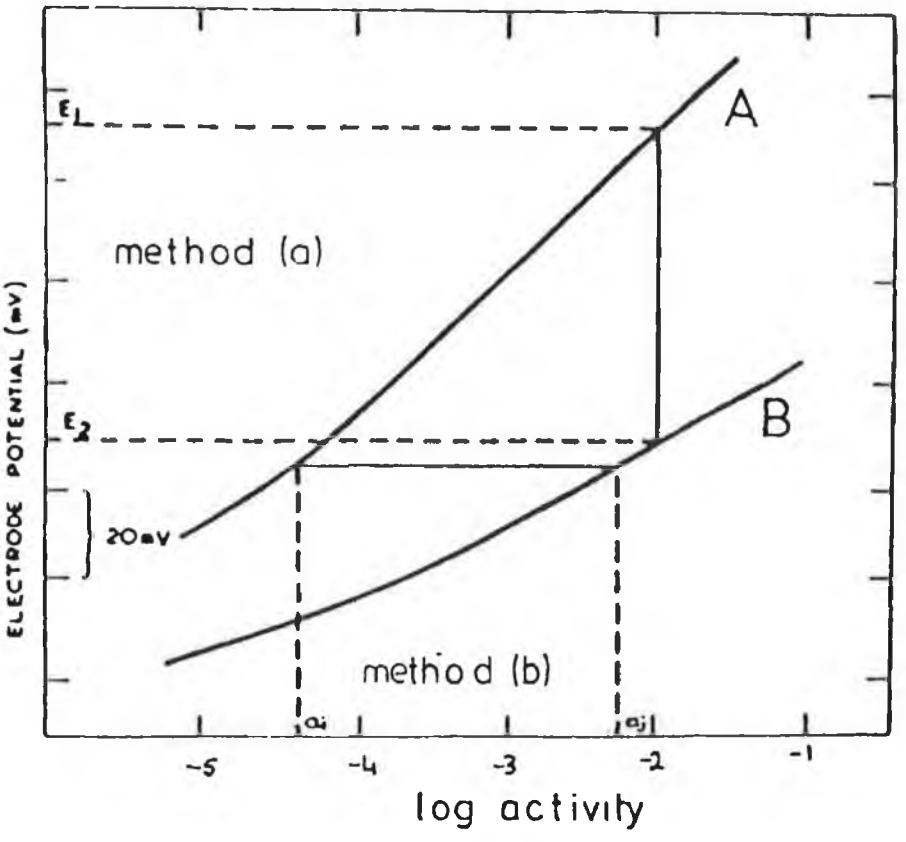

Figure 5.10:- *Estimation of selectivity coefficient (k_{ij}^{Pot}) using the mixed solution method, [6].*

5.3.5.2 Mixed Solution Method

Here the calibration curve is recorded in (a) the absence and (b) the presence of a fixed level of interfering ion (e.g. $a_j = 0.01$ M) throughout the calibration range of a fixed level of the primary ion. As the activity of the primary cation falls, the interfering ion j exerts its influence until complete interference sets in, and is seen as a horiziontal plateau at which the potential is constant (Figure 5.10). The two linear portions are extrapolated to calculate the activity of the primary ion a_i at the intercept and the selectivity coefficient is calculated from equation (**5.34**) where a_j is the constant background interference activity. If drift of the potential is observed in the plateau region when ion (j) provides high interference, then the value of a_i can be taken at the point where the two curves differ by 18 mV. In the case where $z_j = 2$ i.e. divalent ion selectivity a value of 8.9 mV should be used.

5.3.5.3 Selectivity Coefficient Determination for SCISEs, CWEs, HFE's.

The selectivity coefficients (k_{ij}^{Pot}) were determined by the separate solutions method using 10^{-2} M chloride solutions of the cations involved. Response time measurements involved the injection of 225 μL of 1 M LiCl into 25 mL of 10^{-3} M LiCl, to give a ten-fold change in concentration.

5.3.6 Redox Responses

The response of any electrochemical reaction which involves a transfer of charge to or from species in solution can be defined as

$$\text{oxidant} + ne^- \rightleftharpoons \text{reductant} \qquad (5.35)$$

$$E_{cell} = S\log\frac{[\text{oxidant}]}{[\text{reductant}]} \qquad (5.36)$$

where E_{cell} is the measured value of the cell potential, E^o is the formal potential for the reaction. A plot of potential (E_{cell}) Vs. the quantity [oxidant]/[reductant] or the ratio of the concentration of the two species in solution should give a theoretical slope of 59.2 mV for a one electron system. In order to investigate the ideality of the response at a platinum, glassy carbon, or polymer coated substrate

electrodes, an oxidant/reductant couple was chosen whose standard potential falls within the semiconducting range of the polymers polythiophene or polyoctylthiophene i.e.less than approximately 0.9 V. The redox couple based on the potassium salts of iron ferric/ferro cyanate was found to be suitable.

$$\underset{\text{(FeIII)}}{Fe(CN)_6^{3-}} + e^- \rightleftharpoons \underset{\text{(FeII)}}{Fe(CN)_6^{4-}} \qquad E^o = 0.36V \qquad (5.37)$$

The redox sensitivity of the different electrodes was examined by measuring the potential of the redox couple FeII/FeIII in various ratios with the total Fe concentration being 10^{-3} M, and in the presence of a constant background ionic concentration of 10^{-1} M LiCl. The potential vs. log ([Fe(III)]/[Fe(II)]) was then plotted and the slope determined. The ratio was changed from 10/1 to 1/1 to1/10.

5.4 Results and Discussion

5.4.1 Ionic Response of Electrodes with Lithium Selective Membranes

5.4.1.1. (CPE)Pt/PT and (CPE)Pt/POT

The cationic response of the galvanostatically polymerised platinum electrodes to LiCl was examined prior to coating with the lithium selective cocktail. Even after four days of conditioning of the (CPE)Pt/PT electrode in 0.1M LiCl, a poor cationic response of 17.65 and 35.65 mV/dec was obtained. Hysteresis on measuring potentials from 10^{-1} to 10^{-4} M and then from 10^{-4} to 10^{-1}M was significant with large differences in slope also being noted, (Figure 5.11a). Previously a slope of 39.4 mV/dec had been achieved for a similarly prepared electrode [61]. In order to reduce this hysteresis effect and to try and improve the electrode response, the electrode was conditioned for a further 16 hours in 10^{-4} M LiCl, (Figure 5.11b) The performance of a PPy electrode was previously shown to be affected by the concentration of conditioning solution, with a decrease in initial potential and an improvement of slope being seen with a decrease in concentration of conditioning solution [57].

This time a best slope of 39.6 mV/dec. was obtained and although hysteresis was still evident, it was decided at this stage to coat with the lithium selective PVC membrane. After allowing the PVC membrane to dry for 12 hours and subsequently conditioning for 12 hours in 0.1 M LiCl, the electrode's response to LiCl was measured.

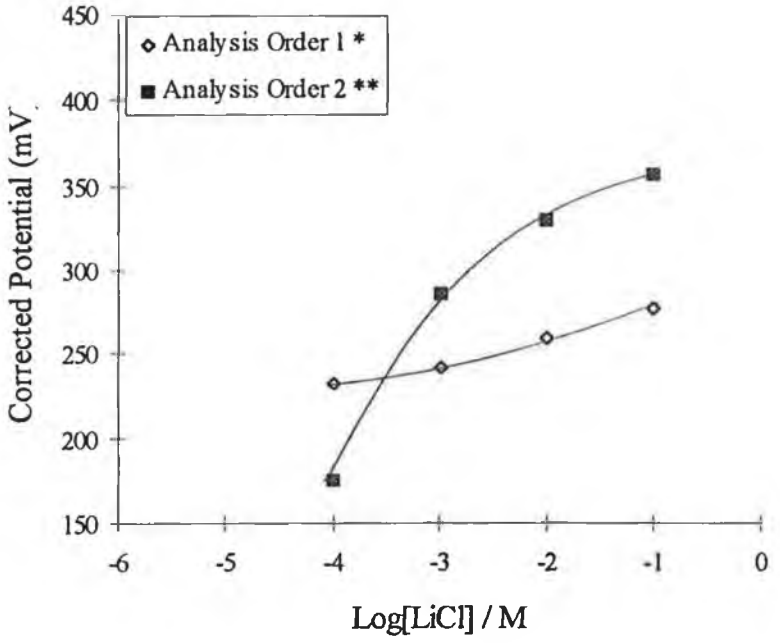

Figure 5.11 (a):-*Potentiometric Response of (CPE)Pt/PT electrode to LiCl after 4 days conditioning in 0.1 M LiCl, in the presence of no background electrolyte.*

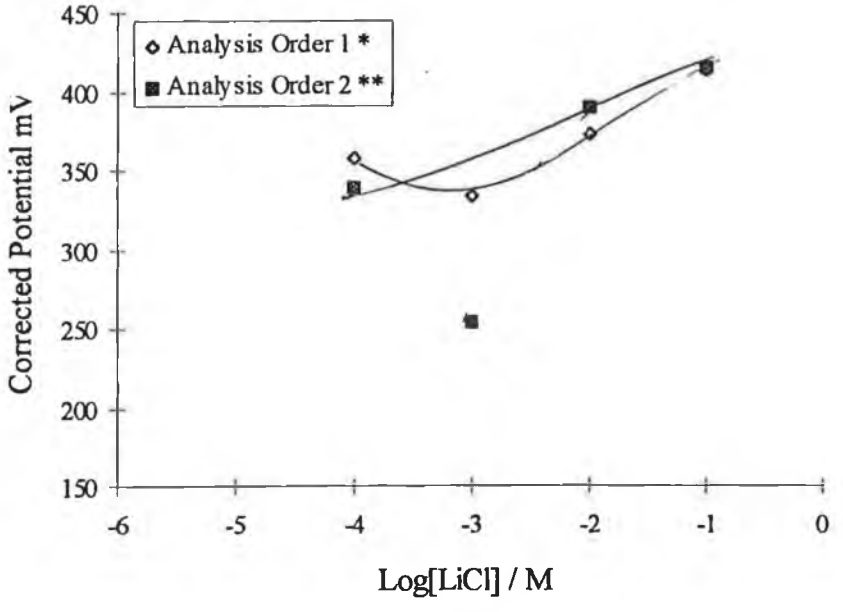

Figure 5.11 (b):-*Potentiometric Response of (CPE)Pt/PT electrode to LiCl after a further 12 hours conditioning in 10^{-4} M LiCl, in the presence of no background electrolyte.*

* Analysis Order 10^{-1} - 10^{-4} M

** Analysis Order 10^{-4} - 10^{-1} M

The (CPE)Pt/POT electrode exhibited a slope of 41.1 mV/dec. after 20 hours conditioning in 0.1M LiCl and was coated with the lithium selective cocktail at this stage (Figure 5.12).

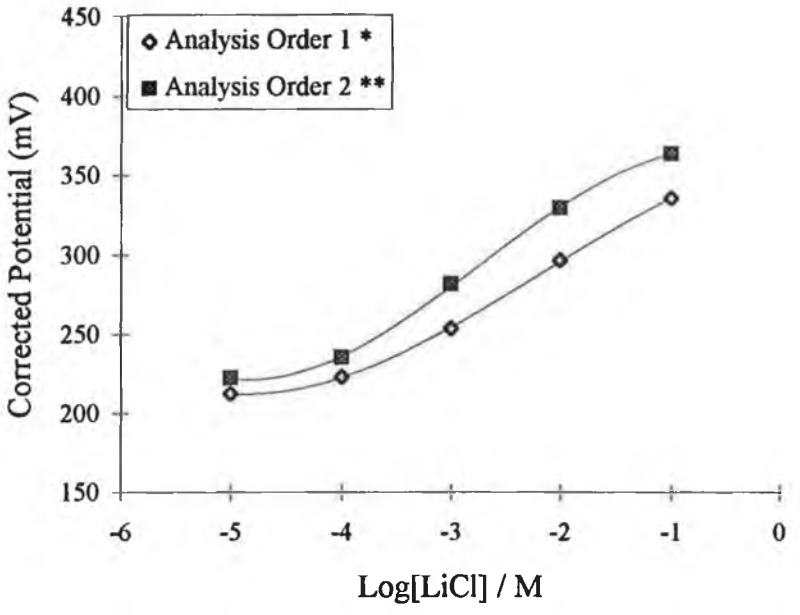

Figure 5.12:-Potentiometric Response of (CPE)Pt/POT electrode to LiCl after 20 hrs. conditioning in 0.1 M LiCl, in the presence of no background electrolyte.

* Analysis Order 10^{-1} - 10^{-5} M

** Analysis Order 10^{-5} - 10^{-1} M

5.4.1.2 Ionic Response of (SC)Pt/PT/PVC(Li^+), (SC)Pt/POT/PVC(Li^+) and (CWE)Pt/PVC(Li^+)

The response characteristics of the three different lithium selective electrodes measured at 23°C are outlined in Table 5.3. The coated wire electrode, (CWE)Pt/PVC(Li^+), shows a slightly better cationic response, with a mean slope of 56.5 mV/dec. compared to 56 mV/dec. for (SC)Pt/PT/PVC(Li^+) and 56.25 mV/dec. for (SC)Pt/POT/PVC(Li^+). However, slightly superior selectivity along with lower limits of detection are displayed by the (SC)Pt/PT/PVC(Li^+) electrode. The theoretical slope for a monovalent ion is 58.8 mV/dec. at 23°C Selectivity is generally in the order $Li^+ > Na^+ > K^+ > NH_4^+ > Mg^{2+}$. Improved selectivity has previously been described for PVC electrodes incorporating

polpyrrole (PPy) as the conducting polymeric solid contact [1], compared to corresponding conventional ISE's.

Table 5.3 Cationic Response of Lithium Containing Electrodes.

Electrode	Slope (mV/dec.)	LOD (M)	K_{Li^+,Na^+}	K_{Li^+,K^+}	K_{Li^+,NH_4^+}	$K_{Li^+,Mg^{2+}}$
Pt/PT	35.15	-	-	-	-	-
Pt/POT	41.15	-	-	-	-	-
Pt/PT/PVC (Li^+)	56.00	2.09×10^{-4}	-1.28	-1.29	-1.30	-2.27
Pt/POT/PVC (Li^+)	56.25	2.09×10^{-4}	-1.22	-1.28	-1.30	-2.32
Pt/PVC (Li^+)	56.50	3.25×10^{-4}	-1.24	-1.28	-1.28	-2.32

Hysteresis:- Both the (CWE)Pt/PVC(Li^+) and the (SC)Pt/POT/PVC(Li^+) electrode exhibited a difference between potential values on going from 10^{-1} to 10^{-6} M LiCl (analysis order 1) and then returning from 10^{-6} to 10^{-1} M (analysis order 2). On reading the potentials a third time (analysis order 3), very little further difference is noted between solutions of the same concentration. This effect is not evident with the (SC)Pt/PT/PVC(Li^+) electrode where potential values of solutions of the same concentration are very similar. This point is illustrated in Figure 5.13(a), 5.13(b) and 5.13(c) for (SC)Pt/PT/PVC(Li^+), (SC)Pt/POT/PVC(Li^+) and (CWE)Pt/PVC(Li^+) electrodes respectively where the response to LiCl at varying concentrations is shown. The existence of hysteresis effects during initial electrode use should therefore be considered and the electrode should be calibrated prior to use with sufficient measurements of standards.

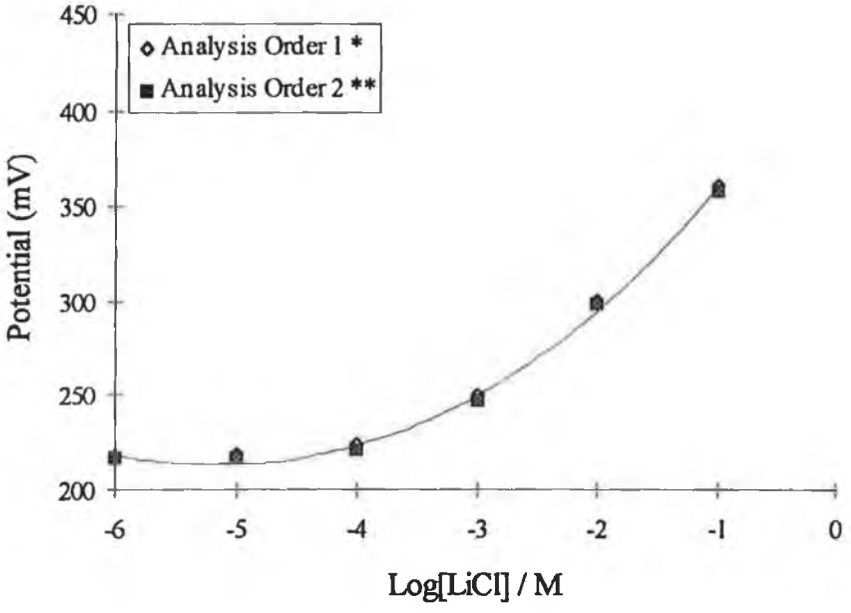

Figure 5.13a:-Potentiometric response of (SC)Pt/PT/PVC(Li^+) electrode to LiCl in the presence of 0.1 M KNO_3 background electrolyte.

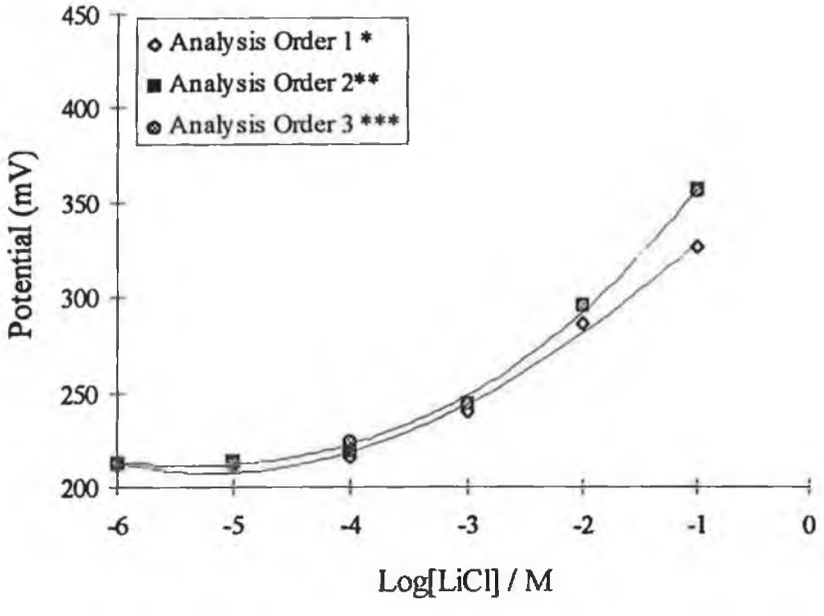

Figure 5.13b:-Potentiometric response of (SC)Pt/POT/PVC(Li^+) electrode to LiCl in the presence of 0.1 M KNO_3 background electrolyte.

* Analysis Order 10^{-1} - 10^{-6} M

** Analysis Order 10^{-6} - 10^{-1} M

*** Analysis Order 10^{-1} - 10^{-6} M

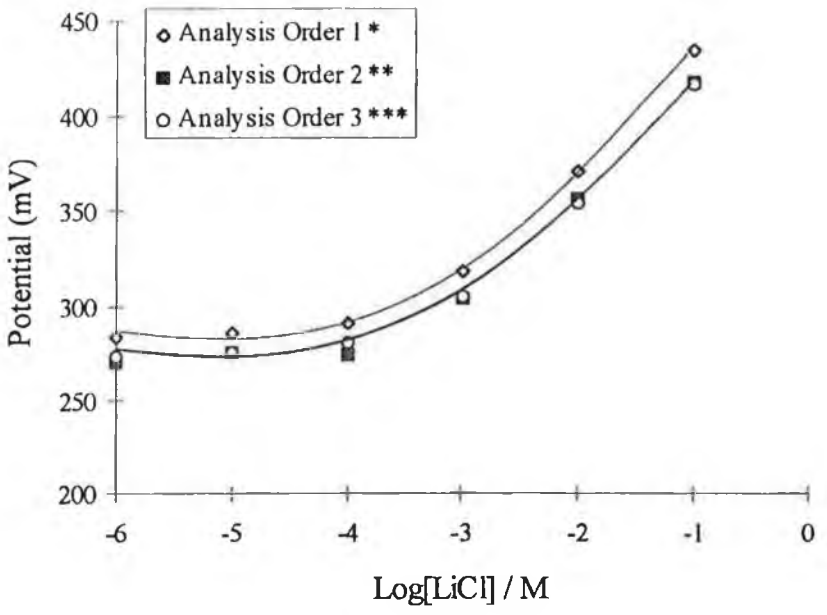

Figure 5.13c:-Potentiometric response of (CWE)Pt/PVC(Li^+) electrode to LiCl in the presence of 0.1 M KNO_3 background electrolyte

5.4.2 Time Response

Similar response times were observed for the SCISEs and the CWEs studied. The (SC)Pt/PT/PVC(Li^+), (SC)Pt/POT/PVC(Li^+) and the (CWE)Pt/PVC(Li^+) showed response times of under 10 s, including the time needed for mixing of the added solution. It is encouraging that the response times are similar to the corresponding CWEs , since an extra conduction process is envisaged for the SC electrodes.

5.4.3 Stability

The long term stability of the electrode potentials is of great importance in practical applications of ion-selective electrodes. Typically the performance of many CWEs is characterised by irreproducible potentials, noise and overshoot of potentials, with such problems generally occurring during the first few days. One of the main purposes of this work was thus to investigate the possibilities of producing a stable SCISE having PT or POT as the solid contact. The stability of

the electrode potentials for the (SC)Pt/PT/PVC(Li^+), (SC)Pt/POT/PVC(Li^+) and the (CWE)Pt/PVC(Li^+) are shown in Figures 5.14(a), (b) and (c) respectively.
For the (CWE)Pt/PVC(Li^+) electrode, Figure 5.14(c), a continuous steady decrease in potential was observed for 7 days after the initial 53 mV drop observed during the first 12 hours, with a further 132 mV decrease being observed over these final 7 days. So overall the electrode cannot be considered stable with approximately a 20 mV decrease in potential each day. CWEs have been previously shown to be unstable [19]. Since the coupling between the metal and the coating in CWEs can be described as capacitive and the contact potential is distributed between the capacitors of the two surfaces, the sensitivity of the capacitive coupling to external substances penetrating between the coating and the metal is detrimental to stability. Behaviour which resembled a discharging capacitor was noted with all of the (CWE)Pt/CWEs studied. After the gradual drift to lower potentials over a number of days, the electrodes were removed from the analyte solution and placed in new solutions of 0.1 M LiCl. The potentials of the electrodes were found to have returned to approximately their original values. The reason for such behaviour is unclear at this point but it is possibly due to some internal boundary effect.

For the (SC)Pt/PT/PVC(Li^+) electrode an initial sharp decrease in potential of 50 mV occurred during the first 48 hours, (Figure 5.14(a)). The rate of change in potential then reduced slightly and continued decreasing at the new level for the remaining three days, with the final potential after the 5 days stability study being 94 mV lower than the original potential value on day 1. This electrode would appear to be slightly more stable than the CWE especially after a number of days when the initial drift seen is reduced to about 10 mV/day. A 10 mV drift/day however cannot be seen as ideal electrode behaviour. When the electrode was transferred into a fresh solution of LiCl at the end of the stability study, the immediate potential change observed for the (CWE)Pt/PVC(Li^+) electrode was not witnessed, but instead it assumed the same potential it had before its transfer.

The drift observed may be due to a further anionic equilibration between the layers, with any remaining BF_4^- from the polymerisation passing through the PVC layer trying to set up an equilibrium with the Cl^- anions, which would permeate the PVC membrane from the LiCl solution a lot more slowly than the Li^+ cation, thus causing a drift in potential. It has previously been observed that measurements on conducting polymers doped with BF_4^-, on a platinum substrate,

yield higher initial potentials than those doped with other anions [65]. In this work BF_4^- was used as the doping ion during polymerisation and although the electrode was undoped after polymerisation, some residual BF_4^- may have remained in the polymer layer giving a slightly higher initial potential than would exist if the polymer was totally undoped.

With the (SC)Pt/POT/PVC(Li^+) electrode, a potential within ±12 mV of the potential reached within 2 days of the beginning of the study was maintained. Again a large initial potential change of 104 mV was observed during the first 48 hours of the stability study, before a levelling off became apparent. This electrode appears to be the most stable of the three electrodes examined and again the capacitor discharge effect was not observed on transferring the electrode into a new solution.

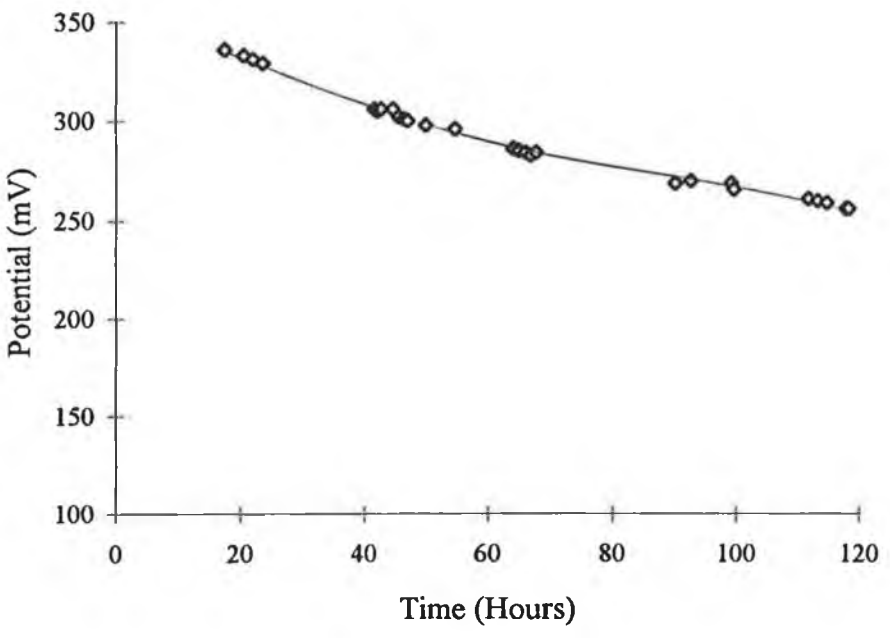

Figure 5.14(a):-Stability study of (SC)Pt/PT/ISE(Li^+) in 0.1 M LiCl in the presence of 0.1 M KNO_3.

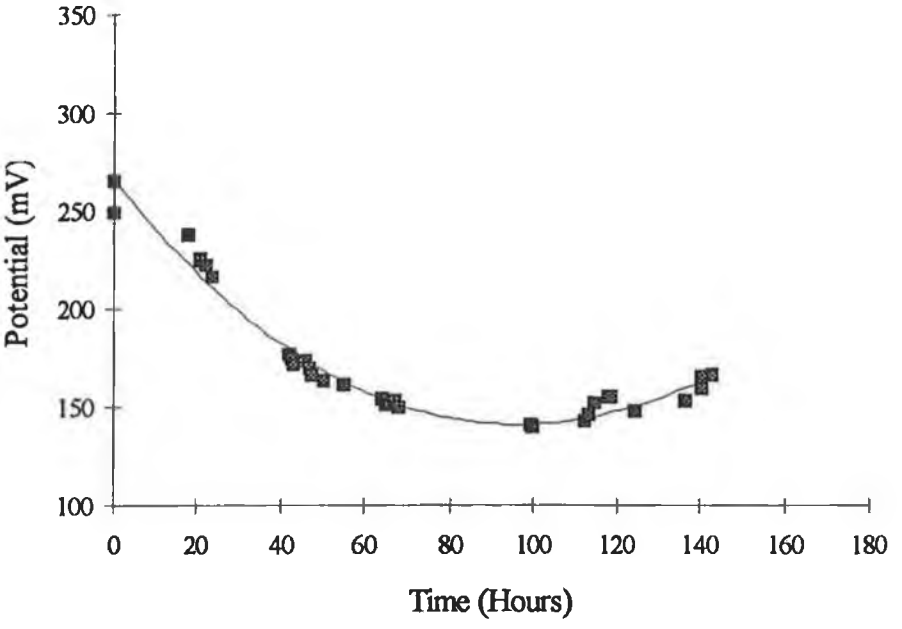

Figure 5.14(b):-Stability study of (SC)Pt/POT/ISE(Li^+) in 0.1 M LiCl, in the presence of 0.1 M KNO_3.

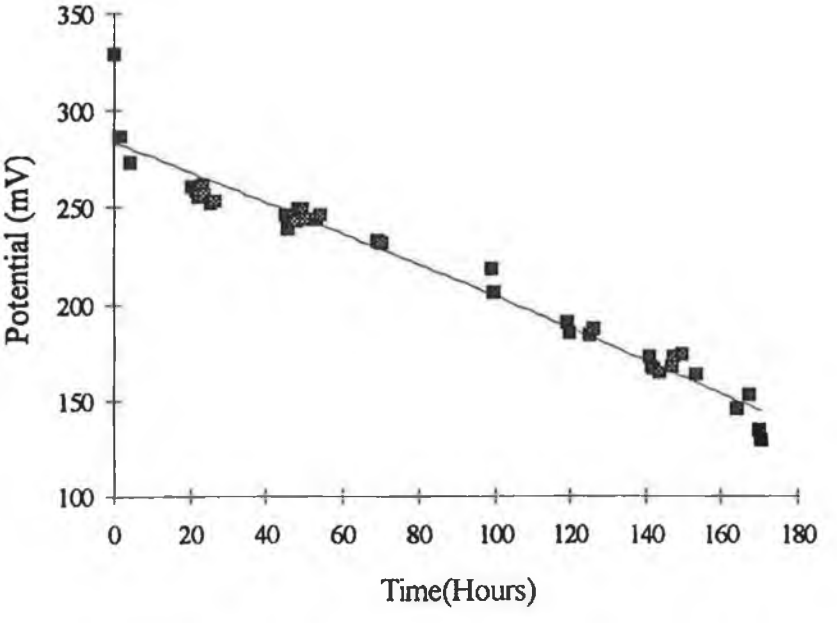

Figure 5.14(c):-Stability study of (CWE)Pt/ISE(Li^+) in 0.1 M LiCl, in the presence of 0.1 M KNO_3.

5.4.4 Oxygen Dependence

The potential of CWEs is also known to be dependent on the partial pressure of oxygen [66, 67]. Table 5.4 shows the change in potential of 10^{-1} M LiCl solutions which had been allowed to reach a steady potential in open stirred solutions, before purging with nitrogen for 2 hours.

Table 5.4 Effect of O_2 on Electrode Potential.

Electrode Type	Electrode	Initial Potential (mV)	Final Potential (mV)	ΔE (mV)
	Pt	329	249	80
(CPE)	Pt/PT	347	295	52
(CPE)	Pt/POT	311	289	22
(SC)	Pt/PT/PVC (Li^+)	253	227	26
(SC)	Pt/POT/PVC (Li^+)	320	306	14
(CWE)	Pt/PVC(Li^+)	329	311	18

From these results, we can see that the bare platinum electrode is affected the most by the presence of O_2. Unlike the polypyrrole system previously described [1], where the (CPE)Pt/PPy electrode in which the PPy was in its doped form, displayed no potential change, both PT and POT do exhibit a potential decrease when purged with N_2. The (CPE)Pt/PT electrode showed a larger potential change than the (CPE)Pt/POT electrode. The potential changes are however smaller than that seen for the Pt electrode on its own. This suggests that by coating the Pt electrode with these semiconducting polymers the effect of O_2 on the platinum electrode can be reduced.

The effect of O_2 on the electrodes is further reduced when each of the semi-conducting polymers is coated with the PVC-ionophore cocktail suggesting that both semi-conducting polymer layers are more permeable to O_2 than the ionophoric PVC layer. The (CWE)Pt/PVC(Li^+) electrode displays an 18 mV drop in potential under the same conditions indicating the capability of oxygen to penetrate the PVC membrane to the platinum surface. The polypyrrole layers

used in analogous work had an estimated thickness of 8 μm [1] whereas the polymer layers in this work are approximately 0.25 μm [62]and this could account for the increased influence of oxygen on the rest potential. All electrodes showed a tendency to return to approximately their original potential upon cessation of nitrogen purging.

5.4.5 Redox Response

The results of the redox response measurements are summarised in Table 5.5. The bare Pt electrode displayed a Nernstian response whereas the (CPE)Pt/PT and (CPE)Pt/POT electrodes displayed a sub Nernstian response but with some electronic conduction being evident. This was to be expected since both polymers used in this system are in their undoped/semiconductive state. The fact that a response is obtained indicates that some electronic transmission to the Pt layer is possible. When the PVC(Li^+) layer was added no redox response was observed, since there is no mechanism present for electron transport in the PVC. Hence the PVC layer can protect the inner Pt or semiconducting polymer layer from the effects of strong oxidising or reducing agents in solution.

Table 5.5 Redox Response

Electrode Type	Electrode	Slope (mV/decade)
	Pt	58.2
(CPE)	Pt/PT	30.0
(CPE)	Pt/POT	35.1
(SC)	Pt/PT/PVC (Li^+)	-0.5
(SC)	Pt/POT/PVC (Li^+)	-1.5
(CWE)	Pt/PVC(Li^+)	-0.5

5.4.6 Effect of Conditioning Solution on Electrode Response

A PT polymeric film was prepared as previously described and was conditioned for 2 days in KCl after synthesis. A cationic sub-Nernstian slope was obtained ie 36.25 mV/dec. At this stage a Na^+ selective PVC-ionophore cocktail was added to the electrode to yield a (SC)Pt/PT/PVC(Na^+) electrode. After drying, the electrode was conditioned for 24 hours in NaCl before its response to NaCl was examined, Figure 5.16. A slope of 56.72 mV/dec was obtained and a selectivity coefficient of Na^+ against K^+ was calculated to be -1.65 indicating that the electrode was responding selectively to its primary ion.

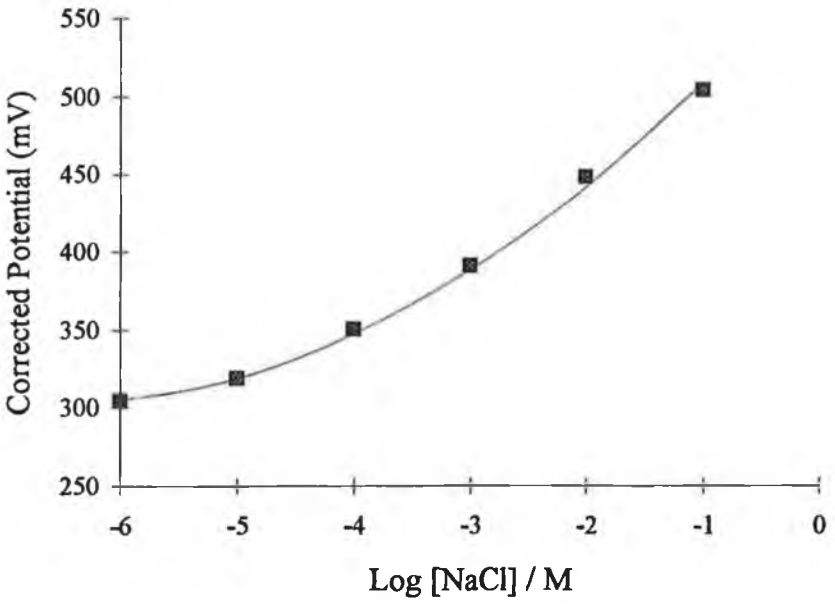

Figure 5.16:-Response of (SC)Pt/PT/PVC(Na^+) electrode to NaCl in the presence of no background electrolyte.

5.4.7 Conclusion

Electrode systems incorporating the semiconductive polymers PT and POT as a solid contact between a platinum substrate and a PVC layer containing a lithium selective ionophore have been successfully made and compared to a CWE using the same ionophore. Both types of electrode give comparatively the same lithium response with a slope of approximately 56 mV/decade and the (SC)Pt/PT/PVC(Li^+) electrode shows slightly superior lithium selectivity over a number of cations. Stability, although not ideal at this stage, was better for the solid contact electrodes compared to the CWE, with the (SC)Pt/POT/PVC(Li^+) electrode showing the best stability. The partial pressure of oxygen in analyte solutions was found to have an influence on solid contact electrodes which is in direct contrast with the findings of the electrically conducting doped PPy and may be a consequence of the thinner conducting polymer layers used in this work. Redox results suggest that electronic information can be conducted through the polymer layers and this would appear to be involved in the mechanism of information transmission in the overall electrode system.

5.5 Comparison of Chloride Selective Solid Contact Electrodes and Coated Wire Electrodes

The next stage of the work involved trying to ascertain whether a cation sensitive electrode such as (CPE)Pt/PT or (CPE)Pt/POT could be made anion selective by the addition of an anion selective PVC membrane. The anion which was to be determined was chloride and it was decided to keep the nature of the cation constant throughout all of the work so again lithium was used.

5.5.1 Ionic Response

The cationic response of both polymer layers was again examined prior to coating. The (CPE)Pt/PT electrode was conditioned for 4 days in 0.1 M LiCl. The response was very poor compared to that obtained previously [61], with a slope of 28.37 mV/dec being obtained. The electrode was conditioned for a further 36 hours in 10^{-4} M LiCl. Again the response was not very good and the electrode was conditioned for a further 36 hours in 0.1M LiCl before an adequate response was obtained with a slope of 35.1 mV/dec. Hysteresis was again evident but this did not seem to have really affected the final (SC)Pt/PT/PVC(Li^+) electrode response, so it was decided to coat with PVC containing Cl^- selective ion-exchanger ionophore , PVC(Cl^-) at this stage. The cationic response of (CPE)Pt/POT was not as good as that previously obtained, with a slope of 31.70mV/dec. being observed, but it was decided to go ahead with it after 27 hours conditioning in 0.1 M LiCl. Electrochemically synthesised conducting polymer electrodes are susceptible to changes in polymerisation conditions, and all parameters must be rigidly adhered to if reproducible films are to be prepared. Parameters such as the presence of oxygen, presence of water and polymerisation temperature can greatly affect the properties of the layer produced.

The PVC layers were allowed to dry for at least 12 hours before being conditioned in 0.1 M LiCl. No background electrolyte was used in any of the measurements since NO_3^- and SO_4^{2-} were both found to interfere significantly with the chloride response. Therefore, all values quoted have been corrected for liquid junction potential using the Henderson equation. All slopes have been calculated over three decades with four points between 10^{-1} and 10^{-4} M.

The results for the chloride selective electrodes are shown in Table 5.6 with data obtained from the response curves 5.17(a), (b) and (c) for the (SC)Pt/PT/PVC(Cl^-), (SC)Pt/POT/(Cl^-) and the (CWE)Pt/PVC(Cl^-) respectively.

Table 5.6 Ionic Response of Chloride Electrodes

Electrode Type	Electrode	Slope (mV/Decade)	L.O.D. (M)
(CPE)	Pt/PT	35.15	-
(CPE)	Pt/POT	31.70	-
(SC)	Pt/PT/PVC (Cl^-)	-61.95	3.20×10^{-5}
(SC)	Pt/POT/PVC (Cl-)	-62.55	1.40×10^{-5}
(CWE)	Pt/PVC(Cl^-)	-63.45	7.93×10^{-6}

Both solid contact electrodes showed near Nernstian anionic response with (SC)Pt/PT/PVC(Cl^-) giving the best response ie. -61.96, compared to the coated wire version, (CWE)Pt/PVC(Cl^-) which gave a slope of -63.45. However, the Pt/PVC(Cl^-) electrode showed a better L.O.D. Hysteresis did not seem to be a problem with any of the three electrodes, with similar potential values being obtained for each electrode when the potential was measured from 10^{-1} to 10^{-6} M, and in reverse from 10^{-6} to 10^{-1} M. Selectivity measurements for different anions were not carried out since the Cl^- ionophore was found not to be particularly Cl^- selective. Any anions examined interferred significantly with the Cl^- response and no suitable background salt for selectivity measurements could be obtained. The aim of this section of the work was to establish whether the principle of reversing a cation selective electrode could be carried out. Therefore the lack of selectivity displayed by the particular ion-exchanger used is not really detrimental to the findings at this stage but for future work, where ion sensors are being developed, like with all ISEs initial ion selectivity of the ionophore or ion-exchanger is crucial.

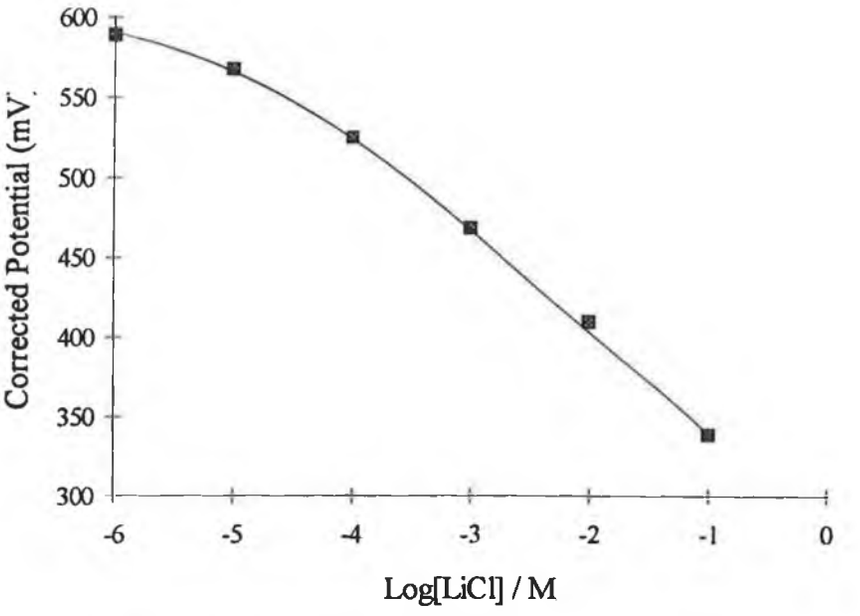

Figure 5.17(a):- *Response of (SC)Pt/PT/PVC(Cl^-) electrode to LiCl in the presence of no background electrolyte.*

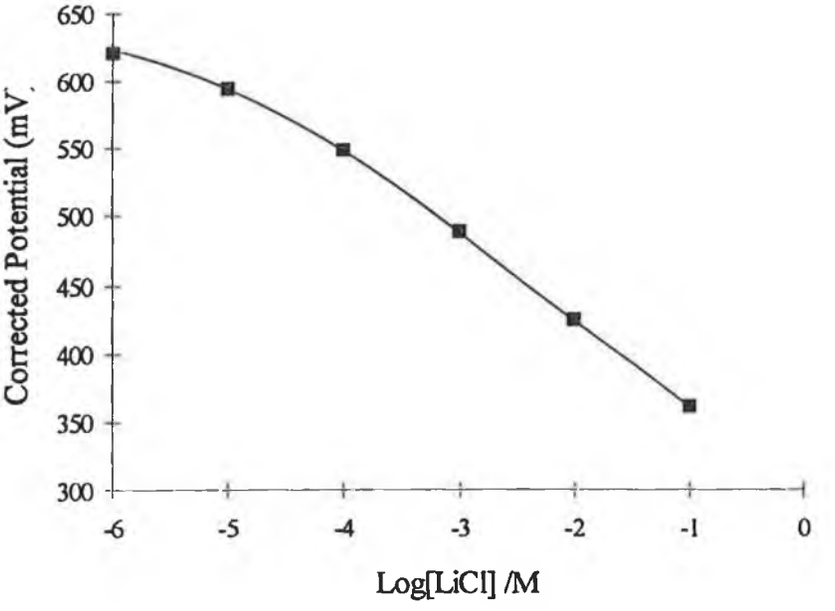

Figure 5.17(b):- *Response of (SC)Pt/POT/PVC(Cl^-) electrode to LiCl in the presence of no background salt.*

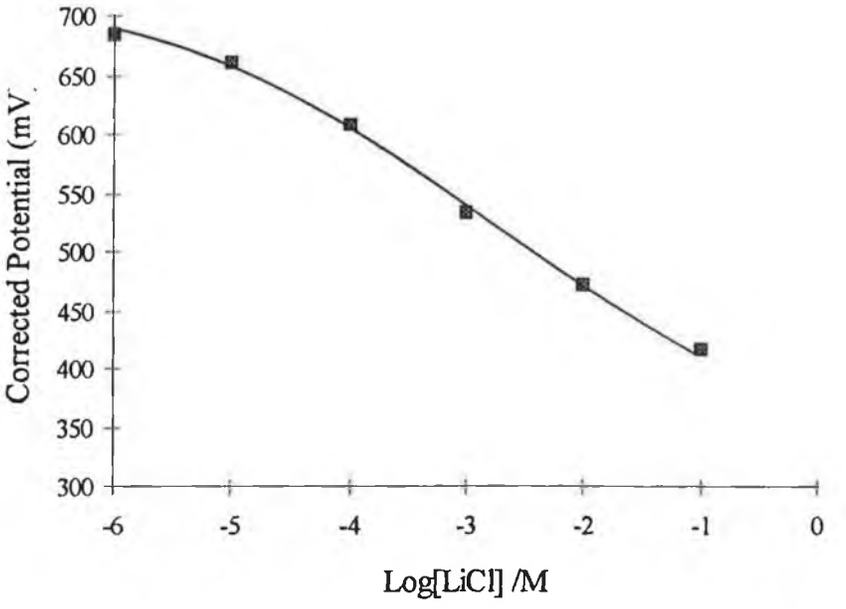

Figure 5.17(c):- Response of (CWE)Pt/PVC(Cl^-) electrode to LiCl in the presence of no background electrolyte.

5.5.2 Stability

The stability studies for the (SC)Pt/PT/PVC(Cl^-), (SC)Pt/POT/PVC(Cl^-) and (CWE)Pt/PVC(Cl^-) are shown if Figures 5.18(a), (b) and (c) respectively. The (SC)Pt/PT/PVC(Cl^-) electrode like its lithium analogue shows a continuous decrease in potential over the duration of the seven day stability study (Figure 5.18(a)). The final rate of the potential decrease is established within the first 10 hours unlike the (SC)Pt/PT/PVC(Li^+) electrode which took 48 hours to reach its final rate of potential change. This however could be an ionophore effect. The final potential was 119 mV less than the initial potential, and still decreasing at a rate of about 15 mV/day. This decrease in potential could be due to a further decrease in BF_4^- anion concentration in the electrode system as was previously discussed.

The (SC)Pt/POT/PVC(Cl^-) electrode showed very good stability over an 8 day stability study (Figure 5.18(b)). A final potential value of $\pm$10 mV was achieved in under 24 hours with no continuous decrease during this time. This ability to stay at approximately the same potential over a number of days was also

exhibited by the Li^+ analogue of this solid contact material ie (SC)Pt/POT/PVC(Li^+)

The (CWE)Pt/PVC(Cl^-) electrode, after an initial 212 mV decrease in the first 40 hours, maintained a final potential within ±16 mV of this value for a remaining 4 days, but with larger variations in potential between days than those observed for (SC)Pt/POT/PVC(Cl^-) (Figure 1.6c). Again a return of the potential to its original value was seen when the electrode was transferred to a new solution of LiCl at the end of the stability study, illustrating the difficulities in obtaining stable CWE potentials.

So it can be concluded again from these stability studies that the POT solid contact electrode offers the most stable system, but in general the Cl^- electrodes appear to be more stable than their Li^+ equivalents.

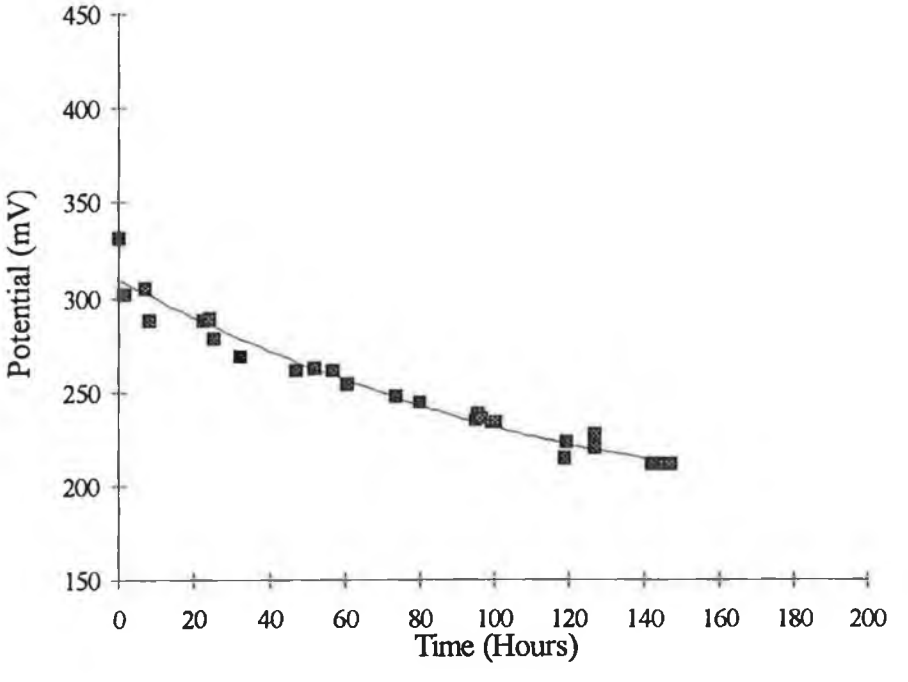

Figure 5.18(a):-Stability study of (SC)Pt/PT/PVC(Cl^-) in 0.1 M LiCl in the presence of no background electrolyte.

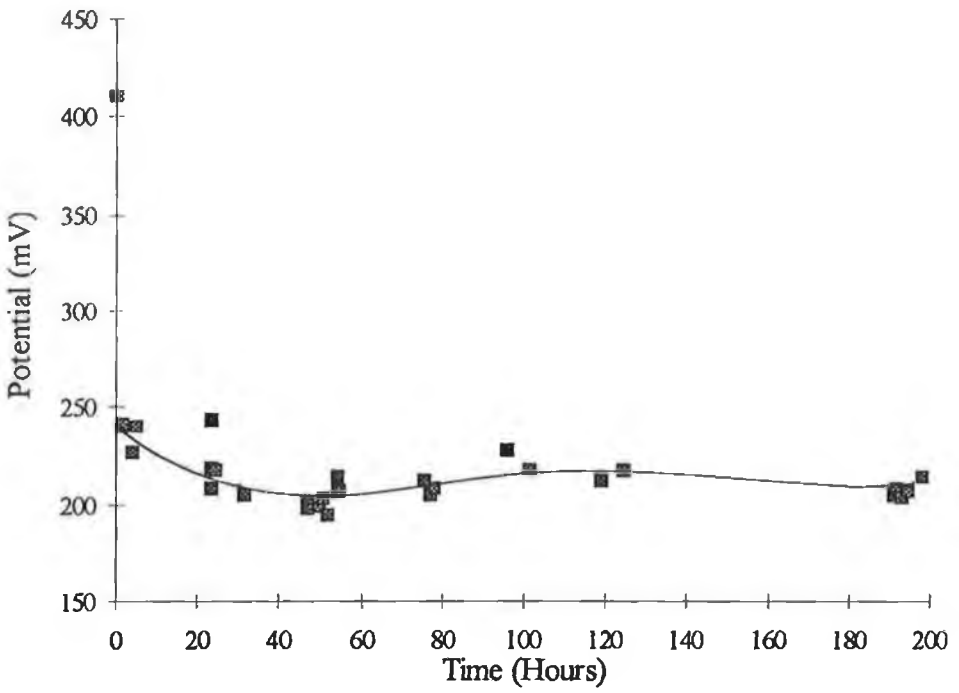

Figure 5.18(b):-Stability study of (SC)Pt/POT/PVC(Cl^-) in 0.1 M LiCl in the presence of no background electrolyte.

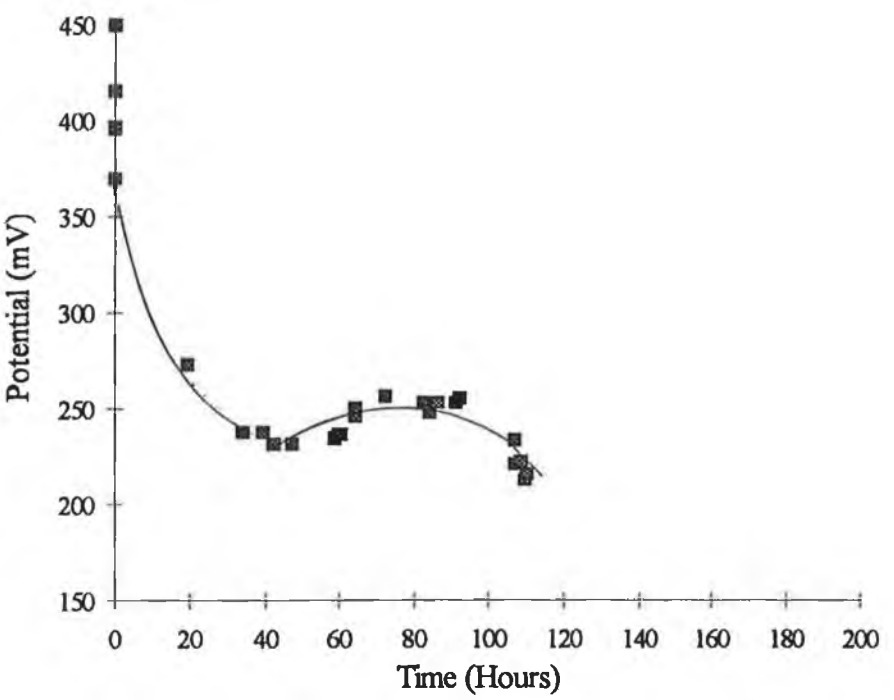

Figure 5.18(c):-Stability study of (CWE)Pt/PVC(Cl^-) in 0.1 M LiCl in the presence of no background electrolyte.

5.5.3 Oxygen Study

The effect of the presence of O_2 on the various electrodes is demonstrated in Table 5.7, where the change in potential of each electrode over a 2 hour period in which the electrode solution, 0.1 M LiCl was purged with N_2. The chloride CWE shows a slightly bigger potential decrease to that observed for the lithium CWE ie 36 mV vs 18 mV, but again the potential reduction is an indication that the PVC ionophore layer is to a certain extent O_2 permeable. The potential change is found to be decreased with the addition of the PVC(Cl^-) onto the solid contact electrodes. This is a similar effect to that observed with the Li^+ selective analogues. PT or POT as earlier stated do not block the permeation of O_2 to the Pt surface but do reduce it and a combination of both semi-conducting polymer and PVC reduces the influence of O_2 on the overall electrode response.

Table 5.7 Effect of O_2 On Electrode Potentials

Electrode Type	Electrode	Initial Potential (mV)	Final Potential (mV)	ΔE (mV)
	Pt	329	249	80
(CPE)	Pt/PT	347	295	52
(CPE)	Pt/POT	311	289	22
(SC)	Pt/PT/PVC (Cl^-)	213	196	17
(SC)	Pt/POT/PVC (Cl^-)	320	306	14
(CWE)	Pt/PVC(Cl^-)	333	297	36

5.5.4 Redox Response

Table 5.8 shows the redox responses of the different combinations of electrodes which also incorporate the chloride selective membrane. The electronic conduction observed with Pt/PT and with Pt/POT in the form of a sub-Nernstian redox response, is non-existent once the PVC(Cl^-) layer forms the redox solution/electrode interface indicating the inability of the PVC to provide a mechanism of electronic conduction and that electronic transmission cannot occur between the PVC and the semiconducting polymer layers. These results

corroborate the conclusions drawn in section 5.4, that the PVC layer has the potential to protect the inner conducting polymer layer from the effects of stong oxidising or reducing agents in sample solutions.

Table 5.8:- Redox Response of Electrodes Incorporating Chloride Ionophore.

Electrode Type	Electrode	Slope (mV/Decade)
	Pt	58.2
(CPE)	Pt/PT	30
(CPE)	Pt/POT	35
(SC)	Pt/PT/PVC (Li^+)	-1.5
(SC)	Pt/POT/PVC (Li^+)	-0.5
(CWE)	Pt/PVC(Li^+)	-1.5

5.5.5 Conclusion

The successful conversion of a cation sensitive electrode ie Pt/PT and Pt/POT to an anion sensitive electrode was carried out by the addition of a chloride selective PVC membrane to the solid contact electrodes. The coated wire electrodes displayed the best chloride sensitivity and the POT solid contact electrode exhibited the best stability. No redox sensitivity was shown by any of the PVC coated electrodes due to the absence of any electronic conduction mechanism. This is also an indication that the initial ionic analyte concentration variation is transmitted through the PVC ionophore membrane by ionic conduction.

5.6 Discussion to sections 5.4 and 5.5, Solid Contact Lithium and Chloride Selective Electrodes.

The experiments described in sections 5.4 and 5.5 were carried out to determine whether PT and POT could be incorporated into an electrode between a Pt substrate and a PVC ion-selective membrane to produce a functioning electrode and to build up a picture of the mechanism of operation of such electrodes. From the ionic response studies (section 5.4.1 and 5.5.1) it was clear that a semi-conducting PT or POT electrode exhibiting sub-Nernstian cation sensitivity could be made either cation (Li^+) or anion (Cl^-) selective by the addition of a PVC layer containing the appropriate ionophore. Such electrodes were capable of giving near Nernstian responses to their primary ion.

None of the stability studies (section 5.4.3 and 5.5.2) gave results for electrodes which could be classed as stable i.e $\pm$ 2 mV/day, but the inclusion of the Pt or POT semi-conducting layers in the electrodes was found to produce electrodes which were more stable than their coated wire equivalents. The lack of stability of the CWEs was demonstrated by a constant reduction in potential with time, but with a return of the potential to its original value when the electrodes were transferred to a fresh solution. The exact reason for such behaviour is not understood but it could be due to an internal boundary effect. No such behaviour was shown by any of the solid contact electrodes giving an initial indication of an alternative, potentially less erratic, mechanism of conduction being involved in the solid contact electrodes. The POT solid contact electrodes showed the best stability, with a maximum variation after the initial potential decrease, which was displayed by all of the electrodes of $\pm$ 12 mV/day. The overall lack of day to day stability exhibited by these electrodes could be a consequence of the effect of variations of the partial pressure of O_2 on the electrode potentials.

The chloride selective electrodes displayed improved stability compared to their lithium counterparts for all three electrode types i.e. (SC)Pt/PT/PVC(Cl^-), (SC)Pt/POT/PVC(Cl^-) , (CWE)Pt/PVC(Cl^-). This could be an effect of the particular ion-exchanger used, but the failure of KONE to release information on the characteristics of these ionophores precludes further comment. Alternatively this difference in stability may be due to slight mechanistic variations between the generation of a cationic response and the generation of an anionic response.

The results obtained from the redox studies (section 5.4.5 and 5.5.4) are very important from the point of view of describing a possible mechanism for the solid contact electrodes. The fact that both (CPE)Pt/PT and (CPE)Pt/POT electrodes display a response although not Nernstian, to the presence of a redox couple is indicative of electronic conduction in the PT or POT layers to the Pt substrate. This is a vital piece of information as it indicated that both PT and POT have the capability to behave as an electron exchanger which is absent in CWEs. No redox response is displayed by the Pt/CWE electrodes and the addition of the PVC ionophore layer to the semi-conducting polymers results in the removal of the redox sensing capabilities of the electrode. This is also an important feature of the solid-contact electrode since a mixed ionic and redox response is obviously undesirable [57]. The lack of selectivity and sub-Nernstian responses exhibited by potentiometric electrodes made using conducting polymers which has been ascribed to a mixed redox-ionic response is effectively eliminated by the addition of the ionically conducting PVC-ionophore layer.

The potentiometric response displayed by the electrically polymerised PT and POT, both in this work and in previous research [61], strongly suggest that PT and POT behave preferentially as cation exchangers in their undoped semi-conductive state. From the potentiometric studies carried out, potentials of the polymer electrodes were in the range 0.1 to 0.45 V, which are below the oxidation potential for PT and POT. Hence the polymers are believed to remain in their undoped state during these measurements. The potential at which these electrodes operate, coupled with the redox response results, give an indication that changes in sample ion concentrations, can be transmitted to electronic conduction at the Pt substrate because of the mixed response of the PT and POT layers.

By collating the data obtained with these electrodes an analogous interface diagram to that presented for the PPy solid contact system [1] can be drawn.

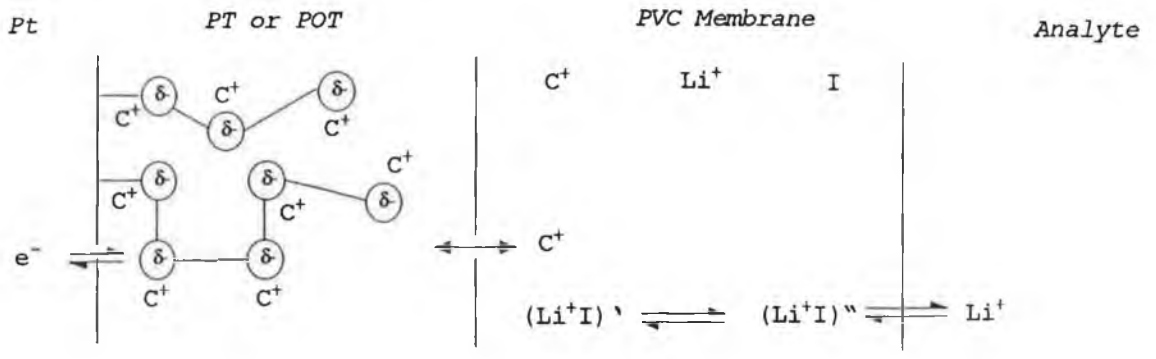

Diagram 5.1:- *Schematic diagram of the charge transfer processes between the three interfaces of the PT or POT solid contact lithium selective electrode.* C^+ = *conditioning cation,* δ^- =*charge on sulphur atoms of thiophene rings,* I = *ionophore.*

The following charge transfer processes are thought to occur

i Li$^+$ or Cl$^-$ exchange at the PVC/analyte solution interface

$$Li^+_{(aq)} + I_{(m)} \rightleftharpoons Li^+ I_{(m)} \qquad (5.38a)$$

or

$$Cl^-_{(aq)} + I_{(m)} \rightleftharpoons I_{(m)} Cl^- \qquad (5.38b)$$

where (aq) is the aqueous phase, (m) represents the PVC membrane phase and I is the ionophore.

ii Transport of the charged complex within the bulk PVC layer :

$$(Li^+I)' \rightleftharpoons (Li^+I)'' \qquad (5.39a)$$

or

$$(I\,Cl^-)'_m \rightleftharpoons (I\,Cl^-)''_m \qquad (5.39b)$$

where (") is the external side and (') is the internal side of the PVC membrane.

iii Exchange of ions at the PT or POT/PVC interface.

iv Electron transport within the PT or POT

v Electron transfer at the Pt/PT or Pt/POT interface

vi Electron flow within the metal.

The PT and POT layers in their undoped state are cation sensitive [61]. This sensitivity has been attributed to a possible interaction between the electron donating sulphur atoms of the thiophene rings forming the polymer backbone with cations. Therefore a cation equilibrium is set up at the Pt/PT ot Pt/POT

interfaces, in contrast to the anion equilibrium illustrated by Cadogan et al [1]. A constant bulk concentration of Li^+ both in the PT or POT and in the lithium selective PVC membrane is providing a sufficient driving force to control a local equilibrium at this interface and thereby maintain a constant gradient of electrical potential.

In the chloride selective solid contact electrodes, the cation potential is maintained by both the Li^+ in the PT or POT as before and also with the ion exchanger which is a component of the ionophoric cocktail. Therefore again there is a sufficient driving force to control a local equilibrium at the SC/PVC interface.

So in both the cationic and anionic selective electrodes a cationic equilibrium is set up at the PT/PVC/solution interfaces and throughout the bulk PVC membrane during conditioning with the possibility of some neutral salt formation between the Li^+ and the Cl^- anion especially in the (SC)Pt/PT/PVC(Cl^-) or (SC)Pt/POT/PVC(Cl^-) electrodes not being ruled out. A disruption of this equilibrium by a change in PVC membrane ion concentration results in the ultimate electronic conduction of a change through the electropolymer to the Pt substrate.

From a stability view point the most important process of the solid contact electrode is that described by process iii where effectively the transfer of ionic to electronic information is accomplished. The apparent lack of such an interface in CWEs has been offered as an explanation for the lack of stability of CWEs.

In conclusion, the inclusion of a a mixed ion/e^- conducting electropolymer such as PT or POT, has the power to "unblock" the interface between the ionically conducting PVC-ionophore membrane and the electronically conducting substrate.

5.7 Hybrid-Film Electrodes

Introduction

Up to this point the solid contact approach for a solution to the blocked interface problems, among others, of the CWE, has involved a three tier electrode approach ie. a substrate like Pt or GC coated with conducting polymer and then subsequently coated with the traditional PVC layer containing the ionophore of interest. A mixture of the two polymers, conducting and PVC to form a hybrid-film electrode which would have the inherent properties of both the electronically conducting PPy, PT or POT and the ionically conductive PVC cocktail has not been extensively examined due to solubility problems of PPy and PT in THF and most organic solvents, the solvent which is used in casting PVC ISEs. However, POT is a member of the polyalkylthiophene (PAT) family which is known for solubility in organic solvents, is slightly soluble in THF, so it was decided to utilise this property to examine the possibilities of such a system.

The incorporation of a conducting polymer into a membrane which was then used in a conventional ISE arrangement has previously been described by Pearson et al [56]. In the electrodes described doped PPy which had been prepared either chemically or electrochemically was ground to a fine powder in an agate mortar and was then mixed with an approximately equal weight of either PVC or silver sulphide. After further grinding of the mixtures to give homogeneous PPy-PVC binder mixtures THF was added and the resulting disc produced after evaporation was used in a conventional ISE arrangement. The ion-selective nature of the membrane was provided solely by the presence of the doped PPy. All of the electrodes of this format except one gave a sub-Nernstian anionic responses with a cationic response being seen for an electrode whose PPy component had been prepared by cycling to -0.75 V on the reverse scan. Undoping to such low levels may cause an influx of cations into the membrane to effect electroneutrality. The sub-Nernstain anionic responses were attributed to the possibliity of insufficient numbers of electroactive sites being available in the surface layers of the membrane. The work described in this section involves the mixing of chemically polymerised POT, (POT)c, with a lithium selective ionophore in different ratios and the assessment of each combination as a lithium selective electrode. So unlike the work described by Pearson et al [56] a solid contact configuration will be used which contains both ionically and electronically conducting materials.

Results and Discussion

It must be noted that the electrode containing 50% POT looked different to the other combinations. The film was not smooth like the others but appeared crumpled. This may have been due to the two different polymers drying at unequivalent rates causing the film to stretch.

5.7.1 Ionic Response

5.7.1.1 Hybrid-film Electrodes on Platinum.

The first electrode of this type examined, used a Pt substrate. It was composed of approximately 10% POT and 90% PVC(Li^+). It yielded a sub-Nernstian cationic response to Li^+ with a slope of 43.75 mV/dec., (Figure 5.19). It displayed good stability over the latter 5 days of a 7 day stability test (Figure 5.20) and showed no redox response to various ratios of the FeII and FeIII redox couple. The cationic response although sub-Nernstian, along with the apparent stability of the electrode and most importantly the lack of redox response of the electrode with this combination of electroactive and ionically active components was very encouraging. However, the black polymeric layer did not adhere very well to the Pt substrate and it actually fell off before selectivity measurements could be made. Therefore, further examination was carried out using GC as the substrate. This inability of $(POT)_c$ to adhere well to Pt was previously reported [68].

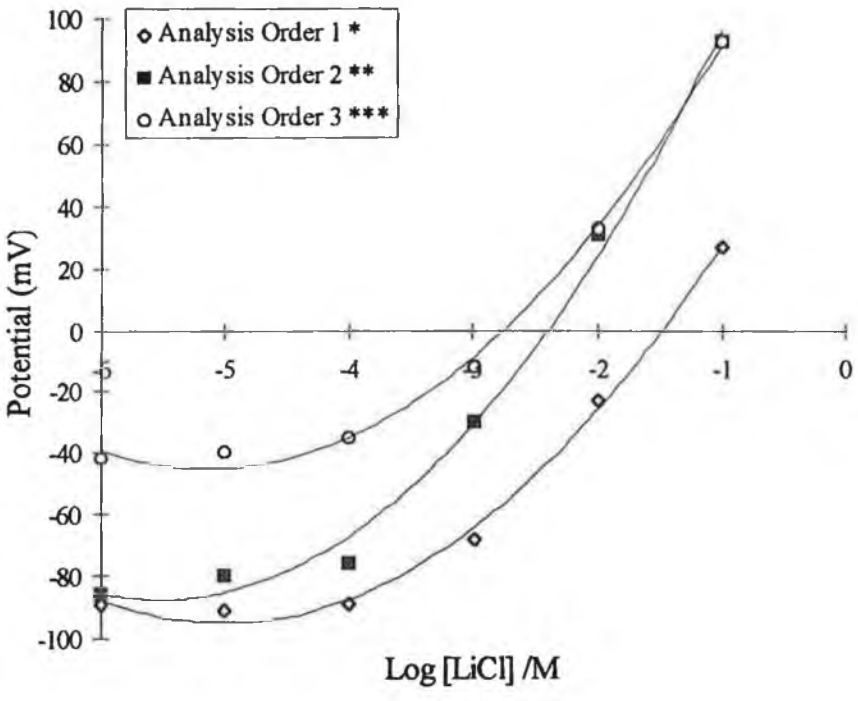

Figure 5.19:- *Potentiometric response of a (HFE)Pt/10%POT, 90%PVC(Li) electrode to LiCl, in the presence of a background electrolyte of 0.1 M KNO_3*

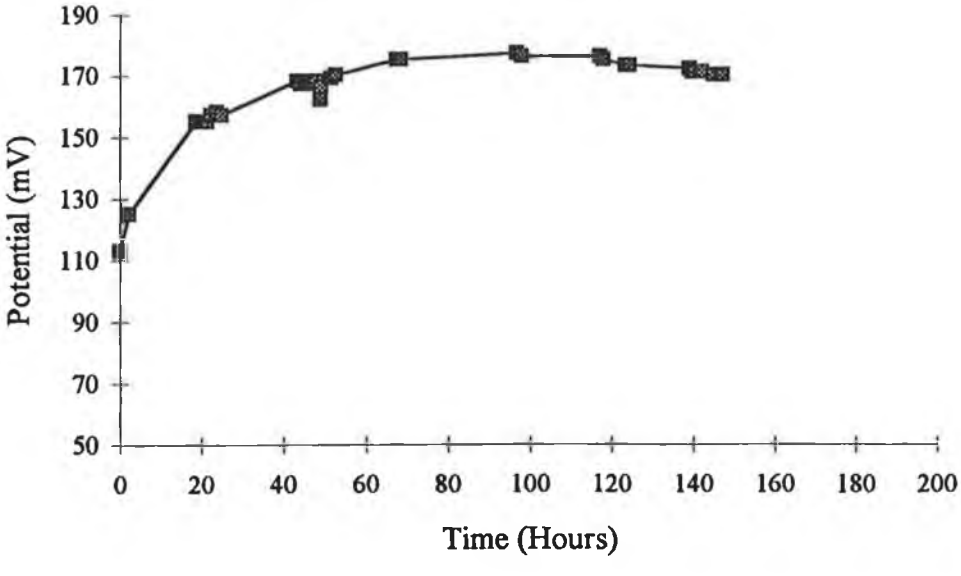

Figure 5.20:- *Stability study with (HFE)Pt/10%POT, 90%PVC(Li) electrode in 0.1 M LiCl, in the presence of 0.1 M KNO_3*

5.7.1.2 Hybrid-film POT Electrodes Using Glassy Carbon as Substrate.

The ionic response of the various hybrid-film electrodes on glassy carbon is summarised in Table 5.9, with data obtained from the response curves 5.21(a)-(i).

Table 5.9 Ionic Response of Hybrid-film Electrodes on GC.

Electrode Name.	% POT	Slope mV/ Dec	LOD (M)	K_{Li^+,Na^+}	K_{Li^+,K^+}	K_{Li^+,NH_4^+}	$K_{Li^+,Mg^{2+}}$
(a)	0	56.00	2.11×10^{-4}	-1.24	-1.29	-1.33	-2.33
(b)	5	56.00	2.59×10^{-4}	-1.27	-1.29	-1.39	-2.39
(c)	10	56.75	1.66×10^{-4}	-1.31	-1.46	-1.49	-2.43
(d)	15	57.75	1.78×10^{-4}	-1.40	-1.48	-1.61	-2.58
(e)	20	55.50	1.57×10^{-4}	-1.37	-1.47	-1.57	-2.49
(f)	25	56,75	1.76×10^{-4}	-1.40	-1.47	-1.62	-2.45
(g)	50	20.75	3.30×10^{-4}	+0.14	+0.18	-0.55	-0.28
(h)	75	23.00	1.40×10^{-4}	+0.03	+0.05	+0.04	-1.03
(i)	100	6.85	-	-0.10	0.00	+0.02	-1.00

For electrodes containing between 0 and 25% POT a near Nernstian response was obtained (Figures 5.21(a) - 5.21(f)). All of these electrodes also displayed Li^+ selectivity over Na^+, K^+, NH_4^+ and Mg^{2+}. For electrodes prepared with 50 - 100% POT a poor cationic response was observed with slopes of 20.8 and 23.0 being obtained for 50 and 75% POT respectively (Figure 5.21(g) and (h)) and a more anionic response being observed for the 100% POT (Figure 5.21(i)). Lithium selectivity was non-existent for these three electrodes.

Of the electrodes containing between 0 and 25% POT, the 15% POT electrode, (HFE)GC/15%POT,85%PVC(Li^+) gave the best slope and marginally better selectivity coefficient values. A slope of 57.75 mV/dec. was obtained for LiCl compared to 56.0 mV/dec. for the GC coated wire version, or (CWE)GC/0%POT,100%PVC(Li^+) electrode. The selectivity values obtained for this electrode are also superior to those obtained for the (CWE)GC/0%POT,100%PVC(Li^+) electrode with k_{LiNa}^{Pot} of -1.40 compared to -1.24 being obtained. These selectivity and slope values are also better than those obtained for the solid contact electrodes prepared with both PT and POT described earlier. However a different substrate was used i.e. Pt, and for a direct comparison to be made PT and POT solid contacts should be prepared by

electropolymerisation on GC. The LOD of 1.78×10^{-4} M is also an improvement on that obtained with the analogous CWE and SC lithium selective electrodes discussed in section 5.3.

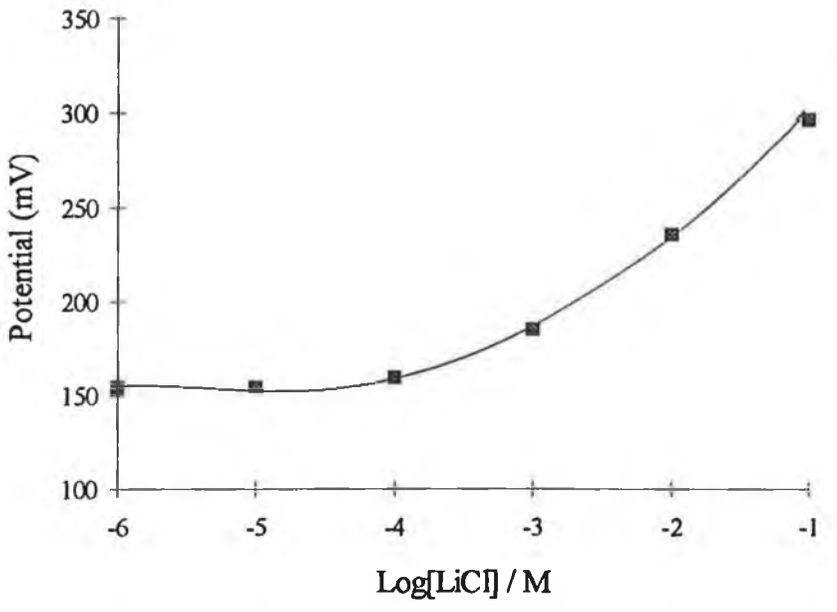

Figure 5.21(a):- *Potentiometric response of a (CWE)GC/0%POT, 100%PVC(Li^+) electrode to LiCl, in the presence of 0.1 M KNO_3*

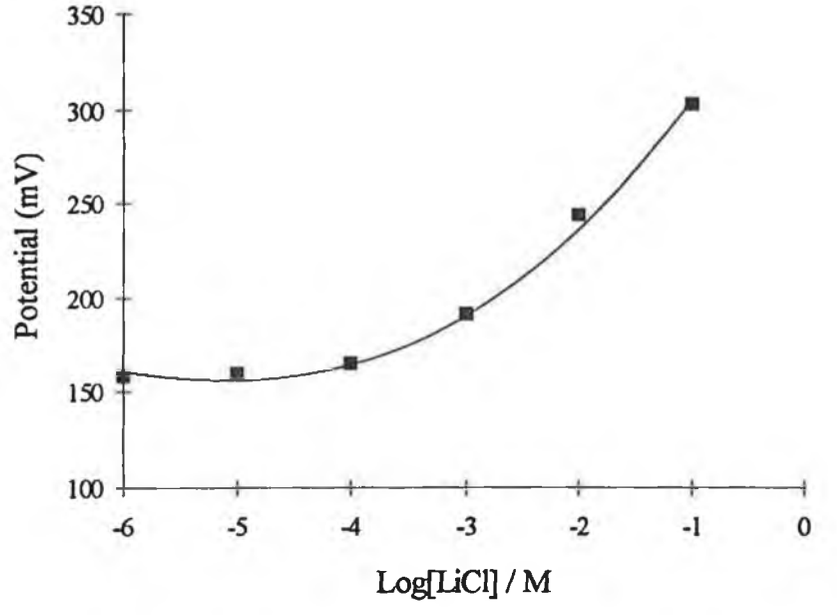

Figure 5.21(b):- *Potentiometric response of a (HFE)GC/5%POT, 95%PVC(Li^+) electrode to LiCl, in the presence of 0.1 M KNO_3*

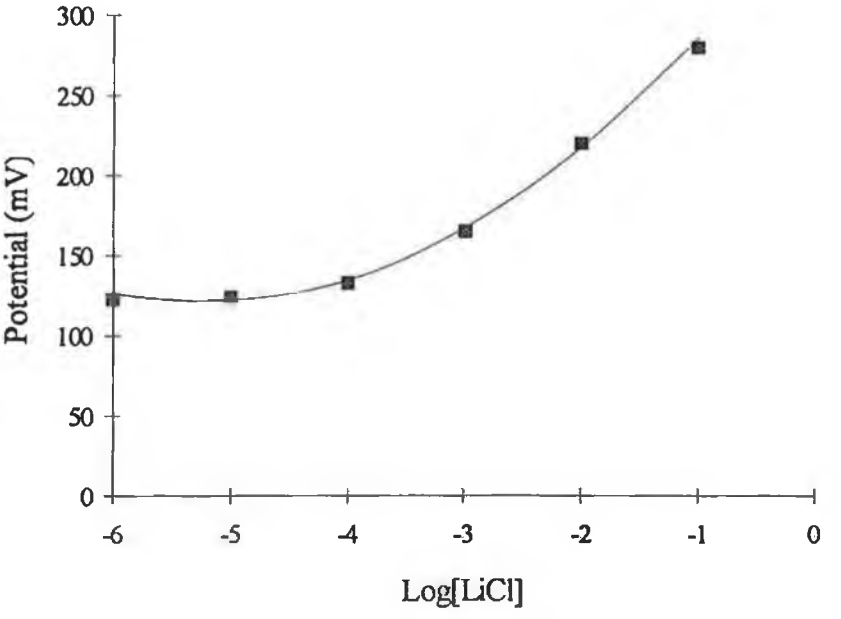

Figure 5.21(c):- *Potentiometric response of a (HFE)GC/10%POT, 90%PVC(Li^+) electrode to LiCl, in the presence of 0.1 M KNO_3*

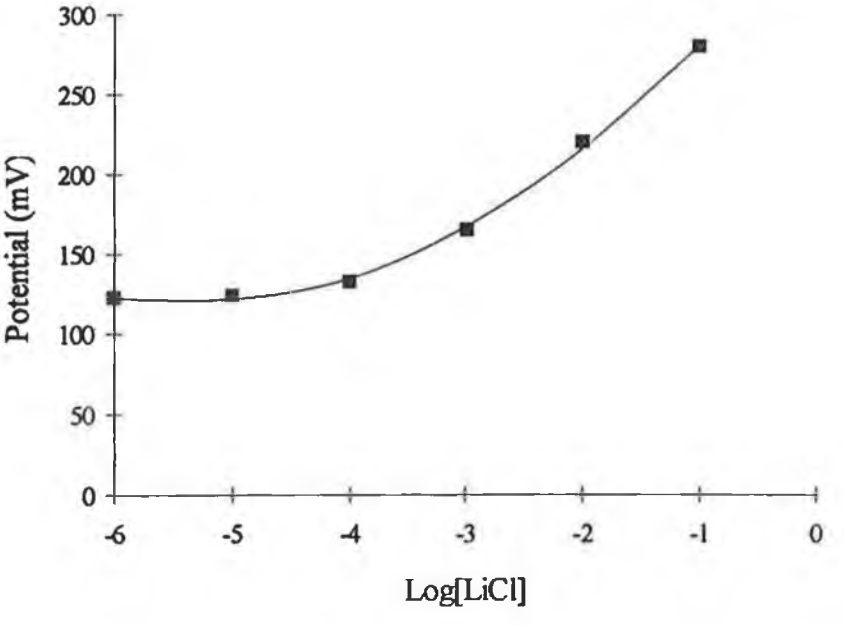

Figure 5.21(d):- *Potentiometric response of a (HFE)GC/15%POT, 85%PVC(Li^+) electrode to LiCl, in the presence of 0.1 M KNO_3*

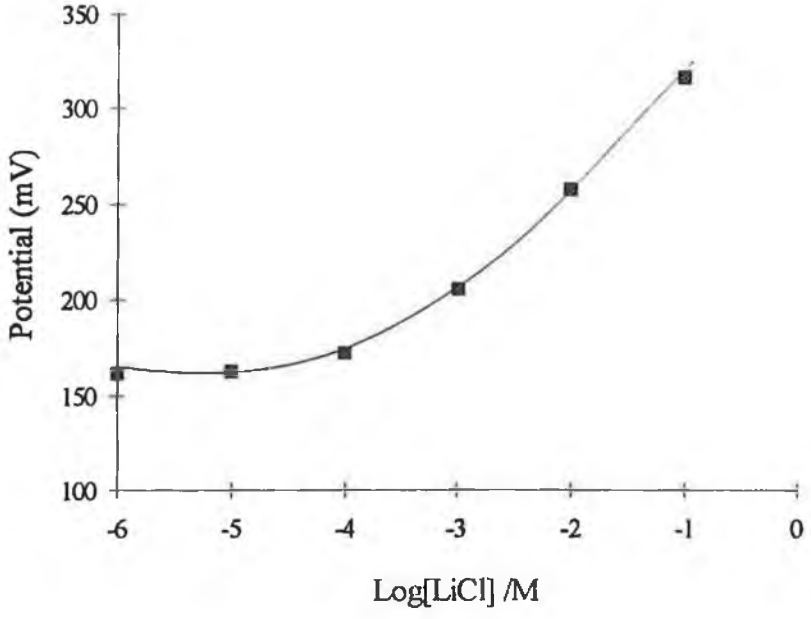

Figure 5.21(e):- *Potentiometric response of a (HFE)GC/20%POT, 80%PVC(Li^+) electrode to LiCl, in the presence of 0.1 M KNO_3*

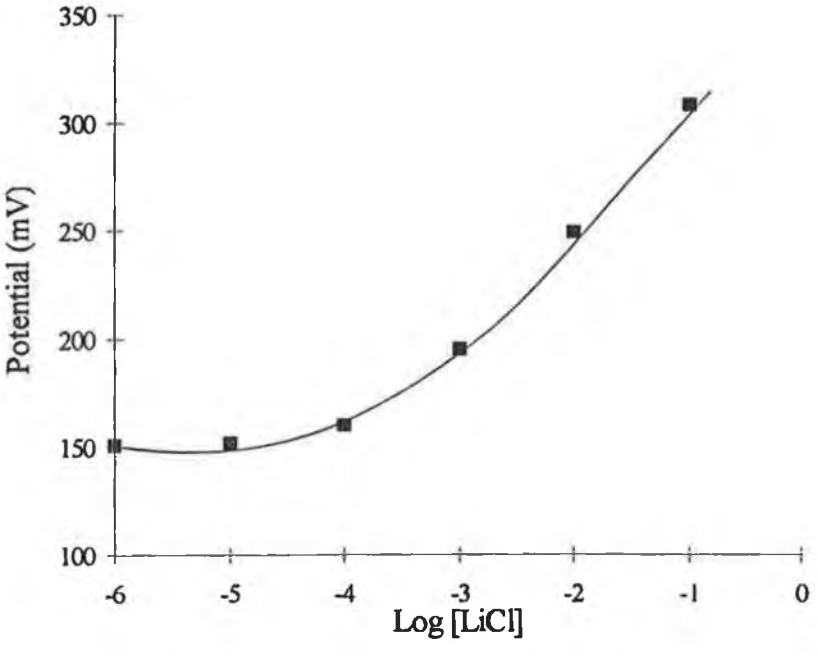

Figure 5.21(f):- *Potentiometric response of a (HFE)GC/25%POT, 75%PVC(Li^+) electrode to LiCl, in the presence of 0.1 M KNO_3*

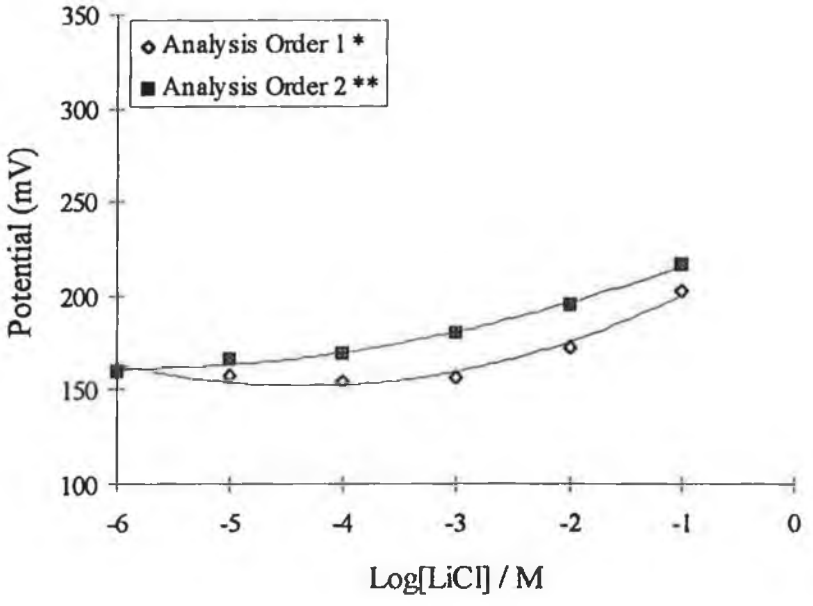

Figure 5.21(g):- *Potentiometric response of a (HFE)GC/50%POT, 50%PVC(Li^+) electrode to LiCl, in the presence of 0.1 M KNO_3*

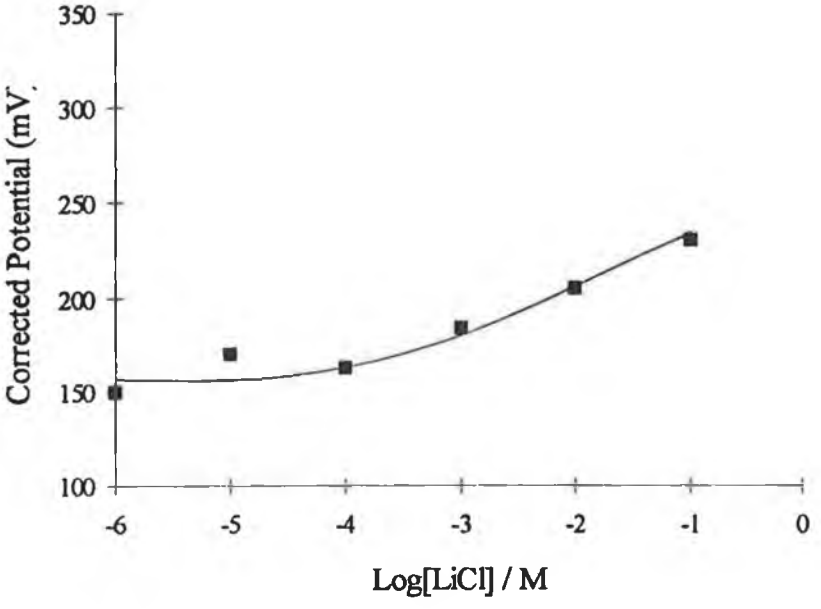

Figure 5.21(h):- *Potentiometric response of a (HFE)GC/75%POT, 25%PVC(Li^+) electrode to LiCl, in the presence of no background electrolyte.*

* Analysis Order 10^{-1} - 10^{-6} M

** Analysis Order 10^{-6} - 10^{-1} M

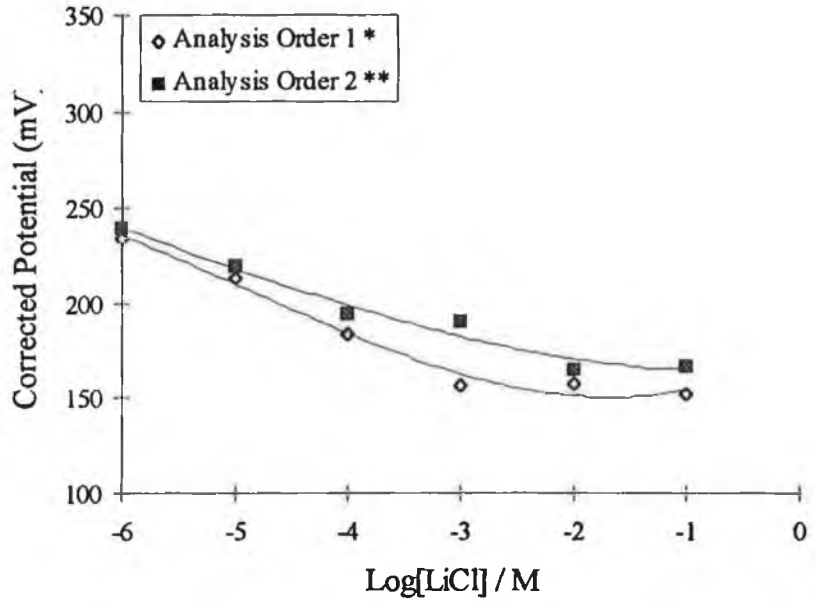

Figure 5.21(i):- *Potentiometric response of a (CPE)GC/100%POT, 0%PVC(Li^+) electrode to LiCl, in the presence of no background electrolyte.*

* Analysis Order 10^{-1} - 10^{-6} M

** Analysis Order 10^{-6} - 10^{-1} M

Hysteresis was not evident with any of the hybrid-film electrodes from 0 to 25% POT, with very stable potential readings being achieved immediately when the magnetic stirrer was turned off. All electrodes had a response time of under 10 seconds.

5.7.2 Stability

The (HFE)GC/15%POT, 85%PVC(Li^+) electrode showed very good stability over the latter 6 days of a seven day stability test (Figure 5.22(a)), with a potential difference of only 2 mV over the last three days. The coated wire electrode on this substrate also displayed good stability but a constant upward drift of between 2 and 4 mV/day was noticed from the third day onwards (Figure 5.22(b)). It would appear therefore that the hybrid-film electrode is slightly more stable than its CWE equivalent. The return of the electrode to its original potential after the stability test was not observed with the GC/PVC(Li^+) electrode and the initial upward increase in potential during the first couple of days of the stability study is possibly associated with an equilibration of the LiCl throughout the bulk of the membrane.

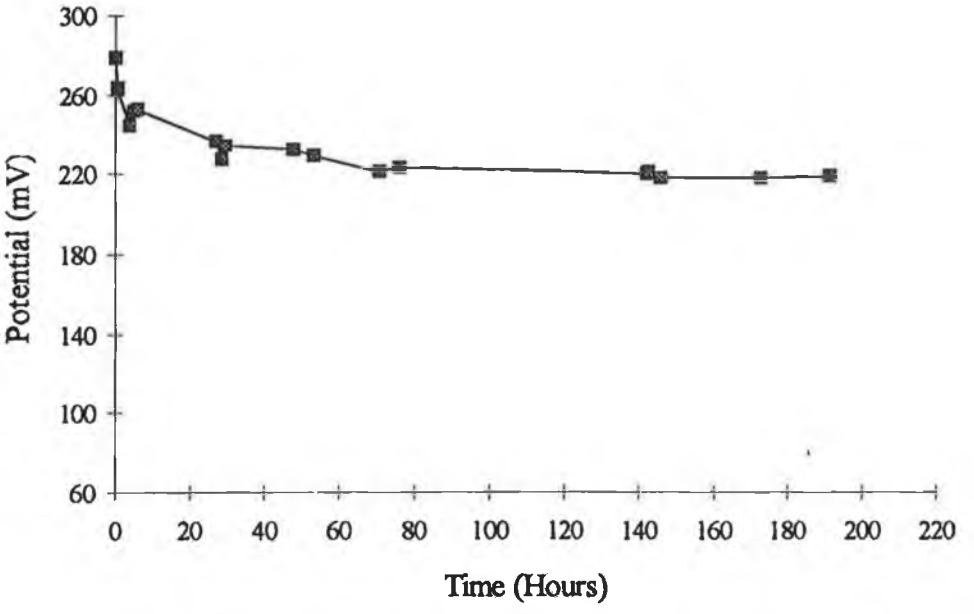

Figure 5.22(a):- Stability study of (HFE)GC/15%POT, 85%PVC(Li^+) in 0.1 M LiCl, in the presence of a fixed background solution of 0.1 M KNO_3.

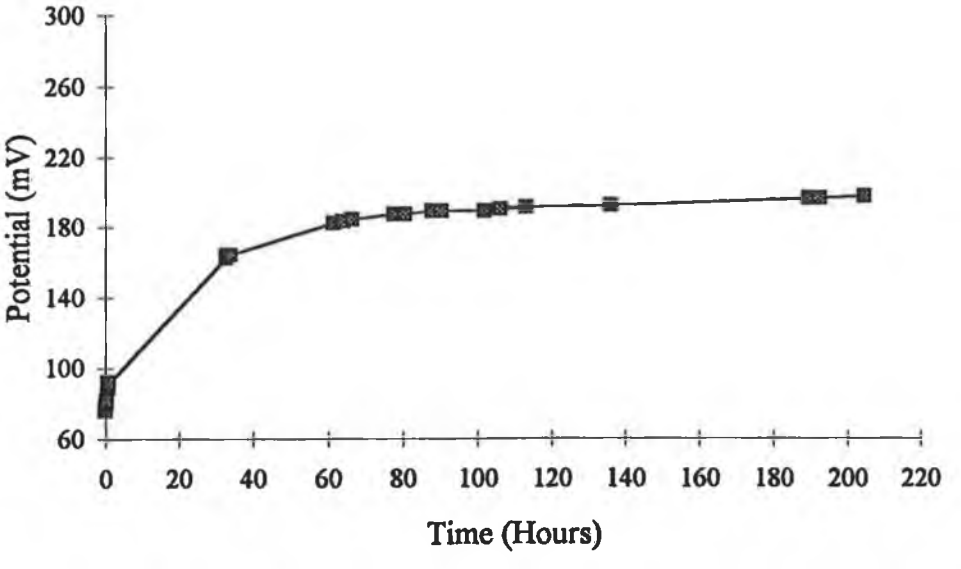

Figure 5.22(b):- Stability study of (CWE)GC/100%PVC(Li^+) in 0.1 M LiCl, in the presence of 0.1 M KNO_3

5.7.3 Oxygen Dependence

From Figure 5.23(a) it can be seen that oxygen bears no influence on the absolute potential of the (HFE)GC/15%POT, 85%PVC(Li^+) electrode. The reason for this being that oxygen was found not to affect the GC substrate (Figure 5.23(b)) in the same way it affects Pt with no decrease in potential being observed upon purging with nitrogen. Glassy carbon has been suggested to be a suitable substrate for electrodeposition of heteroatomic compounds due to its large electrochemical working range and the fact that it gives strong adherent films [48]. Such a positive characteristic would also appear to be applicable to GC electrodes coated with chemically prepared (POT)c. The lack of effect of the partial pressure of sample oxygen on the GC substrate displayed here could be a contributing factor to the improved stability observed for the hybrid-film electrodes compared to the Pt/SC electrodes of sections 5.4 and 5.5.

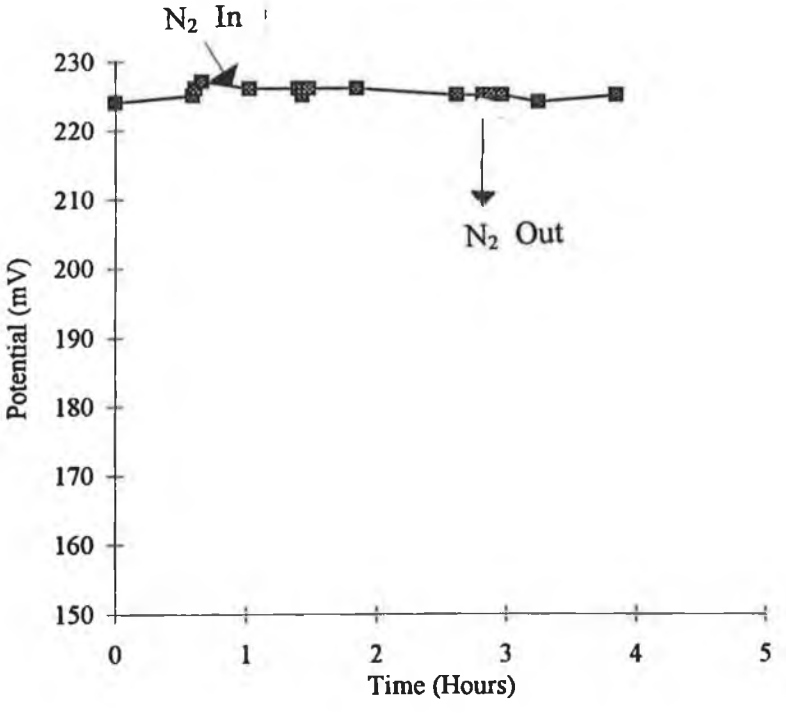

Figure 5.23(a):- *Effect of removal of O_2 from a 0.1 M LiCl solution on the (HFE)GC/15%POT, 85%PVC(Li^+) electrode, in the presence of 0.1 M KNO_3.*

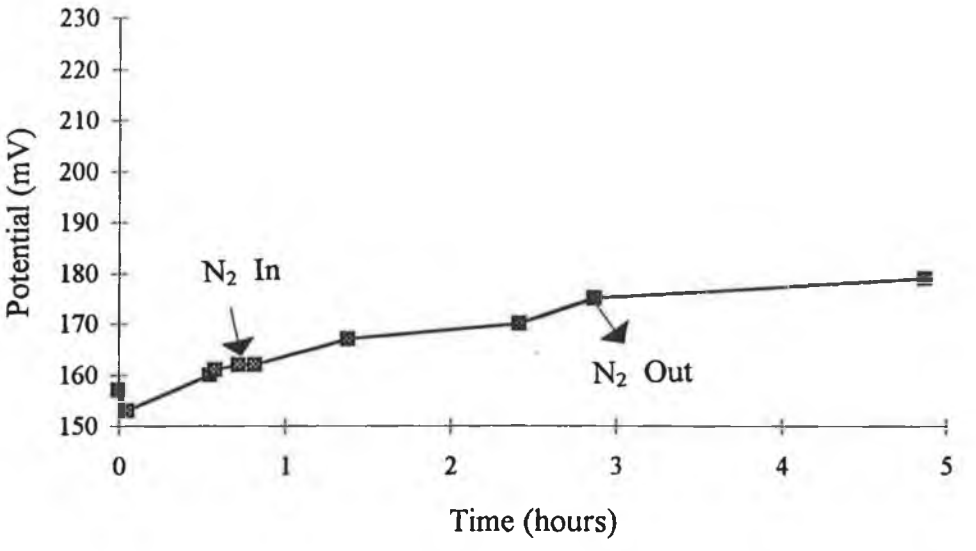

Figure 5.23(b):- Effect of removal of O_2 from a 0.1 M LiCl solution on an uncoated GC electrode, in the presence of 0.1 M KNO_3.

5.7.4 Redox Response

None of the electrodes between 0 and 50% POT displayed any sort of redox response, giving evidence, that the PVC part of the membrane rather than the (POT)c is dominating the cationic response process displayed in the potentiometric curves, to the changes in its environment. The analyte ion concentration recognition process would be purely ionic and changes in ion concentration are then transmitted through to the Pt substrate by an electronic process similar to the solid contact described for the POT in the solid contact electrodes (Table 5.10). Since both the (HFE)GC/75%POT, 25%PVC(Li^+) and (CPE)GC/100%POT display some redox response indicates that the (POT)c is electronically semi-conducting and hence electronic conduction from the solution directly through to the GC substrate is possible.

At higher POT compositions, where a redox response is noted, the semiconductive nature of the POT appears to be the dominant recognition species and hence electronic conduction from the solution directly through to the GC substrate occurs.

Table 5.10:- Redox response of glassy carbon hybrid-film electrodes.

Electrode Type	Electrode	Slope (mV/decade)
	GC	57.6
(CWE)	GC/100%PVC(Li^+)	0.5
(HFE)	GC/15%POT,85%PVC(Li^+)	1.5
(HFE)	GC/50%POT,50%PVC(Li^+)	0.5
(HFE)	GC/75%POT,25%PVC(Li^+)	20.0
(CPE)	GC/100%POT	21.5

5.8 Hybrid-film Electrode containing Chloride ionophore, GC/15%POT,85%PVC(Cl^-).

One hybrid-film electrode containing 15% PVC (Cl^-) was prepared. The dry weight of 100 µL PVC(Cl^-) was 14.28 m, so for the 15% POT electrode a weight of 2.14 mg POT was used along with 85 µL of the cocktail. The layer did not dry as evenly as its comparable (HFE)GC/15%POT,85%PVC(Li^+) hybrid-film electrode with two thinner patches in the film over the (HFE)GC surface. The film did not appear as black as that obtained with the (HFE)GC/15%POT,85%Li^+ electrode, and small water droplets were noticed to have adhered to the electrode surface upon removal from the aqueous 0.1 M LiCl conditioning solution. The (HFE)GC/15%POT,85%Li^+ film appeared to be more hydrophobic with no moisture remaining upon removal from the conditioning solution.

The response to LiCl with no background salt is shown in Figure 5.24, with an average slope of 61.50 mV/decade being obtained. Potential reproducibility was not as good with the (HFE)GC/15%POT,85%PVC(Li^+) electrode. A negative redox response slope was obtained with a slope of 20 mV/dec. The polymeric film was found to be dark green after the redox measurements had been made. The 15%POT,85%PVC(Cl^-) had previously been noticed to trap some of the FeIII during redox measurements, giving a yellow colour to a layer which should have been clear. This colour remained in the film even after a week long conditioning period in 0.1 M LiCl. Time did not permit a further examination of this type of electrode. The occurence of a redox response for this electrode is in contrast to the lack of redox sensitivity of the (HFE)GC/15%POT, 85%PVC(Cl^-)

electrode. The actual apparent absorption of FeIII by the POT layer by visual inspection may have contributed to the response seen here, as the incorporation of a redox component within the membrane or in close contact with the semi-conducting POT will make conduction a lot simpler than in the case of the non Fe permeable POT, PVC(Li^+) mixture.

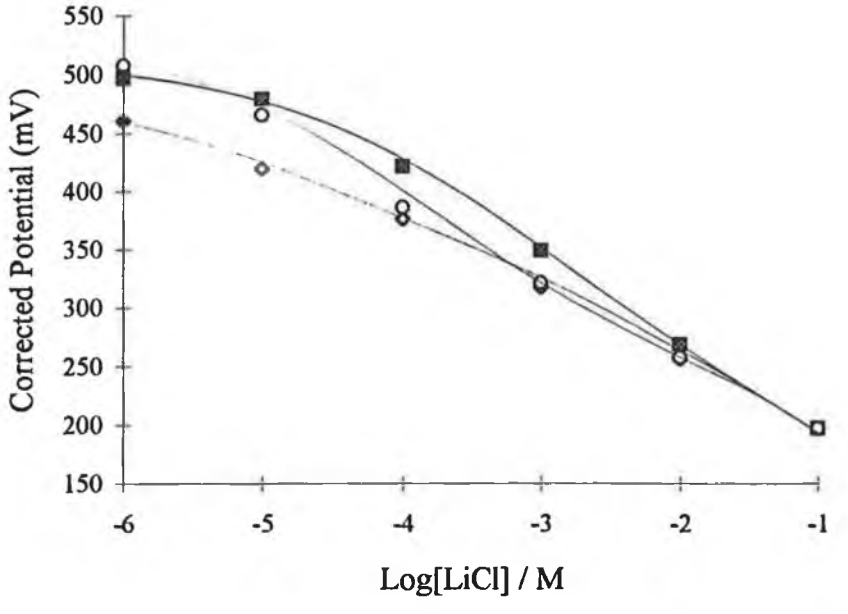

Figure 5.27:- *Potentiometric response of (HFE)GC/15%POT, 85%PVC(CI) electrode to LiCl in the presence of no background interferent.*

* Analysis Order 10^{-1} - 10^{-6} M

** Analysis Order 10^{-6} - 10^{-1} M

*** Analysis Order 10^{-1} - 10^{-6} M

5.9 Overall Discussion

The near Nernstian cationic response and the fact that cationic selectivity occur with the hybrid-film electrodes in the absence of any redox response with a POT percentage less than or equal to 25% is very encouraging. It indicates that the PVC(Li^+) component of the membrane plays the predominant role in cationic recognition for these membrane compositions. If (POT)c was playing the dominant role, cationic selectivity would not be expected and as illustrated with (CPE)GC/100% POT, the cationic response would actually be very poor or non-existent for this thickness of film. The improved response and selectivity values

for (HFE)GC/15%POT over its coated wire equivalent is a possible indication of the presence of an additional information transmission mechanism for concentration changes. The small percentage of (POT)c appears to play a role in transferring electronic information to the Pt metal substrate in a more efficient manner than in the CWE.

The 100% (POT)c electrode does not display any real cationic sensitivity, in this work, whereas it was observed previously [61] with a slope of approximately 50mV/dec and this could be due to a number of factors. Firstly, a different substrate was used i.e. Pt instead of GC, although this factor should not reduce cation sensitivity to practically zero but would be expected to alter it slightly. Secondly, the thickness and density of the polymer layer which was approximately 150 μm compared to just 3 μm in the earlier work, could simply be too large to allow sufficient transport of cations through the film during conditioning, thereby preventing electrostatic interaction with the sulphur group of the polyoctylthiophene taking place, a process which is considered of paramount importance in the ability of these polymers to perform as cation sensitive materials. Since POT has a relatively low ionic/electronic conduction which manifests itself in non-Nernstian cationic and redox responses, a thick film may prevent effective signal transfer. From the redox response results for the GC/100%POT electrode where a slope of 21.5 mV/dec is seen, it is apparent that some electronic conduction is possible with even this dense membrane.

With the (HFE)GC/15%POT, 85%PVC(Li^+) electrode, there is a larger percentage of polymer through which cations can freely move i.e. PVC, and hence Li^+ is introduced into the film in a more comprehensive way and can interact more easily with the sulphur groups of the POT. This introduces the possibility of electronic transfer of ionic concentration changes in the film to the GC substrate. The percentage of POT would appear not to be large enough to exert its own cationic sensing abilities on the overall results as a decrease in selectivity, not an increase as observed, would be expected if the POT was playing a role in the solution cationic recognition process . The way in which the polymer dries on the electrode surface may also play an important role in the electrode characteristics, with perhaps the POT having a greater tendency to adhere to the GC substrate resulting in a predominantly electronically conductive interface. The lack of a redox response for this electrode is a beneficial characteristic since it means it is not susceptible to interference from the presence of a redox couple and it is responding solely to the presence of the Li^+ cation.

The over all stability of both the (HFE)GC/15%POT, 85%PVC(Li^+) and (CWE)GC/0% POT, 100%PVC(Li^+) are improved from the (CWE)Pt//PVC(Li^+) and Pt/ CWE electrodes with the potential of the (HFE)GC/15%POT, 85%PVC(Li^+) electrode being particularly stable i.e. 2-4 mV/day after 2 days and initial potential changes not being as great i.e. 30 mV, as those witnessed for the Pt electrodes. The increased stability could be a substrate effect, with GC not being as susceptible to potential changes with oxygen partial pressure changes. The slightly better stability for the (HFE)GC/15%POT compared to the (CWE)GC/100% PVC(Li^+) points to the possible existence of an additional ionic/electronic conduction mechanism being involved in the membrane containing (POT)c. This coupled to the selectivity and cationic response curve add to this proposition. A diagram of the possible nature of the conduction process is presented in diagram 5.2.

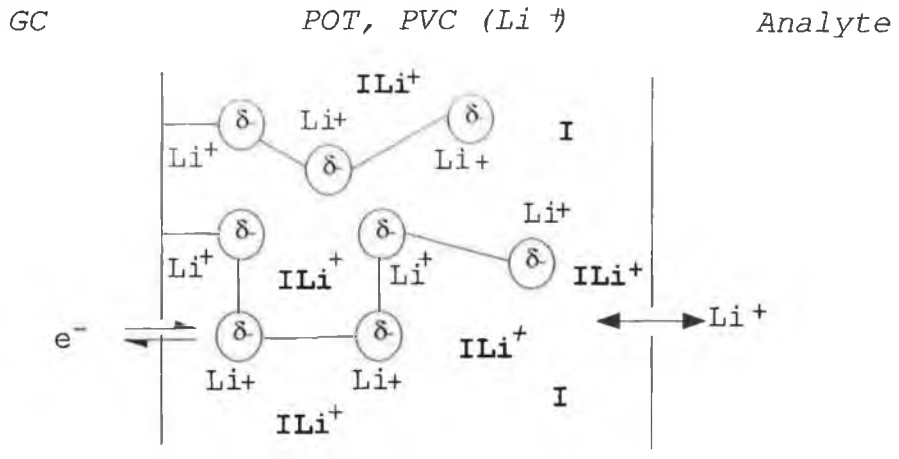

Diagram 5.2:- *Schematic conduction mechanism of hybrid-film POT, PVC(Li^+) electrodes. I=Ionophore.*

5.10 Conclusion

A new type of Lithium selective electrode has been produced using chemically synthesised POT and a lithium selective ionophore. It displays superior Li^+ response, selectivity, L.O.D. and stability to either CWE, or solid contact electrodes incorporating electrically polymerised PT or POT. It requires the use of a cheaper substrate i.e. GC instead of Pt, which is not susceptible to potential changes with variations in the partial pressure of oxygen in the analyte solutions. Further work will be required to elucidate the exact nature of the conduction processes of this type of electrode.

5.11 References

1. A. Cagogan, Z. Gao, A. Lewenstam, A. Ivaska, and D. Diamond. Anal. Chem., 64 (1992) 2496.
2. R.W. Cattrall, and I.C. Hamilton, Ion-Selective Electrode Rev., 6 (1984) 125.
3. W.E. Morf, "*The Principles of Ion-Selective Electrodes and of Membrane Transport*", Elsiever, Amsterdam, (1981) 3.
4. E.P Serjeant, in "*Potentiometry and Potentiometric Titrations*", Wiley, New York, (1984) 105.
5. W.E Morf in ref 3 above, 60.
6. G.J. Moody and J.D.R. Thomas (Eds.) "*Selective Ion-Sensitive Electrodes*", Merrow, Watford, (1971).
7. D. Ammann, W.E. Morf, P.Anker, P.C. Meier, E. Pretsch, and W. Simon, Ion-Selective Electrode Rev., 5 (1983) 3.
8. P. Oggenfuss, W.E. Morf, U. Oesch, D. Ammann, E. Pretsch, W. Simon, Anal. Chim. Acta, (1986) 299.
9. G.J. Moody and J.D.R. Thomas, Selective Electrode Rev., 13 (1991) 227.
10. J. Janata, M. Josowicz and D. M. De Vaney, Anal. Chem., 66 (1994) 207 R.
11. J. Janata, Anal. Chem., 64 (1992) 196 R.
12. R.L.Solsky, Anal. Chem., 62 (1990) 21R.
13. J. Janata, Anal. Chem., 62 (1990) 33 R.
14. R.L.Solsky, Anal. Chem., 60 (1988) 106R.
15. M.A. Arnold and R.L.Solsky, Anal. Chem., 58 (1986) 54R.
16. H.Hirata and K. Date, Talanta, 17 (1970) 883.
17. R.W. Cattrall and H. Freiser, Anal. Chem., 43 (1971) 1905.
18. H. Hirata and K. Date, Anal. Chem., 43 (1971) 279.
19. R.W. Cattrall D.M. Drew and I.C. Hamilton, Anal. Chim. Acta, 76 (1975) 269.
20. R.W Cattrall, D.M. Drew, Anal. Chim. Acta, 77 (1975) 9.
21. A. Hulanicki, R. Lewandowski and M. Maj, Anal. Chim. Acta, 69 (1974) 409.
22. H. Tamura, K. Kimura and T. Shono, Anal. Chem., 54 (1982) 1224.
23. M. Trojanowicz, Z. Augustowska, W. Matuszewski, G. Moraczewska and A. Hulanicki, Talanta, 29 (1982) 113.
24. H. James, G. Carmack and H. Freiser, Anal. Chem., 44 (1972) 856.
25. B.P Nikolskii, and E.A. Materova, Ion-Selective Electrode Rev., 7 (1985) 3.
26. R.P. Buck, in "*Ion-Selective Electrodes in Analytical Chemistry*" Vol 1,. H. Freiser (ed.), Plenum, New York, (1990) 58.

27. F. Oehme in "*Sensors, a Comprehensive Survey*" Vol. 2, (eds.) W. Gopel, J. Hesse and J. N. Zemal (eds.), V.C.H., Weinheim, (1991).
28. M.A. Ratner and D.F. Shriver, Chem. Rev., 88 (1988) 109.
29. R.W. Murray, in "Electroanalytical Chemistry", Vol. 13, A.J. Bard (ed.), Marcel Dekker, New York, (1991) 191.
30. R.J. Forster, J.G. Vos, M.E.G. Lyons, J.Chem. Soc., Faraday Trans., 87, 23 (1991) 3761.
31. T.A. Skotheim (ed.) "*Handbook of Conducting Polymers*", Marcel Dekker, New York, (1986).
32. H. Shirakawa, E.J. Louis, A.G. Mac Diarmid, C.K. Chiang, A.F. Heeger, J. Chem. Soc. Chem Commun., (1977) 578.
33. C.K. Chiang Y.W. Park, A.J. Heeger, H.Shirakawa, E.J. Louis, and A.G. Mac Diarmid, J. Chem. Phys., 69 (1978) 5098.
34. R.B. Kauer, and A.G. Mac Diarmid, Sci. Am., 258 (1988) 60.
35. L.H. Van Vlack, "*Elements of Materials Science and Engineering*", 5th Edition, Addison-Wesley Publishing Company, US, (1985).
36. J. Heinze, Top. Curr. Chem., 152 (1990) 1.
37. E.M. Genies, G. Bidan, and A.F. Diaz, J. Electroanal. Chem., 149 (1983) 101.
38. R.J. Waltman, J. Bargon, and A.F. Diaz, J. Phys. Chem., 87 (1983) 1459.
39. G. Tourillon and F. Garnier, J. Electroanal. Chem., 135 (1982) 173.
40. P. Marque, J. Roncali, and F. Garnier, J. Electroanal. Chem., 218 (1987) 107.
41. Q. X. Zhou, C. J. Kolaskie and L.L. Miller, J. Electroanal. Chem., 223 (1987) 283.
42. S. Bruckenstein, A.R. Hillman, J. Phys. Chem., 95 (1991), 10748.
43. I.C. Lee, J. Electroanal. Chem., 340 (1990) 333.
44. G.L. Duffitt and P.G. Pickup, J. Chem. Soc., J. Chem. Soc., Faraday Trans., 88 (1992) 1417.
45. G.G. Wallace, and Y.P. Lin, J. Electroanal. Chem., 247 (1988) 145.
46. C. Iwakaura, Y. Kajiya, and H. Yoneyama, J. Chem. Soc., Chem. Commun., (1988) 1019.
47. J.M. Slater, J. Paynter, and E.J. Watt, Analyst, 118 (1993) 379.
48. P.R. Teasdale, G.G. Wallace, Analyst, 118 (1993) 329.
49. M.D. Imisides, R. John, P.J. Riley, G.G. Wallace, Electroanalysis, 3 (1991) 879.
50. G. Bidan, Sens. and Actuators B, 6, (1992) 45.
51. A. Ivaska, Electroanalysis, 3 (1991) 247.
52. S. Dong, Z. Sun, and Z. Lu, Analyst, 113 (1988) 1525.

53. S. Dong, Z. Sun, and Z. Lu, J. Chem. Soc., Chem. Commun., (1988) 993.
54. Z. Lu, Z. Sun and S. Dong, Electroanalysis, 1 (1989) 271.
55. A. Cadogan, A. Lewenstam and A. Ivaska, Talanta, 39 (1992) 617.
56. J. F. Pearson, J.M. Slater and V. Jovanovic, Analyst, 117 (1992) 1885.
57. J. Bobacka, Z. Gao, A. Ivaska, and A. Lewenstam, J. Electroanal. Chem., 368 (1994) 33.
58. A. Lewenstam, J. Bobacka, A. Ivaska, J. Electroanal. Chem., 368 (1994) 23.
59. T.Okako, H. Hayashi, K. Hiratini, H. Sugihara and N. Koshizaki, Analyst, 116 (1991) 923.
60. A.E. Karagozler, O.Y. Ataman, A. Galal, Z.-L. Hue, H. Zimmer, H.B. Mark Jr., Anal. Chim Acta, 248 (1991) 163.
61. J. Bobacka, A. Lewenstam, and I. Ivaska, Talanta, 40 (1993) 1437.
62. J. Bobacka, M. Grzeszczuk and I. Ivaska, Electrochimica Acta, 37 (1992) 1759.
63. K.Y. Jen, R. Oboodi, and R.L. Elsenbaumer, Polym. Mater. Sci. Eng., 53 (1985) 79.
64. IUPAC Recommendations for Nomenclature of Ion-selective Electrodes, Pure and Appl. Chem., 48 (1976) 127.
65. J. Bobacka, personal communication.
66. K. Toth, E. Graf, G. Horvai, E. Pungor and R.P Buck, Anal. Chem., 58 (1986) 2741.
67. M. Mai-Zurawska, A. Hulanicki, Anal. Chim. Acta, 136 (1982) 395.
68. J. Bobacka, A. Ivaska, M. Grzeszczuk, Synth. Met., 44 (1991) 21.